

# Sheffield Hallam University

*Design, analysis and testing of non metallic rockbolt bearing plates.*

WILLIAMS, Karen M.

Available from the Sheffield Hallam University Research Archive (SHURA) at:

<http://shura.shu.ac.uk/20543/>

## A Sheffield Hallam University thesis

This thesis is protected by copyright which belongs to the author.

The content must not be changed in any way or sold commercially in any format or medium without the formal permission of the author.

When referring to this work, full bibliographic details including the author, title, awarding institution and date of the thesis must be given.

Please visit <http://shura.shu.ac.uk/20543/> and <http://shura.shu.ac.uk/information.html> for further details about copyright and re-use permissions.

CITY CAMPUS FOND STREET  
SHEFFIELD S1 1WB

101 531 906 8  


BEN  
376717

Sheffield Hallam University  
**REFERENCE ONLY**

**Fines are charged at 50p per hour**

14 OCT 2002 9pm.
26 SEP 2005 4.38

ProQuest Number: 10701190

All rights reserved

INFORMATION TO ALL USERS

The quality of this reproduction is dependent upon the quality of the copy submitted.

In the unlikely event that the author did not send a complete manuscript and there are missing pages, these will be noted. Also, if material had to be removed, a note will indicate the deletion.



ProQuest 10701190

Published by ProQuest LLC (2017). Copyright of the Dissertation is held by the Author.

All rights reserved.

This work is protected against unauthorized copying under Title 17, United States Code  
Microform Edition © ProQuest LLC.

ProQuest LLC.  
789 East Eisenhower Parkway  
P.O. Box 1346  
Ann Arbor, MI 48106 – 1346

**Design, analysis and testing of non metallic  
rockbolt bearing plates**

Karen Margaret Williams B.Eng.

A thesis submitted in partial fulfilment of the requirements of  
Sheffield Hallam University  
for the degree of Doctor of Philosophy

February 1998

Collaborating Organisation: AMS Anchoring Systems Ltd





## Abstract

Non metallic bearing plates have been identified as the weakest component in GRP rockbolting systems used in UK coal mines. A literature review revealed a shortage of information on the design of rockbolting components, particularly the design of the non metallic bearing plates.

Over twenty parameters concerning the design and testing of non metallic rockbolt bearing plates have been investigated using Finite Element Analysis and laboratory testing. The parameters included bearing plate depth, central hole diameter, external diameter, material, coned angle for both solid and webbed bearing plates. The designs have been evaluated by comparing the load / plate volume to consider the efficient use of the material. The experiments were designed using Taguchi and one factor at a time methodologies. Interactions between some parameters have been investigated. Reasons for the observed effect of parameters have been suggested.

A modification of the BS 7861 test is proposed which more closely simulates the colliery failure mechanism and hence gives a better measure of a bearing plate's suitability for use in a coal mine. The modified test uses a 100 mm hole in the steel support plate as specified by American Standard F432 for steel rockbolt bearing plates, not the 55 mm hole as specified by BS 7861.

Optimum values for important parameters have been determined for a 100 mm hole in the steel support plate as proposed in this research and for the 55 mm hole diameter specified by BS 7861. The results produced can be used to design a bearing plate for use in a coal mine with optimum depth and coned angle.

## Acknowledgements

I would like to thank Mr M. Hubbard, Dr T.D. Campbell, Mr A.G. Evans and Dr D.W Clegg for their supervision during this project. Thanks are also expressed to Mr J. Callender and Dr B. Worthington for their advice.

The assistance from the technical staff was much appreciated and in particular I would like to thank Messrs J. Stanley, S. Brandon, R. Wainwright, T. O'Hara, J. Ross Smith, M. Muldownie and K. Wright.

Finally I would like to thank Mr J. Bowler of Thoresby colliery, Mr S. Lang of Whitemoor colliery and Mr A. Hardy of the Union of Democratic Mineworkers for helpful discussions about the problem.

# Contents

Abstract	ii	
Acknowledgements	iii	
Nomenclature	vi	
Index to figures	vii	
Index to tables	xi	
<b>1</b>	<b>Introduction and Literature Review</b>	<b>1</b>
1.1	Introduction	1
1.2	Objectives of research	3
1.3	Overview of types of rockbolts	3
1.4	UK Coal mining	7
1.5	Installation of rockbolts in UK coal mines	8
1.6	Literature Review	10
<b>2</b>	<b>Problem Definition</b>	<b>27</b>
2.1	Observations from a visit down Thoresby colliery	27
2.2	Deformed bearing plates used in the coal mines	31
2.3	Design Specification	34
<b>3</b>	<b>Methodology</b>	<b>37</b>
3.1	Finite Element analysis methodology	37
3.2	Tensile testing of polymer material	45
3.3	Strain gauge methodology	46
3.4	Taguchi experimental design	48
3.5	Overview of approach used to investigate design and testing parameters	57
3.6	Laboratory test on bearing plates	58
<b>4</b>	<b>Finite Element results</b>	<b>59</b>
4.1	Comparison of strain gauge and FE results	59
4.2	Two level Taguchi experiment	60
4.3	Multiple level Taguchi experiment on solid bearing plate designs	62
4.4	Multiple level Taguchi experiment on webbed bearing plate designs	63
4.5	One Factor at a time results	64
4.6	Stress / strain distribution in FE models of bearing plates	77
<b>5</b>	<b>Laboratory testing</b>	<b>89</b>
5.1	Introduction to laboratory testing	89
5.2	Diameter of hole in steel support plate	90
5.3	Radius on edge of hole in steel support plate	97
5.4	Rate of loading	97
5.5	Different nut diameters	98
5.6	Different diameters of hole in the centre of bearing plate	101
5.7	Different external diameter and shape of bearing plate	103
5.8	Load applied to nut via threadform	104
5.9	Bearing plate at an inclined angle of 10°	104

5.10	AMS green circular plate	105
<b>6</b>	<b>Material selection</b>	<b>108</b>
6.1	Materials for use in a bearing plate	108
6.2	Material selection criteria	108
6.3	Material selection charts	110
6.4	Manufacturing techniques	115
6.5	Material data	116
<b>7</b>	<b>Discussion</b>	<b>119</b>
7.1	Finite Element results and method	119
7.2	Taguchi method and results	126
7.3	One factor at a time results	135
7.4	Failure mechanisms of bearing plates from collieries and laboratory tests	155
7.5	Material selection	171
7.6	Summary of how results can be used to design bearing plates for use in coal mines	173
<b>8</b>	<b>Conclusions</b>	<b>182</b>
8.1	Geometry of bearing plate	182
8.2	Laboratory testing parameters	184
8.3	Stress and strain distribution	185
8.4	Methodology	185
8.5	Materials	186
8.6	Further Work	186
	References	188
<b>A1</b>	Appendix 1 - Further FE results	<b>II</b>
<b>A2</b>	Appendix 2 - Orthogonal arrays and drawings of bearing plate designs	<b>XXXIV</b>
<b>A3</b>	Appendix 3 - Material selection charts, abbreviations and tensile specimen dimensions	<b>XXXVII</b>
<b>A4</b>	Appendix 4 - Calculation of load to cause crushing of coal	<b>XLII</b>

## Nomenclature

$A_1, A_2$	Sum of results for parameter A at levels 1 and 2
$C_M$	minimum cost guideline
$C_R$	cost per unit weight of the material / cost per unit weight of steel
$D_R$	Rockbolt diameter
$E_Y$	Young's modulus
$E_R$	Rock mass deformation modulus
F-test	Ratio of variances
$I_1, I_2, I_3$	First, second and third strain invariants
$N_T$	Total number of results
$S_{BP}$	Bearing plate surface area
SS	Sum of squares
$V_A$	Variance for parameter A
$k_{\text{foundation}}$	stiffness of bearing plate foundation on tunnel wall
$k_{\text{plate}}$	stiffness of bearing plate
$k_{\text{tie}}$	stiffness of rockbolt tie on tunnel surface
$\epsilon_{xx}$	principal strain in x direction
$\epsilon_{yy}$	principal strain in y direction
$\epsilon_{zz}$	principal strain in z direction
$\rho$	density
$\nu_A$	degrees of freedom for parameter A
$\nu$	Poisson's ratio
$\nu_{RM}$	Poisson's ratio of rock mass

### Parameters investigated in Taguchi and one factor at a time tests

A	Diameter of central hole in bearing plate
B	Depth of bearing plate at the centre
C	Coned or Flat shape
D	Webbed or solid
E	Material
F	Diameter of hole in steel support plate
G	External diameter of nut
H	External diameter of bearing plate
I	Coned angle
J	Coned shape
K	Number of radial webs
L	Number of circumferential webs
M	Web thickness
N	Depth of bearing plate over edge of hole in steel support plate
O	Position of circumferential webs
P	Temperature
Q	Time in service
R	Distance between diameter of hole in steel support plate and diameter of nut
S	Rate of loading
T	Radius on edge of hole on steel support plate
U	Square or circular shape
V	Inclined angle of bearing plate
W	Load applied to nut via threadform or via top of nut

## Index to Figures

<b>Chapter 1</b>	<b>Introduction and Literature Review</b>	
Figure 1.1	Typical design of bearing plate used in UK coal mines	2
Figure 1.2	Types of rockbolts used in mining engineering	4
Figure 1.3a	A full column resin anchored rockbolt	6
Figure 1.3b	A point resin anchored rockbolt	6
Figure 1.4	Plan layout of longwall retreat mining	7
Figure 1.5	Typical non-metallic rockbolt installed in a UK coal mine	9
Figure 1.6	Resin capsule used for rockbolting	16
Figure 1.7	Testing of non-metallic rockbolt bearing plates	21
<b>Chapter 2</b>	<b>Problem Definition</b>	
Figure 2.1	Rockbolt assembly with a failed plywood plate	29
Figure 2.2	Failed Weldgrip bearing plate	32
Figure 2.3	Failed cracked Weldgrip bearing plate	33
Figure 2.4	Failed Mai bearing plate	34
Figure 2.5	Minimum diameter of bearing plate central hole to allow 18° out of alignment movement of the rockbolt	35
<b>Chapter 3</b>	<b>Methodology</b>	
Figure 3.1	Load, restraint and mesh on webbed bearing plate	38
Figure 3.2	Parameters investigated in Taguchi and one factor at a time tests	49
Figure 3.3	Apparatus used for laboratory tests on bearing plates	58
<b>Chapter 4</b>	<b>Finite Element Results</b>	
Figure 4.1	Circumferential strain in Weldgrip bearing plate from strain gauges and Finite Elements	59
Figure 4.2	Vertical strain in Weidmann bearing plate from strain gauges and Finite Elements	60
Figure 4.3	Variation of load / volume with diameter of hole in steel support plate	64
Figure 4.4	Variation of load / volume with diameter of hole in steel support plate for coned and flat plates	65
Figure 4.5	Variation of load / volume with depth of bearing plates for different diameters of hole in the steel support plate	66
Figure 4.6	Variation of load / volume with coned angle for different diameters of hole in the steel support plate	66
Figure 4.7	Variation of load / volume with coned angle for different depths of bearing plates with a 55 mm hole in the steel support plate	67
Figure 4.8	Variation of load / volume with coned angle for different depths of bearing plate with a 120 mm hole in the steel support plate	68
Figure 4.9	Optimum coned angle for different depths of bearing plate with different diameters of hole in the steel support plate	69
Figure 4.10	Drawing, design number 1	69
Figure 4.11	Drawing, design number 2	70
Figure 4.12	Drawing, design number 3	70
Figure 4.13	Drawing, design number 4	71
Figure 4.14	Variation of load / volume with diameter of nut	72

Figure 4.15	Variation of load / volume with diameter of the central hole in the bearing plate	73
Figure 4.16	Variation of load / volume with number of radial webs for different diameters of hole in the steel support plate	74
Figure 4.17	Distribution of Tresca stress in a flat bearing plate of depth 10 mm with a 55 mm hole in the steel support plate	79
Figure 4.18	Stress at restraint for different diameters of hole in steel support plate	80
Figure 4.19	Distribution of Tresca stress in a coned bearing plate of depth 30 mm coned angle 30° with a 70 mm hole in steel support plate	81
Figure 4.20	Distribution of radial stress in a webbed bearing plate with a 100 mm hole in the steel support plate	83
Figure 4.21	Distribution of circumferential stress in Weldgrip bearing plate with 120 mm hole in steel support plate	85
Figure 4.22	Variation of tensile circumferential stress on lower surface of bearing plate with different diameters of hole in steel support plate	88
<b>Chapter 5</b>	<b>Laboratory testing</b>	
Figure 5.1	Failure mechanism of Weldgrip bearing plate when tested with 60 mm hole in steel support plate	90
Figure 5.2	Failure mechanism of Weidmann bearing plate when tested with 60 mm hole in steel support plate	91
Figure 5.3	Cracks in a failed Weidmann bearing plate tested with 140 mm hole in steel support plate	94
Figure 5.4	Peak load carried in laboratory tests on Weldgrip and Weidmann bearing plates using different diameters of hole in steel support plate	95
Figure 5.5	Sketch of steel support plate with radius on edge of hole	97
Figure 5.6	Plot of load carried against crosshead deflection for Weldgrip bearing plate and Mai nut with a 100 mm hole in the steel support plate	99
Figure 5.7	Failed Weldgrip bearing plate tested with 120 mm hole in steel support plate and Mai nut	100
Figure 5.8	Failed Weldgrip bearing plate with a smaller diameter of hole in the centre of the bearing plate	103
Figure 5.9	Failed AMS bearing plate, 2 months after testing	106
Figure 5.10	AMS bearing plate after complete failure	107
<b>Chapter 6</b>	<b>Material selection</b>	
Figure 6.1	Material selection chart of Young's modulus and ductility	111
Figure 6.2	Stress against strain for material used in Weldgrip and Weidmann bearing plates	117
Figure 6.3	Secant modulus against strain for material used in Weldgrip and Weidmann bearing plates	117
Figure 6.4	Secant modulus against strain for material obtained from Campus database	118
Figure 6.5	Stress against strain for material obtained from Campus database	118

<b>Chapter 7</b>	<b>Discussion</b>	
Figure 7.1	Failure mechanism of Weldgrip bearing plate when tested with 55 mm hole in steel support plate	156
Figure 7.2	Circumferential crack in Weldgrip bearing plate of external diameter 98 mm when tested with 70 mm hole in steel support plate	162
Figure 7.3	Bearing plate test proposal	169
<b>Chapter 8</b>	<b>Conclusions</b>	
<b>Appendix 1</b>	<b>Further Finite Element Results</b>	
Figure A1.1	Variation of load / volume with diameter of hole in steel support plate for a webbed bearing plate	V
Figure A1.2	Variation of load / volume with diameter of hole in steel support plate for different materials	VI
Figure A1.3	Variation of load / volume with depth of bearing plate	VII
Figure A1.4	Variation of load / volume with coned angle for different depths of bearing plate for a 70 mm hole in the steel support plate	VIII
Figure A1.5	Variation of load / volume with coned angle for different depths of bearing plate for a 100 mm hole in the steel support plate	IX
Figure A1.6	Variation of load / volume with depth of bearing plate for different coned angles with a 100 mm hole in the steel support plate	IX
Figure A1.7a	Variation of load / volume with bearing plate depth and nut diameter with 100 mm hole in the steel support plate	X
Figure A1.7b	Variation of load / volume with bearing plate depth and nut diameter with 55 mm hole in steel support plate	XI
Figure A1.8	Variation of load / volume with nut diameter for coned and flat plates	XII
Figure A1.9	Variation of load / volume with nut diameter and coned surface area	XIII
Figure A1.10	Variation of load / volume with distance between nut and support plate hole	XIV
Figure A1.11	Variation of load / volume with nut diameter for three different materials	XIV
Figure A1.12	Variation of load / volume with nut diameter for three different materials	XV
Figure A1.13	Variation of load / volume with nut diameter for different diameters of hole in the centre of the bearing plate	XVI
Figures A1.14 -A1.22	Drawings of webbed bearing plates, webbed design numbers 1-9	XVII - XXV
Figure A1.23a	Comparison of webbed designs 1-9 using a 55 mm hole in steel support plate, evaluated on basis of load / volume	XXVI
Figure A1.23b	Comparison of webbed designs 1-9 using a 55 mm hole in steel support plate, evaluated on basis of load	XXVII
Figure A1.24a	Comparison of webbed designs 1-9 using a 70 mm hole in the steel support plate, evaluated on basis of load / volume	XXVII
Figure A1.24b	Comparison of webbed designs 1-9 using a 70 mm hole in the	XXVIII

	steel support plate, evaluated on basis of load	
Figure A1.25a	Comparison of webbed designs 1-9 using a 100 mm hole in the steel support plate, evaluated on basis of load / volume	XXVIII
Figure A1.25b	Comparison of webbed designs 1-9 using a 100 mm hole in the steel support plate, evaluated on basis of load	XXIX
Figure A1.26	Variation of load / volume with web thickness for webbed design number 4, with a 100 mm hole in the steel support plate	XXX
Figure A1.27	Variation of load / volume with web thickness for webbed design number 4, with a 55 mm hole in the steel support plate	XXX
Figure A1.28	Variation of load / volume with web thickness for design number 8, with a 100 mm hole in the steel support plate	XXXI
Figure A1.29	Variation of load / volume with web thickness for design number 9, with a 55 mm hole in the steel support plate	XXXII
Figure A1.30	Comparison of materials at 25°C and 40°C	XXXII
Figure A1.31	Comparison of different materials over different periods of time	XXXIII
<b>Appendix 2</b>	<b>Orthogonal arrays and drawings of bearing plates designs</b>	
Figures A1.1 - A1.17	Drawings of bearing plate models in 2 level Taguchi experiment	XXXIV
Figures A1.18 - A1.28	Drawings of bearing plates in multiple level Taguchi experiment on solid bearing plate designs	XXXV
Figures A1.29 - A1.40	Drawings of bearing plates in multiple level Taguchi experiment on webbed bearing plate designs	XXXVI
<b>Appendix 3</b>	<b>Material data</b>	
Figure A3.1	Tensile testing specimens	XXXVII
Figure A3.2	Material selection chart showing ductility and Young's modulus	XXXVIII
Figure A3.3	Material selection chart showing flammability and Young's modulus	XXXIX
Figure A3.4	Material selection chart showing tensile strength and maximum service temperature	XL

## Index to Tables

<b>Chapter 1</b>	<b>Introduction and Literature Review</b>	
Table 1.1	Specification for steel roofbolts	10
Table 1.2	Specification for steel ribbolts	11
Table 1.3	Specification for GRP rockbolts	11
Table 1.4	Performance of a steel cable bolt and DAPPAM GRP cable bolt, Pakalnis (1994)	14
Table 1.5	Typical properties of resins used during rockbolting	16
Table 1.6	Typical properties of steel bearing plates used in civil engineering	20
Table 1.7	Allowable failure loads of steel bearing plates, BS 7861	22
Table 1.8	Testing of bearing plates, diameter of unsupported span, external diameter of nut	23
<b>Chapter 2</b>	<b>Problem Definition</b>	
Table 2.1	Proportion of bearing plates that had failed and were of no further use	30
Table 2.2	Design Specification	35
<b>Chapter 3</b>	<b>Methodology</b>	
Table 3.1	Example of verification procedure used to compare stresses at nodes	43
Table 3.2	Example of iterative procedure used to determine performance comparison load	44
<b>Chapter 4</b>	<b>Finite Element Results</b>	
Table 4.1	Results from two level Taguchi experiment	61
Table 4.2	Results from multiple level experiment on bearing plate design	62
Table 4.3	Results from multiple level experiment on webbed bearing plates, using a 100 mm hole in the steel support plate	63
Table 4.4	Comparison of four different designs of solid bearing plates	71
Table 4.5	Comparison of solid and webbed designs, with the same external dimensions	75
Table 4.6	Magnitude of deflection in positive y direction of bearing plate FE models	86
Table 4.7	Tensile circumferential stress on lower surface of bearing plate with different diameters of bearing plate central hole	87
Table 4.8	Comparison of radial and circumferential stress in Weldgrip bearing plate with different external diameters of bearing plate	88
<b>Chapter 5</b>	<b>Laboratory testing</b>	
Table 5.1	Load carried in laboratory tests on Weldgrip plate with different radius on edge of hole	97
Table 5.2	Peak load carried by Weldgrip bearing plate at different rates of loading	98
Table 5.3	Comparison of load carried by Weldgrip bearing plate with Mai and Weldgrip nuts and two different diameters of hole in the steel support plate	101
Table 5.4	Comparison of load carried by the Weldgrip bearing plate with	102

	different diameters of central hole in the bearing plate	
Table 5.5	Comparison of load carried by Weldgrip bearing plate with different external diameter and plan shape of bearing plate	103
Table 5.6	Load carried by Weldgrip bearing plate with 100 mm diameter of hole in steel support plate when load applied to nut directly and via threadform	104
Table 5.7	Load carried by Weldgrip bearing plate with 100 mm diameter of hole in the steel support plate, supported flat and at an inclined angle of 10°	105
<b>Chapter 6</b>	<b>Material selection</b>	
Table 6.1	Material selection criteria	109
<b>Chapter 7</b>	<b>Discussion</b>	
Table 7.1	Design specification for non metallic bearing plates	173
Table 7.2	Load carried by bearing plate FE models with a 100 mm hole in the steel support plate	178
<b>Chapter 8</b>	<b>Conclusions</b>	
<b>Appendix 1</b>	<b>Further Finite Element Results</b>	
Table A1.1	Results from two level Taguchi experiment	II
Table A1.2	Results from multiple level experiment on webbed bearing plates, using a 55 mm hole in the steel support plate	III
Table A1.3	Results from multiple level experiment on webbed bearing plates varying the thickness of only the central webs	IV
Table A1.4	Load and load / volume carried by bearing plates with different external diameters of bearing plate	XVI
<b>Appendix 2</b>	<b>Orthogonal arrays and drawings of bearing plate designs</b>	
Table A2.1	L16 orthogonal array used for 2 level Taguchi experiment	XXXIV
Table A2.2	L9 orthogonal array used for multiple level Taguchi experiment on solid bearing plate designs	XXXV
Table A2.3	L9 orthogonal array used for multiple level Taguchi experiment on webbed bearing plate designs	XXXVI
<b>Appendix 3</b>	<b>Material data</b>	
<b>Appendix 4</b>	<b>Load to cause crushing of coal</b>	
Table A4.1	Compressive strength of coal	XLII
Table A4.2	Load to cause crushing of coal	XLII

# **CHAPTER 1**

## **1. INTRODUCTION AND LITERATURE REVIEW**

### **1.1 Introduction**

This thesis investigates the design and testing of non metallic bearing plates that are used in conjunction with glassfibre (GRP) rockbolts to support the walls in coal mines. A rockbolt is a bolt approximately 2 m long and 22 mm diameter which is inserted and secured into a hole drilled in rock or coal and prevents excessive movement of the rock. Figure 1.1 shows a typical design of bearing plate used in UK coal mines, with a short length of rockbolt of diameter 22 mm. This bearing plate has an external diameter of 147 mm and a maximum thickness of 18 mm.

This research originates from a real problem of failed bearing plates that is being encountered in coal mines. Many failed bearing plates were seen down Thoresby colliery and some have been collected and are presented in Chapter 2. The methodology used to investigate the design and testing methods of bearing plates includes Finite Element Analysis, Taguchi experimental design and laboratory testing. The methodology used is described in Chapter 3.

Chapter 1 provides a general overview of types of rockbolts and their application and installation. The literature review looks briefly at steel rockbolts, cable bolts and in more depth at glassfibre (GRP) rockbolts and components. The literature review ends with a review in detail of bearing plate design, testing and application.

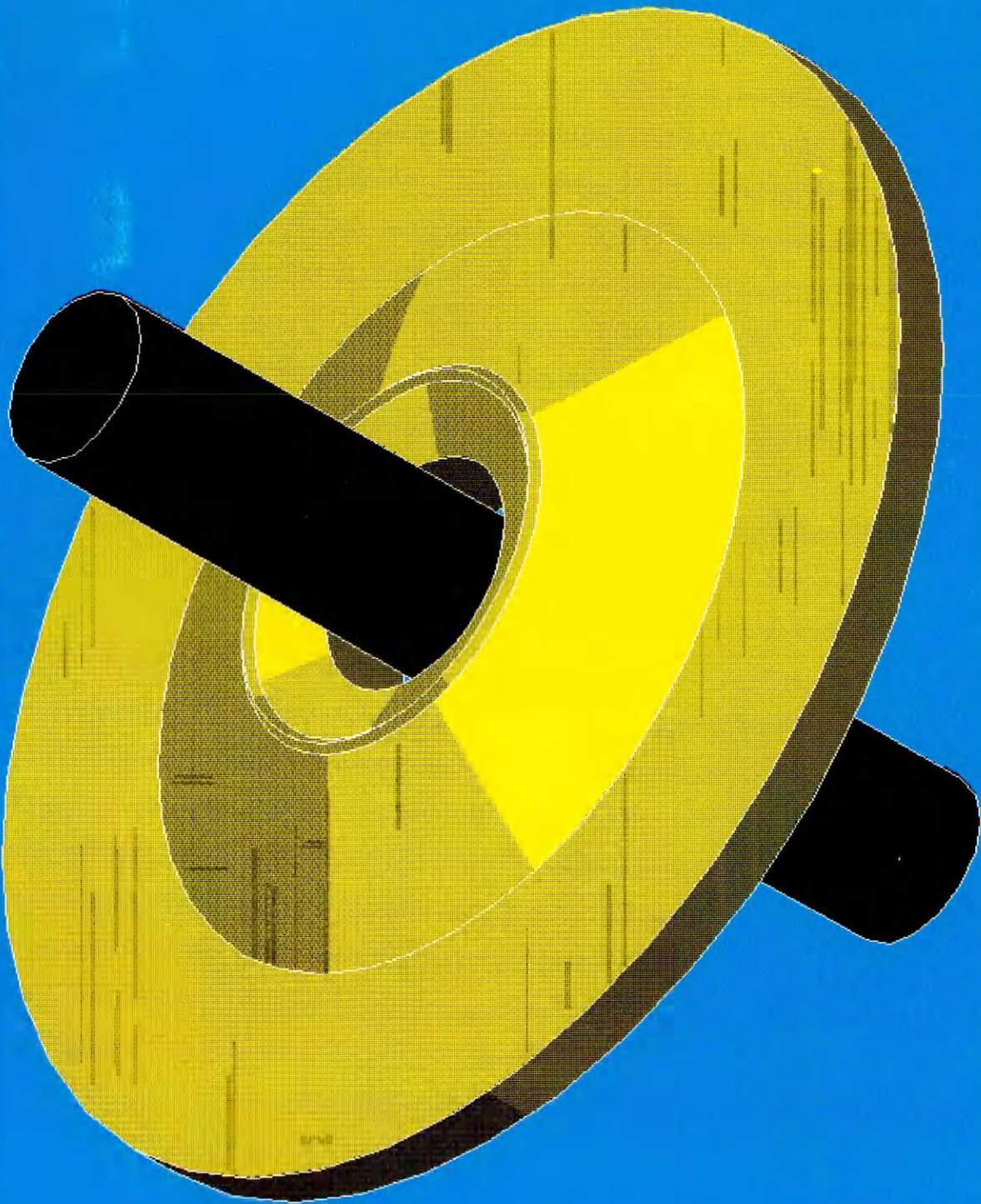


Figure 1.1 Typical design of bearing plate used in UK coal mines.

## **1.2 Objectives of research**

The objectives of this research were to understand the parameters concerning the design and testing of a non-metallic bearing plate for use in UK coal mines, and hence to provide information and guidelines on the design of these bearing plates. Another objective was to propose a bearing plate test which as closely as possible simulates loading down the mine, and hence can be used to evaluate whether a bearing plate performs adequately.

## **1.3 Overview of types of rockbolts**

There are numerous articles which review the different kinds of rockbolts available and the different applications of the rockbolts, Daws (1987), Daws (1988), Tague D. (1990); a brief summary follows.

There are many different types and categories of rockbolts used in mining and civil engineering. In mining a 'roofbolt' is a rockbolt that is used in the roof. A ribbolt is a rockbolt that is used in the rib (wall). Rockbolts in UK coal mines are all made from steel unless the rockbolt will be cut through by the coal cutter. In this case the rockbolts are made from glassfibre (GRP) so that they are cuttable without creating sparks or damaging the coal cutting equipment. GRP rockbolts are also used for civil engineering applications if corrosion is a problem. Figure 1.2 shows the range of different rockbolts that are used in mining engineering.

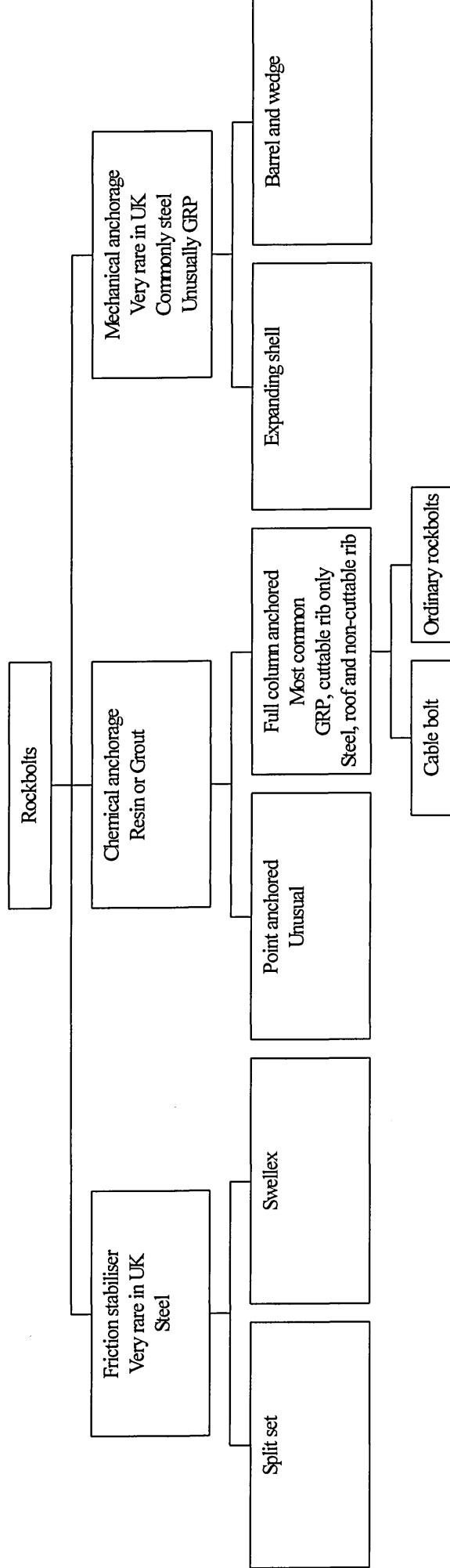


Figure 1.2 Types of rockbolts used in mining engineering.

The usual way of classifying rockbolts is by their means of anchorage in the rock. The three main types of rockbolt are:-

- Mechanical anchors
- Friction stabilisers
- Resin anchors

There are two main designs of mechanical anchors, the 'slot and wedge type' and the 'expanding shell type'. These all involve an anchorage with the rock at the distal (far) end of the borehole. These are usually point anchored rockbolts, i.e. where the full length of the rockbolt is not anchored. This type of rockbolt requires the anchorage point to be in strong competent rock. If used in soft rock (e.g. coal) the wedge grips can cause failure of the rock next to the grips, Hoek (1995). Hence for geological reasons these rockbolts are not widely used in UK coal mines.

Another type of anchorage in rock is the friction stabiliser. Friction stabilisers rely on frictional forces within the borehole for their anchorage. Friction stabilisers are usually anchored along the full length of the rockbolt. Friction stabilisers have the limitation of low anchorage resistance per unit length of rockbolt and hence are not used as primary roof support mechanisms, Daws (1988).

The majority of rockbolts used in the UK today are resin anchored. Resin anchored rockbolts can be used in weak rock where mechanical anchors are unsuitable. When weak roof conditions are encountered in the USA, combination rockbolts using resin anchorage and mechanical anchorage are used. Daws (1987) explains how full column

resin bonded rockbolts can be used for applications where mechanical anchors and friction stabilisers are both unsuitable.

Resin anchored rockbolts can be point anchored or full column resin bonded. Point resin anchored rockbolts are secured with resin at the distal end of the rockbolt. Full column resin anchored rockbolts are secured with resin along the full length of the rockbolt. When rockbolts were first introduced to the UK they were almost all point anchored rockbolts. Most rockbolts currently used in UK coal mines are full column resin anchored.

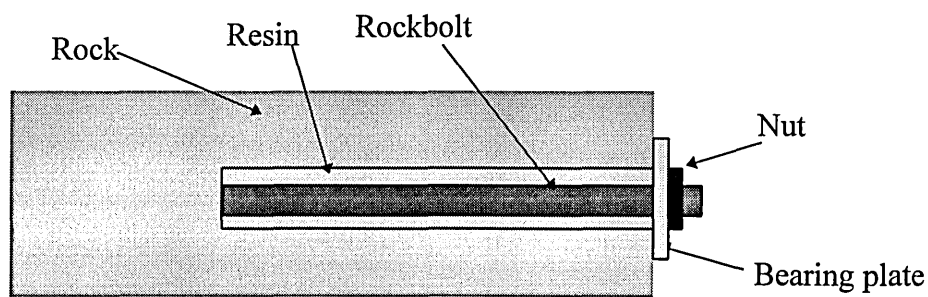


**Figure 1.3a.** A *full* column resin anchored rockbolt.

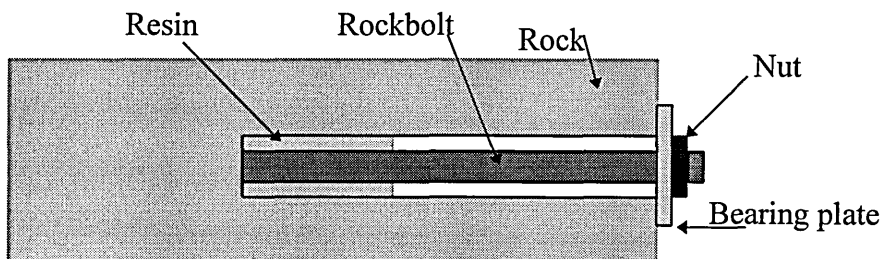


**Figure 1.3b.** A *point* resin anchored rockbolt.

The portion of the nut in contact with the bearing plate is circular. This circular region of the nut is sometimes called the conical seat.

The details of the Rock Mechanics and the theory behind the design of rockbolting systems in a coal mine is outside the scope of this research. However there is much literature available that gives an introduction to the application of rockbolting, e.g.

Sykes G. (1989), Gale W.J. (1991), Siddall R.J.(1992), Eaton (1988). These papers include a discussion of suitable installation densities of rockbolts, and the most appropriate rockbolt for the particular geology.

#### **1.4 Coal Mining in the UK**

Tunnels in a coal mine are usually called 'roadways'. A roadway would typically be around 4m wide and 2m high. Coal mining in the UK usually operates by longwall retreat mining. This involves driving two parallel roadways approximately 1500 m long, although possibly as long as 3000 m. Roadways are supported using both steel and GRP rockbolts. A 'face' is then driven between the two roadways and the face 'retreats back', excavating the coal from between the two roadways. The area behind the face is called the "Goaf", this area is allowed to cave in. The term 'Longwall' refers to the 1500 m long wall (length of the roadways); the alternative is 'Shortwall' which may be only 200m long.

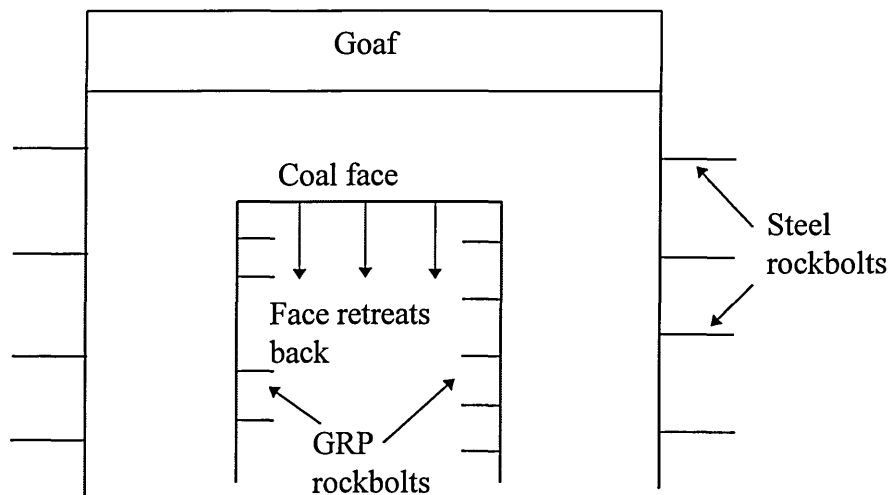


**Figure 1.4** Plan layout of Longwall Retreat Mining

The rockbolts used in the rib that will later be cut through are made from GRP to reduce the danger of sparks. Steel rockbolts can withstand higher loading and also have a cost advantage. GRP rockbolts are only used in ribs which are later cut through. GRP

rockbolts do not cause problems with sparks and also do not damage the cutting equipment, hence they are 'cuttable'. The GRP rockbolts that are inserted first are the ones that are cut through last. Hence there is a large variation in the length of time that the rockbolts are likely to be in service. The longest that any rockbolt is likely to be in service for is 2 years, Hardy (1995).

### **1.5 Installation of Rockbolts in UK coal mines**

HSE (1996b) gives guidelines on the installation of rockbolts. British Coal Operating Instructions (OI/30) (1993) gives guidelines on the minimum density of rockbolts to be used in the coal rib. Rockbolts along the coal rib should be spaced not more than 1.5 m apart. The vertical distance between rows should not exceed 1 m. British coal (1993) also mentions that the ribbolts should be installed within the range of horizontal to 45° upwards. However BS 7861 specifies that the rockbolt conical seat and bearing plate arrangement should be able to accommodate up to 18° out of alignment from the perpendicular. Hence the extra 27° may mean that the conical seat is not in full circumferential contact with the bearing plate and so the loading of the bearing plate would not be completely symmetrical. In practice the problem is lessened because the walls and roof in a coal mine tend not to be clearly defined Lang (1995). Hoek (1995) gives a possible solution to the problem of not having full circumferential contact by using a tapered wedge shaped washer with the bearing plate.

Steel roofbolts are normally 2.4 m long and steel ribbolts are normally 1.8 m long. GRP ribbolts are normally 1.2 m long. All rockbolts are normally 22 mm diameter. In a roadway 4m wide 7 roofbolts would typically be installed across the roof. Extra rockbolts are often installed if the particular geology and mine layout requires extra support.

The installation procedure used in UK coal mines is basically as follows. A hole is drilled in the rock (roof or rib) approximately 50 mm shorter than the length of the bolt. The drilled hole usually has a diameter of approximately 6 mm greater than the bolt. The hole is usually drilled using wet flushing, or less often, air flushing. Resin capsules are inserted into the borehole. The fast setting (red) resin capsule is inserted first and then the slow setting (green) resin capsule, as shown in figure 1.5.

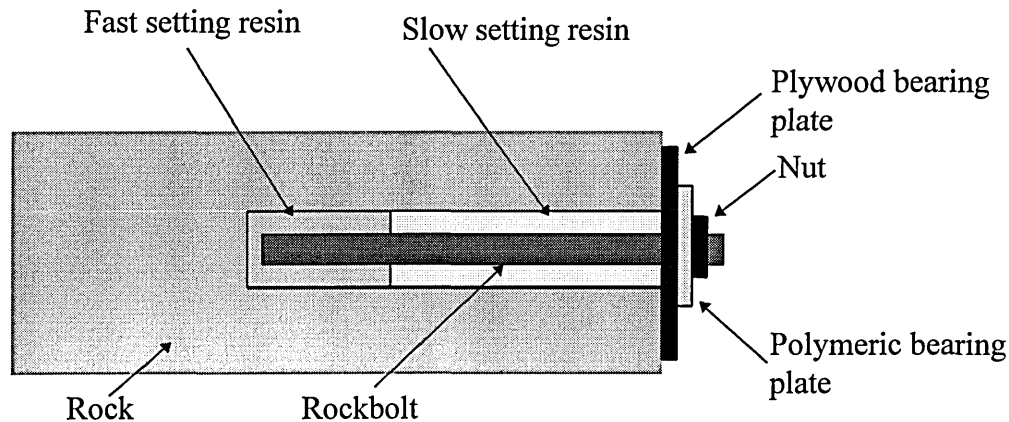


**Figure 1.5** Typical non-metallic rockbolt installed in a UK coal mine

When installing roofbolts, a plastic retainer is used to prevent the resin capsules falling out. The rockbolt is inserted into the borehole. Steel bearing plates and nuts are used with steel rockbolts. For GRP rockbolts, a plywood plate is fitted first with a polymeric plate and nut on top. A mesh is also sometimes used which is stretched between the rockbolts and provides support over a greater area of rock / coal. The rockbolt is rotated and rips open the resin capsules. Once the rockbolt has reached the top of the borehole it is rotated for a further 10 seconds (mixing time) or until the ‘break out torque’ of the nut is reached. The operator then pauses for approximately 20 seconds for the fast setting resin to set (setting time). The nut is then tightened up and produces a pre-tension in the rockbolt. Then the slow setting resin sets and the rockbolt is anchored along its full length.

The plywood plate typically has a bearing area of approximately  $0.09\text{m}^2$  (1 square foot).

The polymeric bearing plate would typically have a bearing area of  $0.02\text{m}^2$ .

## **1.6 Literature Review**

### **1.6.1 Rockbolts**

BS 7861 on rockbolting specifies many dimensional and loading requirements for both steel and GRP rockbolts. The standard also specifies Fire Resistance tests and Electrical Resistance tests and states that the rockbolts shall be threaded.

To comply with BS 7861 steel roofbolts and components should have the properties outlined in table 1.1, (compiled from the text in BS 7861, when tested in accordance with the tests specified in BS 7861).

Minimum diameter of bolt	21.7 mm
Minimum length of bolt	1.8 m
Minimum length of thread	150 mm
Area of steel bearing plate	150 mm × 150 mm or 100 mm × 100 mm
Minimum load of threaded end of rockbolt	295 kN
Yield strength of bolt	640 N/mm <sup>2</sup> - 720 N/mm <sup>2</sup>
Tensile strength of bolt	≥ 20% more than yield strength
Elongation at maximum force	≥ 8 %
Elongation after fracture	≥ 18 %
Minimum shear strength	250 kN
Minimum load of bearing plate - flatten pull through	140 - 200 kN 210 - 290 kN
Break out torque (For high torque roofbolts)	95 -175 Nm 125 - 185 Nm
Bond strength (over 125 mm)	200 kN
Minimum system stiffness at loads 50 kN to 150 kN	70 kN/mm

**Table 1.1** BS 7861 Specification for steel roofbolts

To comply with BS 7861 steel roofbolts shall have a raised ribbed surface. The nut shall have a 'break out' torque facility to limit the torque applied to the nut. The conical seat should allow an out of alignment angle of 18° from the perpendicular, whilst still in full circumferential contact with the bearing plate.

The requirements for steel ribbolts are very similar, the differences are given in table 1.2.

Minimum length of bolt	1.2 m
Break out torque	40 - 125 Nm

**Table 1.2** BS 7861 Specification for steel ribbolts

To comply with BS 7861 GRP rockbolts should have the properties as outlined in table 1.3. For GRP rockbolts a break out torque facility on the nut is not essential but if there is a 'break out' feature it shall break out at the torque specified in table 1.3. As with the steel rockbolts the conical seat and bearing plate shall allow 18° of out of alignment from the perpendicular.

minimum diameter of bolt	21.5 mm
minimum length of bolt	1.2m
minimum length of thread	150 mm
minimum load of threaded end of bolt	60 kN
minimum tensile load of bolt	300 kN
minimum shear strength	120 kN
minimum load bearing plate	50 kN
break out torque facility	40 to 125 Nm
minimum bond strength over 450 mm	245 kN

**Table 1.3** BS 7861 Specification for GRP rockbolts

### 1.6.2 Cable Bolting

Cable bolts are used in mining applications where support is needed in addition to the normal rockbolts. Cable bolts are longer than normal rockbolts and so provide support

over a greater depth of rock. If a previous roadway passes above or below, this area may need additional reinforcement as offered by cable bolts. Cable bolts are also used in conjunction with steel arches at junctions to roadways. Cable bolts are often used when the bolt is required to have some shear resistance. HSE (1996a) gives guidance on the use of cablebolts.

### 1.6.3 GRP Rockbolts

Reddish et al (1994) mentions the problem of the smooth surface of the GRP rods when they are manufactured by pultrusion. He reports several methods of solving this problem. One method that is not very effective is to dip the bolts into resin and then apply some coarse sand. This method tends to bring part of the coating off the bolt when tested, and so gives unsatisfactory results. Another method of producing a rough surface is to use a nylon sleeve or peel ply. This sleeve allows resin to leak through, when the sleeve is removed a rough texture is left. This is the most common means of producing a rough surface. Reddish et al (1994) reports that an effective but more expensive method called 'pull moulding' can also be used to produce a rough surface.

Benmokrane (1996) conducted pull out tests to determine the bond strengths of different types of GRP rockbolts in cement grout. The importance of the surface of the GRP rockbolt was noted. Daws (1995) also conducted pull out tests on GRP cable bolts and concluded that the surface of the GRP cable bolt was of critical importance in determining the bond strength of the cable bolt. Daws (1995) observed that the tendency for an anti-sparking coating to flake away from the rockbolt severely reduced the bond strength.

It is claimed by Conley (1992) that the problem of smooth surfaces on the GRP rockbolts has been solved in the AROA (Applied Research of Australia Pty Ltd) rockbolt by using the “matched die process”. This method is similar to pultrusion, involving wetting out glass fibres in a resin bath. The rod is then compressed by high pressure dies to form the rockbolt. The threads and surface deformations are produced by the dies. The problem of producing satisfactory threads on a GRP rockbolt was also identified. It is claimed, Conley (1992), that the thread on this rockbolt can carry a relatively high load because some of the glass filaments are deformed into the thread surface.

Conley (1992) discusses tests on a GRP rockbolt supplied by AROA. Creep tests were carried out on the glassfibre material. A creep rate of 0.9 microstrain per hour is quoted when loaded to 70% of yield strength. Yielding then took place at 200 or 250 microstrain. This corresponds to a lifetime of only 225 hours or 9.4 days at 70% of yield strength. This compares to a maximum lifetime of 2 years in UK coal mines.

Howarth (1992) describes the Highly Oriented Polyethylene bar (HOPE) which is used instead of GRP bolts as a cuttable rib reinforcement in some Australian coal mines. Howarth reports that the HOPE bar has been used successfully. However creep tests on the HOPE bar show that it has very poor creep behaviour. Howarth concludes that the HOPE bar should only be used for low stress or short duration applications.

Pakalnis (1994) performed tests on the 'DAPPAM' GRP cable bolt. The DAPPAM cable bolt is a 10 stranded rockbolt. Table 1.4 gives some mechanical properties of the DAPPAM and a comparable steel cable bolt.

	DAPPAM cable bolt	Steel cable bolt
Tensile strength	289 kN	245 - 267 kN
Shear strength	89 kN	245 - 267 kN
Critical bond length	39 cm	102 - 112 cm
Specific gravity	2.1	7.85

**Table 1.4** Performance of a steel cable bolt and DAPPAM GRP cable bolt, Pakalnis (1994)

Hence Pakalnis (1994) identified that the DAPPAM GRP rockbolt performed as well as the steel rockbolt in tension, but the shear properties of the GRP rockbolt are much worse than the steel rockbolt. Ludvig (1983) also identified that GRP rockbolts have much lower shear strengths than steel rockbolts.

Reddish et al (1994) looks at the performance of GRP rockbolts using laboratory tests. The question of whether it is worthwhile pre-tensioning GRP rockbolts was identified. Strain gauges were installed on the side of boreholes and on rockbolts. Two tests were carried out, one with a pre-tensioned rockbolt and one with a non pre-tensioned rockbolt. The results suggest that pre-tensioning is possibly not worthwhile. The pre-tension appears to put the rock into compression at the proximal end (near to the nut and bearing plate) but the rock may be in tension at the distal end of the rockbolt.

Reddish et al (1994) identified the problem of damage to the glassfibre if the torque applied to the rockbolt is too large. A torque above 68 Nm may cause damage to the glassfibre, Reddish et al (1994). Hence the pre-tension that can be achieved with GRP rockbolts is much less than for the steel rockbolts.

Reddish et al (1994) also identifies two different methods for testing the shear properties of GRP rockbolts. The need for the test to be thoroughly specified is identified. The

dimensions between the testing blocks used in a shear test should be very small (<1 mm), to avoid testing the tensile and not the shear properties of the GRP, Reddish et al (1994).

Conley (1992) identifies 4 aspects of an installed rockbolt which can limit the rockbolts' performance.

1. the strength of the rockbolt / rock bond
2. the tensile strength of the bolt
3. capacity of the bearing plate
4. capacity of the nut and thread system

These observations are based upon experience of rockbolting in coal mines. The colliery rockbolting engineer stated that at Thoresby colliery the load carried by the bearing plate limited the GRP rockbolts performance. The bearing plate fails before the other rockbolting components, this is described in more depth in Chapter 2. Hence the capacity of the bearing plate is the topic concentrated upon in this thesis.

#### 1.6.4 Resins and Grouts

Most rockbolts used in the UK are resin or grout anchored. The resin is polyester based and the grout is cement based. Resin is usually inserted into the borehole in capsules. Eaton (1993) notes that when resin was first used for anchoring rockbolts, it was installed using pumps. However resin capsules were found to be more convenient, safer, quicker to install and created less wastage. Daws (1991) reports on trials at Pen y Clip tunnel using pumps to insert the resin.

Eaton (1993) explains how the resin capsules contains two compounds, the mastic and the catalyst.

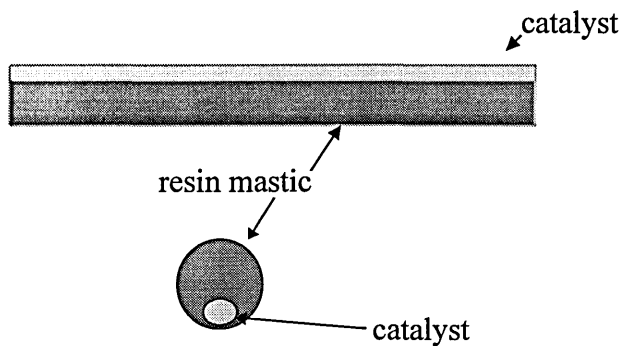


**Figure 1.6** Resin capsule used for rockbolting

When the rockbolt is inserted the capsule is broken open and the resin is mixed and then sets after a certain length of time. The length of the setting time can vary with various environmental factors, e.g. temperature. Different formulations of resins are available to provide different setting times.

Eaton (1993) reports that the Celtite AT resin, which is commonly used in the UK coal mining industry has the following properties.

Unconfined compressive strength	80 MPa minimum
Compressive modulus of elasticity	11 GPa minimum
Compressive creep	0.12% maximum

**Table 1.5** Typical properties of resins used during rockbolting

Eaton (1993) mentions that when the resin is loaded it is by compression. Hence the performance of the resin in tension is not considered relevant. The need for the resin annulus around the bolt to be as small as possible is identified. Hence the diameter of the hole drilled in the rock must be as close to the diameter of the rockbolt as possible.

Grout usually has a greater bond strength than resins. The disadvantage of grout is that it takes longer to install. Grout is often used with cable bolts, since cable bolts are used

for secondary support a long installation time is not a problem. Grout is rarely used with ordinary rockbolts.

Fabjanczyk (1992) shows how poor load transfer from the rock to the resin / grout or from the resin / grout to the rockbolt, increases the load on the end fitting and bearing plate.

#### 1.6.5 Polymer mesh

If a polymer mesh is used, it is suspended from the steel mesh used on the roof and spread over the coal rib before the GRP rockbolts are installed. The GRP rockbolts are pushed through the gaps in the mesh, the bearing plate and nut secures the mesh to the rib. The polymer mesh is a cuttable mesh which does not produce sparks when cut. The mesh helps to hold back loose material. Naylor (1994) demonstrates a polymer mining grid's compliance with the flame retardant regulations. Naylor (1994) also explains that there are two ways to install the polymer mesh on to the rib. The mesh can be installed straight from a roll of mesh or it is sometimes cut to size, depending upon the heading machine and bolting pattern.

#### 1.6.6 Threaded end fittings

There is a variety of different end fittings available for GRP rockbolts. End fittings currently used on GRP rockbolts in the UK are almost invariably threaded nuts. Hoek (1995) states that the threads on rockbolts should be as coarse as possible because a fine thread may be easily damaged and may cause installation problems. End fittings that rely on frictional grip properties are available, but they tend to be used only on cable bolts.

Reddish (1994) describes the development of GRP rockbolt end fittings used in the UK. The end fittings used today are moulded FRP nuts designed to withstand 70 -100 kN. Swiss made products which have higher end loading capacity are available, but they are more expensive.

Reddish et al (1994) mentions that some systems have eliminated the use of nuts and simply have a solid end to the rockbolt which is driven into position. A disadvantage of a solid end rockbolt is that it does not allow the rockbolt to be pre-tensioned or even for the bearing plate to be secured firmly against the rock. Lang (1995) suggested that it was the inability to secure the bearing plate firmly that limited the use of the solid end rockbolt.

#### 1.6.7 Bearing Plates

There is a variety of different bearing plates used in civil engineering and mining engineering. They are often known by many different names, including header plate, patch plate, domed washer plate, face plate, rockbolt plate, rock bolt plate, bolt end plate, bolt plate, plate washer and mine roof plate. In UK coal mines two bearing plates are typically used in conjunction with GRP rockbolts. A large plywood plate bears against the coal or mesh and a smaller polymeric plate is fitted between the plywood plate and the nut.

This thesis focuses on the design of the smaller polymeric bearing plate used in conjunction with GRP rockbolts. The following review of bearing plate literature includes literature on steel bearing plates as well as non metallic bearing plates.

Schach (1979) notes that the saucer or domed shaped plate is quite successful. The domed plate has an increased surface area in contact with the rock after deformation, hence Schach claims that crushing of the rock is inhibited. Douglas (1983) and Norris (1981) report that some bearing plates are designed to deform when loaded, and provide a visual indication that rock movement is taking place. Bell (1992) mentions that the bearing plate must be large enough to prevent deformation to the rock. This problem is particularly important with the GRP rockbolts that are used in the coal rib because of the low compressive strength of coal (approximately  $30 \text{ MN/m}^2$ ). O'Grady (1994) identified that the support load carried by a rockbolt is limited by the capacity of the bearing plate and of the rock itself. This was observed from experience of rockbolting in coal mines. Norris (1981) identifies that the compressive strength of the rock determines the amount of bending that the bearing plate undergoes. Norris (1981) identifies that the lower the compressive strength of the coal, the more likely that the coal fails before the bearing plate. If the coal fails the greater the diameter of the support given to the bearing plate and hence the more the bearing plate bends. This conclusion has been expanded by the calculations given in Appendix 4.

Douglas (1983) reports that there are a wide range of different shapes of bearing plates. Plates available are round or square, flat or coned, solid or webbed. It is thought, Daws (1994), that the shape of the bearing plate is insignificant and it is only the bearing surface area that is important. There seems to be no literature on the detailed design of bearing plates. Most of the bearing plates used are made from steel. A minority of the bearing plates used in coal mines are polymeric (only if they need to be cuttable).

Tague (1990) gives recommended minimum sizes for steel bearing plates for use in coal mines of  $100 \times 100 \times 12$  mm thick. Douglas (1983) gives some typical dimensions of steel rockbolt bearing plates used in civil engineering.

size of plate (length of side or diameter)(mm)	working load of bolt (kN)	thickness (mm)
125-150	80	7
150-200	150	10
200-250	300	12

**Table 1.6** Typical dimensions of steel bearing plates used in civil engineering, Douglas (1983)

One of the problems with the use of bearing plates is the uneven surface of the rock, causing load not to be spread evenly over the surface of the plate or the coal. Douglas (1983) describes how a solution for this problem has been used in civil engineering. Resin is spread onto the uneven rock behind the bearing plate and forms a flat surface allowing the load to be spread over the rock more evenly. Douglas (1983) claims that it is necessary to ensure that the resin is separated from the bearing plate and end fitting by means of a 'bond breaker', (lubrication, aluminium foil, or waterproof paper). The aluminium foil would not be appropriate for use in a coal mine.

Norris (1981) identified the problem of bearing plates and end fitting arrangements which do not allow sufficiently large out of alignment angles. This can lead to bending of the rockbolt which reduces the rockbolt's performance. He also suggests that the coefficient of friction between the nut / end fitting and bearing plate needs to be as low as possible.

BS 7861 gives the following definition for a bearing plate (domed washer plate)

“Accessory which when used in conjunction with a rockbolt, nut and conical seat, facilitates load distribution, ensures correct alignment and reduces weathering around the mouth of the rockbolt hole.”

#### 1.6.7.1 BS 7861 test on rockbolt non-metallic bearing plates

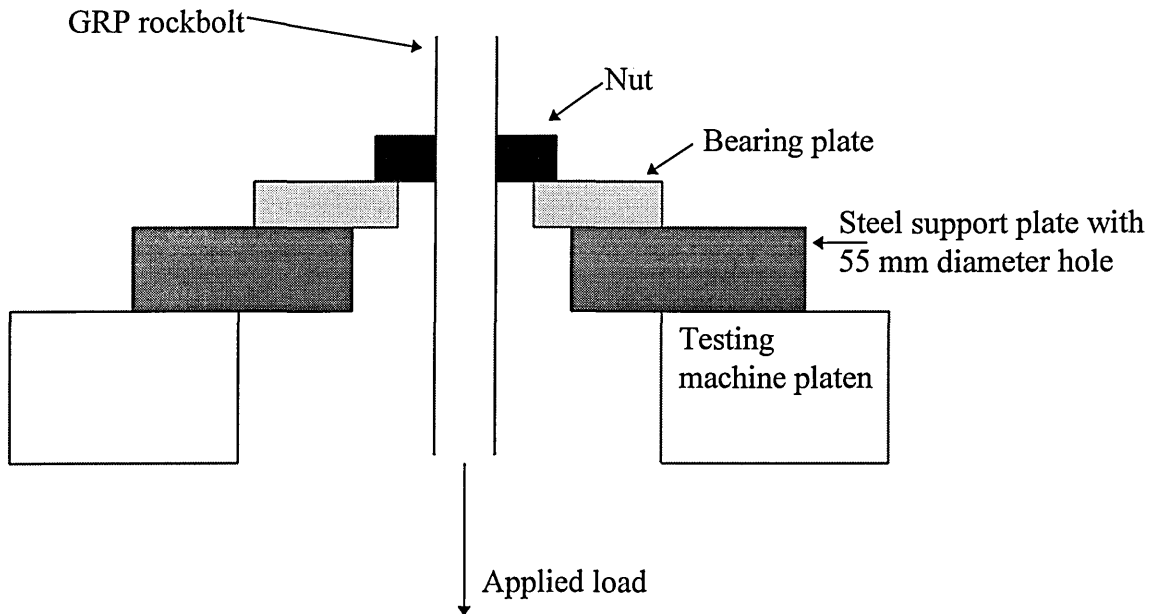


**Figure 1.7** Testing of non-metallic rockbolt bearing plates

To comply with BS 7861 the bearing plate shall fail by allowing the nut and conical seat assembly to pull through the centre of the bearing plate. The bearing plate should not fail suddenly, but progressively. The non metallic bearing plate should withstand a load of at least 50 kN. The bearing plate should fail before the threaded end of the ribbolt and before the polymeric nut. The polymeric nut should fail before the threaded end of the rockbolt. The rate of loading of the tests is not specified. The radius at the edge of the steel support plate is not specified.

The failure mechanism is important as well as the failure loads. For reasons of safety it is necessary for the components to fail in a progressive manner. It should be possible to see the deformation of the plate / nut whilst the plate and nut is still withstanding load.

The test on steel rockbolt bearing plates in BS 7861 is very similar, but a 70 mm diameter of hole in the steel support plate is used instead of a 55 mm hole. The steel bearing plate used with the steel bolts, conical seat, and nut shall fail first by flattening out, then the bolt, nut and conical seat shall pull through the bearing plate, without failure of the threads. Hence the failure is progressive. Table 1.7 gives the minimum and maximum loads that the steel bearing plates should flatten and pull through at, as specified by BS 7861.

	flatten	pull through
maximum test load	200 kN	290 kN
minimum test load	140 kN	210 kN

**Table 1.7** Allowable failure loads of steel bearing plates, BS 7861

## 1.6.7.2 Summary of world-wide rockbolt bearing plate tests

	Diameter of hole in steel support plate used when testing bearing plate (mm)	Diameter of nut or punch used to test bearing plates (mm)
British Standard (steel plate)	70	actual nut
British Standard (polymeric plate)	55	actual nut
British Standard Cable bolting single cable bolt strand gripping assembly	80	actual nut
British Standard Cable bolting double cable bolt strand gripping assembly	100	actual nut
Plate at an angle of 10°	135	
American Standard (steel plate)	101.6 +/- 1.6 mm	actual nut or a punch 45 mm external diameter
Canadian Standard (steel plate)	101.6 +/- 1.6 mm	actual nut or a punch 45 mm external diameter
German Standard (steel plate)	50 <M20	
Tests carried out at an angle of 15°	60 M20 to M24	
	70 M27 to M33	
Ogata (1985) (steel plate)	M18 42, 52, 62	31.2 mm
	M22 52, 62, 72	37 mm
	M24 52, 62, 72	41.6 mm
	M27 62, 72, 92	47.3 mm
		(across flats)

**Table 1.8** Testing of bearing plates, diameter of unsupported span, external diameter of nut.

Table 1.8 summarises world-wide rockbolt bearing plate test methods. The American, Canadian and German Standards make no mention of polymeric or non metallic bearing plates and refer solely to steel bearing plates for use with steel rockbolts. The rate of loading of the bearing plate is not specified in these standards. The American and Canadian Standards specify that the load should be applied either to the rockbolt from

below or to the nut / punch from above. The American and Canadian standards are almost identical to each other. The German standard specifies that the bearing plate should be inclined at an angle of  $15^\circ$ , and the British standard on cablebolting includes a test with the bearing plate at an inclined angle of  $10^\circ$ . All other standard tests specify that the bearing plate is tested flat i.e. at an inclined angle of zero.

Ogata (1985) looked at the load to cause different deflections of steel bearing plates with different diameters of hole in the steel support plate and different sizes of nuts.

A number of researchers Reznik (1996), Rukovodstvo (1977), Trofimenkov et al (1983) have performed bearing plate tests on different soils to determine soil / rock deformation moduli. These tests assume a rigid bearing plate and hence do not consider deformation of the bearing plate.

The Canadian Standard also includes a test on the header plate, which is a bearing plate of larger surface area than the standard bearing plate (equivalent to the plywood plate for GRP rockbolts). This test is the same as the Canadian test on the smaller bearing plates, except that the specified diameter of the hole in the steel support plate is 152.4 mm (6 in), (instead of 101.6 mm). The header plate referred to in the Canadian standard is a steel bearing plate of similar external dimensions as the plywood bearing plates used with GRP rockbolts. BS 7861, the German standard and American standard do not mention a test for the larger header plates or plywood plates.

The end fitting and bearing plate is particularly important with point anchored rockbolts because it is the only means of transferring load onto the rockbolt at the proximal end of

the rockbolt. Most of the rockbolts currently used are intended to be full column resin bonded rockbolts. A theory has been proposed, Hassani (1995), that for full column resin bonded rockbolts, the end fitting and bearing plate are completely unnecessary, as in theory they do not carry any load. However as the photographs of failed bearing plates shown in figures 2.2, 2.3 and 2.4 show, the argument that the bearing plate is not important because it does not come under any load is a fallacy. Also due to problems of resin leaking into crevices, the rockbolt may not be completely full column resin bonded. There is also a possibility that the operators may not install all the necessary resin capsules. Bell (1992) states that if a bearing plate and end fitting is used on a full column resin bonded rockbolt, the end fitting prevents the rockbolt from debonding from the borehole.

Oreste (1996) recognised that the stiffness of the rockbolt bearing plate was very important to the rockbolt performance. Oreste (1996) gives the following expression for the stiffness of the bearing plate foundation of the tunnel wall.

$$k_{foundation} = \frac{E_R S_{BP}}{(1 - \nu_{RM}^2) D_R} \quad (1.1)$$

where

- $D_R$  - rockbolt diameter
- $E_R$  - rock mass deformation modulus
- $S_{BP}$  - bearing plate surface area
- $\nu_{RM}$  - Poisson's ratio of rock mass
- $k_{foundation}$  - stiffness of the bearing plate foundation of the tunnel wall

Oreste (1996) combines the stiffness of the bearing plate foundation on the tunnel wall with the stiffness of the bearing plate to find the stiffness of the bolt tie on the tunnel surface. This suggests that the bearing plate is a very important part of the rockbolting system.

$$\frac{1}{k_{tie}} = \frac{1}{k_{plate}} + \frac{1}{k_{foundation}} \quad (1.2)$$

$k_{plate}$  - stiffness of the bearing plate

$k_{tie}$  - stiffness of the bolt tie on the tunnel surface

These equations also relate the surface area of the bearing plate to the stiffness of the rockbolt system. However calculations are not used in practice to determine the minimum surface area of bearing plates to be used in coal mines, Lang (1995).

Dunham (1991) mentioned the problem of bearing plates which have sharp edges cutting through the mesh near to the mouth of the rockbolt holes. It is not stated whether this occurred with the steel or non-metallic mesh and bearing plates. A comparison of the costs of rockbolting components is presented. Rockbolt bearing plates can be seen to be only a small proportion of the total cost of a rockbolt installation.

There is some literature, Schach (1979), Douglas (1983), that mentions various designs of bearing plate available. However there does not appear to be any detailed study of the design or performance of the bearing plates. Most research that has taken place on the subject of rockbolting is concerned with the design of the rockbolting system, not the components. However there has recently been more interest in the rockbolting components, Bigby (1997), Eaton (1993), Reddish (1994), but no detailed study on the design of the bearing plates.

## CHAPTER 2

### 2. PROBLEM DEFINITION

#### 2.1 Observations from a visit down Thoresby colliery

The roadways seen on the route to the coal face were supported by steel arches; with corrugated panels between the arches to hold back loose material. In several places along the roadways there were signs of distortion to the steel arches, particularly flattening at the peak of the archways. In steel archway supported roadways, there is no means of knowing about the roof movement before the archways has distorted. Up to a metre of roof movement may have taken place before the archways distorted.

At junctions between two roadways, major deformation of steel girders had taken place. In places the large I beams had greatly distorted and twisted through up to 90°. At a junction between roadways, steel cable bolts had been used to provide support extra to the steel arches.

Telltale monitoring roof movement were present in the rockbolted roadways. A telltale is used to measure roof movement it can measure to the nearest millimetre. Telltales are installed in the roof every 20 metres along the roadway, using the normal rockbolting equipment. The telltale consists of two steel tubes with coloured bands painted on. A cable is attached to a steel tube and the other end of each cable is fixed into the rock at a depth of 2.5m and 5m. The telltale is fitted so that just the two tubes are protruding from the borehole. If the roof starts to move downwards, part of the coloured bands are covered up by the rock or the other tube. This gives an indication of the depth at which the rock movement is originating from.

On entering the rockbolted roadway it was noted that the rockbolts in the coal rib were made from GRP and in the roof and other rib they were made from steel. The steel rockbolts were fitted with steel bearing plates, nuts and straps. The GRP rockbolts were fitted with large plywood bearing plates, polymeric/GRP bearing plates and polymeric nuts. The GRP rockbolts seen had a large plywood plate approximately  $300 \times 300$  mm. This was bearing against the rock, then there was a polymeric plate secured by a threaded polymeric nut. There was no polymeric mesh installed on this roadway.

#### 2.1.1 Observations of deformation to bearing plates and coal rib

There were no signs of any damage to the roof that was supported by steel rockbolts. The telltales installed at every 20 metres along the roadway showed only a few millimetres of roof movement. The rib supported by steel rockbolts showed very little deformation and very little damage to the steel bearing plates and nuts. The rib reinforced with GRP rockbolts showed signs of a large amount of deformation, particularly at the upper third of the rib. There were a large number of polymeric bearing plates in the coal rib that had severe deformations and cracks.

Most of the plywood plates installed on the coal rib were starting to 'butterfly', 'lifting off' from the rock on two opposite edges, as shown in figure 2.1. This was affecting the way that load was transferred to the polymeric bearing plate. After the plywood plate had 'butterflied' the loading of the polymeric bearing plate was not symmetrical.

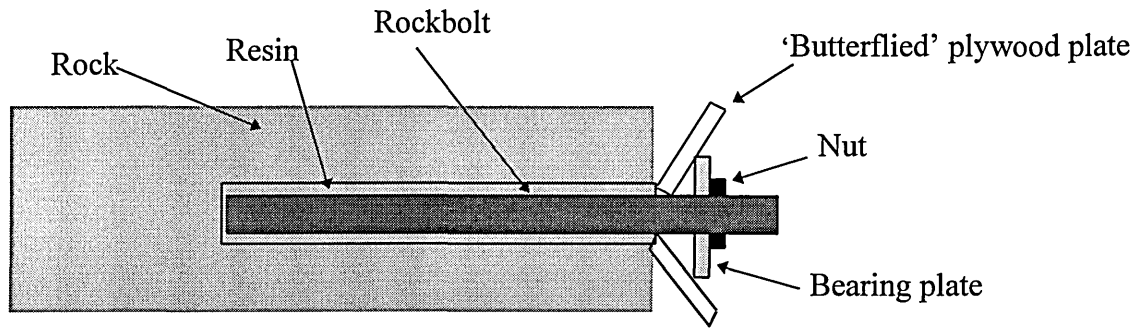


**Figure 2.1** Rockbolt assembly with a failed plywood plate

Two different types of polymeric/GRP bearing plate were seen down Thoresby colliery. There was a white square shaped plate supplied by Weldgrip Ltd (figures 2.2, 2.3). There was also a circular bearing plate made in a black or beige glassfibre material supplied by Mai Systems Ltd (figure 2.4).

Most of the circular Mai bearing plates seen had cracks present. Many of the Mai bearing plates had broken and fallen off the rockbolts and could be seen lying in two or more pieces on the floor. Many other Mai bearing plates were seen to be bending and 'lifting off' at the edges. On rockbolts with missing polymeric plates, the polymeric nut was usually still present and had frequently been forced through the centre of the plywood plate.

There were no signs of cracks in the white square Weldgrip bearing plates. The square Weldgrip plates had failed by bending outwards at the edges and yielding in the centre. There were signs of a large amount of deformation to the Weldgrip bearing plates before the nut had forced its way through the centre.

The GRP rockbolts had been installed with a large amount of thread left protruding into the roadway. This meant that additional bearing plates and nuts could be installed if the original ones had failed. On many of the rockbolts a second polymeric bearing plate had been fitted leaving the original nut in place and the polymeric plate if it was still in one piece. Most of the polymeric bearing plates on the area seen had had to be replaced. For rockbolts on which a second bearing plate had been fitted, the nut had been pulled into the coal rib, or the coal rib had moved outwards around the rockbolt and nut.

Table 2.1 gives some estimates on the proportion of the different bearing plates that had deformed and were of no further use, according to a colliery rockbolting engineer. The Weidmann webbed plates that had been installed on other roadways tended to fail by 'flattening out'. Very few of the Weidmann plates had completely failed, complete failure was by cracking of the circumferential webs. The use of the webbed Weidmann plate had been very successful at Thoresby although there was still room for improvement. The Weidmann webbed plate had survived intact down the mine for much longer than the Mai or Weldgrip plates had. The colliery rockbolting engineer was of the opinion that the green Apex/AMS bearing plates were useless, and hence the Apex/AMS bearing plates are no longer in use at Thoresby colliery.

Bearing plate	Cracked and / or deformed	Of no further use
Weldgrip / Mai	90 %	40 %
Weidmann	50 %	5 %

**Table 2.1** Proportion of bearing plates that had failed and were of no further use

The GRP rockbolts could be installed within 5° out of alignment. However many of the rockbolts seen had much larger out of alignment angles due to the large movements of part of the coal rib. Some of the rockbolts seen had out of alignment angles of more than

18°. BS 7861 specifies 18° as the angle away from the perpendicular which the bearing plates, nuts and conical seats must be able to accommodate.

The major problem with the GRP rockbolting system was the poor performance of the polymeric bearing plates, according to the colliery rockbolting engineer.

## **2.2 Deformed bearing plates used in the coal mines**

When describing the different failure mechanisms of the bearing plate, the surface of the bearing plate in contact with the rock is described as the 'lower surface' and the surface of the bearing plate on which the nut sits is described as the 'upper surface'.

Figure 2.2 shows a Weldgrip bearing plate that has been used down Whitemoor colliery. The view shown is of the lower surface of the bearing plate. This bearing plate has failed by deformation to the centre of the bearing plate, and the nut used with it (the small Mai nut) has been pulled through the centre of the bearing plate. Bending of the bearing plate has taken place. Deformation to the centre of the bearing plate can be seen. This is the most common method of deformation of the Weldgrip bearing plates used in UK coal mines. Other failed Weldgrip bearing plates are similar, some show more bending than others and different amounts of localised deformation at the centre. Some Weldgrip bearing plates show unsymmetrical bending, probably because the bearing plate was loaded at an inclined angle.

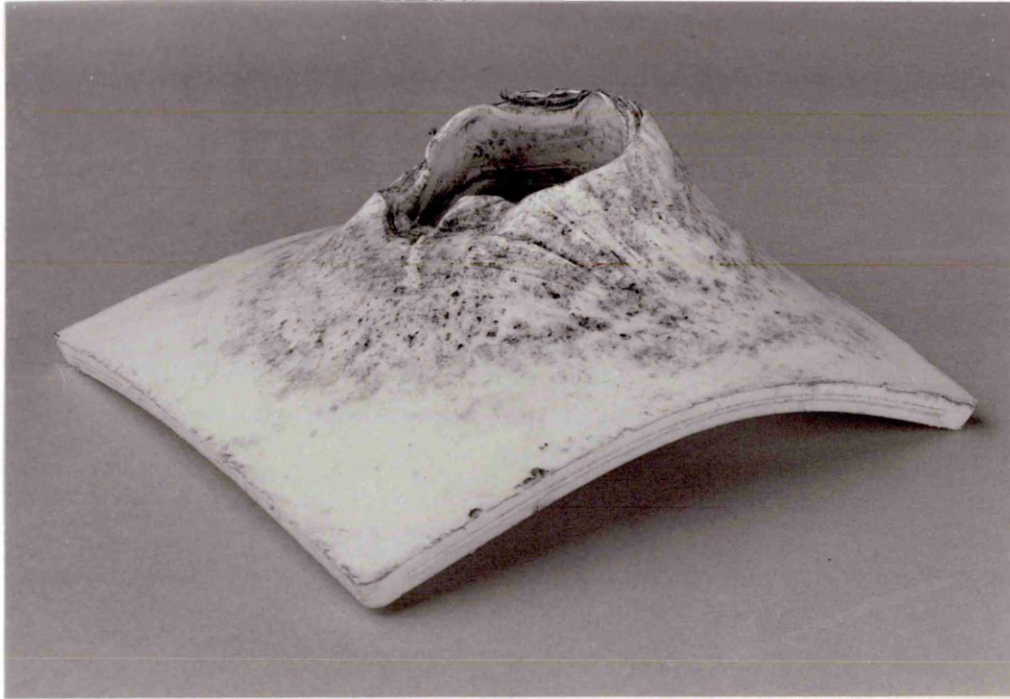


**Figure 2.2** Failed Weldgrip bearing plate

The threadforms are not the same on different manufacturer's rockbolts, hence the correct nut has to be used with the rockbolt. However this may not be the correct nut to go with the particular bearing plate. It is common for one manufacturer's bearing plate to be used with another manufacturer's nut and rockbolt.

Figure 2.3 shows a Weldgrip bearing plate that has been used down Whitemoor colliery in conjunction with a Mai nut. The view shown is of the lower surface of the bearing plate. This bearing plate has also failed by allowing a nut to pull through the centre, however a crack has formed in the bearing plate spreading outwards from the centre. The crack appears to have formed on the lower surface of the bearing plate and has spread to the upper surface. On close inspection of the crack, small cavities can be seen possibly because of the difficulty of injection moulding thick sections. Crack formation is a much more unusual failure mechanism than the nut simply pulling through the

bearing plate. The crack formation is possibly caused by a greater length of time that the nut was embedded in the centre of the bearing plate, giving time for creep deformation to take place. Failure of the plywood plate by 'butterfling' (figure 2.1) would cause unsymmetrical loading of the bearing plate and may induce the type of failure shown in figure 2.3.



**Figure 2.3** Failed cracked Weldgrip bearing plate

Figure 2.4 shows the upper surface of a Mai bearing plate that has been used down Thoresby colliery. The failure mechanism can be clearly seen. In Mai bearing plates seen down the mine, cracks appeared to initiate from the lower surface of the bearing plate. This is the typical failure mechanism of the Mai bearing plates. A small amount of bending of the Mai bearing plate has taken place before fracture.

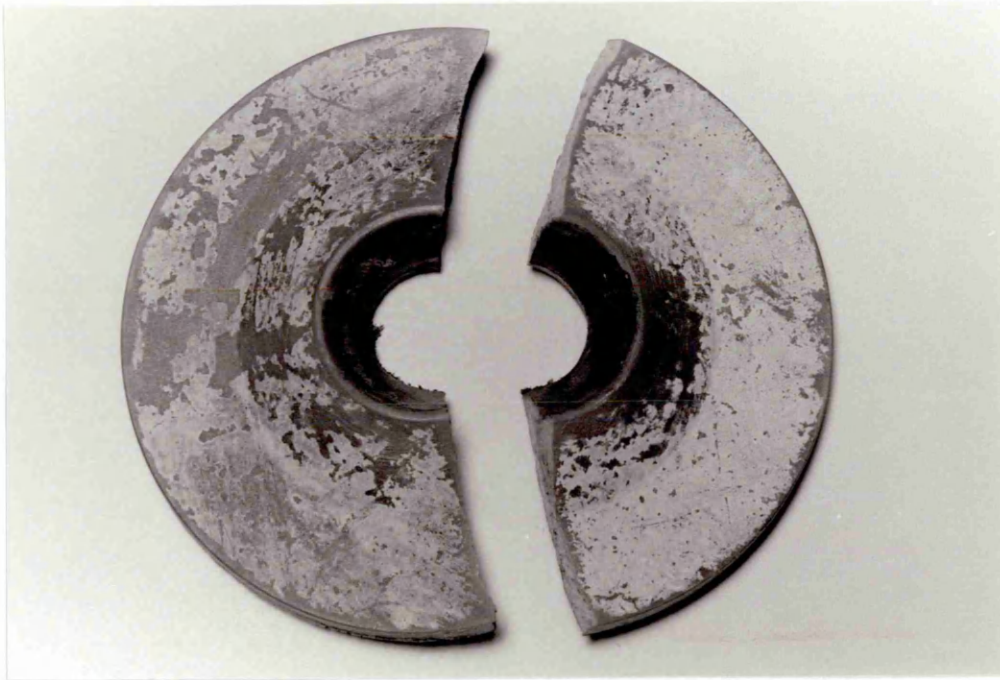


**Figure 2.4** Failed Mai bearing plate

Colliery rockbolting engineers prefer a progressive failure mechanism to sudden crack formation and sudden failure. Hence the failure mechanism of the Weldgrip plate is preferable to the failure mechanism of the Mai plate.

### **2.3 Design specification**

BS 7861 on rockbolting gives minimum performance levels for bearing plates and rockbolting components to be used in coal mines. Table 2.2 gives a specification for a bearing plate to comply with BS 7861. Another design specification based upon BS 7861 and results in this thesis is presented in table 7.1.

	BS 7861 specification
Performance	50 kN when tested with 55 mm hole in steel support plate allows an out of alignment angle of at least 18°
Materials	non-metallic
Target product cost	not specified
Life in service	not specified
Size	not specified
Safety	flame retardancy properties anti-sparking properties nut fails before bearing plate
Environment	not specified

**Table 2.2** Design Specification for non metallic bearing plates based upon BS 7861

One of the specifications in BS 7861 is that the bearing plate should allow 18° out of alignment movement of the rockbolt away from the perpendicular. For a given depth of bearing plate at the centre, there is a minimum clearance between the central hole in the bearing plate and the rockbolt diameter to still allow 18° out of alignment. Figure 2.5 gives the minimum diameter of the bearing plate central hole for different depths of bearing plate and different rockbolt diameters, that I have calculated on the basis of the geometry.

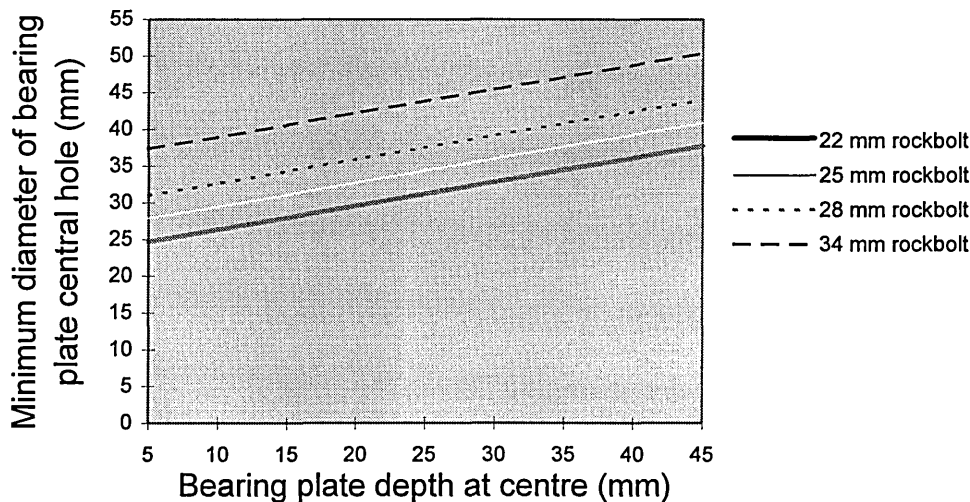


**Figure 2.5** Minimum diameter of bearing plate central hole to allow 18° out of alignment movement of the rockbolt.

The standard diameter of GRP rockbolts currently used in coal mines is 22 mm. However due to the threadforms glued onto the rockbolt, the rockbolt diameter at the proximal end (next to the bearing plate and end fitting) is often around 28 mm. There have recently been discussions, Hurt (1994), Daws (1994) about the possibility of using larger diameters of rockbolt of around 34 mm. A larger diameter of rockbolt has been suggested because this may mean that fewer rockbolts are required.

BS 7861 also specifies that the bearing plate and conical seat assembly should allow  $18^\circ$  out of alignment whilst the conical seat is still in full circumferential contact with the bearing plate. Hence existing designs are produced with a curved underside to the nut (conical seat) and a curved concave shape to the upper surface of the bearing plate. This allows the nut to transfer the load to the bearing plate whilst still in full circumferential contact with the bearing plate.

## **CHAPTER 3**

### **3. METHODOLOGY**

#### **3.1 Finite Element Analysis methodology**

The Finite Element Method is a well established technique that has been used for many years. Zienkiewicz (1977) and Lewis (1991) provide much more detail about the method which involves approximation of the model by dividing the model up into a finite number of elements, by a process of discretization.

The Finite Element Analysis required for this research was undertaken using ABAQUS version 5.4 FEA software and Patran version 3 as a pre and post processing package. The computers used were Sun Sparc workstations. The models were drawn and mesh and boundary conditions created using the Patran software and ABAQUS was used as the analysis package. Patran and ABAQUS are both general purpose, widely used software packages.

The elements used were 8 noded quadrilateral elements or 6 noded triangular elements. These 8 noded and 6 noded elements were used because they are generally considered to be more accurate than 4 noded / 3 noded elements. The majority of elements used were quadrilateral elements. Some triangular elements were used on the coned designs of bearing plate to prevent large skew angles of the elements. The aspect ratio of the mesh was kept as close to unity as possible and was always less than 5. The bandwidth of the mesh was reduced by means of the Cuthill McKee optimisation method, described by ABAQUS (1994). For the webbed bearing plate models, (e.g. figure 3.1) the mesh density on the outer webs (large diameters) was much lower than on the inner webs

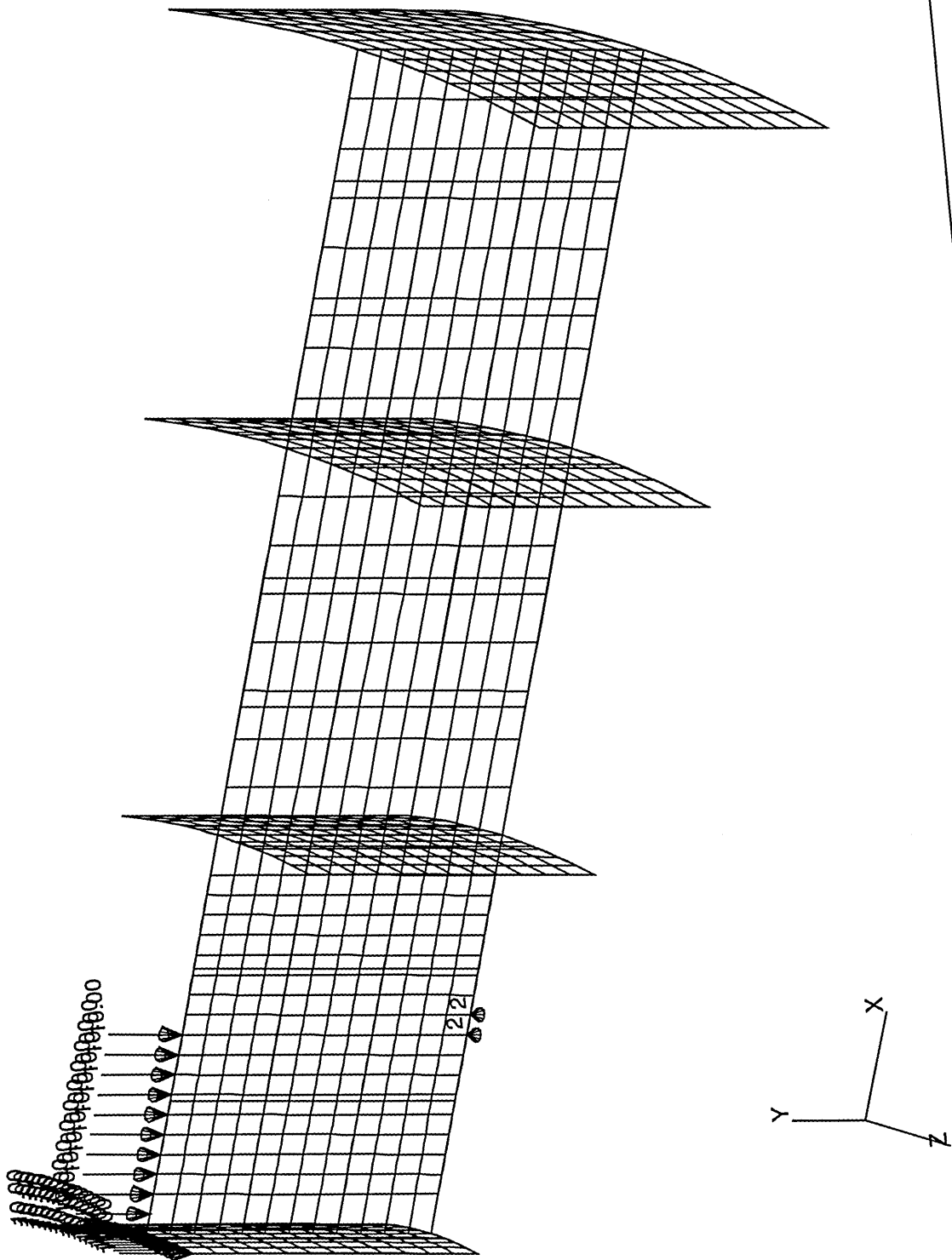


Figure 3.1 Load, restraint and mesh on webbed bearing plate.

(small diameters) because of the lower stress levels / gradients at the outer webs. However to ensure node connectivity the vertical mesh density was kept constant.

The solid designs of bearing plate were modelled using 2D axisymmetric elements. The webbed designs were modelled using 2D shell elements. The shell elements used were all thick shell elements as recommended by the ABAQUS manuals, because the thickness of the shells (webs) was usually more than 1/15 of a characteristic length of the shell. Thick shell elements calculate transverse shear effects which thin shell elements do not.

All the bearing plate FE models were circular plates. For all the FE models x was the radial direction, y was the vertical direction (perpendicular to the bearing plate) and z was the circumferential or tangential direction (see figure 3.1).

Figure 3.1 shows a segment of a webbed bearing plate modelled using shell elements. The model shown in figure 3.1 has 20 radial webs, hence the segment shown is 1/20th of the bearing plate. The elements used are all 8 noded quadrilateral elements. The mesh shown in figure 3.1 is a typical mesh used for a webbed bearing plate, with a higher mesh density close to the centre than at the outer edges of the bearing plate.

The boundary conditions applied were restraints on the lower surface of the bearing plate (the surface in contact with the rock / steel support plate) and load on the upper surface of the bearing plate (the surface in contact with the nut). The point loads and restraints are shown on figure 3.1. The load was applied as point loads at all of the nodes on the upper surface of the bearing plate within the specified nut diameter. The

load was evenly distributed between these nodes. The node spacing of the mesh in the region where the nut acts was constant to ensure that the load was evenly distributed. Pressure loads could not be used because ABAQUS does not enable pressure loads to be applied to the edge of shell elements. Hence for consistency all loads applied were point loads. The load applied to all FE models acted in the negative y direction, perpendicular to the bearing plate and hence the models had an out of alignment angle of zero.

The restraint applied prevented movement of the plate in the y direction. This restraint was applied to the two nodes on the lower surface of the plate at a diameter greater than the support plate hole diameter. Unfortunately the restraint could not be applied at points and had to be applied at nodes. The first restrained node was usually within 0.25 mm of the specified radius for support and in no model was further than 0.75 mm away. Hence in all cases the support plate hole diameter modelled using FEA was slightly larger than the nominal diameter. Only two nodes were restrained so that most of the bearing plate was not prevented from moving in the positive y direction. It was found that if three or more nodes were restrained, the bearing plate was prevented from moving in the positive y direction and tensile stresses were produced. The way in which the load and restraints were applied simulates the loading of the bearing plate in the laboratory test and not in the coal mines. The exact loading of the bearing plate in the coal mine is not known. The loading of each bearing plate in the coal mines will vary due to the different surface of the coal.

In the models of the webbed designs only a segment was modelled, as shown in figure 3.1. The segments consisted of one radial web and half of the circumferential webs on either side of the radial web. Boundary conditions were applied at the 'cut' edges of the

segment to simulate the restraint from the other webs. These boundary conditions were produced by declaring local co-ordinate systems at the ‘cut’ edges of the segment. The ‘cut’ edges were then restrained from translating in the z direction and from rotation in the x and y directions of the local co-ordinates.

For the webbed bearing plates, the load applied to the segment modelled was multiplied by the number of segments to calculate the total load. Similarly the volume of the segment was multiplied by the number of segments to calculate the total volume of the webbed bearing plate.

### 3.1.1 Hypoelastic material model

All the FE models used non linear static analysis, which considers both material non linearity and geometric non linearity (large displacement analysis). The material non linearity was modelled using the Hypoelastic material model. The Hypoelastic material model considers non linear elastic behaviour, as found in many polymer materials. ABAQUS can successfully model the two forms of non linearity together. The analysis performed was at stresses and strains below yield, hence elastic analysis. The variation of secant modulus, Poisson’s ratio and the three strain invariants for the uniaxial case were entered for the material definition. The material data was entered into the ABAQUS input files directly because Patran does not support the Hypoelastic material model. The first, second and third strain invariants for the uniaxial case are given by the following expressions:-

$$I_1 = \epsilon_{xx} + \epsilon_{yy} + \epsilon_{zz} \quad (3.1)$$

$$I_2 = -\epsilon_{xx}\epsilon_{yy} - \epsilon_{xx}\epsilon_{zz} - \epsilon_{yy}\epsilon_{zz} \quad (3.2)$$

$$I_3 = \epsilon_{xx}\epsilon_{yy}\epsilon_{zz} \quad (3.3)$$

from Boresi (1993).

where

$\epsilon_{xx}$  is the principal strain in the x direction

$\epsilon_{yy}$  is the principal strain in the y direction

$\epsilon_{zz}$  is the principal strain in the z direction

The three strain invariants were calculated for the uniaxial case from uniaxial test data using the above equations.  $\epsilon_{yy}$  and  $\epsilon_{zz}$  were calculated from the value of  $\epsilon_{xx}$  based on the Poisson's ratio effect i.e.  $\epsilon_{yy} = -\nu\epsilon_{xx}$  and  $\epsilon_{zz} = -\nu\epsilon_{xx}$ .

The material data used for modelling existing designs of bearing plates and the comparison with strain gauge results was obtained from tensile testing of specimens, these results are given in figures 6.2 and 6.3. All other material data used was obtained from the Campus database compiled by most major material manufacturers, the main results are given in figures 6.4 and 6.5.

### 3.1.2 Verification of Finite Element results

Three techniques were used to verify the Finite Element results. Firstly the reaction forces produced were compared with the loads applied. The difference between the load applied and the reaction force produced was always less than 1%.

The second verification technique was to refine the mesh and re-analyse to check that the results were consistent. The mesh was refined by using more elements of the same type but of a smaller size, (h refinement). The predicted maximum deflection produced by the original and refined mesh was compared (see table 3.2) and further modifications made if the difference was considered excessive. The difference between the two meshes was typically less than 4%. The maximum difference accepted was 6.4%.

The third verification technique was to re-analyse each model to give stresses at nodes instead of at element integration points. Element integration points are generally considered to give more accurate results than nodes but, the maximum deflection when the stress and strain were calculated at nodes instead of at element integration points, was identical in most cases and never more than 0.2% different. The stresses at the nodes calculated on the basis of adjacent elements were compared for errors. An example of this verification is given in table 3.1 for test 2 in the Taguchi 2 level experiment. The elements examined for this verification were all only 1 or 2 elements away from either the restraint or the load, so as to be in an area of fairly high stress gradient. The variation between adjacent elements was typically less than 5%. However for elements with low stress levels below  $5 \text{ MN/m}^2$ , the percentage difference was often larger. Table 3.1 shows a large percentage difference between the radial stresses, but the magnitude of the difference is not excessively large. If there was a large variation between adjacent elements, the mesh was refined and verified again.

Node	Element	Radial stress ( $\text{MN/m}^2$ )	Vertical stress ( $\text{MN/m}^2$ )	Circumferential stress ( $\text{MN/m}^2$ )
439	185	2.571	-20.89	-26.89
439	186	3.65	-21.09	-27.55
439	187	2.088	-22.29	-26.81
439	188	3.425	-22.08	-27.43
399	196	1.265	-15.12	-20.22
399	198	1.667	-15.22	-20.19
417	187	2.390	-12.81	-24.55
417	189	-0.6483	-14.98	-26.32

**Table 3.1** Example of verification procedure used to compare stresses at nodes

### 3.1.3 Performance comparison of FE models of bearing plate designs

The results from the Finite Element Analysis used to compare the bearing plate designs was a performance comparison load for each of the designs. It was not possible to find the load to cause complete failure using FEA, as would be obtained if using laboratory tests. The performance comparison used for each of the designs was the maximum deflection of the bearing plate, in the negative y direction. After Finite Element Analysis of existing bearing plates, a performance comparison of 1 mm deflection was chosen. This maximum overall deflection invariably occurred on the upper surface of the bearing plate, at the centre (on the edge of the hole). The reasons for this choice of performance comparison are discussed in section 7.1.3. A deflection of 1 mm was chosen to be at a high level of loading, but without the stress or strain in the bearing plate reaching yield. The load to cause a deflection of 1 mm was estimated for each bearing plate model, the load applied was iterated until the maximum overall deflection of the plate in the negative y direction was within +/- 0.009 mm (+/- 1%) of 1 mm. The non linear material behaviour meant that iterations were necessary as the load applied and deflection produced is not a straight line relationship. Table 3.2 gives an example (for test 2 in the Taguchi 2 level experiment), of the iterative procedure used for all bearing plate designs.

Load applied (N)	Deflection produced (mm)
1440	-0.3168
4464	-1.137
3888	-0.9663
4017.6	-1.004
refined mesh	4 % difference
4017.6	-0.9655
4161.6	-1.005

**Table 3.2** Example of iterative procedure used to determine performance comparison load

The iterative procedure shown in table 3.2 produced a deflection within 0.005 mm of 1 mm. ABAQUS gives values of deflection to 4 significant figures. Table 3.2 shows that for this example, there was a 4 % difference in the value of maximum deflection between the two meshes.

A criticism of the method used here is that it is an iterative method and hence required large numbers of FE runs. However to provide a valid comparison between the different bearing plate designs it was necessary to be able to compare the designs using the same performance criteria.

The volume of material used in all of the bearing plate designs was calculated using the Patran software package. The load/volume ( $\text{N}/\text{mm}^3$ ) was used as the main performance comparison to give an indication of the efficiency of the design in terms of distribution of material. In order to understand the effect of the parameters more fully, load (N) was also used as a performance comparison.

### **3.2 Tensile testing of polymer material**

In order to model existing designs of bearing plates using Finite Element Analysis, material data was required. This was obtained from tensile tests on the material. The results from this testing, including a stress / strain graph and the variation of secant modulus with strain for the material used in the Weldgrip and Weidmann bearing plates are given in figures 6.2 and 6.3.

Tensile specimens of the Weldgrip plate material were cut from the edges of solid Weldgrip bearing plates. The geometry of the webbed Weidmann bearing plate was

such that it was not possible to cut tensile specimens out directly. Tensile specimens of the webbed Weidmann bearing plate material were obtained by putting 2 Weidmann bearing plates into a Leesona granulating machine to produce small granules of the material. The granules were then compression moulded into a rectangular block using a Moore's press. Tensile specimens were then machined from the rectangular blocks. It is possible that the regranulation and subsequent compression moulding of the material in the Weidmann bearing plate may have distorted the properties.

Tensile test specimens were machined to the dimensions specified in BS 2782, part 3, Method 320C. The dimensions of the specimens used are given in Appendix 3, figure A3.1. The dimensions were checked using a micrometer. The samples were tested according to BS 2782 using a JJ Lloyd Testing Machine and chart recorder. The specimens were tested with a crosshead speed of 5 mm/min. This relatively slow speed is recommended by BS 2782 for measuring the stress / strain behaviour. This is the standard crosshead speed used when testing the bearing plates. The gauge length of the tensile specimens was 50 mm. A total of five specimens of each material were tested, as recommended by BS 2782.

### **3.3 Strain gauge methodology**

In order to validate the Finite Element results strain gauges were attached to a Weldgrip and Weidmann bearing plate. The strain gauged Weldgrip plate was first turned into a circular plate so that it could be modelled using axisymmetric elements, which were used for all other solid bearing plate designs. The centre point of the strain gauge was positioned over the co-ordinates of a node to enable comparison of the strain gauge and Finite Element results. The strain gauges were positioned in an area of relatively high

strain levels, but not in a position where the strain gauges might be crushed by the nut or steel support plate. The strain gauges used were supplied and recommended by Techni Measure Ltd (code number FLA-2). These gauges were made from a Copper / Nickel alloy called Advance or Constantan. The adhesive used for the Weldgrip bearing plate was Cyanoacrylate as recommended by Techni Measure, the adhesive used for the Weidmann bearing plate was polyester P2 adhesive because the Cyanoacrylate adhesive failed to secure the strain gauge to the Weidmann bearing plate material. The gauges chosen were as short as possible (2 mm gauge length) to minimise the change in strain along the length of the gauge.

The monitoring equipment used for the strain gauge measurement was a Measurements Group Strain Indicator P3500 and a Switch and Balance Unit SB10. The gauge factor of the gauges used was 2.12. The strain gauges were connected to the monitoring equipment using a Quarter Bridge circuit. The bearing plate was connected to the monitoring equipment and left for a few minutes for the temperature to stabilise. The load was applied to the bearing plate during the strain gauge experiments using a Mayes 100 kN testing machine. The load was applied to the Weldgrip bearing plate using the same manufacturers' nut. The bearing plate was supported by a steel plate with a 55 mm hole. A preload of 0.5 kN was applied and the strain gauge reading recorded. This initial reading and preload was subtracted from the subsequent strain gauge readings. The load was applied in increments of 0.5 kN and strain gauge readings were taken. A comparison of the strain gauge and FE results for the Weldgrip bearing plate is given in figure 4.1.

### **3.4 Taguchi Experimental Design**

The Taguchi experimental design method is a well reported methodology, Ross (1988), Logothetis (1989). Many of the concepts promoted by Taguchi had already been established and used by statisticians for many years before. The Taguchi experimental design method involves identifying relevant parameters and levels to be investigated, and fitting these parameters into an orthogonal array as shown in Appendix 2, table A2.1.

The Taguchi experimental design method was used as a way of looking at a large number of parameters concerning the design and testing of non metallic bearing plates and assessing their relative significance without requiring excessive numbers of Finite Element models. Some of the parameters investigated are shown in figure 3.2.

### Parameters investigated

The sketch below is a cross-section of a solid coned bearing plate design. All designs looked at in the Taguchi and one factor at a time experiments are circular designs. Some designs are solid as shown below and others are webbed. Some designs are flat and others are coned as shown below. Some of the coned designs have straight sided cones as shown below whilst others have a convex curve and others have a concave curve.

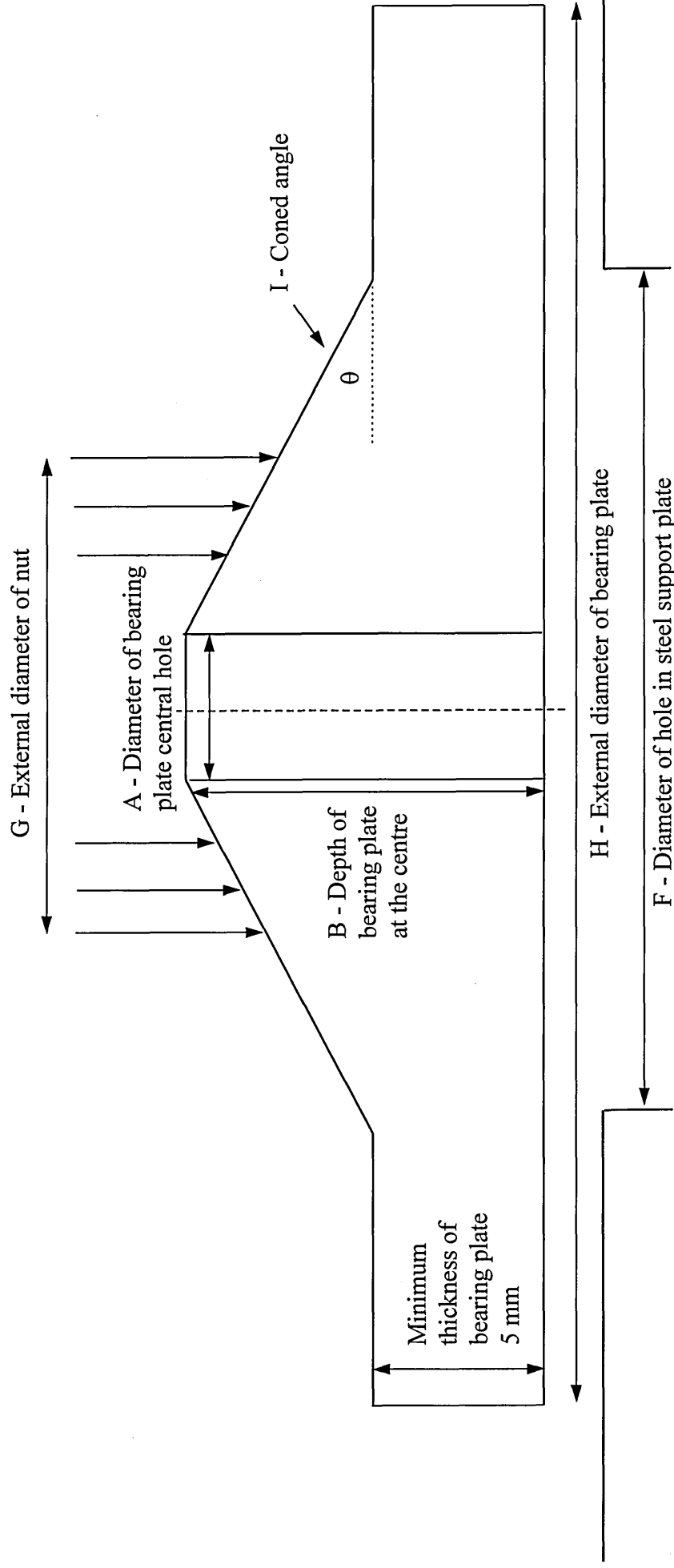


**Figure 3.2** Parameters investigated in Taguchi and one factor at a time experiments

### 3.4.1 Two level Taguchi experiment

The parameters were first investigated using a Taguchi 2 level experiment, which means that two values of each parameter were investigated. Two different values of eight parameters were investigated using only 16 tests (FE models).

The validity of a Taguchi experiment is dependent upon correctly identifying the relevant parameters and their interactions at the experiment design stage. In the two level Taguchi experiment the following parameters and values were used and interactions assumed.

<u>Parameters</u>	<u>Level 1</u>	<u>Level 2</u>
A Diameter of central hole in bearing plate	A1 25.85 mm	A2 34.0 mm
B Depth of bearing plate at the centre	B1 10 mm	B2 35 mm
C Coned or flat shape	C1 flat	C2 coned
D Webbed or solid shape	D1 solid cross section	D2 webbed
E Materials	E1 polypropylene	E2 polyamide 6
F Diameter of hole in steel support plate	F1 55 mm	F2 100 mm
G External diameter of nut	G1 40 mm	G2 56 mm
H External diameter of bearing plate	H1 150 mm	H2 200 mm

### Interactions

FG  
EF  
EG  
AG

The Taguchi tests involved varying the values of the different parameters, and obtaining results from Finite Element Analysis for the load carried by the designs (to cause 1 mm deflection). The 'output parameter' or parameter used for comparison was the load per unit volume of material. The most successful designs were indicated by a high value of

load per unit volume. This 'output parameter' was chosen because the main objective of the experiments was to maximise the load bearing capacity of the bearing plates in a cost effective manner. Including the volume of material enables the analysis to consider efficient distribution of material.

The values for the two levels of the parameters given above were chosen as extremes of the values that could be sensibly chosen. The diameters of the hole in the centre of the bearing plate given as parameter A, are the minimum diameters to still allow 18° out of alignment based upon the bearing plate depths given as parameter B (see figure 2.5). The bearing plate depths are slightly larger and slightly smaller than the depths of bearing plate designs currently available. The coned angle used was 30° for all coned designs in the 2 level Taguchi experiment. There were 12 radial and 4 circumferential webs for all webbed designs in the 2 level Taguchi experiment. The webs had a constant thickness of 3 mm. The coned angle, number of webs and web thickness was held constant throughout the two level Taguchi experiment, to enable comparisons of other parameters to be made. Two materials suggested by both Plascams and CMS material selection packages were used. The material data required was obtained from the Campus materials database. The material data used in most FE models is given in figures 6.4 and 6.5. The diameter of hole in the steel support plate used when testing non metallic bearing plates specified in BS 7861 is 55 mm. A larger diameter of hole in the steel support plate of 100 mm which causes a different failure mechanism (see section 5.2) was compared. The American and Canadian rockbolting standards (table 1.8) specifies a hole diameter of 100 mm. The two values of external diameter of nut are the minimum and maximum values of nut diameters available from UK suppliers. The diameter of the bearing plates currently available in the UK is approximately 150 mm. A diameter of

200 mm would offer a larger surface area of bearing plate in contact with the rock, hence spreading the load over a larger area of rock, which has an advantage from a Rock Mechanics point of view.

Four interactions were included in the design of the Taguchi 2 level experiment. With the benefit of hindsight these were not ideal choices as is discussed in section 7.3.4. The interactions included in the experiment design and the reasons for their inclusion are given below.

FG - Diameter of hole in steel support plate and diameter of nut. This was included because both parameters affect the distance between the support and load.

EF - Material and diameter of hole in steel support plate. This was included because it was expected that the difference in stiffness of the material would make more difference with a larger diameter of hole in the steel support plate than a small hole.

EG - Material and diameter of nut. This was included because it was anticipated that different material stiffness may make more difference with smaller diameters of nut.

AG - Diameter of central hole in bearing plate and diameter of nut. This was included because they both affect the surface area of the bearing plate over which the load is applied.

Before the 2 level Taguchi experiment could be performed, the parameters and their expected interactions were assigned to an orthogonal array. This was done using a technique of linear graphs as explained by Ross (1988). Table A2.1 in Appendix 2

shows an L16 orthogonal array that the above parameters have been assigned to. An L16 orthogonal array requires 16 tests (FE models) to be carried out. The orthogonal array gives the levels of each parameter to be used for each test. Figures A2.1 - A2.16 show the 16 bearing plate designs used for the Taguchi 2 level experiment.

The results from the Taguchi experiments were analysed using 'Analysis of Variance' (ANOVA). The application of ANOVA is explained in detail by Ross (1988), a brief summary is included here. The sum of squares SS was calculated for each parameter.

For parameter A the sum of squares is :-

$$SS_A = \frac{(A_1 - A_2)^2}{N_T} \quad (3.4)$$

where

$A_1$  - sum of results at level 1

$A_2$  - sum of results at level 2

$N_T$  - total number of results

As the 'output parameters' used (load / volume and load) are 'higher the better' output parameters, the best level for parameter A is given by the higher sum of results, either  $A_1$  or  $A_2$ .

The variance was calculated for each parameter. For parameter A the variance  $V_A$  is:-

$$V_A = \frac{SS_A}{v_A} \quad (3.5)$$

where

$v_A$  - degree of freedom for parameter A

Confidence levels were obtained by means of the 'F-test' method. 'F-test' is the ratio of variances. The variance of each parameter was compared with the error variance, to give an F ratio for each parameter. The larger the F ratio the larger the confidence level. The confidence level for each parameter was obtained from standard tables of F ratios, Ross (1988). A 90 % confidence level means that with at least 90 % confidence level or

probability the parameter is significant compared to the error. The error in the 2 level Taguchi experiment was determined by means of an empty column in the orthogonal array. The error in the multiple level Taguchi experiment was obtained by ‘pooling up’ the least significant parameters.

$$F = \frac{V_A}{V_E} \quad (3.6)$$

where

$V_E$  - variance of the error

After completing the Taguchi 2 level experiment and analysing the results a confirmation test was performed (figure A1.17). This involved selecting the ‘best’ level for each parameter (determined by the highest value of the sum of results) and performing a test using this combination.

### 3.4.2 Multiple level Taguchi experiments

#### 3.4.2.1 Multiple level Taguchi experiment for solid bearing plates

The parameters which were found to be most significant in the 2 level Taguchi experiment (see table 4.1) were further investigated using multiple level Taguchi experiments. The multiple level Taguchi experiment on solid bearing plates investigated three levels of four parameters concerning the design of solid coned bearing plates as shown below.

<u>Parameters</u>	<u>Level 1</u>		<u>Level 2</u>		<u>Level 3</u>	
F Diameter of hole in steel support plate	F1	55 mm	F2	65 mm	F3	75 mm
B Depth of bearing plate at the centre	B1	15 mm	B2	25 mm	B3	35 mm
I Coned angle	I1	15°	I2	30°	I3	45°
J Coned shape	J1	straight	J2	concave	J3	convex

These three levels of four parameters were fitted into an L9 orthogonal array as shown in table A2.2. An L9 array requires 9 tests (Finite Element models) to be carried out. Parameters F and B were examined in more detail than in the 2 level Taguchi experiment. Parameter I looked at different coned angles. Parameter J is a discrete parameter investigating straight convex and concave shaped cones. The radius of curvature for the convex and concave shaped cones was kept constant at 100 mm to enable comparison. For the convex and concave shaped coned plates the dimensions at each end of the curve were calculated as for a straight sided cone and a concave or convex curve was created between the two points. In the convex shaped bearing plates, the material curves outwards adding extra material compared to a straight shaped plate. In the concave shaped plate, the bearing plate curves inwards removing material compared to a straight shaped plate. Figures A2.18 - A2.26 show bearing plate designs for each of the 9 tests in this multiple level Taguchi experiment. The material used for these tests was polypropylene. No interactions were included in the design of this multiple level Taguchi experiment, because none had been identified by the 2 level Taguchi experiment.

#### 3.4.2.2 Multiple level Taguchi experiment for webbed bearing plates

This multiple level Taguchi experiment investigated three levels of four parameters concerning the design of webbed bearing plates. The parameters investigated are shown below.

<u>Parameters</u>	<u>Level 1</u>		<u>Level 2</u>		<u>Level 3</u>	
K Number of radial webs	K1	4	K2	12	K3	20
L Number of circumferential webs	L1	3	L2	4	L3	5
M Web thickness	M1	3 mm	M2	4 mm	M3	5 mm
E Materials	E1	polypropylene	E2	polyamide 6	E3	polycarbonate

These parameters were fitted into an L9 orthogonal array as shown in table A2.3. The depth of the designs in this multiple level Taguchi experiment was kept constant at 20 mm, and all of the designs were flat (not coned) plates. Parameters K and L investigated the number of radial and circumferential webs respectively. These webs were equidistantly spaced. Parameter M investigated the effect of varying the web thickness. The web thickness of all the webs in the model, both radial and circumferential were varied. The two materials used in the 2 level Taguchi experiment (polypropylene and polyamide 6) were again compared and polycarbonate was also investigated. The webbed multiple level Taguchi experiment was carried out with both a 100 mm and 55 mm hole in the steel support plate and repeated thickening only the central webs. There were no interactions included in the design of the webbed multiple level Taguchi experiment. Figures A2.28 - A2.36 show bearing plate designs for the webbed multiple level Taguchi experiment.

There were no empty columns in the design of either of the multiple level Taguchi experiments, the three levels of four parameters filled the L9 orthogonal array, making the experiments highly efficient. The multiple level Taguchi experiments were analysed using ANOVA. The 'best' levels for each parameter were obtained and used to produce a confirmation model for each Taguchi experiment.

### 3.5 Overview of approach used to investigate design and testing parameters

An overview of the methodology and order that the parameters were investigated in is shown below. A 2 level Taguchi experiment was performed initially. The parameters which were found to be significant in the 2 level Taguchi experiment were further investigated using two multiple level Taguchi experiments. The parameters which were shown to be significant and some possible interactions suggested by the Taguchi experiments were then investigated further using a one factor at a time approach. Finally some parameters which had a small significance in the Taguchi experiments were further investigated in case missed interactions had previously obscured the results.

#### 2 level Taguchi experiment

Identification of design / testing parameters

Identification of probable interactions between parameters

#### Multiple level Taguchi experiment for solid bearing plates

#### Multiple level Taguchi experiment for webbed bearing plates

#### One factor at a time approach

F - Diameter of hole in steel support plate

B - Depth of bearing plate

I - Coned angle

Interaction between above parameters

K - Number of radial webs

O - Number and position of circumferential webs

M - Variation of web thickness

Interaction of webbed parameters

Comparison of webbed and solid bearing plate designs

G - Diameter of nut

A - Diameter of central hole in bearing plate

Interactions of minor parameters

Variation of thickness above edge of support plate hole

### 3.6 Laboratory tests on bearing plates

Tests on existing designs of bearing plate were performed using a Denison 67 kN testing machine. The bearing plate was positioned on a steel plate with a central hole. Load was applied to the bearing plate via a nut and conical seat arrangement. Figure 3.3 shows the apparatus used for tests on bearing plates. A chart of load against crosshead deflection was produced. Unless otherwise specified the results were obtained using a rate of loading of 5 mm/min, using the Weldgrip nut and with a sharp edge on the edge of the hole in the steel support plate of radius less than 0.4 mm. For all bearing plate tests the 'failure load' was taken as the peak load carried.

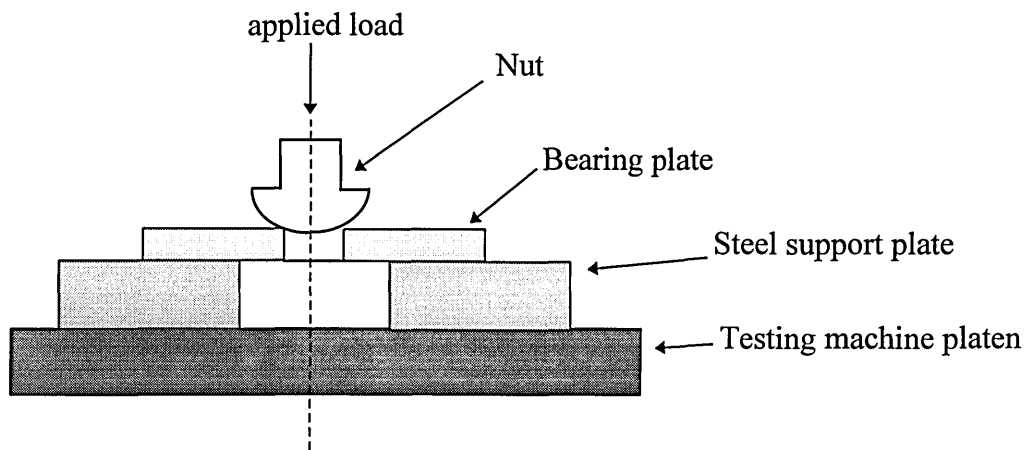


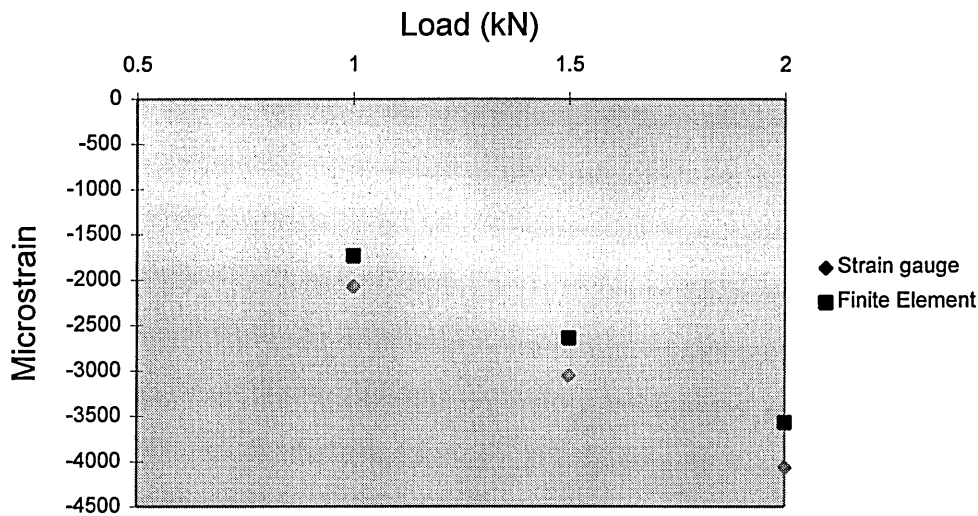
**Figure 3.3** Apparatus used for laboratory tests on bearing plates

## CHAPTER 4

### 4. FINITE ELEMENT RESULTS

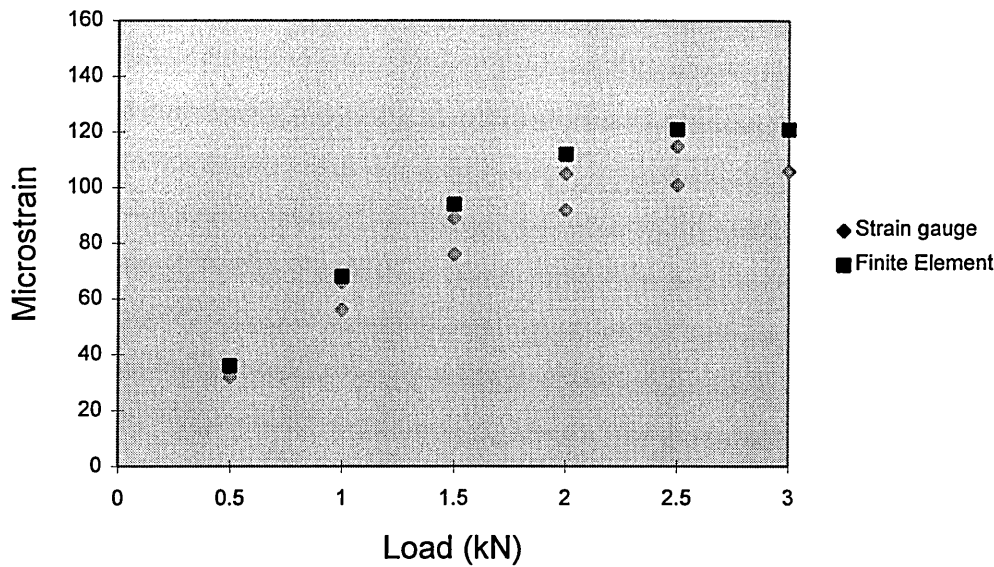
#### 4.1 Comparison of strain gauge and FE results

Figure 4.1 gives a comparison of the circumferential strain in the Weldgrip bearing plate, obtained by strain gauges and Finite Element Analysis. The strain was measured on the upper surface of the Weldgrip bearing plate on a region of reasonably high strain but not so close to the nut to risk crushing the strain gauges. The diameter of the hole in the steel support plate was 55 mm and the nut used to apply the load was the Weldgrip nut.



**Figure 4.1** Circumferential strain on upper surface of Weldgrip bearing plate

Figure 4.2 gives a comparison of the vertical strain in a circumferential web of the Weidmann webbed bearing plate, obtained by strain gauges and Finite Element Analysis. The diameter of the hole in the steel support plate was 140 mm and the nut used to obtain the results was the Weidmann nut. The strain was measured in a position where cracks occurred in laboratory tests (see figure 5.3).



**Figure 4.2** Vertical strain on web of Weidmann bearing plate

#### **4.2 Two level Taguchi experiment**

The Taguchi two level experiment investigated eight parameters concerning the design and testing of a bearing plate. The eight parameters are presented in table 4.1, in order of significance as found in the experiment. The value presented in the 'best' column is the value out of the two levels of the parameter investigated that gave the higher value of load / volume ( $\text{N}/\text{mm}^3$ ). The value given in the 'worst' column is the value which gave the lower value of load / volume. The confidence level gives an indication of the parameters relative significance in the experiment. For the parameters where no confidence level is given, the confidence level is below 90%. The error in the experiment was evaluated by means of an empty column in the orthogonal array. It was found that four parameters had a significance greater than the error and four parameters had a significance of less than the error.

parameter	best level	worst level	confidence level
F - Diameter of hole in steel support plate	55 mm	100 mm	99 %
B - Depth of bearing plate at the centre	35 mm	10 mm	99 %
C - Coned or flat shape	coned	flat	95 %
D - Webbed or solid	webbed	solid	95 %
Error			
E - Material	polypropylene	polyamide 6	< 90%
H - External diameter of bearing plate	150	200	< 90%
A - Diameter of central hole in bearing plate	25.85 mm	34 mm	< 90%
G - External diameter of nut	56 mm	40 mm	< 90%

**Table 4.1** Results from 2 level Taguchi experiment

A confirmation test was carried out to verify the results from the 2 level Taguchi experiment. The values used for the confirmation experiment were the ‘best’ value for each parameter. A drawing of the Taguchi 2 level confirmation test is given in Appendix 2, figure A2.17. The confirmation test model gave a higher value of load / volume than any of the 16 test models used in the 2 level experiment, hence the

confirmation test confirmed the experiment. The Taguchi 2 level experimental results were also evaluated by comparing the load carried, these results are given in table A1.1.

### **4.3 Multiple level Taguchi experiment on solid bearing plate designs**

The first multiple level Taguchi experiment looked at three levels of four parameters, for solid designs of bearing plates. Table 4.2 gives the four parameters in order of significance.

Parameter	Best level	Intermediate level	Worst level	Confidence level
F - Diameter of hole in steel support plate	55 mm	65 mm	75 mm	99 %
B - Depth of bearing plate at centre	25 mm	35 mm	15 mm	99 %
I - Coned angle	30°	45°	15°	95 %
J - Coned shape	straight	concave	convex	< 90 %

**Table 4.2** Results from multiple level Taguchi experiment on solid bearing plate designs

A confirmation test was carried out after the multiple level Taguchi experiment. A drawing of the model used for the confirmation test is given in figure A2.27. The confirmation test used the values of each parameter that gave the 'best' result in the multiple level Taguchi experiment. It is worthy of note that one of the designs in the multiple level Taguchi experiment produced a higher value of load / volume than the confirmation test.

There was no empty column included in the multiple level Taguchi experiment, which meant that there was no measure of error, but the experiment was efficient as the maximum number of parameters and levels were investigated with the minimum number of tests.

#### **4.4 Multiple level Taguchi experiment for webbed bearing plate designs**

The webbed multiple level Taguchi experiment looked at three levels of four parameters, concerning the design of webbed bearing plates. Table 4.3 gives the parameters in order of significance.

Parameter	Best level	Intermediate level	Worst level	Confidence level
Number of radial webs	12	20	4	< 90 %
Material	polypropylene	polyamide 6	polycarbonate	< 90 %
Web thickness	5	4	3	< 90 %
Number of circumferential webs	5	4	3	< 90 %

**Table 4.3** Results from multiple level Taguchi experiment on webbed plate designs using a 100 mm hole in the steel support plate

In the multiple level Taguchi experiment with a 100 mm hole in the steel support plate, none of the parameters had a confidence level of more than 90 %.

Tables A1.2 and A1.3 give further results on the webbed multiple level Taguchi experiment. The experiment was repeated using a 55 mm hole in the steel support plate and repeated again varying the thickness of only the webs at the centre of the bearing plate.

#### 4.5 One Factor at a time results

A one factor at a time method means that one factor is varied whilst all others remain constant. Hence direct comparisons can be made easily. A one factor at a time approach was used to gather information about parameters over a large number of points. Unless otherwise specified, for all the one factor at a time tests, the material used was polypropylene, the nut diameter was 56 mm, the diameter of the central hole in the bearing plate was 34 mm, the external diameter of the bearing plate was 150 mm and the bearing plate was a solid (not webbed) design.

##### 4.5.1 Diameter of hole in steel support plate

The diameter of the hole in the steel support plate was shown to be a very significant parameter in the Taguchi experiments. Hence it was further investigated using a one factor at a time approach. Figure 4.3 shows the variation of load / volume with diameter of hole in the steel support plate for a very simple flat plate of depth 10 mm. The hole diameter specified in BS 7861 is 55 mm. Figure 4.3 shows that the bearing plate carries a larger amount of load (before deflecting by 1 mm) with a small hole in the steel support plate than with a large hole in the steel support plate. Clearly the variation is non-linear.

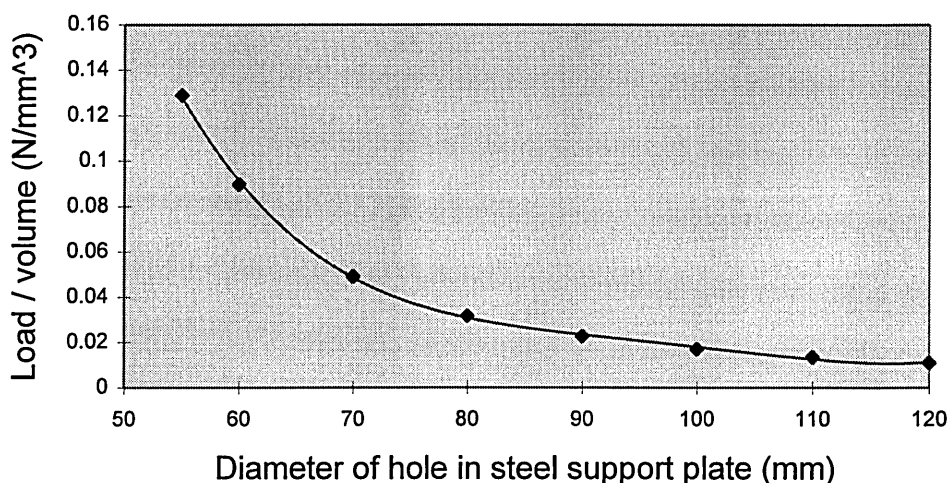


**Figure 4.3** Variation of load / volume with diameter of hole in steel support plate.

The diameter of the hole in the steel support plate was also investigated for coned plates of depth 30 mm and a flat plate of depth 30 mm, these results are given in figure 4.4. The curves shown in figure 4.4 are not parallel to each other. Hence the rate of decrease in load carried with increasing diameter of hole in the steel support plate is different for coned plates than for flat plates.

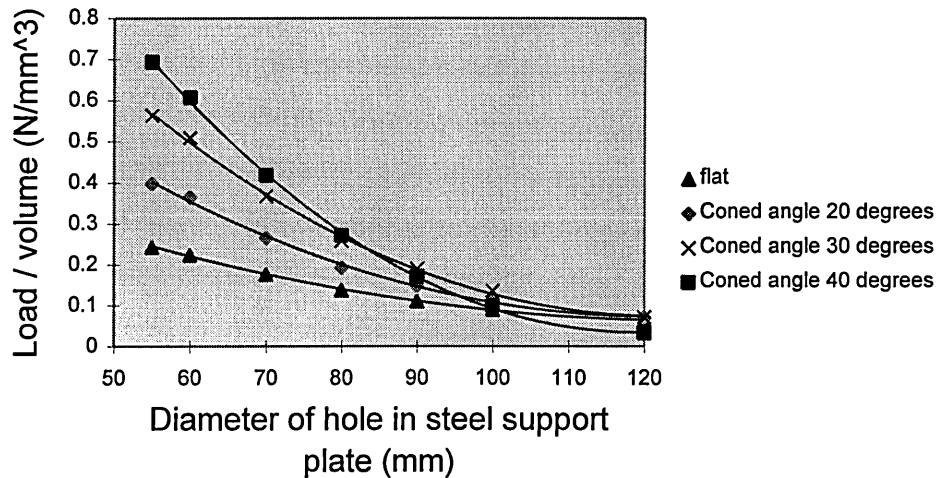


**Figure 4.4** Variation of load / volume with diameter of hole in steel support plate for coned and flat plates.

Appendix 1, figures A1.1 and A1.2 show the variation of diameter of hole in the steel support plate for a webbed bearing plate and for different materials. It can be seen in figure A1.1 that the results for a hole diameter underneath a circumferential web do not seem to fit the curve very well.

#### 4.5.2 Depth of bearing plate

Figure 4.5 shows the variation of load / volume with depth of the bearing plates, for five different diameters of hole in the steel support plate. These results are for flat plates, where the thickness of the plate is the same at the outside edge as in the centre of the plate. Notice that the curves for different diameters of hole are not parallel to each other.

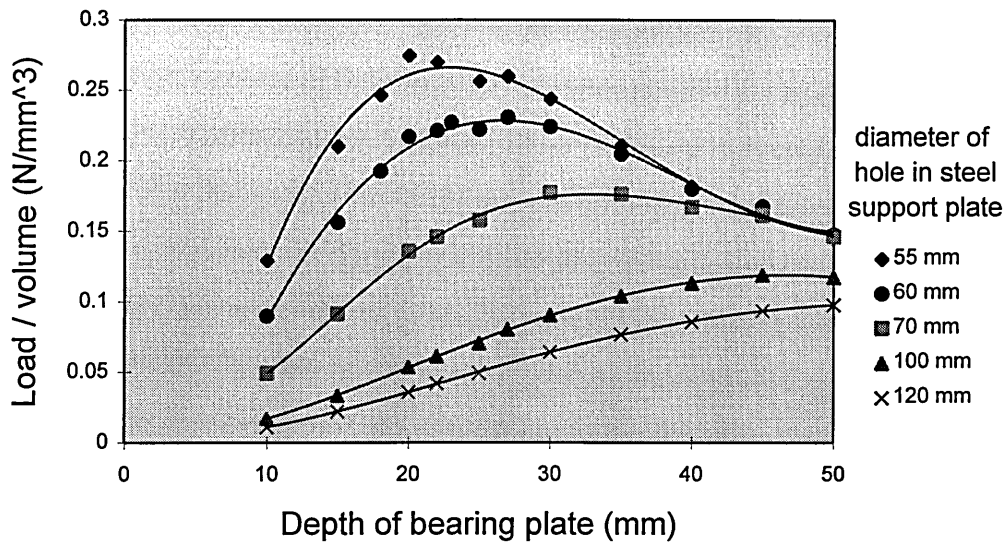


**Figure 4.5** Variation of load / volume with depth of bearing plates for different diameters of hole in the steel support plate

Figure A1.3 gives the same results as figure 4.5, plotted on the basis of load.

#### 4.5.3 Coned angle of bearing plate

Figure 4.6 shows the variation of load / volume with coned angle of the bearing plates for three different diameters of hole in the steel support plate. All of the models used in figure 4.6 had a depth of 30 mm.

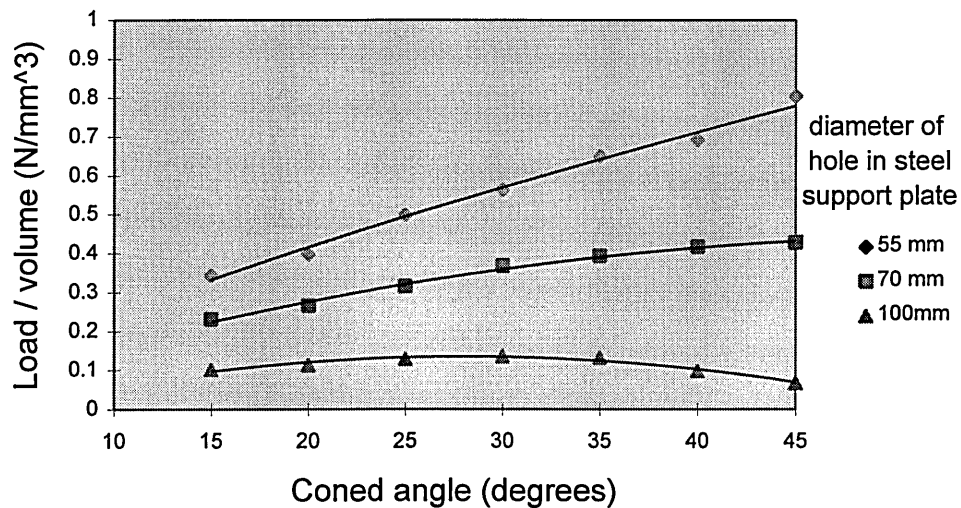


**Figure 4.6** Variation of load / volume with coned angle for different diameters of hole in the steel support plate

#### 4.5.4 Interaction between diameter of hole in steel support plate, depth of bearing plate and coned angle

The results presented in sections 4.5.2 and 4.5.3 show that there is an interaction between the depth of the bearing plate and the diameter of the hole in the steel support plate, and an interaction between the coned angle and the diameter of the hole in the steel support plate. The following results examine a three way interaction between the depth of the bearing plate, the coned angle and the diameter of the hole in the steel support plate.

Figure 4.7 shows the variation of load / volume with coned angle for four different depths of bearing plates with a 55 mm hole in the steel support plate. The coned angle of zero corresponds to a flat plate, of constant thickness.

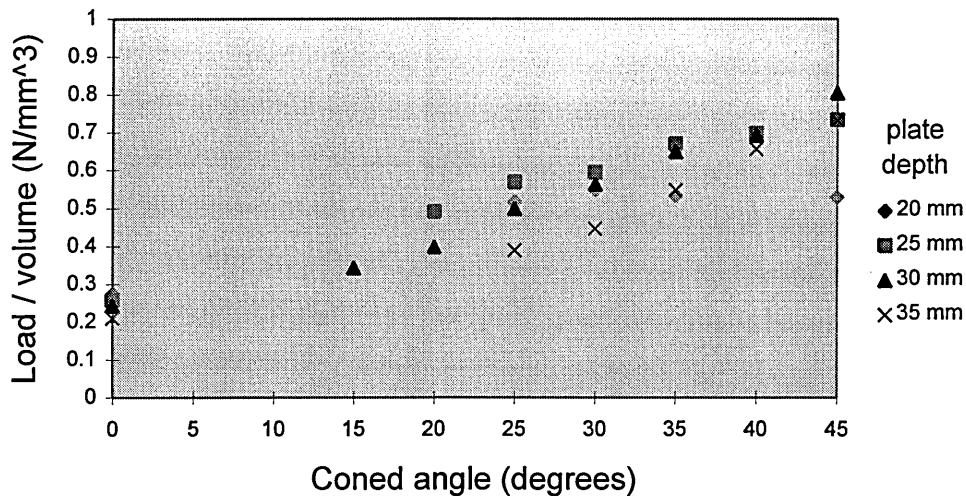


**Figure 4.7** Variation of load / volume with coned angle for different depths of bearing plate with a 55 mm hole in the steel support plate

The results in figure 4.7 show that for a 55 mm hole in the steel support plate, all coned plates perform better on a load / volume basis than flat plates of the same depth at the centre.

Figure 4.8 shows the variation of load / volume with coned angle for seven different depths of bearing plates with a 120 mm hole in the steel support plate. The variation shown in figure 4.8 is clearly very different to the variation shown in figure 4.7.

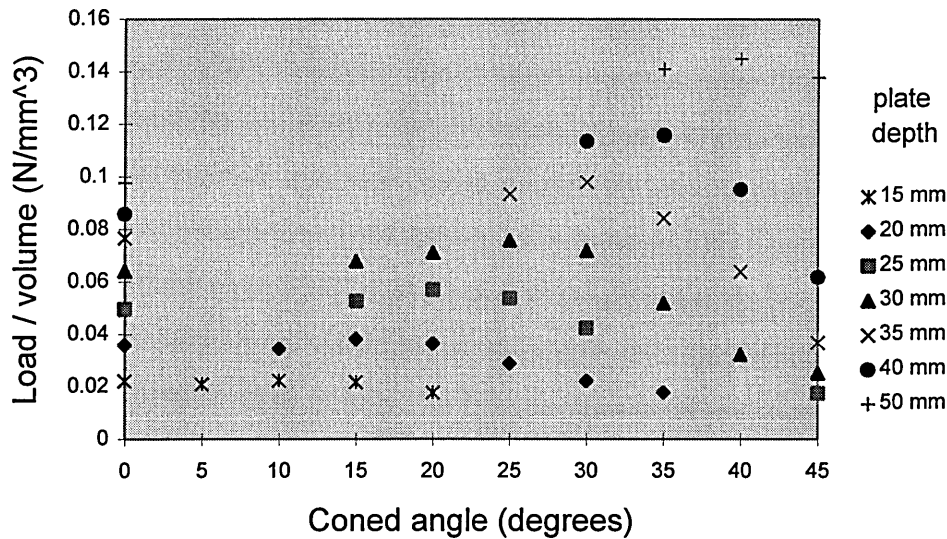


**Figure 4.8** Variation of load / volume with coned angle for different depths of bearing plate with a 120 mm hole in the steel support plate

The results shown in figure 4.8 show that for a 120 mm hole in the steel support plate, the coned plates perform better on a load / volume basis than the flat plates, but the difference is not as large as with a 55 mm hole in the steel support plate.

Further results are given in figures A1.4 and A1.5 for the variation of load / volume with coned angle for different depths of bearing plate when tested with steel plates with 70 mm and 100 mm diameter holes. Results are given in figure A1.6 for the variation of load / volume with depth of bearing plate for different coned angles.

Figure 4.9 shows the optimum coned angle for different depths of bearing plates with different diameters of hole in the steel support plate. The optimum coned angle was

extracted from figures 4.7, 4.8, A1.4 and A1.5 as the peak value of the coned angle on each curve.

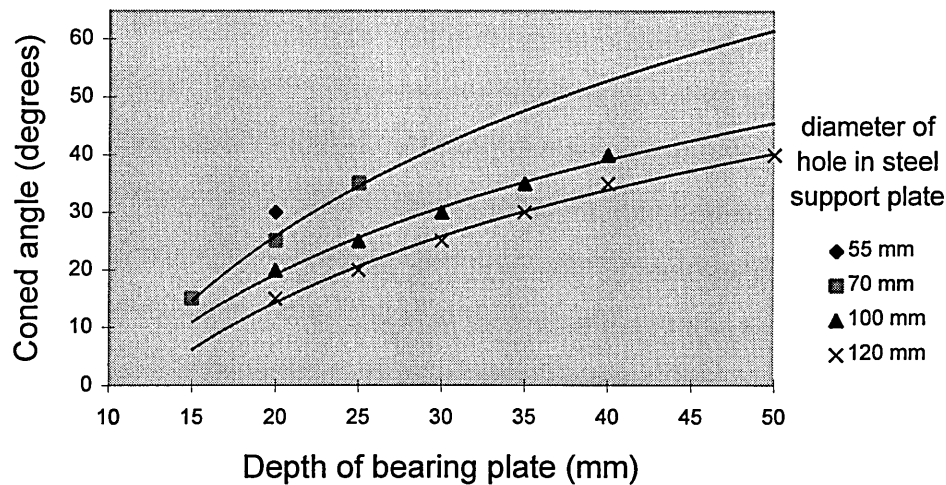
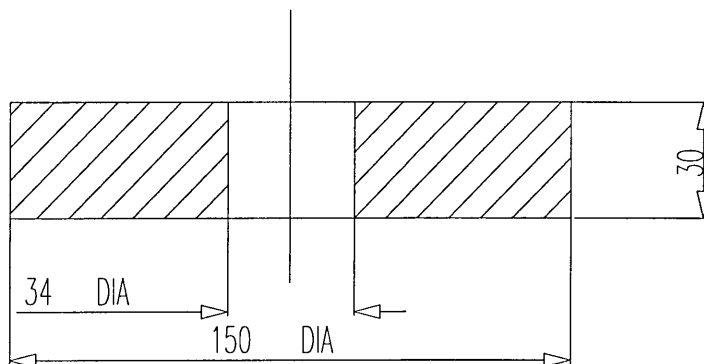


**Figure 4.9** Optimum coned angle for different depths of bearing plate with different diameters of hole in the steel support plate

#### 4.5.5 Increasing thickness of plate above edge of support plate hole

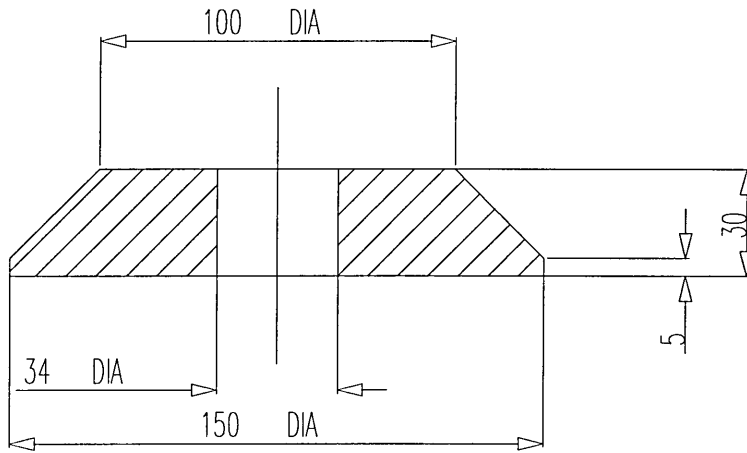
Some designs were examined which had a greater thickness above the region supported by the steel support plate. Figures 4.10, 4.11, 4.12 and 4.13 show some bearing plate designs which were compared with a 100 mm hole in the steel support plate. The design shown in figure 4.10 is a simple flat plate with a constant depth of 30 mm across the bearing plate's diameter.



All dimensions in mm

**Figure 4.10** Design number 1

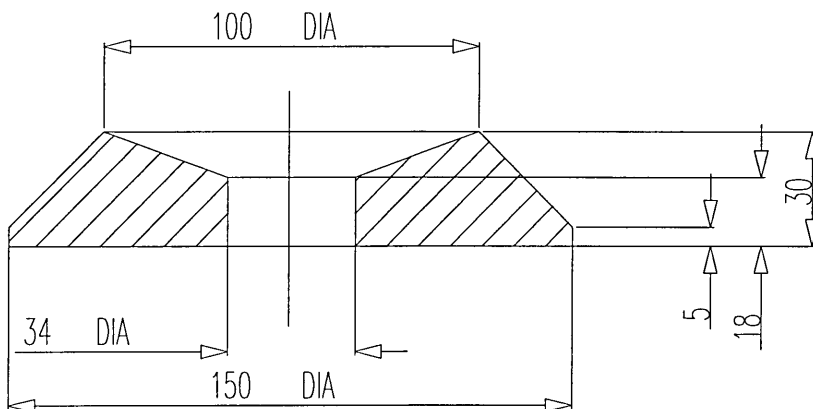
Figure 4.11 shows a design with a constant thickness of 30 mm from the centre to the region supported by the steel support plate. This design then slopes down at an angle of  $45^\circ$  to a thickness of 5 mm at the outside edge.



All dimensions in mm

**Figure 4.11** Design number 2

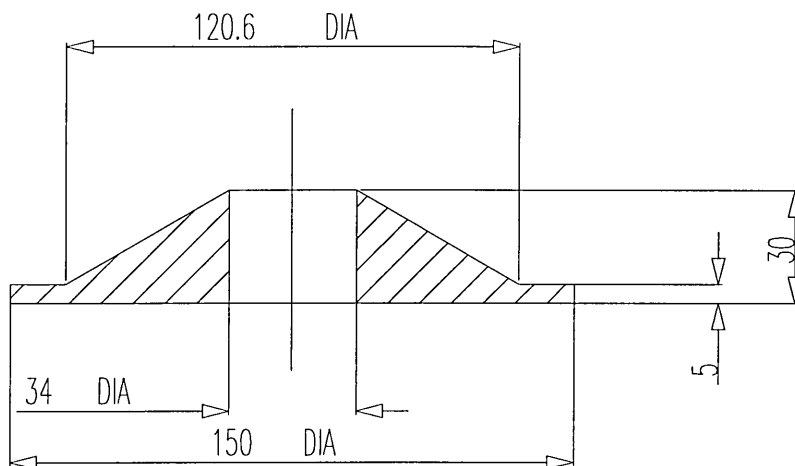
Figure 4.12 shows a design which is thicker over the edge of the hole in the steel support plate, (when used with a 100 mm hole). This design also tapers down at an angle of  $45^\circ$  to a thickness of 5 mm at the outside edge. This design also has a reduced thickness at the centre tapering down at an angle of  $20^\circ$  to a thickness of 18 mm.



All dimensions in mm

**Figure 4.12** Design number 3

Figure 4.13 shows a coned design of bearing plate similar to the coned plates investigated earlier. This plate has a thickness of 30 mm at the centre but tapers down at an angle of  $30^\circ$  and hence has a thickness of only 10.95 mm over the edge of the hole in the steel support plate.



All dimensions in mm

**Figure 4.13** Design number 4

Table 4.4 shows the variation in load (to cause 1 mm deflection) and volume and hence load /volume for each of the four designs presented above when tested with a 100 mm hole in the steel support plate.

	Load (N)	Volume (mm <sup>3</sup> )	Load / volume (N/mm <sup>3</sup> )
Design 1 (Figure 4.10)	45,600	502,905	0.09067
Design 2 (Figure 4.11)	44,070	369,500	0.11927
Design 3 (Figure 4.12)	25,942	337,900	0.07677
Design 4 (Figure 4.13)	25,986	191,500	0.1357

**Table 4.4** Comparison of four different designs of solid bearing plates

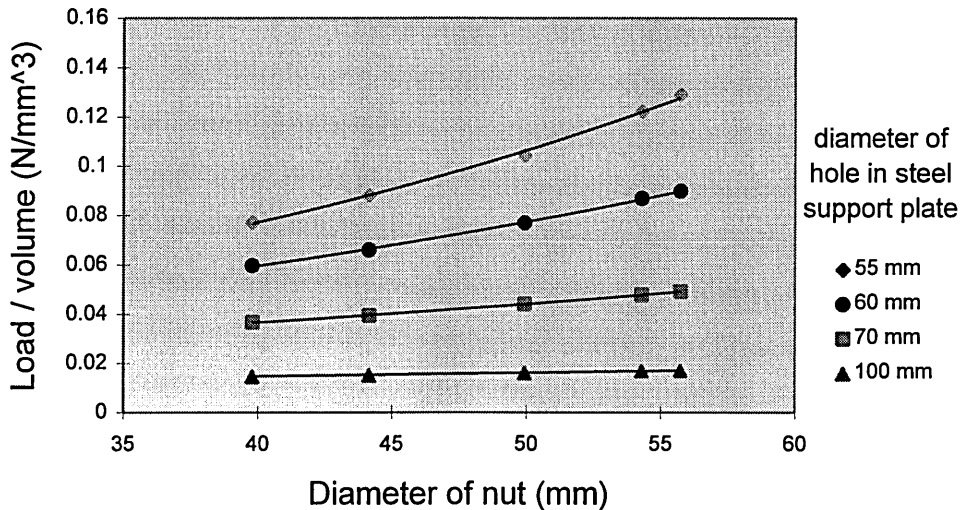
#### 4.5.6 Size of nut / volume of nut

The effect of varying the external diameter of the nut and conical seat was investigated.

A range of external diameters of the nut was investigated. The minimum nut diameter investigated was 40 mm which is the minimum diameter of nut available commercially.

Similarly the maximum diameter of nut which was investigated was 56 mm which is the maximum diameter of nut available commercially.

Figure 4.14 shows the variation of load / volume with diameter of the nut for a flat bearing plate design of depth 10 mm for four different diameters of hole in the steel support plate.



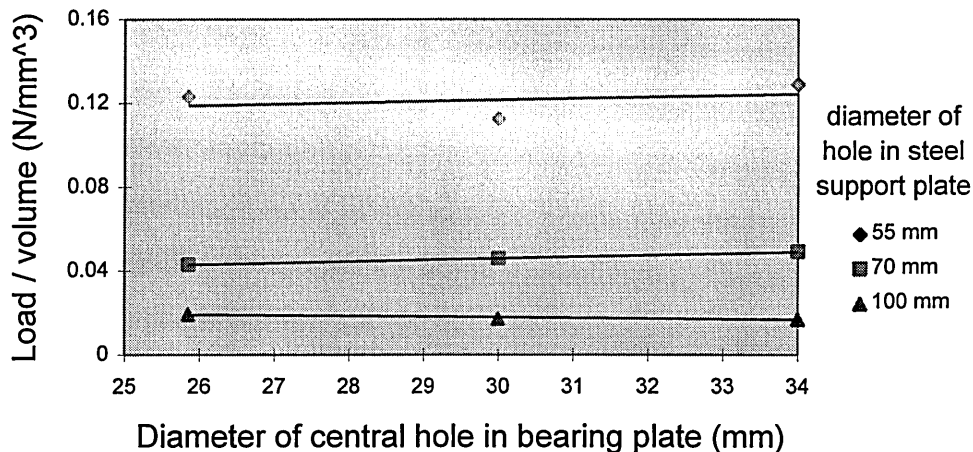
**Figure 4.14** Variation of load / volume with nut diameter for four different diameters of hole in the steel support plate

Figure 4.14 shows the variation of the nut diameter compared on a load / volume basis. Since the volume of the bearing plate is not changing figure 4.14 is simply showing the variation in the load carried by the bearing plate with different sizes of nut.

Appendix 1, figures A1.7 - A1.13 give further results for the variation of nut diameter. Results comparing the total volume of material in the bearing plate and nut, results for coned plates and flat plates and results comparing the surface area of the bearing plate that load is applied over for coned plates and flat plates are given. A comparison of the distance 'r' between the diameter of the hole in the steel support plate and the diameter of the nut is given.

#### 4.5.7 Diameter of central hole in bearing plate

The diameter of the central hole in the bearing plate is a parameter that had a significance of less than the error in the 2 level Taguchi experiment. Hence a simple comparison was made using a one factor at a time approach, to evaluate the parameters effect individually. Figure 4.15 shows the variation of load / volume with diameter of the central hole for three different diameters of hole in the steel support plate. As shown in figure 4.15 a bearing plate with a large central hole performs marginally better than a bearing plate with a small central hole when tested with a 70 mm and 100 mm hole in the steel support plate. This was true when the diameter of the bearing plate central hole was evaluated on a load / volume basis and on a load basis.



**Figure 4.15** Variation of load / volume with diameter of central hole in bearing plate

#### 4.5.8 Number of radial webs

Figure 4.16 shows the variation of load / volume with number of radial webs for three different diameters of hole in the steel support plate. The number of circumferential webs was held constant at 4 equally spaced webs. The depth of the bearing plates was held constant at 20 mm.

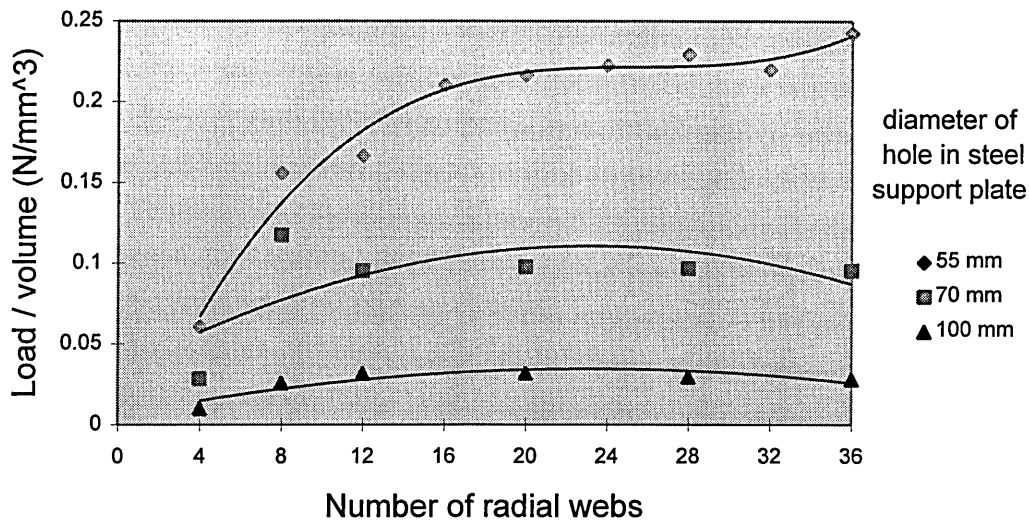


**Figure 4.16** Variation of load / volume with number of radial webs for different diameters of hole in the steel support plate

#### 4.5.9 Number of circumferential webs

The number of circumferential webs and their positions was also varied. Figures A1.14 - A1.22 show different designs of webbed plates with different numbers of circumferential webs at different diameters, including designs with the webs concentrated closer to the centre. A comparison of these designs is given in figures A1.23 - A1.25. In general the designs with the circumferential webs concentrated closer to the centre performed better than the designs with webs evenly spaced. The optimum configuration of the circumferential webs was found to depend on the diameter of the hole in the steel support plate.

#### 4.5.10 Thickening of different webs

The effect of thickening the different webs in webbed bearing plate designs was investigated. Initially all webbed bearing plates had a web thickness of 3 mm. Figures A1.26, A1.27, A1.28 and A1.29 give some results on the effect of thickening or reducing the thickness of the different parts of a webbed bearing plate. The results show that the effect of increasing the radial or circumferential web thickness depends upon the

number of radial and circumferential webs. The results suggest that whether it is better to thicken up the radial webs or the circumferential webs depends upon the number of radial and circumferential webs in the design. In general it was found to be better to increase the thickness of the webs close to the centre and decrease the thickness of the webs at the outer edge of the bearing plate.

#### 4.5.11 Comparison of solid and webbed designs

To be able to compare the difference between webbed and solid plates by a one factor at a time method, solid and webbed plates with the same external dimensions were produced. Table 4.5 gives a comparison between solid and webbed designs with the same external dimensions.

Constant parameters	<u>Solid Plate</u>	<u>Webbed plate</u>	
Flat plate Depth 20 mm Polypropylene 55 mm hole in steel support plate	Load - 92,055N Volume - 335,270 mm <sup>3</sup> Load / volume - <b>0.275 N/mm<sup>3</sup></b>	Load - 28,969N Volume - 83,844 mm <sup>3</sup> Load / volume <b>0.346 N/mm<sup>3</sup></b>	12 radial 3 circumferential webs (webbed design 6 - see figure A1.19)
Coned Plate Depth 20 mm Coned angle 45° Polypropylene 55 mm hole in steel support plate	Load - 53,271 N Volume 100,500 mm <sup>3</sup> Load / volume - <b>0.530 N/mm<sup>3</sup></b>	Load - 28,044 N Volume - 58,752 mm <sup>3</sup> Load / volume - <b>0.477 N/mm<sup>3</sup></b>	36 radial webs 3 circumferential webs (webbed design 9 - see figure A1.22)
Flat plate Depth 20 mm Polypropylene 100 mm hole in steel support plate	Load - 18,020 N Volume - 335,270 mm <sup>3</sup> Load / volume - <b>0.0537 N/mm<sup>3</sup></b>	Load - 4,850 N Volume - 113,352 mm <sup>3</sup> Load / volume - <b>0.0428 N/mm<sup>3</sup></b>	12 radial 5 circumferential webs (webbed design 5 - see figure A1.18)
Coned plate Depth 40 mm Coned angle 30° Polypropylene 100 mm hole in steel support plate	Load - 57,504 N Volume - 330,900 mm <sup>3</sup> Load / volume - <b>0.174 N/mm<sup>3</sup></b>	Load - 13,104 N Volume - 106,188 mm <sup>3</sup> Load / volume - <b>0.123 N/mm<sup>3</sup></b>	12 radial webs 5 circumferential webs best web thickness (webbed design 8 - see figure A1.21)

**Table 4.5** Comparison of solid and webbed designs, with the same external dimensions

The webbed coned plate results given in table 4.5 are for the best arrangement of webs investigated with the best web thickness used. The flat webbed plates are for the best arrangements of webs investigated. The results in table 4.5 clearly show that the solid designs of bearing plate are producing a higher value of load / volume than the webbed designs of bearing plate.

#### 4.5.12 Materials / Temperature and time effects

Results are given in figures A1.30 and A1.31 comparing different materials, and comparing some materials at 40°C and over a longer period of time. The results show that the materials that perform best are those with a high value of secant modulus, hence the stiffer materials.

#### **4.6 Stress / strain distribution in FE models of bearing plates**

The performance of the different designs investigated using Finite Element Analysis was compared mainly on the basis of a maximum deflection of 1 mm in the negative y direction. However some general observations of the stress levels in the bearing plates have been made. These observations were made by inspection of plots of Tresca stress and strain, and stress and strain in the XX (radial), YY (vertical, perpendicular to bearing plate) and ZZ (circumferential) directions in the models. Hoechst (1994) recommends the Tresca (Maximum Shear Stress) criteria for use with polymeric materials. However there are a number of articles, Mears et al (1969), Wronski (1977), Raghava et al (1973) which suggest that polymeric materials do not obey either the Tresca or Von Mises criterion, because of the differences between compressive and tensile yield strengths and pressure dependence effects. There does not seem to be a clear consensus on which yield criteria is appropriate for polymeric materials, Freire (1980), with different criteria possibly required for different polymers. The Tresca criteria was used in this research because it is supported by the Patran software and appears to provide as good a comparison as any other criteria.

When describing the stress / strain distribution and the different failure mechanisms in the bearing plate, the surface of the bearing plate in contact with the rock or steel support plate is described as the 'lower surface' and the surface of the bearing plate on which the nut sits is described as the 'upper surface'.

To enable comparisons of the stress distribution to be made between the different models, a standard load of 2 kN was applied. The material used for these comparisons

was polypropylene, with a yield stress of  $33 \text{ MN/m}^2$ , a yield strain of 3.5% and stress/strain behaviour as shown in figure 6.5.

#### 4.6.1 Flat bearing plate of depth 10 mm with 55 mm hole in steel support plate

Figure 4.17 shows a displaced plot with the distribution of Tresca stress in a simple flat solid bearing plate of depth 10 mm, external diameter 150 mm, central hole diameter 34 mm, made from polypropylene, tested with a 55 mm hole in the steel support plate and a nut of external diameter 56 mm. The load applied to this bearing plate to produce this plot was 2 kN, spread over 31 nodes. The view shown is a cross section through half of the circular plate with the axes of revolution on the left, focusing on the area close to the centre, where the highest stress and strain occur.

Inspection of the stress distribution in figure 4.17 shows that the maximum Tresca stress occurs on the lower surface of the bearing plate in the area around the restraint. It can be seen that the peak stress is localised in a very small area around the restrained nodes and on the deflected material closest to the restraint. The second area of stress concentration shown in figure 4.17 occurs in the region on the upper surface of the bearing plate, underneath the nut where the load is applied. The stress levels in the middle of the bearing plate are lower than the stress on the upper and lower surfaces. The stress levels at the outer regions, diameter  $> 100 \text{ mm}$  are very low, less than  $2 \text{ MN/m}^2$ . For a given load, less deflection occurs with a 55 mm hole in the steel support plate than for a larger hole.

Figure 4.18 shows the Tresca and Von Mises stress at the restraint (the edge of the hole in the steel support plate) for different diameters of hole in the steel support plate when

FRINGE PLOT LC=1.62 RES=1.1 (TRESCA - 1) MSC/PATRAN R-1.4 ABAQUS 20 - May - 97 15:49:09

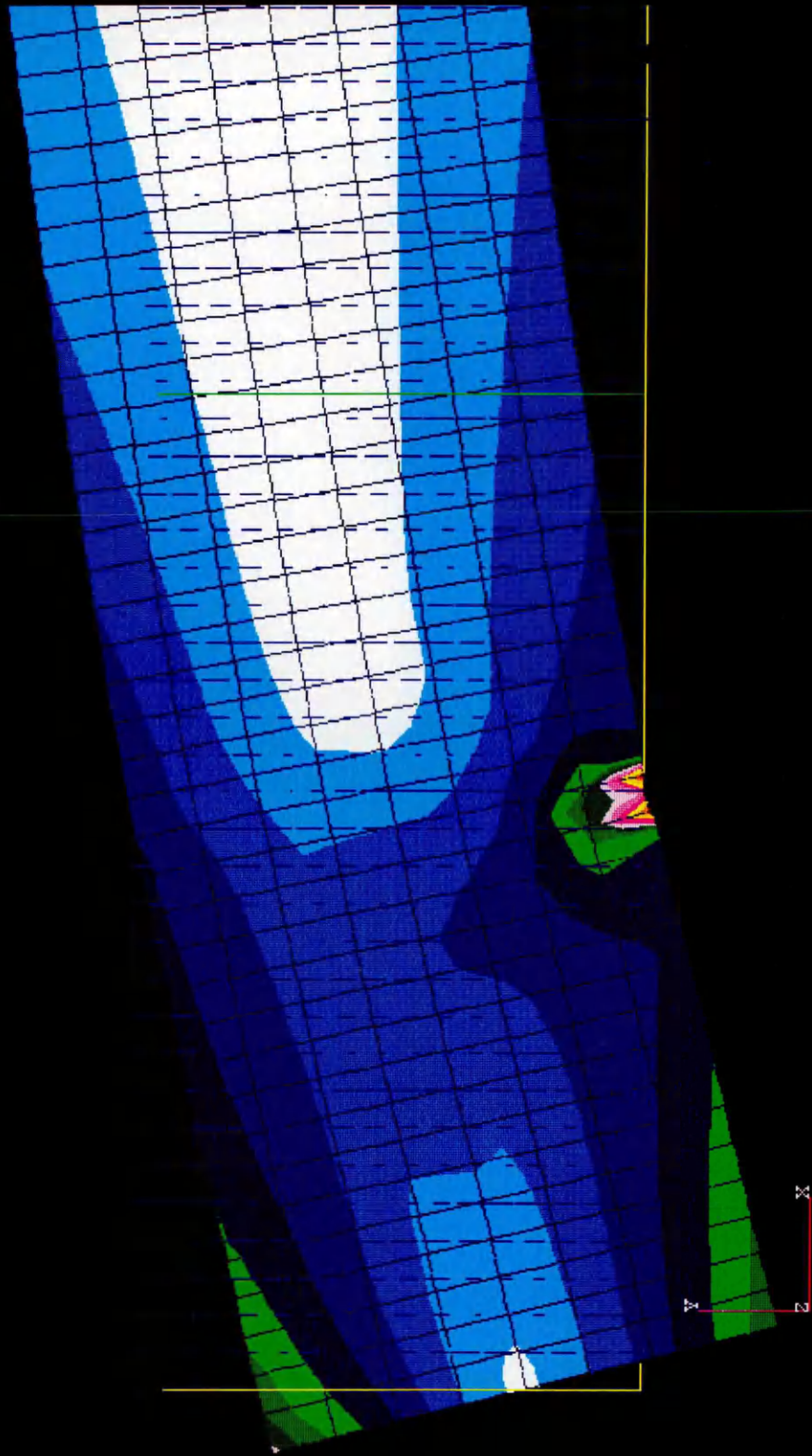
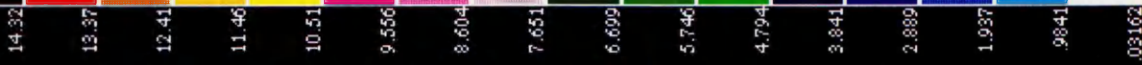
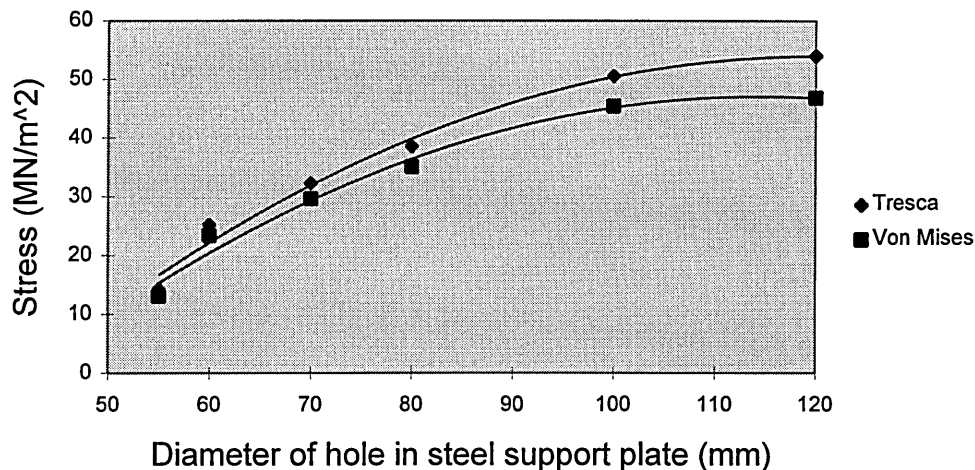


Figure 4.17 Distribution of Tresca stress in a flat bearing plate of depth 10 mm with a 55 mm hole in the steel support plate.

a standard load of 2 kN was applied. These results are based on a solid flat bearing plate of depth 10 mm made from polypropylene. Figure 4.18 shows that the stress at the edge of the hole increases with increasing diameter of hole in the steel support plate.



**Figure 4.18** Stress at restraint for different diameters of hole in steel support plate

#### 4.6.2 Coned bearing plate of depth 30 mm with 70 mm hole in steel support plate

Figure 4.19 shows the Tresca stress distribution in a coned bearing plate of depth 30 mm, coned angle 30°, external diameter 150 mm, central hole diameter 34 mm, made from polypropylene, tested with a 70 mm hole in the steel support plate and a nut diameter of 56 mm. The load applied to the bearing plate to produce this plot was 2 kN spread over 16 nodes.

In the coned bearing plate shown in figure 4.19 a stress concentration around the restraint can be clearly seen. However the maximum stress is underneath the nut, not around the restraint. This maximum stress is concentrated in a very small area at the tip of the coned plate. The stress levels at large diameters > 100 mm is very low less than 0.7 MN/m<sup>2</sup>.

PRINCE PLOT IC=1.24 RES=1.1 (TRESCA - 1) MSC/PATRAN R - 1.4 ABAQUS 20 - May - 97 16:34:12

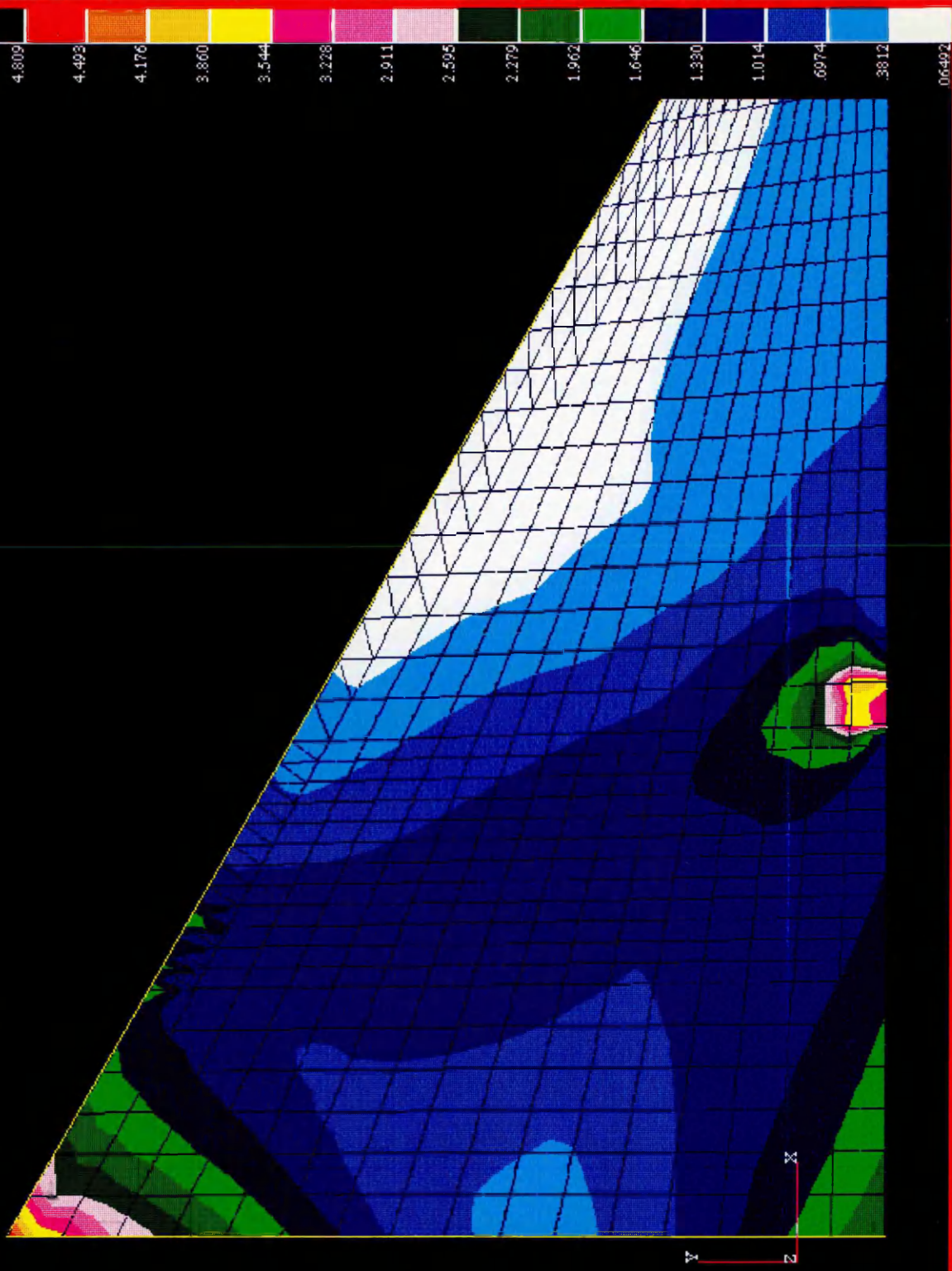


Figure 4.19 Distribution of Tresca stress in a coned bearing plate of depth 30 mm, coned angle 30 degrees, with a 70 mm hole in the steel support plate.

If the bearing plate is coned the stress under the nut is more than for a flat bearing plate of the same central depth. The larger the coned angle the larger the stress under the nut, because of the smaller volume of material in the region directly beneath the nut. For some coned bearing plates the maximum stress occurred underneath the nut not around the restraint. The larger the coned angle the more likely the maximum stress occurs underneath the nut, not around the restraint.

#### 4.6.3 Webbed bearing plate with 20 radial webs, 4 circumferential webs and a 100 mm hole in steel support plate

Figure 4.20 shows the radial (XX) stress distribution in a webbed bearing plate design. This bearing plate has 20 radial webs and 4 circumferential webs, a web thickness of 3 mm and is supported with a 100 mm hole in the steel support plate. It is a flat bearing plate of depth 20 mm, made from polypropylene, with an external diameter of 150 mm and a central hole diameter of 34 mm. Only  $1/20^{\text{th}}$  of the bearing plate was modelled as shown in figure 4.20. One of the 20 radial webs can be seen in the XY plane and  $1/20^{\text{th}}$  of the 4 circumferential webs can be seen in the YZ plane. The load applied to this bearing plate model to produce this plot was 2 kN, hence the load applied to the segment modelled was  $2000/20 = 100$  N.

The stress concentration around the restraint can be seen in figure 4.20 (radial 2, the region between the 2<sup>nd</sup> and 3<sup>rd</sup> circumferential webs from the centre). The stress in the outermost webs (hoop 4, radial 3) is very low. The stress in the circumferential webs is higher in the webs closer to the centre and decreases further from the centre. Within the support plate hole diameter the radial stress is predominantly tensile on the lower surface of the bearing plate; on the upper surface of the bearing plate the radial stress is predominantly compressive.

FRINGE PLOT LC=1.12 RES=1.1 (XIK - COMP) MSC/PATRAN R-1.4 ABAQUS 22-May-97 10:55:51

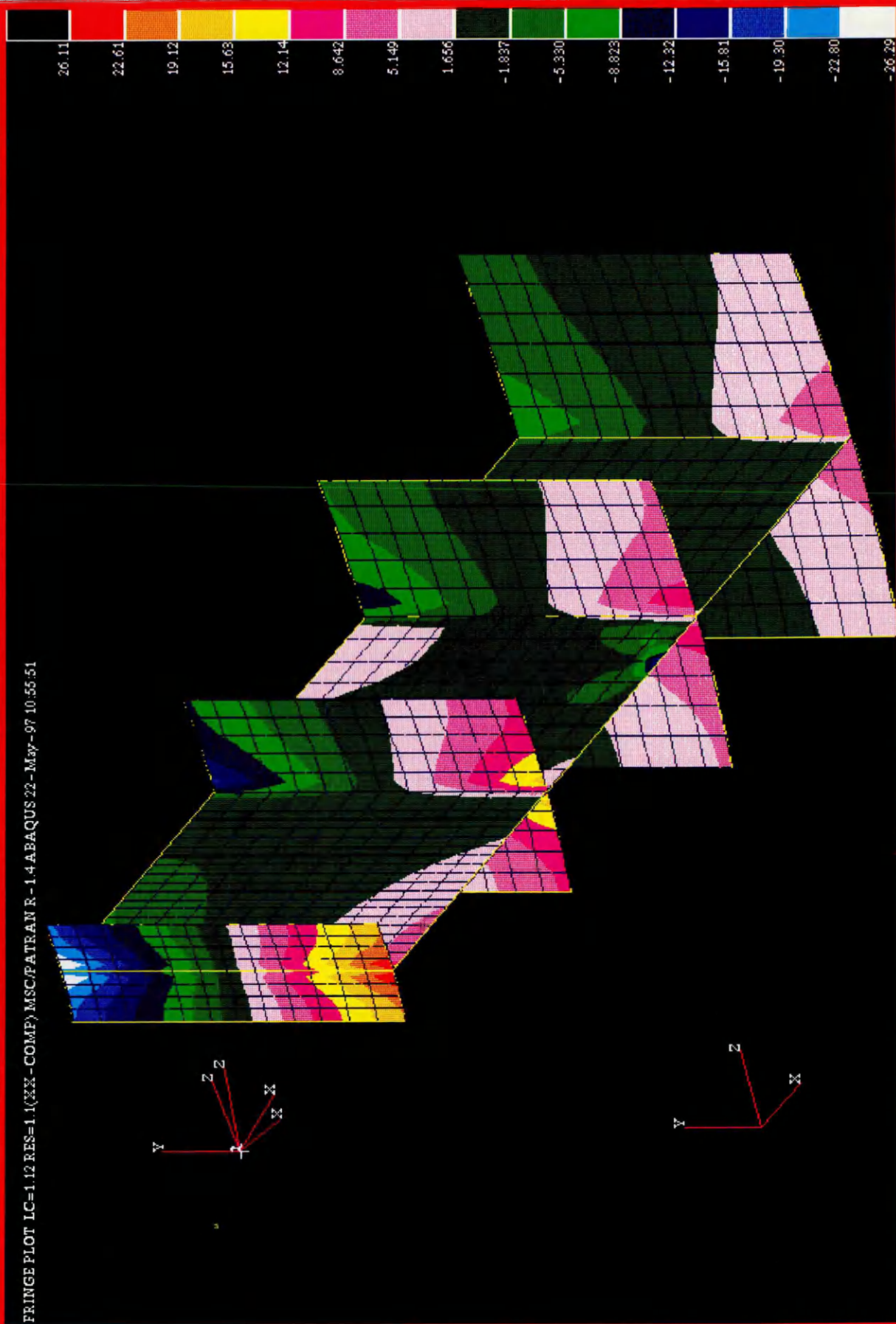


Figure 4.20 Distribution of radial stress in a webbed bearing plate with a 100 mm hole in the steel support plate.

There are many similarities between the stress distribution in the webbed bearing plates and in the solid bearing plates. The stress levels at large diameters, (beyond the support plate hole diameter) are low in both the solid and webbed models. There is a stress concentration around the restraint for both solid and webbed bearing plate models, the stress levels around the restraint are generally larger in the webbed bearing plate models for the same load, probably due to the lower thickness of material in the webbed bearing plate. If the thickness of webs in the bearing plate around the restraint is reduced, stress levels around the restraint are increased.

#### 4.6.4 Weldgrip bearing plate with 120 mm hole in steel support plate

Figure 4.21 shows a displaced plot with the distribution of circumferential (ZZ) stress in the Weldgrip bearing plate with a 120 mm hole in the steel support plate. The Weldgrip bearing plate was modelled as a circular bearing plate using axisymmetric elements, in the same way as all the other solid designs of bearing plates. The material data used for this analysis was obtained from tensile testing of specimens of the Weldgrip material, the stress / strain behaviour of this material is given in figure 6.2, the yield stress of this material is approximately  $25 \text{ MN/m}^2$ . The load applied to this bearing plate to produce this plot was 2 kN.

The circumferential stress on the upper surface of the bearing plate within the support plate hole diameter is compressive as shown in figure 4.21. The circumferential stress on the lower surface of the bearing plate is tensile, with the exception of the region directly around the restraint which has localised compressive circumferential stress. The tensile circumferential stress on the lower surface has a maximum value of  $13.2 \text{ MN/m}^2$

FRINGE PLOT IC=1,35 RES=1,1(ZZ-COMP) MSC/PATRAN R - 1.4 ABAQUS 2.2 - May - 97 10:40:49

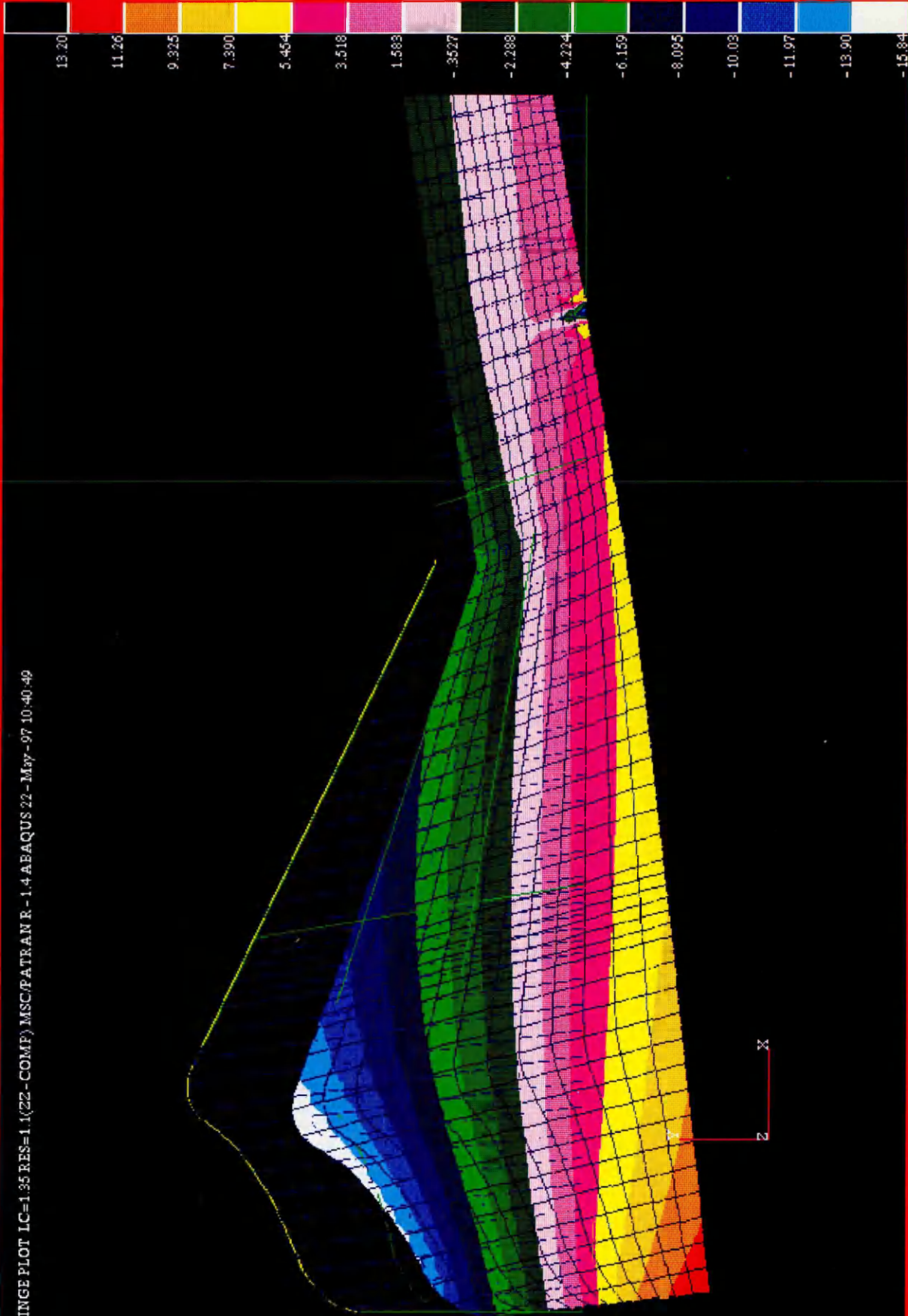


Figure 4.21 Distribution of circumferential stress in Weldgrip bearing plate with a 120 mm hole in the steel support plate.

at the centre of the bearing plate. The stress levels in regions of the bearing plate with diameters greater than the support plate hole diameter are low.

The Weldgrip bearing plate tested in the laboratory with a 120 mm hole in the steel support plate carried a peak load of 11.6 kN. Failure occurred by the formation of radial cracks on the lower surface of the bearing plate extending from the centre of the bearing plate to the ring supported by the steel support plate. Inspection of the stress levels in figure 4.21 shows that the maximum compressive stress on the upper surface is greater than the maximum tensile stress on the lower surface. However the ratio of compressive yield strength / tensile yield strength is around 1.3 or 1.4 for most polymers. Hence the tensile stress on the lower surface is closer to yield than the compressive stress on the upper surface.

#### 4.6.5 Further stress / strain distribution observations

There is a tendency for the outer regions of the bearing plate FE models beyond the support diameter to ‘lift off’ the supporting surface, deflecting in the positive y direction as can be seen in figures 4.17 and 4.21. The edges ‘lift off’ more with the thin bearing plates than with the thicker bearing plates. The edges of the Weldgrip and Weidmann bearing plates in laboratory tests were also observed to ‘lift off’. Table 4.6 shows the magnitude of deflection in the positive y direction at the specified diameters for the Weldgrip bearing plate with small and large external diameters of bearing plate.

Bearing plate external diameter	Deflection at diameter :-	
	98 mm	147 mm
98 mm	1.479 mm	n / a
147 mm	0.2993 mm	0.7642 mm

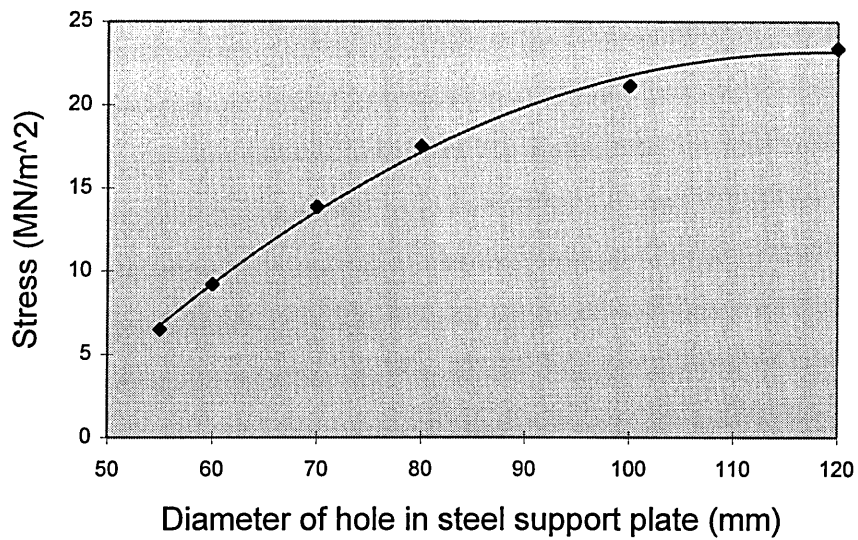
**Table 4.6** Magnitude of deflection in positive y direction of Weldgrip bearing plate FE models

Table 4.7 shows the tensile circumferential stress on the lower surface of the bearing plate at the centre for different diameters of central hole in the bearing plate. The smaller the diameter of the central hole in the bearing plate, the larger the tensile circumferential stress on the lower surface of the bearing plate.

Diameter of hole in centre of bearing plate	30 mm	34 mm
1 mm deflection (Load)	25.57 MN/m <sup>2</sup> (2934 N)	24.49 MN/m <sup>2</sup> (2864 N)
Load of 2 kN	21.20 MN/m <sup>2</sup>	21.15 MN/m <sup>2</sup>

**Table 4.7** Tensile circumferential stress on lower surface of bearing plate with different diameters of central hole.

Figure 4.22 shows the variation of the maximum tensile circumferential stress on the lower surface of the bearing plate with different diameters of hole in the steel support plate, when a standard load of 2 kN is applied. These results are for a flat plate of depth 10 mm made from polypropylene. Figure 4.22 shows that the larger the hole in the steel support plate, the larger the tensile circumferential stress on the lower surface of the bearing plate. In all cases the maximum tensile circumferential stress occurred on the lower surface of the bearing plate at the centre.



**Figure 4.22** Variation of circumferential stress on lower surface of bearing plate with different diameters of hole in steel support plate.

Models of the Weldgrip bearing plate were produced with an external diameter of 147 mm and also with a smaller external diameter of 98 mm as used in section 5.7. Table 4.8 shows that for a constant load, the tensile radial stress underneath the nut was larger for the smaller diameter bearing plate than the larger diameter of bearing plate. Also the tensile circumferential stress on the lower surface of the bearing plate was greater with a smaller diameter of bearing plate.

	98 mm	147 mm
Tensile radial stress underneath nut on upper surface of bearing plate	1.757 MN/m <sup>2</sup>	0.6151 MN/m <sup>2</sup>
Tensile circumferential stress on lower surface of bearing plate.	15.41 MN/m <sup>2</sup>	7.543 MN/m <sup>2</sup>

**Table 4.8** Comparison of radial and circumferential stress in Weldgrip bearing plate with different external diameters of bearing plate.

## CHAPTER 5

### 5. LABORATORY TESTING

#### 5.1 Introduction to laboratory testing

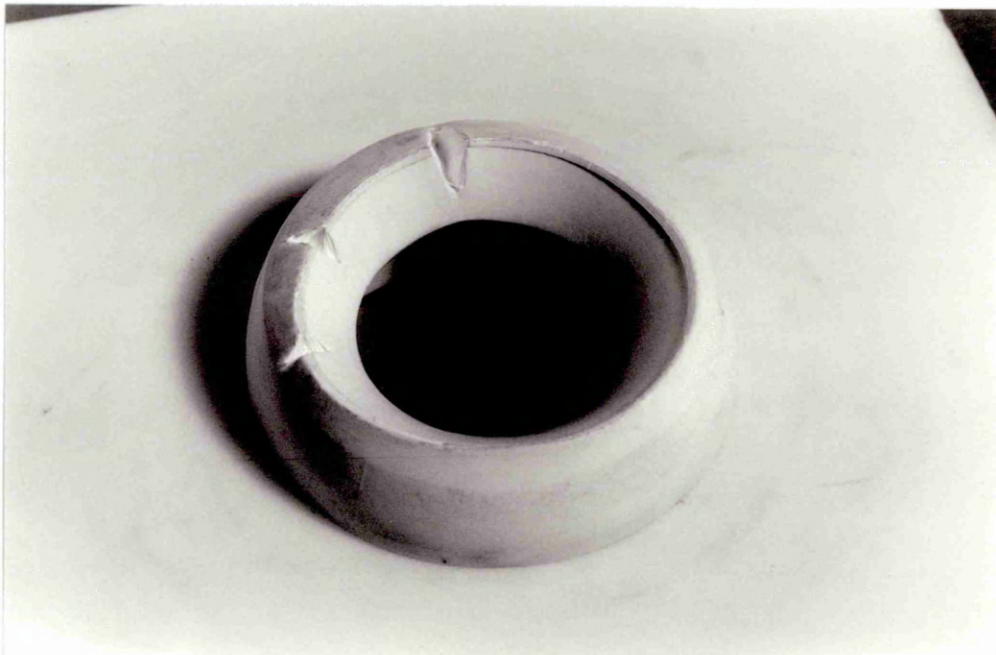
Laboratory tests were carried out on existing designs of bearing plates in order to identify a test on the bearing plates, which as closely as possible simulates the failure mechanism and loading conditions encountered in coal mines. Tests on bearing plates with different diameters of hole in the steel support plate were performed in order to investigate the effect of the different diameter of hole at a higher level of loading than was possible using FEA. Some parameters that could not be investigated using FEA, (e.g. rate of loading, radius on edge of hole in steel support plate and inclined angle of bearing plate) were investigated using laboratory tests. The laboratory tests demonstrated actual failure mechanisms rather than just initial loading.

The laboratory tests were carried out as described in section 3.6 and figure 3.3. To allow valid comparisons to be made from the laboratory testing results, parameters other than the one being investigated were held constant. Therefore unless stated otherwise the rate of loading used was 5 mm/min, the nut used was the larger Weldgrip nut (which had an external diameter of 56 mm), the load was applied perpendicular to the bearing plate, i.e. with an out of alignment angle of zero and the edge of the hole in the steel support plate had a sharp edge of radius less than 0.4 mm. For all bearing plate tests the 'failure load' was taken as the peak load carried. For tests where the nut diameter was greater than the diameter of the hole in the steel support plate, the tests were not continued to push the nut through the support plate hole because this would have been testing the strength of the nut not the bearing plate. The steel support plate had a larger external diameter than the bearing plates.

## **5.2 Diameter of hole in steel support plate**

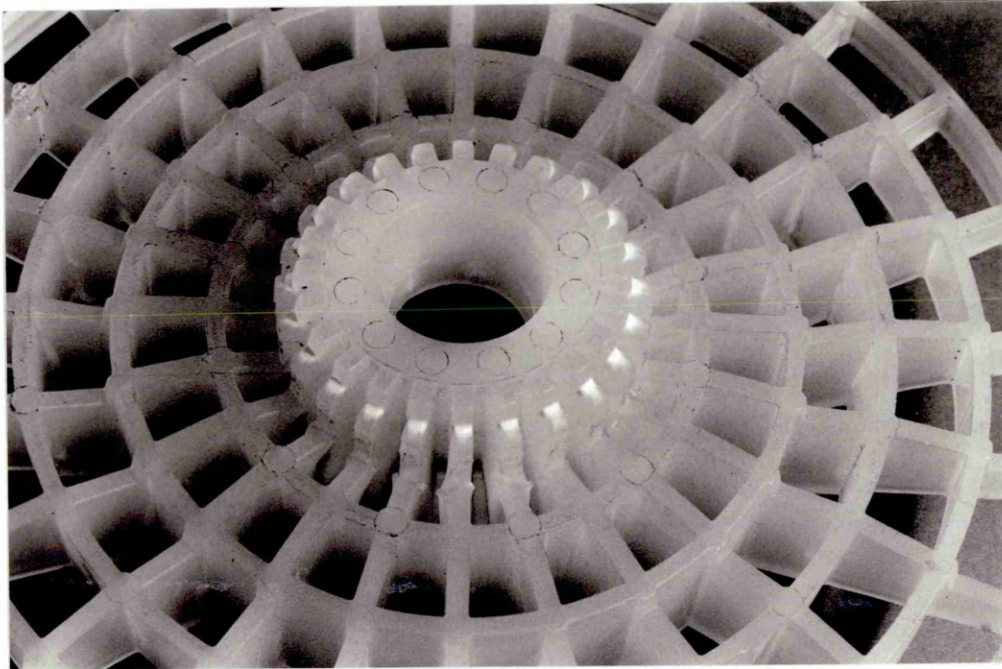
Tests were carried out on the Weldgrip bearing plate with a 55 mm hole in the steel support plate as specified by BS 7861. The peak load carried in these tests was 63 and 64.6 kN. The failure was by shearing which occurred next to the edge of the support plate hole. Cracks can be seen in the sheared material on the lower surface of the bearing plate. This failure mechanism was very similar to the failure mechanism of bearing plates tested with a 60 mm hole.

Figure 5.1 shows the failure mechanism produced when testing the Weldgrip bearing plate with a 60 mm hole in the steel support plate. The view shown is of the central part of the lower surface of the bearing plate. The bearing plate has sheared next to the edge of the hole in the steel support plate. Cracks have formed on the sheared material on the lower surface of the bearing plate. The peak load carried in this test was 49.6 kN.



**Figure 5.1** Failure mechanism of Weldgrip bearing plate when tested with a 60 mm diameter hole in the steel support plate

Figure 5.2 shows the failure mechanism produced when testing a webbed bearing plate design supplied by Weidmann, using a 60 mm hole in the steel support plate. The failure mechanism is again by shearing of the polymer material adjacent to the edge of the hole in the steel support plate. The peak load carried in this test was 57.3 kN. There is no sign of any cracks in the sheared material around the restraint.



**Figure 5.2** Failure mechanism of Weidmann webbed bearing plate when using a 60 mm hole in the steel support plate.

The bearing plate material at a diameter greater than 60 mm did not appear to be affected by the deformation at the centre. No bending or cracks could be seen on the outer regions of either the Weldgrip or Weidmann bearing plates after the removal of the load.

A test was also carried out on the Weldgrip bearing plate with a 70 mm hole in the steel support plate. This bearing plate carried a peak load of 38 kN. A shear failure with some

bending of the outer region was produced, cracks were again produced on the sheared material on the lower surface of the bearing plate.

The Weidmann bearing plate tested with a 70 mm hole in the steel support plate also failed by shearing. No bending or cracks were produced on the outer region of the bearing plate. The failure mechanism of the Weidmann bearing plate with a 70 mm hole in the steel support plate is very similar to the failure mechanism with a 60 mm hole shown in figure 5.2.

Tests were also performed on the Weldgrip bearing plate using an 80 mm hole in the steel support plate. During the test the bearing plate was seen to bend downwards at the centre as the load was applied. The corners of the bearing plate were seen to lift off. After the peak load was reached a crack was heard to form on the lower surface of the bearing plate. The load carried by the bearing plate dropped suddenly. However on removal of the load the bearing plate returned to almost its original shape. A circular indent can be seen on the lower surface of the bearing plate, caused by the edge of the steel support plate. One large crack and some small cracks can be seen on close inspection of the lower surface of the bearing plate, extending radially outwards from the centre of the bearing plate (edge of the hole).

The Weidmann bearing plate tested with an 80 mm hole in the steel support plate failed by the formation of cracks. The cracks spread from the lower surface of the bearing plate, next to the edge of the support plate hole, up through the circumferential webs at an angle of approximately  $45^\circ$ . There were no cracks present in webs at a diameter of more than 80 mm. At the centre of the bearing plate in the thick material there was a

vertical crack extending upwards from the lower surface of the bearing plate. This crack extended through one of the injection points.

The failure mechanism produced when testing the Weldgrip bearing plate with a 100 and 120 mm hole in the steel support plate was similar to that produced with an 80 mm hole in the steel support plate. The bearing plates were seen to bend and the peak load was reached. Cracks were produced on the lower surface of the bearing plate extending in the radial direction from the centre of the bearing plate. On removal of the load the Weldgrip bearing plates tested with a 100 and 120 mm hole returned to almost their original shape. The radial cracks produced when testing with a 120 mm hole in the steel support plate were larger than the cracks produced when testing with a 100 mm hole.

The Weidmann webbed bearing plates tested with a 100, 120 and 140 mm hole in the steel support plate also failed by the formation of cracks. There were no cracks at a diameter of more than the support plate hole diameter. The cracks spread upwards from the lower surface of the bearing plate at an angle of approximately 45°. Again these cracks did not break through on the upper surface of the bearing plate. At the centre of the bearing plate in the thick material there was a vertical crack extending upwards from the lower surface of the bearing plate. In all cases the vertical crack at the centre of the Weidmann bearing plate extended through one of the injection points that the bearing plate had been moulded from. Figure 5.3 shows the cracks formed in a failed Weidmann bearing plate tested with a 120 mm hole in the steel support plate.

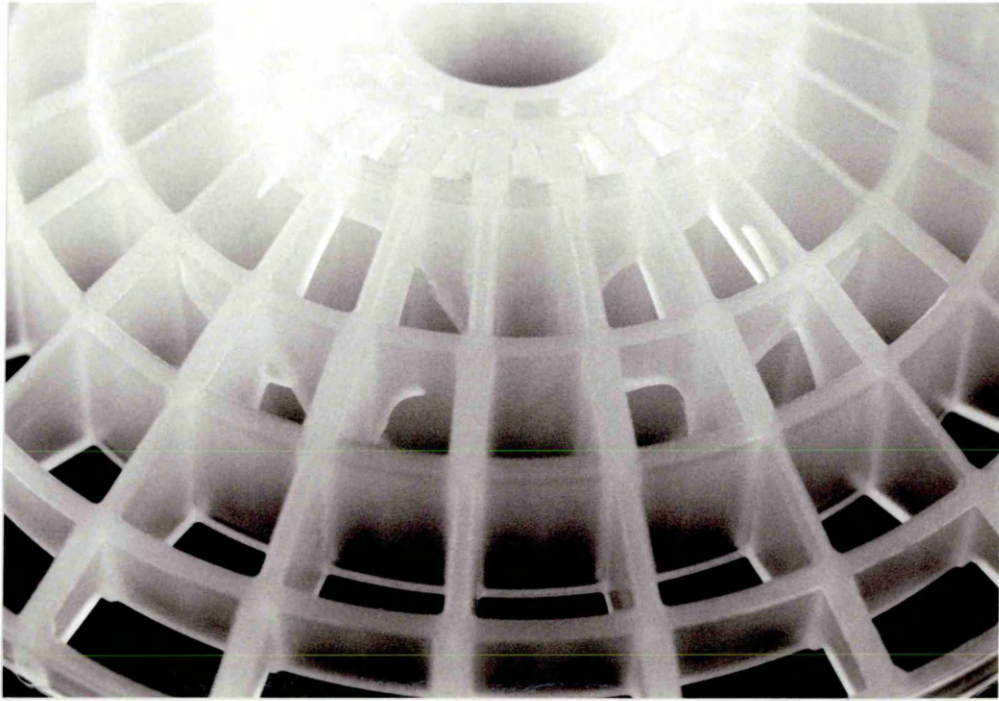


**Figure 5.3** Cracks in a failed Weidmann bearing plate tested with a 120 mm hole in the steel support plate

The load carried by the bearing plates with different diameters of hole in the steel support plate varied enormously. Figure 5.4 shows the peak load carried by the Weldgrip and Weidmann bearing plates and a green circular plate supplied by AMS Ltd (figures 5.9, 5.10), with different diameters of hole in the steel support plate. These results were all obtained using the Weldgrip nut and a rate of loading of 5 mm/min.

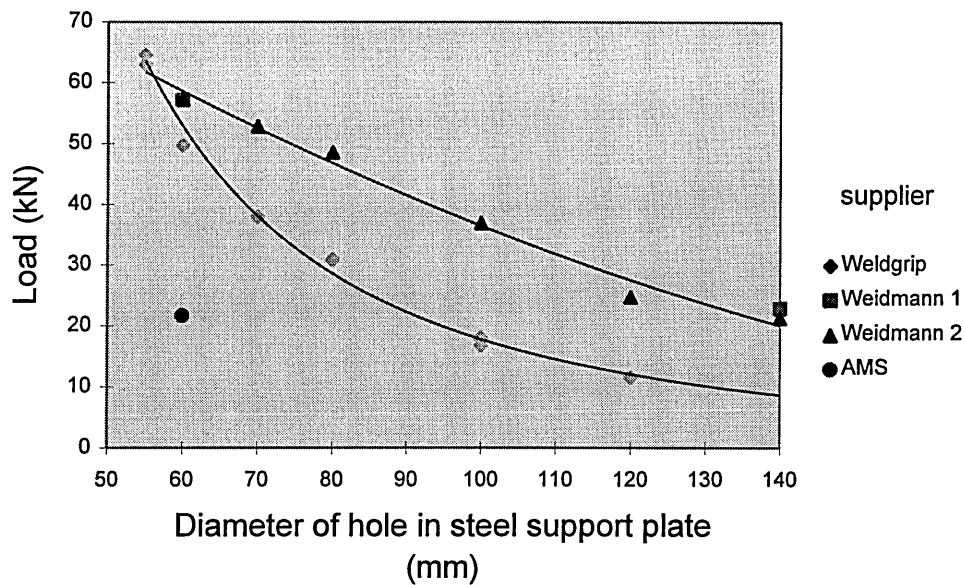


**Figure 5.4** Peak load carried in laboratory tests on Weldgrip, Weidmann and AMS bearing plates using different diameters of hole in the steel support plate

Figure 5.4 shows that bearing plates carry much more load when tested with small holes in the steel support plate than large holes. The shear type failure corresponds to a small hole in the steel support plate. The bending failure occurs with a large hole in the steel support plate. The transition from bending to shear failure occurs between hole diameters of 70 and 80 mm.

Notice that the curves for the different designs of bearing plate are not parallel to each other. With a 60 mm hole in the steel support plate the Weidmann bearing plate carried 7.7 kN more load than the Weldgrip bearing plate. However with a 120 mm hole in the steel support plate the Weidmann bearing plate carries 13.2 kN more load than the Weldgrip bearing plate.

Two versions of the Weidmann webbed bearing plate were tested. The only difference between the two designs being the central region underneath the nut. Weidmann 2 has

extra material in the central region compared to Weidmann 1. It can be seen in figure 5.4 that there is hardly any difference in the load carried between the two Weidmann designs. This is probably because with both a 140 mm and 60 mm hole in the steel support plate, the failure did not take place in the area underneath the nut. As well as modifying the central region of the bearing plate, Weidmann have also produced a new design of nut to go with the two bearing plate designs. However in this thesis the Weldgrip nut has been used to test these bearing plates, because this is a nut that is likely to be used with the bearing plates down the coal mines, and a standard nut allows comparison between the performance of bearing plates.

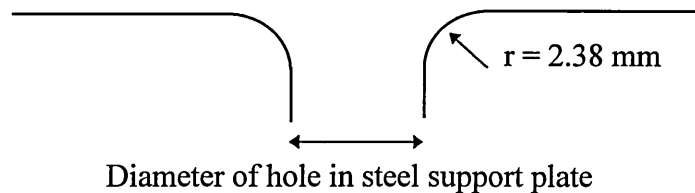
As can be seen in figure 5.4, testing the AMS bearing plates with a 60 mm hole in the steel support plate, produced a much lower peak load than the Weidmann or Weldgrip bearing plates.

Figure 5.4 shows that repetitions of results of the Weldgrip bearing plate produced very little scatter. For the Weldgrip bearing plate with a 100 mm hole in the steel support plate, the standard deviation is only 0.7 kN, with a mean value of 17.6 kN. Unfortunately, due to the limited availability of samples, for some conditions only one test was performed.

Tests on the Weldgrip and Weidmann bearing plates have shown that the failure mechanism with a small hole in the steel support plate is by shearing; and the failure mechanism with a large hole in the steel support plate is by bending with crack formation. Tests have also shown that a higher load is carried with a small hole in the steel support plate than a large hole.

### **5.3 Radius on edge of hole in steel support plate**

The edge of the hole in the steel support plate for all the results presented above has a sharp edge with a radius of less than 0.4 mm. A radius of 2.38 mm was machined onto a steel plate with a 60 mm diameter hole. Table 5.1 shows the load carried when testing the Weldgrip bearing plate with a sharp edge on the steel support plate and with a rounded edge. BS 7861 on rockbolting does not specify a radius on the edge of the hole in the steel support plate.



**Figure 5.5** Sketch showing steel support plate with radius on edge of hole

Sharp edge to hole	2.38 mm radius on edge of hole
49.6 kN	50.4 kN

**Table 5.1** Load carried in laboratory tests on Weldgrip bearing plate with 60 mm hole in the steel support plate

The difference in load capacity is within the variation which would be expected when testing nominally identical plates. The failure mechanism produced with the steel support plate with the 2.38 mm radius edge was practically the same as the failure mechanism produced with the steel plate with a sharp edge (figure 5.1). The only difference was that on very close inspection a radius can be seen on the sheared material on the bearing plate tested with a 2.38 mm radius on the edge of the steel support plate.

### **5.4 Rate of loading**

Table 5.2 shows the load carried by the Weldgrip bearing plate when tested with a 100 mm diameter hole in the steel support plate using the Weldgrip nut at different rates of

loading. 5 mm/min is the standard rate of loading used in all the other tests to allow valid comparisons. The rate of loading is not specified in BS 7861.

Rate of loading (mm/min)			
	5 mm/min	10 mm/min	40 mm/min
	18.1 kN	17.1 kN	17.9 kN
	17.9 kN	17.8 kN	15.4 kN
	16.8 kN		
mean	17.6 kN	17.45 kN	16.65 kN

**Table 5.2** Peak load carried by Weldgrip bearing plate at different rates of loading

The results in table 5.2 do not suggest any significant variation in load carried with different rates of loading. However a different failure mechanism was produced with the different rates of loading. At the slowest rate used of 5 mm/min, the bearing plate underwent a large amount of bending and formed several small cracks (2 - 5 mm) on the lower surface of the bearing plate, at the edge of the hole. With the 10 mm/min rate of loading the bearing plate formed a crack spreading from the centre of the bearing plate to the ring supported by the edge of the hole in the steel support plate. With the 40 mm/min rate of loading the Weldgrip bearing plate formed two cracks. One crack spread from the centre of the bearing plate to the ring supported by the steel support plate, and the other crack spread from the centre of to the outer edge of the bearing plate. Therefore the general trend appears to be that as the rate of loading increases, the failure mechanism of the bearing plate becomes more sudden and more obviously catastrophic.

### **5.5 Different nut diameters**

Weldgrip bearing plates were tested with 100 mm and 120 mm holes in the steel support plate using the smaller Mai nut which has an external diameter of 45 mm instead of the Weldgrip nut, which was the standard nut with an external diameter of 56 mm used for

the other tests. The smaller Mai nut was able to force its way into the centre of the bearing plate. Figure 5.6 shows a plot of the load carried against the crosshead movement for a Weldgrip bearing plate tested with a standard Weldgrip nut, a small Mai nut and a very small AMS end fitting (external diameter 40 mm), when using a 100 mm hole in the steel support plate.

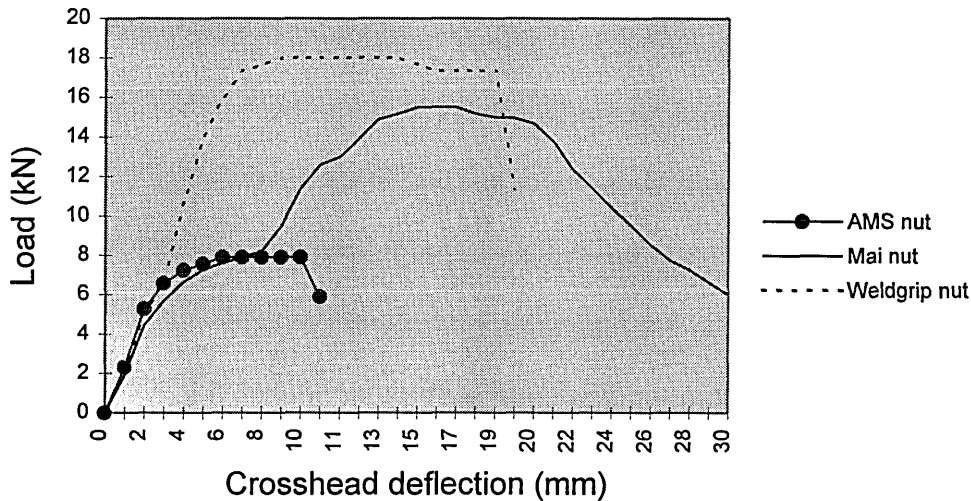


**Figure 5.6** Plot of load carried with crosshead deflection for Weldgrip plate and Mai nut with a 100 mm hole in the steel support plate.

The initial levelling off of the load carried by the Mai nut (shown in figure 5.6) corresponds with the small diameter of nut, initially in contact with the bearing plate, being forced into the centre of the bearing plate. The second increase in the load carried corresponds to the wider part of the nut being forced into the bearing plate centre. After the widest part of the nut had been forced into the centre of the bearing plate the load carried reduced to less than half the peak load. This drop in load carried, corresponds with the formation of two small cracks on the lower surface of the bearing plate. Some bending of the bearing plate was visible after the removal of load for this bearing plate.

When the Weldgrip bearing plate was tested with a 120 mm hole in the steel support plate and the Mai nut, the nut was again forced into the centre of the bearing plate. Failure occurred by the production of cracks. The cracks produced by the Mai nut with a 120 mm hole in the steel support plate were much larger than the cracks produced with the Mai nut and a 100 mm hole in the steel support plate. Figure 5.7 shows the cracks in a Weldgrip bearing plate tested with a 120 mm hole in the steel support plate and a Mai nut. The view shown is of the upper surface of the bearing plate. A crack extended all the way from the centre of the bearing plate to the outer edge of the bearing plate. Another crack extended from the centre to the ring supported by the steel support plate, this crack also spread circumferentially around the bearing plate, above the edge of the hole in the steel support plate. The cracks have broken through onto the upper surface and can be seen on the lower and upper surfaces. For this bearing plate hardly any bending was visible after the removal of load.

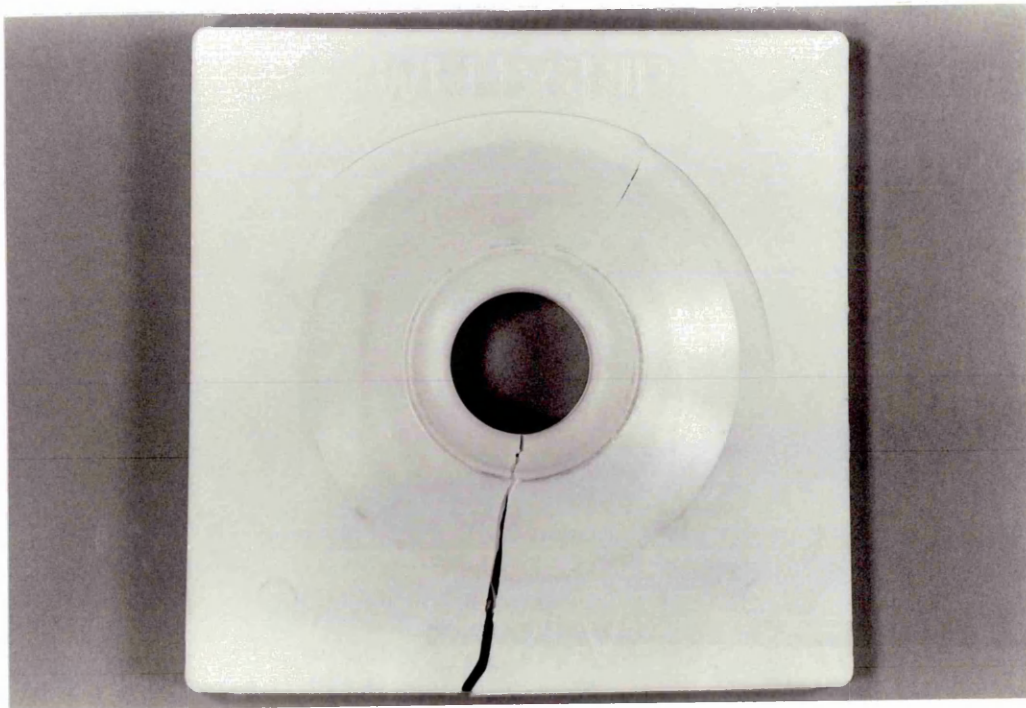


**Figure 5.7** Failed Weldgrip bearing plate tested with 120 mm hole in the steel support plate and Mai nut.

When the Weldgrip bearing plate was tested with the AMS end fitting, the end fitting was not forced into the centre of the Weldgrip bearing plate. Failure occurred by the production of a single radial crack which extended rapidly from the centre of the bearing plate to the outer edge of the bearing plate but did not completely 'break through' on the upper surface.

Table 5.3 compares the load carried by the Weldgrip bearing plate with three different end fittings. The external diameter of the end fittings is given in table 5.3, although it is recognised that the shape of the nut varies as well as the external diameter. The diameter of the central hole in the Weldgrip bearing plate is 31 mm.

Diameter of hole in steel support plate	100 mm	120 mm
Weldgrip nut (56 mm diameter)	18.1 kN, 17.9 kN, 16.8 kN (mean = 17.6 kN)	11.6 kN
Mai nut (45 mm diameter)	(load at which nut forced into centre 8.2 kN) 15.5 kN	(load at which nut forced into centre 6.4 kN) 10.8 kN
AMS end fitting (40 mm diameter)	7.9 kN	

**Table 5.3** Comparison of load carried by Weldgrip bearing plate with Mai, AMS and Weldgrip end fittings and two diameters of hole in steel support plate

### **5.6 Different diameter of hole in centre of bearing plate**

A Weldgrip bearing plate with a smaller diameter of central hole in the bearing plate of 25 mm instead of 31 mm was tested, with a 100 mm hole in the steel support plate and using the Mai nut. Table 5.4 gives a comparison of the load carried by the Weldgrip bearing plate with the two different diameters of hole in the centre of the bearing plate.

Diameter of central hole in bearing plate	25 mm	31 mm
Peak load carried	9.4 kN	15.5 kN

**Table 5.4** Comparison of the load carried by the Weldgrip bearing plate with different diameters of central hole in the bearing plate, using a 100 mm hole in the steel support plate and using the Mai nut

The different diameters of central hole in the bearing plate caused different failure mechanisms of the bearing plate. With the larger standard diameter in the centre of the Weldgrip bearing plate the Mai nut was able to force its way into the centre of the bearing plate. The load carried increased as the wider part of the nut was forced into the centre of the bearing plate. The bearing plate failed by the formation of small cracks extending from the centre of the bearing plates, by approximately 18 mm in the radial direction.

With the smaller diameter of hole in the centre of the Weldgrip bearing plate, the Mai nut did not force its way into the centre of the bearing plate. This bearing plate failed catastrophically by forming large cracks which broke the bearing plate into two pieces very suddenly as shown in figure 5.8. The peak load carried by this bearing plate (immediately before failure) was 9.4 kN, which is higher than the load at which the Mai nut was forced into the centre of the bearing plate tested with the Mai nut and the larger standard diameter of hole in the centre of the bearing plate (table 5.3). However 9.4 kN is less than the peak load carried by the Weldgrip bearing plate with a larger standard diameter of hole in the centre of the bearing plate (see table 5.3 and 5.4).

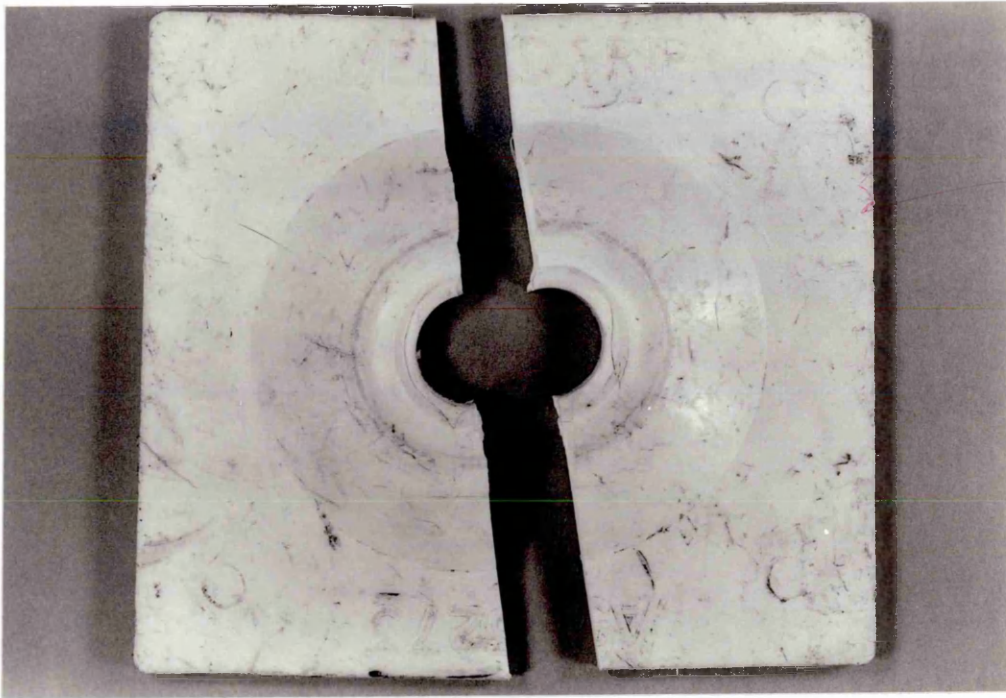


**Figure 5.8** Failed Weldgrip bearing plate with a smaller diameter of hole in the centre of the bearing plate tested with a 100 mm hole in the steel support plate.

### **5.7 Different external diameter and shapes of bearing plates**

The effect of a circular external shape instead of a square external shape and the effect of a smaller external diameter of bearing plate was investigated. Table 5.5 gives a comparison of the load carried by the Weldgrip plate, when tested with a circular shape and smaller external diameter. The failure mechanism between the circular bearing plate of diameter 147 mm and the original square bearing plate appeared identical, however the failure mechanism of the small circular bearing plate was slightly different as discussed in section 7.4.5.

Diameter of hole in steel support plate	Square shape length of side 149 mm (original form)	Circular shape (diameter 147 mm)	Circular shape (diameter 98 mm)
60 mm	49.6 kN	47.8 kN	48.3 kN
70 mm	38 kN	39 kN	37.2 kN
80 mm	30.9 kN	29.2 kN	26.1 kN

**Table 5.5** Comparison of peak load carried by Weldgrip bearing plate with different external diameter and plan shape of bearing plate

### **5.8 Load applied to nut via threadform**

In the majority of tests load was applied directly to the nut which transferred load onto the bearing plate. Table 5.6 gives a comparison of the load carried by the Weldgrip bearing plate when the load was applied to the nut directly or applied to the bolt from above and then transferred to the nut via the threadform.

load applied to nut	load applied to bolt
17.9 kN, 18.1 kN, 16.8 kN	17.7 kN

**Table 5.6** Load carried by Weldgrip bearing plate with 100 mm hole in the steel support plate when load applied to nut directly and via threadform

The failure mechanism was the same when the load was applied to the nut via the bolt and directly to the nut. The load carried by the Weldgrip bearing plate with the two different ways of applying load was practically the same.

### **5.9 Bearing plate at an inclined angle of 10°**

Table 5.7 gives a comparison of the load carried by the Weldgrip bearing plate using the Weldgrip nut with a 100 mm diameter of hole in the steel support plate, with the support plate flat and at an inclined angle of 10°. The steel support plate at an inclined angle had an elliptical shaped hole with a maximum dimension of 102 mm and a minimum dimension of 100 mm. It can be seen that the load carried with the bearing plate at an inclined angle of 10° is less than the load carried with the bearing plate flat. The failure mechanism of the bearing plate tested at an inclined angle was by bending with small cracks forming and spreading from the centre of the bearing plate to the ellipse supported by the steel support plate. The bending observed was not completely symmetrical. However apart from the non symmetrical nature of the bending, the failure mechanism from tests at an inclined angle and flat are almost identical.

Flat	Inclined angle of 10°
17.9 kN, 18.1 kN, 16.8 kN mean - 17.6 kN	15.5 kN, 16.9 kN mean - 16.2 kN

**Table 5.7** Load carried by Weldgrip bearing plate with 100 mm diameter of hole in steel support plate, supported flat and at an inclined angle of 10°

### **5.10 AMS green circular plate**

Tests were also carried out on a circular green bearing plate, supplied by AMS Ltd. This bearing plate was tested with the end fitting supplied by AMS Ltd. The AMS end fitting is a hollow cylinder with an external diameter of 40 mm. Tests on the AMS bearing plate were carried out using a 140 mm hole in the steel support plate. The peak load carried in these tests was 11 kN. Comparisons with figure 5.4 show that this load is approximately half that carried by the Weidmann bearing plate, although it is not really a fair comparison because different end fittings have been used. The end fitting was seen to be forced into the centre of the bearing plate. On the removal of load the end fitting was left in the centre of the bearing plate. A crack was seen to initiate from the boss on the lower surface of the bearing plate during the first week after testing. Figure 5.9 shows a crack in the AMS bearing plate two months after the initial testing. The view shown is of a portion of the lower surface of the bearing plate. The AMS end fitting can be seen in the top left hand corner of the photograph. Localised deformation around the end fitting that occurred at the time of testing can be seen. The crack initiated on the lower surface of the bearing plate, at the centre and spread towards the outer edge; the cracks progress was slowed down to some extent by the boss on the outer edge.

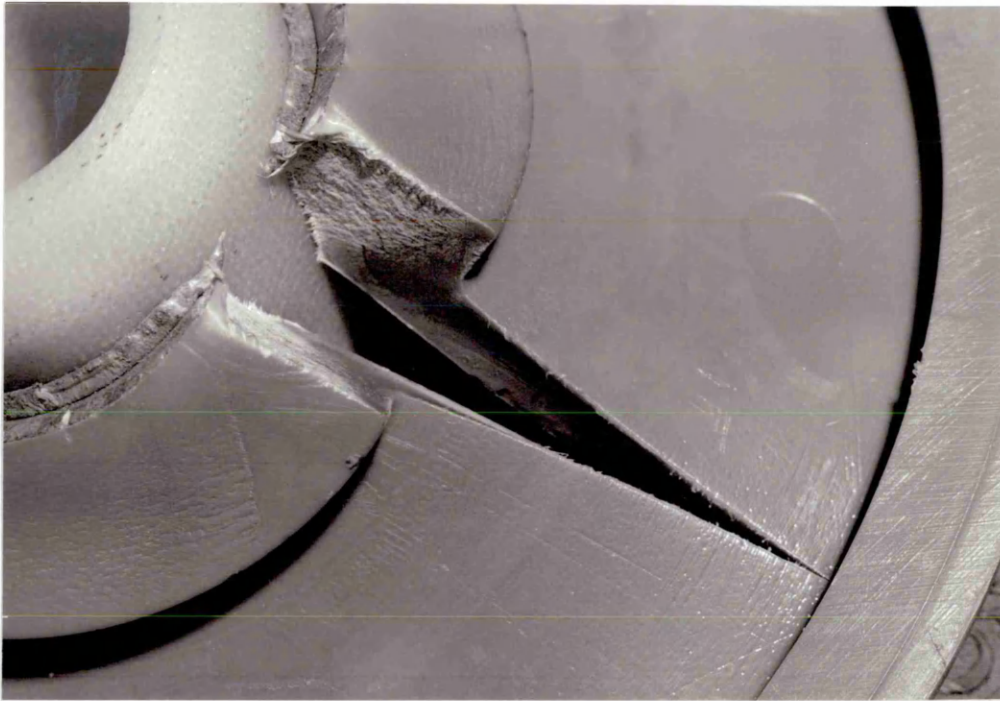


**Figure 5.9** AMS bearing plate 2 months after testing

The crack eventually spread to the outer edge of the bearing plate and another crack initiated on the opposite side of the bearing plate. Figure 5.10 shows the same bearing plate as figure 5.9, after complete failure. This bearing plate finally broke into two halves approximately 18 months after the initial testing. Bearing plates may be installed down the mine for a period of up to 2 years. Hence in the coal mine there is time for failure to take place by slow crack formation and growth.

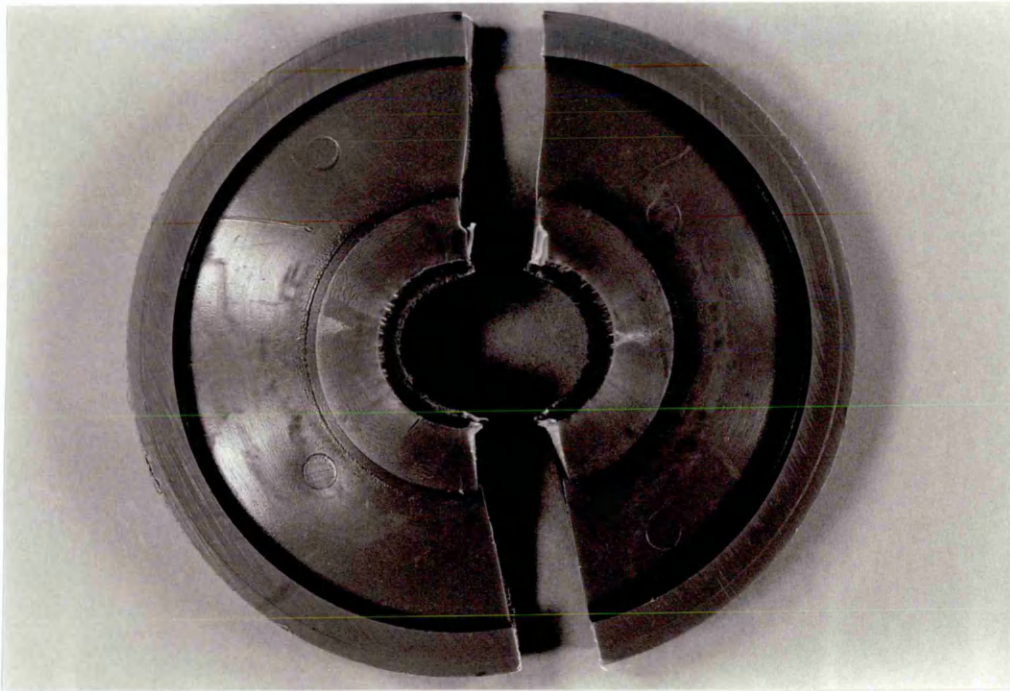


**Figure 5.10** AMS bearing plate after complete failure

For some AMS bearing plates, after the production of cracks, voids were seen in the thick material of the inner and outer bosses. The maximum thickness of the AMS bearing plate (at the inner and outer bosses) is 15 mm. The voids were probably caused by the difficulty of moulding these thick sections.

## **CHAPTER 6**

### **6. MATERIALS**

#### **6.1 Materials for use in a bearing plate**

The Finite Element modelling did not consider all material properties. The calculation of deflection by FEA depends upon geometric factors and the material stiffness (secant modulus). Material was included as a parameter in the FE tests so that the relative significance of the material, compared to other parameters could be obtained. However the FE work did not provide a comprehensive selection of materials, and simply demonstrated that a stiffer material deflected less than a more flexible material.

Watermann (1991) reviews materials for different applications in deep mining. The problem of flame retardancy and long term loading when designing with polymeric materials for use in underground applications is identified. The reason that GRP rockbolts are used in coal mining is because they do not create sparks when cut; in civil engineering applications they are used for their corrosion resistance. Mietz (1997) investigated the possibility of using stainless steels for ground anchors to resist corrosion. However for mining applications rockbolts and components must be non metallic to avoid the danger of sparks.

#### **6.2 Material selection criteria**

Table 6.1 shows some material selection criteria for a material for use in a bearing plate. The first criteria is that the material should not create sparks when cut by the steel coal cutter and therefore the material must be non metallic. Two sets of criteria are proposed, one for a small hole in the steel support plate and one for a large hole in the steel support plate. As shown in figures 5.1 and 5.2 a small hole in the steel support plate

does not realistically simulate the behaviour in the coal mines. Hence the criteria for a large hole in the steel support plate or for use in the coal mines will be concentrated upon here.

<u>Small hole</u> (55 mm - 70 mm) (British Standard laboratory test)	<u>Large hole</u> (80 mm - 140 mm) (Coal mine behaviour)
Non metallic High shear strength / High tensile strength Reasonably high Young's modulus Reasonably high ductility	Non metallic High Young's modulus High ductility High tensile strength

**Table 6.1** Material selection criteria for small and large holes in the steel support plate

For a small hole in the steel support plate as in the BS 7861 test, material properties are required to resist failure by shearing, hence the need for a high shear strength. A high Young's modulus and high ductility is also required but these criteria are not as important as the shear strength.

For a large hole in the steel support plate or for use in the coal mine, a high Young's or secant modulus is required so that the bearing plate does not deflect and bend too easily, under only a small amount of load, in a similar manner to the polyethylene AMS bearing plate (figures 5.9, 5.10). A high ductility is required so that the bearing plate does not fail by the production of cracks at low strain levels in a similar manner to the glassfibre Mai bearing plate (figure 2.4). A relatively high tensile strength is required to resist the formation of cracks on the lower surface of the bearing plate in a similar manner to the Weldgrip bearing plate (figure 5.7, 2.3).

In addition to these main criteria there are a number of other material selection considerations, as listed below.

- Retention of mechanical properties over 2 year period
- Retention of mechanical properties at 40 °C
- Flame retardant properties
- Anti-static properties
- Suitability for manufacturing processes
- Cost

The bearing plates are installed in the mine for a maximum of 2 years, hence the performance of material over a 2 year period needs to be considered. The temperature in the coal mine is often elevated above standard room temperature up to a maximum of about 40°C, hence the performance of materials at elevated temperatures needs to be considered. For reasons of safety and the avoidance of fire, flame retardant and anti sparking properties are required for any material to be used down a coal mine. The suitability of different materials for different manufacturing methods also needs to be considered. The cost of the material is also an issue.

### **6.3 Material selection charts**

Figure 6.1 shows a material selection chart produced by the Cambridge Material Selector (CMS) software showing Young's modulus and ductility's of different types of polymers. A bearing plate material needs to have a high Young's modulus and a high ductility. Figure 6.1 only shows polymeric materials; metallic materials were ruled out because of problems of spark formation. Wood is not an ideal choice because of the unidirectional properties and lower properties perpendicular to the grain. Ceramic materials have high values of Young's modulus but tend to have low ductilities. Composite materials have high values of Young's modulus but the ductility is low compared to other polymers. Elastomers have high ductility's but relatively low values of Young's modulus. Thermosetting materials appear to have relatively low ductility's and most foams have either low ductility's or low Young's modulus. Hence figure 6.1



suggests that thermoplastic materials may be a sensible choice. A list of abbreviations and full names of the polymers is given in Appendix 3 page XLI.

Figure A3.2 shows the same material selection chart of ductility and Young's modulus as figure 6.1 but in much more detail. Figure A3.2 suggests PET, PBT, UPVC, PA, PVC, PC, Nylon, PP, PVDF, CTFE and ACET as possible materials.

A problem when evaluating materials on the basis of cost is that cost fluctuates greatly with time. Ashby (1992) attempts to overcome the problems of inflation and units of currency by defining a relative cost  $C_R$ , as defined in equation 6.1. It is not possible to allow for sudden large variations of the cost of the materials, and it is recognised that the cost is subject to unpredictable change.

$$C_R = \text{cost per kg of material} / \text{cost per kg of mild steel rod} \quad (6.1)$$

The choice of materials was reduced by use of another material selection chart showing Young's modulus and the relative cost per unit volume. Clearly the relative cost per unit volume needs to be as low as possible, and the Young's modulus needs to be as high as possible. A guideline suggested by Ashby (1992) for minimum cost design of plates was used. The guideline was the loci of points for which  $E^{1/3}/C_R\rho = C_M$ . A number of Engineering polymers including PS, PVC and PP were suggested and at a slightly higher cost PC, Epoxy, Polyester and Nylon were suggested. However as shown in figure 6.1, PS has a low ductility.

Figure A3.3 shows another material selection chart showing Young's modulus and flammability. On the chart 'A - very good' refers to materials that are not highly

flammable and 'E - very poor' refers to much more flammable materials. PTFE is shown to have very good anti flammatory properties but is unsuitable because of the high cost per unit volume and low Young's modulus. PTFE is also renowned for its low coefficient of friction which according to Norris (1981) is a good idea for a bearing plate. However this consideration is perhaps quite minor compared to the other parameters. Similarly other materials with good anti flammatory properties have already been ruled out. Figure A3.3 does not greatly narrow down the choice because most of the possible materials are concentrated in the 'C - average' range. Of the possible materials PP PA and PC have better flammability properties than PVC, Epoxies and polyester. Polypropylene has an advantage over polyamide and polycarbonate with better ductility.

Unfortunately the CMS software does not contain details of creep properties and properties at elevated temperatures of 40°C or of anti static properties. As shown in figure A1.30, based on material data from the Campus database, an elevated temperature of 40°C causes a reduction in load carried of up to 60%. Figure A1.31 based on isochronous stress / strain data from the Campus database shows that there is a dramatic drop in load carried over for example one year, to less than a sixth. This shows the importance of considering creep properties when choosing a particular grade of material. Unfortunately by the nature of the tests, creep data takes a long time to acquire and is very expensive to produce. Hence available creep data is often very limited and further work is needed to produce creep data for a material to be used in a bearing plate.

Figure A3.4 shows a material selection chart with tensile strength and maximum service temperature. Clearly the tensile strength of the material is required to be as high as

possible and the maximum service temperature is required to be as high as possible, because the higher the maximum service temperature the less likely that the material will be adversely affected by temperatures of 40°C. Many of the materials shown in figure A3.4 with high tensile strengths have already been ruled out because of low ductilities. Figure A3.4 shows that there is little difference in maximum service temperature for the possible materials. In general thermosetting materials appear to have slightly higher maximum service temperatures than thermoplastic materials, but thermosetting materials are not ideal because of their low ductility. There is some variation in tensile strength with nylons performing well and polypropylene with a lower tensile strength.

The exact choice of material from these charts depends upon the importance placed upon the different parameters. The most suitable material is perhaps one which does not perform too badly on any of the required criteria and performs well on the most important criteria. From the material selection charts it would appear that polypropylene is a suitable material. The ductility of polypropylene and cost per unit volume are very good and the Young's modulus, flammability and maximum service temperature are reasonable. The general term polypropylene covers a wide range of materials which have quite different properties. When choosing a particular grade consideration needs to be given to the criteria raised above.

The grades of materials used for the FE work, polypropylene, polyamide 6 and polycarbonate all have fairly similar values of secant modulus. The fact that the FE work showed the material not to be a highly significant parameter is probably because the three materials chosen have similar values of secant modulus.

#### **6.4 Manufacturing techniques**

The FE design work presented in table 4.5 shows that solid bearing plate designs perform better than webbed bearing plate designs. However the FE analysis did not consider the problems of moulding polymeric components with very thick sections. Injection moulding of thick sections in polymeric components can lead to the formation of voids in the components. Voids were observed in the AMS polyethylene bearing plate, which was injection moulded. A few voids were observed in the Weldgrip bearing plate, which may have been injection moulded or compression moulded. The majority of the Weidmann bearing plate had a thickness of 3 mm or less, the region at the centre of the Weidmann bearing plate had a maximum thickness of 6 mm, no voids were observed in the Weidmann bearing plate. FE models of webbed bearing plates used a thickness of 3 mm as the standard thickness. Hence although the FEA showed that increasing the thickness of webs close to the centre, and having very large thickness of material next to the centre was a good idea, the FE analysis did not consider the problem of moulding these thick components.

Mills (1993) states that for injection moulding it is best to keep the wall thickness constant, preferably between 0.5 and 10 mm. Large thickness of section also increase the amount of time needed for cooling, which increases the cycle time of the component.

Computer packages, for example Moldflow, can be used to investigate whether a mould will fill satisfactorily when using a particular material. Moldflow can also be used to determine the position of weld lines, which occur when molten material injected from

different points meet in the moulding. Weld lines can cause points of weakness in the moulding.

The choice of manufacture method also depends upon the number of components to be produced and the capital cost of the moulding equipment. Approximately 100,000 non metallic bearing plates are used in UK coal mines per year. However the possible market is larger than this because there are civil engineering applications and overseas markets. The Weidmann bearing plate has been widely used for civil engineering applications.

A mould for the production of bearing plates needs to be carefully designed. Correct choices of types of gates is important. The positioning of gates can create weak points in the bearing plate, which may cause cracks to form at specific points as observed in the Weidmann bearing plate.

Ductility, one of the material selection criteria, is not simply a property of the material, but also depends upon the way in which the component is moulded. If there is a large amount of frozen in strain, this increases brittleness and reduces the ductility.

## **6.5 Material data**

### **6.5.1 Material data used for modelling existing designs of bearing plate**

Figure 6.2 shows the variation of stress and strain for the material used in the Weldgrip (solid) and Weidmann (webbed) bearing plates. Figure 6.3 shows the variation of secant modulus with strain for the material used in the Weldgrip and Weidmann bearing plates.

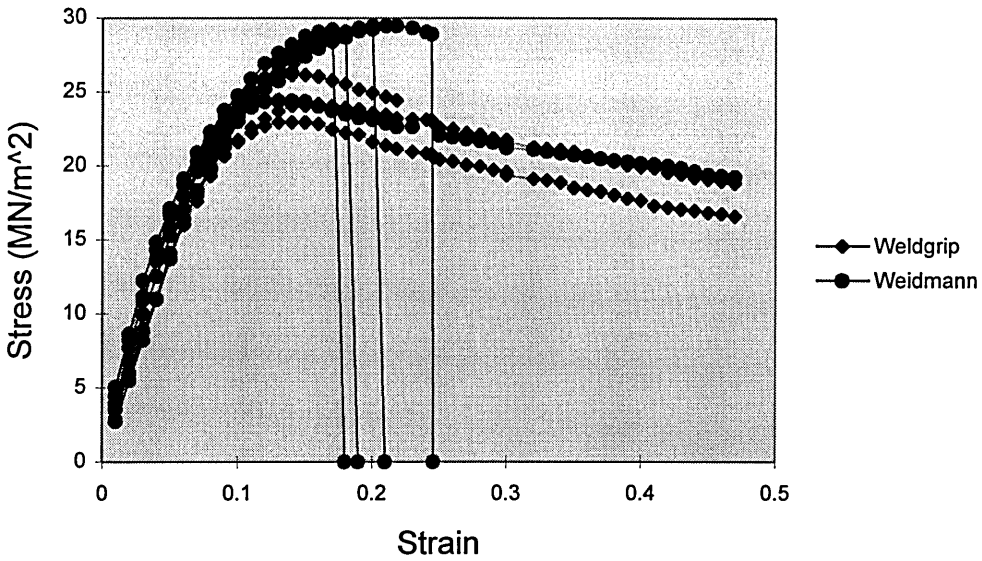


**Figure 6.2** Stress against strain for material used in Weldgrip and Weidmann bearing plates

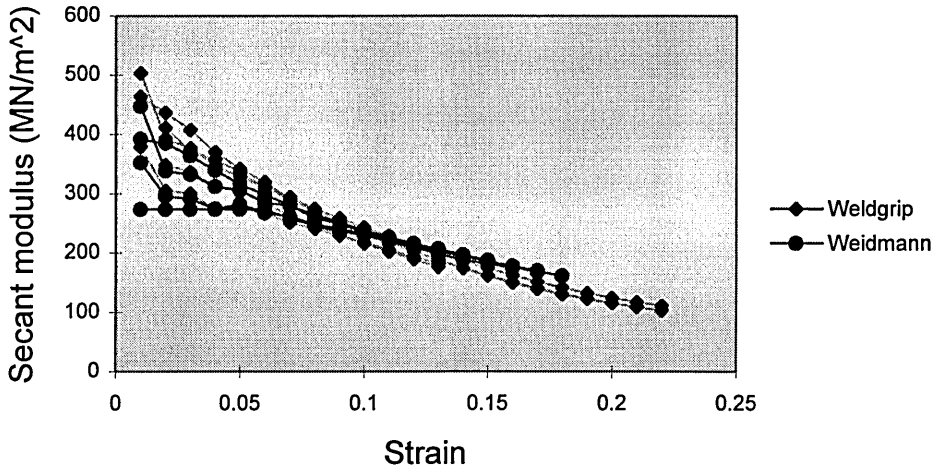


**Figure 6.3** Secant modulus against strain for material used in Weldgrip and Weidmann bearing plates

This data was used to calculate the strain invariants for the uniaxial case. The secant modulus, strain invariants and Poisson's ratio was the required material data to be entered into ABAQUS.

### 6.5.2 Material data obtained from Campus material database

The material data used in the FE models for the Taguchi experiments and the one factor at a time tests, was obtained from the Campus database produced by material manufacturers. Figure 6.4 shows the variation of secant modulus with strain for the grades of polyamide, polycarbonate and polypropylene used in the FE models. Figure 6.5 shows the variation of stress with strain for the same materials as in figure 6.4.

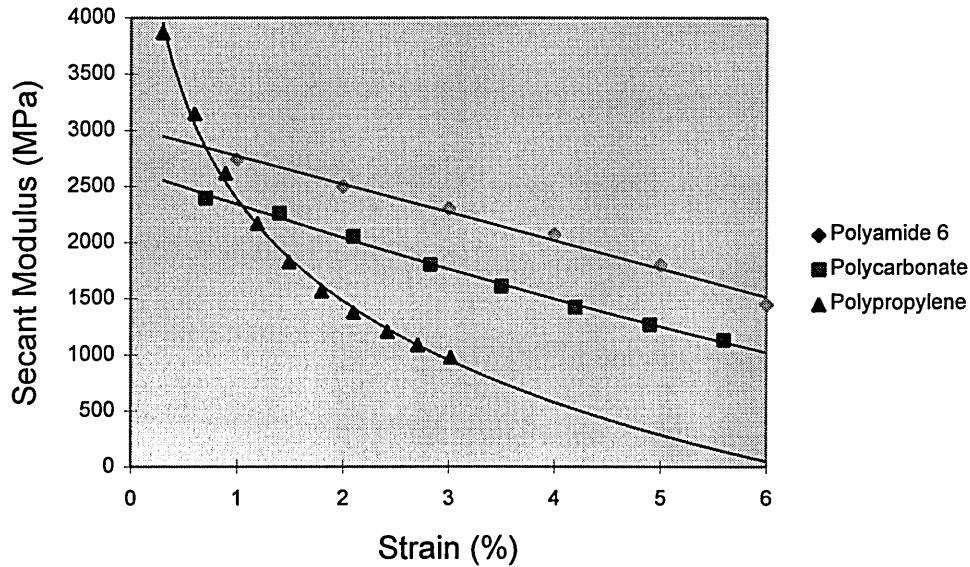


Figure 6.4 Variation of secant modulus against strain

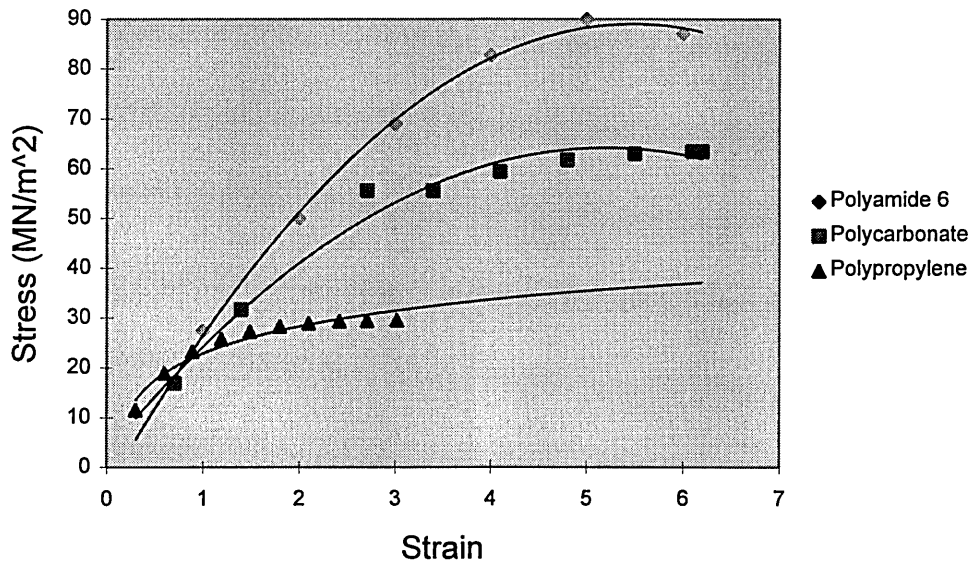


Figure 6.5 Variation of stress against strain

## CHAPTER 7

### 7. DISCUSSION

#### 7.1 Finite Element Results and Method

##### 7.1.1 Comparison of strain gauge and FE results

Strain gauges were attached to existing designs of bearing plate in order to verify that the results from the FEA were reasonably accurate. Figure 4.1 shows circumferential strain in the Weldgrip bearing plate measured by strain gauges and Finite Element Analysis. This strain gauge is consistently measuring strain at a greater magnitude than the Finite Element Analysis. The difference between the strain gauge and Finite Element results is 12 % at 2 kN load. Whilst ideally the strain gauge and Finite Element results would be closer, these results are within the margin of error that may be expected. Figure 4.2 shows vertical strain in a circumferential web of the Weidmann bearing plate, measured by strain gauges and Finite Element Analysis. The difference between the Finite Element and strain gauge results is only 6% at 2 kN load.

##### 7.1.2 Justification of using FEA

Finite Element Analysis (FEA) enabled a large number of different parameters to be compared relatively quickly. It was not possible to compare all of the different design parameters using laboratory testing because of the need to machine too many different bearing plate designs. The webbed designs of bearing plate would be extremely difficult / expensive to machine. However if it had been possible, laboratory test results would have been preferable to the FEA results. Where possible the parameters were evaluated through laboratory testing. This enabled some of the parameters that could not be investigated using FEA to be investigated, e.g. rate of loading, radius on edge of steel support plate hole; and some parameters to be further investigated, e.g. diameter of hole

in steel support plate. Laboratory tests also enabled final failure mechanisms to be investigated instead of initial loading performance. The FEA carried out did not model the nut being pushed into the centre of the bearing plate, or the shearing of the bearing plate next to the steel support plate hole edge at high loads. It was not possible to model plasticity in conjunction with the Hypoelastic material model. Hence laboratory tests were used to confirm the FEA results and to obtain additional information where possible. However the FEA looked at a large number of parameters and so was used as the main method of research. It is recognised that the most important test of a bearing plate's performance is the performance in the coal mine.

Bending Moment and Shear force diagrams and circular plate theory could have been used to look at some of the parameters, but they would not have looked at all of the parameters and been able to compare their relative significance. Hence FEA has the advantage of being able to compare a large number of parameters and their relative significance using the same method. The FEA compares parameters relatively quickly without needing lots of machining of plates or mould making. The strain gauge tests were used to verify that the results from the FE method were acceptable. The comparison of the refined mesh, reaction forces and stresses at nodes was used to ensure that each FE model was valid.

### 7.1.3 Justification of FE Method

The Finite Element models were all evaluated by finding the load to cause a deflection of 1 mm. 1 mm is a small deflection corresponding to a relatively low load level, to ensure that the stresses and strains in the material had not exceeded yield, and hence the Hypoelastic material model was still valid. The deflection measured was the maximum

overall downwards deflection in the bearing plate. This invariably occurred at the centre of the bearing plate on the upper surface. The maximum stress / strain usually occurred at a restrained node. FEA is probably not giving an accurate result at a restrained node. Hence if using the stress /strain as a performance criteria the stress would have to be evaluated at a point other than the restrained node. The maximum overall deflection is possibly a better measure of the bearing plate's performance than the stress at an arbitrary point. Deflection is calculated first by FEA before stress or strain and so deflection FEA results are more accurate than stress or strain FEA results. The failed bearing plate samples from the coal mines all appear to have failed after bending and excessive deflection and not by shearing. As the bearing plate is required to be used in the coal mines it is bending failure that the plate is to be designed against, not shear failure. Hence deflection would appear to be an appropriate measure of the bearing plate's performance, and preferable to the stress or strain at a restrained node or an arbitrary point.

If the bearing plate's material behaviour was linearly elastic the magnitude of the 1 mm deflection would not make any difference to the performance comparison because the load would be proportional to the deflection. As the material behaviour is non linearly elastic the magnitude of the 1 mm deflection does make a difference to the performance comparison. This difference affects the evaluation of the materials but not the evaluation of the bearing plate geometry parameters. The material parameter has been considered in much more depth in Chapter 6.

A criticism of the FE methodology used here is that it only investigated the performance of the model under initial loading conditions. The FE models did not investigate

complete failure or look at plastic deformation of the bearing plate. ABAQUS does not allow plasticity to be modelled in conjunction with hypoelastic behaviour. Another criticism of the FE method is that the loading and support conditions were simplified. The nut and the steel support plate were not modelled themselves; this would have required a much more sophisticated contact surface analysis. If the nut and / or steel support plate had been modelled this would have significantly increased the analysis and model creation time. These simplifications have made it possible to investigate a large number of different parameters, and provide information about the effect of their variation.

Another criticism of the method used is that axisymmetric behaviour was assumed. As shown by the failed samples from the mine in figures 2.2 and 2.3 the loading in the mine is not completely symmetrical and some out of alignment loading takes place. As shown in table 5.7, out of alignment loading reduces the load that the bearing plate carries.

A feature of the approach used is that it was an iterative method and hence required large numbers of FE runs. However this was necessary in order to compare the different models using the same performance criteria.

#### 7.1.4 Stress distribution in bearing plate designs

Plots of bearing plates tested with 55 mm holes in the steel support plate clearly show a stress concentration above the restraint (see figure 4.17). Very little deflection is possible with the small (55 mm) hole in the steel support plate. A plot of the Weldgrip bearing plate with a 55 mm hole in the steel support plate produces a similar stress distribution as shown in figure 4.17, with the maximum Tresca stress in the bearing

plate occurring at the restraint and a second area of stress concentration underneath the nut. The stress in the rest of the bearing plate is very low in comparison to the stress at the restraint and nut. This high concentration of stress around the restraint is compatible with the failure mechanism of the Weldgrip bearing plate tested in the laboratory with a 55 mm hole in the steel support plate, which was by shearing of the material next to the support plate edge.

Inspection of the stress distribution in the bearing plate models, (figures 4.17, 4.19) showed that the stress levels in the outer regions of the bearing plate, at diameters greater than the support plate hole diameter were very low, typically less than  $2 \text{ MN/m}^2$ . This suggests that the outer regions of the bearing plate do not make a large contribution to the bearing plate performance. This is compatible with the FE results based on a performance comparison of 1 mm deflection which suggested that material needs to be concentrated within the support plate hole diameter.

Inspection of the maximum stress in the bearing plate with different diameters of hole in the steel support plate, showed that for a standard load of 2 kN, the stress around the restraint with a large hole in the steel support plate was more than the stress around the restraint for a small hole in the steel support plate (figure 4.18). This occurred despite the fact that with a large hole in the steel support plate the bearing plate was supported over a larger circumference and hence larger area. This is possibly because with the same load but with a larger diameter of hole in the steel support plate there is a larger bending moment above the restraint than with a small diameter of hole.

Despite the fact that (for the same load) the stress around the restraint is greater with a large hole in the steel support plate than a small hole (figure 4.18); it is bearing plates supported with a small hole in the steel support plate that tend to fail because of high shear stress at the restraint (see figures 5.1, 5.2). Bearing plates with a large hole in the steel support plate undergo a large amount of deflection (bending), which causes high tensile circumferential stresses on the lower surface of the bearing plate (see figure 4.21). High tensile circumferential stress on the lower surface of the bearing plate causes the formation of radial cracks on the lower surface of the bearing plate (see figures 2.3 and 5.8). Bearing plates supported with a small hole in the steel support plate do not deflect as much as bearing plates supported with large holes in the steel support plate. Hence the tensile circumferential stress on the lower surface of the bearing plate is not as large with a small hole in the steel support plate as with a large hole. Hence the bearing plate supported with a small hole in the steel support plate does not fail by the formation of cracks on the lower surface of the bearing plate and hence carries more load and eventually fails due to high shear stresses at the restraint, causing shearing of the material (see figure 5.1). The large tensile circumferential stress with a large diameter of hole in the steel support plate observed in figure 4.19 corresponds with the failure mechanisms of the Weldgrip plate when tested with a large diameter of hole in the steel support plate (see figure 5.8). The maximum tensile circumferential stress shown in figure 4.21 occurred on the lower surface at the centre of the bearing plate. From inspection of failed Weldgrip bearing plates it seems likely that the cracks initiated on the lower surface at the centre of the bearing plate. Therefore the stress distribution obtained in the FE models of bearing plates are compatible with the failure mechanism observed in the laboratory with different diameters of hole in the steel support plate.

Higher stress levels around the restraint for webbed bearing plates than for solid bearing plates are not surprising and are probably due to the lower thickness of material in the webbed bearing plates. Inspection of stress levels around the restraint showed, not surprisingly, that reducing the web thickness around the restraint increased stress levels. Inspection of the results of varying the web thickness given in figure A1.27 (based on the load to cause 1 mm deflection) also suggests that reducing the web thickness close to the restraint is not beneficial on a load / volume basis.

The fact that webbed bearing plates have higher stress levels around the restraint than solid bearing plates, is a possible explanation for the difference in performance of the Weldgrip and Weidmann bearing plates at different diameters of hole in the steel support plate in the laboratory (see figure 5.4). The Weidmann bearing plate carries a higher load than the Weldgrip bearing plate at both small and large diameters of hole in the steel support plate. With a 60 mm diameter of hole in the steel support plate, the Weidmann bearing plate carries 7.7 kN more load than the Weldgrip bearing plate. However with a 120 mm hole in the steel support plate the Weidmann bearing plate carries 13.2 kN more load than the Weldgrip bearing plate. Hence the Weidmann bearing plate has a larger advantage in performance with a large hole in the steel support plate. The stress level around the restraint is significant to the failure mechanism of the bearing plate with a small diameter of hole in the steel support plate. As the stress levels around the restraint are more for a webbed bearing plate than a solid bearing plate, the Weidmann webbed bearing plate does not have as large an advantage in comparison to the Weldgrip plate with a small diameter of hole. However with a large diameter of hole in the steel support plate, the failure mechanism is not by shearing at the restraint, hence a higher level of stress around the restraint in a webbed bearing plate is not significant

with a large diameter of hole. The Weidmann bearing plate has a large advantage over the Weldgrip bearing plate with a large diameter of hole but a smaller advantage with a small diameter of hole.

Inspection of stress levels in coned and flat bearing plates showed higher concentrations of stress underneath the nut in coned plates than flat plates. The larger the coned angle, the larger the stress concentration. This is probably due to the small volume of material at the edge of the coned bearing plate. The coned bearing plates used for this research are simplified in that a seat for the nut has not been modelled (see figures 4.19 and 4.21).

## **7.2 Taguchi method and results**

### **7.2.1 Evaluation of Taguchi technique**

The Taguchi experimental technique was used to give an indication of which parameters concerning the design and testing of a bearing plate were the most important and should be investigated further. The advantage of the Taguchi technique is that it produces good indications of a parameters significance and an idea of the best levels for each parameter without the need for an excessive number of tests (FE models). Hence Taguchi methods can be used as a ‘screening’ test to evaluate where further work needs to be done. However there are a number of points that need to be considered when designing and analysing Taguchi experiments, including any possible interactions and the levels chosen for each parameter.

The success of a Taguchi experiment depends upon the experimental design and whether any interactions between parameters have been missed when designing the

experiment. An interaction occurs when two or more parameters are not independent of each other; i.e. the performance of one parameter depends upon the level of another parameter. If a significant interaction is not included in the experimental design, the experimental results may not be correct. If an interaction is not included in the experimental design the interaction will be confounded with other parameters in the orthogonal array, and so information cannot be extracted about the interaction. The results of other factors confounded with the interaction may be false. The Taguchi technique relies on the assumption that in many cases the experiment designer can identify whether parameters are independent or not. The main criticism of the Taguchi method is that the experimental design does not include all possible interactions Callender (1996). Fractional Factorial designs other than Taguchi method designs, e.g. Plackett-Burman, have the same disadvantage of confounding interactions with parameters.

An alternative method instead of the Taguchi method would have been to use a Full Factorial Experiment. To look at the two levels of the eight parameters used in the 2 level Taguchi experiment using a Full Factorial experiment would have required 256 FE models ( $2^8$ ), instead of 16 with the Taguchi experiment. Also to look at the three levels of four parameters used in the multiple level Taguchi experiment would have required 81 tests ( $3^4$ ) instead of 9 using the Taguchi method. The advantage of the Full Factorial experiment is that it would have investigated all of the possible interactions. Full Factorial experimentation is the only technique that investigates all of the possible interactions between parameters.

The relative significance of the parameters in the Taguchi experiment depends upon the values chosen for each level. The 2 level Taguchi experiment used in this research compared two different diameters of hole in the steel support plate, 55 mm and 100 mm; and two depths of bearing plate of 35 mm and 10 mm. These were chosen as extreme values of what may be sensibly chosen. However if depths of 45 mm and 10 mm had been compared, the depth of the bearing plate may have been the most significant parameter in the 2 level experiment.

The results presented in this thesis clearly demonstrate the disadvantage of the Taguchi method, in that many interactions that were not included in the design of the Taguchi experiment have been found to be significant. Also some interactions that were included in the design of the Taguchi experiments were found to have very little effect (see figures A1.2, A1.11, A1.12 and A1.13). However the Taguchi technique did identify the most significant parameters, and it allowed the parameters that would produce the most improvement in load / volume to be focused upon. Hence the Taguchi technique provided a good starting point. With the benefit of hindsight the design of the Taguchi experiment should have included interactions between the diameter of the hole in the steel support plate, the depth of the bearing plates, and the coned angle of the bearing plates. However these could not be expected to have been known before this research.

### 7.2.2 Two Level Taguchi Experiment Results

The results from the 2 level Taguchi experiment are given in table 4.1 when evaluated by comparing the load / volume and in table A1.1 when evaluated by comparing the load. The main differences are that on a load basis a solid design is preferable to a webbed design, an external diameter of 200 mm is preferable to 150 mm and a flat plate

is preferable to a coned plates. These results are reversed for the load / volume results. The different order of significance is also noteworthy. On a load basis the external diameter of the bearing plate is much more significant and the coned angle much less significant than on a load / volume basis.

The diameter of the hole in the steel support plate used when testing bearing plates is clearly an important parameter. The FE results show that the bearing plates perform better with a small hole in the steel support plate than a large hole. A higher load is needed to produce a 1 mm deflection with a small hole in the steel support plate than with a large hole. It is to be expected that a bearing plate supported close to the centre will deflect less easily than a bearing plate supported further away.

The depth of the bearing plate is also an important parameter. Clearly a 35 mm deep plate would perform better than a 10 mm plate when evaluated by comparing the load carried (see table A1.1). However the Taguchi 2 level experiment (table 4.1) shows that the 35 mm bearing plate performs better than the 10 mm plate when evaluated by comparing the load carried / plate volume. Therefore the load carried by the 35 mm deep bearing plate is more than 3.5 times the load carried by the 10 mm deep bearing plate.

When evaluated on a load / volume basis the Taguchi 2 level experiment showed that a coned plate, thicker at the centre of the bearing plate, but thinner at the outer edge is best. However when evaluated on a load basis the flat plate of constant thickness was best. This shows that by taking some material away from the outer edges of the plate, the load carried is reduced. However when the most efficient use of material is

considered by comparing the load / volume, it is better to have a coned not flat plate. The fact that the coned / flat parameter is much less significant in the experiment evaluated by comparing the load, is probably because the load carried does not change enormously with a coned plate instead of a flat plate. It is the decrease in volume that causes a coned plate to perform well on a load / volume basis and hence makes the coned / flat parameter more significant in the experiment evaluated by comparing the load / volume.

The Taguchi 2 level experiment evaluated by comparing the load / volume suggested that a webbed plate was preferable to a solid design of bearing plate. Unfortunately further experimentation showed this to be not entirely true. Some designs of solid and webbed plates are compared in table 4.5 and are discussed further in section 7.3.11. The Taguchi 2 level experiment evaluated by comparing the load carried clearly showed the solid plates to be preferable to the webbed plates.

In the Taguchi two level experiment, a measure of the error was included by means of an empty column in the orthogonal array. The error was found to be more significant than four of the parameters investigated (when evaluated by comparing the load / volume). However the confirmation test performed did confirm the experiment by producing a higher value of load / volume than any of the 16 tests in the Taguchi experiment. Hence this suggests that the most important and significant parameters have been determined and their 'best' level found. However the results for the four least significant parameters are not reliable. The empty column in the orthogonal array is usually used to provide a measure of the experimental error. In this case the error could be caused by any discrepancies in the mesh or modelling technique. Also if any interactions have been missed at the Taguchi experiment design stage, this will mean

that they are confounded with other columns in the orthogonal array and so this could be causing the error.

The Taguchi 2 level experiment and one factor at a time results showed polypropylene to perform better than polyamide 6. The material properties given in figures 6.4 and 6.5 show the polypropylene used has a higher secant modulus and hence is stiffer than the polyamide 6. It is therefore not surprising that the polypropylene carries a higher load before deflecting by 1 mm than the polyamide 6.

The external diameter of the bearing plate clearly has a large effect on the volume of the bearing plate, but also affected the load carried. Hence on a load / volume basis a bearing plate with a small external diameter of 150 mm as opposed to 200 mm is better. However when evaluated on a load basis a bearing plate with a larger external diameter of 200 mm is best. The results given in table A1.1 suggest that a greater external diameter of the bearing plate causes the bearing plate to deflect less easily and carry a greater load. The reason for the low significance of the external diameter of the bearing plate when evaluated by comparing the load / volume, is possibly due to the increase in load of the greater diameter cancelling out the decrease in volume with a smaller diameter.

This experiment is comparing the load carried by the bearing plate evaluated using FEA. The improved bearing area of the plate in contact with the rock is not being considered in this analysis. As shown by equations 1.1 and 1.2, the larger the surface area of the bearing plate, the greater the support offered by the rockbolt to the mine wall. However as the displaced plots shown in figures 4.17 and 4.21 show the outer edges of the plate

have a tendency to simply 'lift off' and so may not be giving any extra support to the rock anyway. Hence the external diameter of the bearing plate is a more complicated parameter than is being considered here.

The Taguchi 2 level experiment suggested that the diameter of the central hole in the bearing plate should be as small as possible. This was found when the diameter of the central hole was evaluated on the basis of load and load / volume. As the significance of this parameter was below the error in this experiment, the parameter was further investigated using a one factor at a time approach.

The Taguchi 2 level experiment suggested that the external diameter of the nut is required to be as large as possible in order to produce a high load from the bearing plate. A larger nut spreads load over a larger portion of the bearing plate and so helps the bearing plate perform better and deflect less easily. However the affect of increasing the nut diameter is not as great as the other parameters affect. The significance of the diameter of the nut parameter was less than the error in the experiment and so further information was gathered using a one factor at a time approach to confirm the Taguchi results.

### 7.2.3 Multiple level Taguchi experiment for solid bearing plate designs

This multiple level Taguchi experiment looked in greater detail at parameters concerning the design and testing of solid coned plates. The variation of load / volume with different diameters of hole in the steel support plate is similar to that found in the 2 level Taguchi experiment but with more detail, the results are given in table 4.2.

The variation of the bearing plate depth was found to be a non linear function. However three points on a graph does not give very much information about the shape of the curve. Hence this important parameter was investigated in more detail using a one factor at a time approach.

The angle of the coned plates was varied in the multiple level Taguchi experiment. In the 2 level Taguchi experiment all bearing plates were either flat or coned with a 30° coned angle. The multiple level Taguchi experiment compared bearing plates with coned angles of 15°, 30° and 45° to the horizontal. The variation of the coned angle was found to be a non linear function. The coned angle was also investigated in more detail using a one factor at a time approach.

The coned shape of the bearing plate was also compared. A straight sided cone appears to be preferable to a concave or convex cone. However the results were very similar. The radius of the coned shape used was 100 mm, this large radius meant that there was only a slight curvature on the side of the cone and hence explains why there is little difference between the shapes.

The confirmation model for the multiple level Taguchi experiment on solid bearing plate designs produced a lower value of load / volume than one of the tests in the multiple level experiment. Hence the confirmation test did not confirm the experiment. The reason for this is almost certainly due to a missed interaction in the experiment. Hence interactions between the three significant parameters in the Taguchi experiment were investigated using a one factor at a time approach.

#### 7.2.4 Multiple level Taguchi experiment for webbed bearing plate designs

This multiple level Taguchi experiment looked at parameters concerning the design of webbed bearing plates. A confirmation test was carried out to verify the results of the webbed multiple level Taguchi experiment. The confirmation test produced a higher level of load / volume than any of the tests in the multiple level Taguchi experiment. Hence the confirmation test confirmed the experiment. This suggests that there are no major interactions between the parameters in the webbed multiple level experiment.

The results from the webbed multiple level Taguchi experiment using a 55 mm hole in the steel support plate are different from the results using a 100 mm hole (table 4.3 and A1.2). This suggests a possible interaction between the diameter of the hole in the steel support plate and parameters in the webbed multiple level Taguchi experiment. Hence these interactions suggested by the Taguchi method were further investigated using a one factor at a time approach.

The variation of the number of radial webs was found to be a non linear function, when evaluated on a load / volume basis with a 100 mm hole in the steel support plate. The number of radial webs was investigated in more detail using a one factor at a time approach.

The stiffer material (polypropylene) with a higher value of secant modulus again performed better than the more flexible materials (polyamide 6 and polycarbonate). These results are based on the material data shown in figure 6.4 at low strain levels.

Clearly a webbed bearing plate with a web thickness of 5 mm will perform better than a bearing plate with a web thickness of 3 mm when evaluated by comparing the load carried. However the webbed multiple level Taguchi experiment showed that a bearing plate with a web thickness of 5 mm on all the webs, radial and circumferential performed better on a load / volume basis than a bearing plate with a web thickness of 3 mm.

Five circumferential webs performed better than three circumferential webs. However this Taguchi experiment considered equally spaced webs and the effect of concentrating the webs closer to the centre was not considered. All of the designs investigated in the webbed multiple level experiment produced a lower value of load / volume than a comparable solid bearing plate. However the number of radial and circumferential webs and the web thickness were investigated in more depth using a one factor at a time approach to see if a webbed bearing plate with material concentrated closer to the centre would perform better than a solid bearing plate.

### **7.3 One Factor at a time**

The one factor at a time results looked at parameters in more detail than in the Taguchi experiments, this allowed parameters to be plotted over a larger number of points.

#### **7.3.1 Diameter of hole in steel support plate**

As the bearing plate volume remains constant when varying the diameter of the hole in the steel support plate, it makes no difference whether the steel support plate hole diameter is evaluated by comparing the load carried or by comparing the load / volume. To enable comparison with other parameters the hole diameter was evaluated on a load / volume basis.

The variation of load carried and load / volume with different diameters of hole in the steel support plate is a non linear function, figures 4.3, 4.4, 5.4, A1.1 and A1.2. The bearing plate carries much more load with a 55 mm diameter hole than with a 100 mm hole in the steel support plate. With the small hole in the steel support plate the steel is supporting the bearing plate much better and so allows the bearing plate to carry a much higher load. As can be seen in figures 4.3, 4.4 and A1.1 varying the diameter of the hole from 55 mm to 60 mm makes a large difference to the amount of load carried, but varying the diameter of the hole from 100 mm to 105 mm makes much less difference to the amount of load carried. The laboratory testing results shown in figure 5.4 support this observation.

The large effect of varying the diameter of the hole in the steel support plate shows the importance of using a standard hole diameter when comparing bearing plate laboratory test results. Clearly it is not valid to compare one manufacturer's bearing plate test results obtained using a 55 mm hole diameter with another manufacturer's obtained using a 60 mm hole diameter.

The effect of varying the hole diameter also shows the importance of the integrity of the edges of the hole drilled when installing the rockbolt in the coal mines. Clearly if the area around the rockbolt hole is not flat close to the rockbolt and so the bearing plate is supported further away from the centre, it will have a detrimental effect on the bearing plates performance down the mine, and allow the bearing plate to deflect much more easily, and hence provide less support to the coal rib. Hence the better the support given by the coal rib to the bearing plate, the better the support given by the bearing plate to

the coal rib. The problem of the coal rib being crushed is examined in Appendix 4 and discussed further in section 7.4.10.

For all bearing plate designs, a small hole in the steel support plate produces a higher load than a large hole in the steel support plate. However the rate of decrease of the load carried with increasing diameter of hole in the steel support plate is different for different designs of bearing plate. The rate of decrease of the load carried with increasing diameter of hole in the steel support plate is greater for coned plates than for flat plates (see figure 4.4). The greater the coned angle the greater the rate of decrease of load carried with increasing diameter of hole in the steel support plate.

The results given in figure A1.1 for the variation of diameter of hole in the steel support plate for a webbed bearing plate, show that the results at diameters of hole in the steel support plate close to a circumferential web position do not fit a smooth curve. The results corresponding to a web position are slightly higher than the expected values, perhaps showing that the bearing plate deflects less easily when supported around the circumferential webs, than when supported just on the radial webs. This suggests a localised interaction between the diameter of the hole in the steel support plate and the position of the circumferential webs.

Figure A1.2 shows the variation of load / volume with diameter of hole in the steel support plate for three different materials. The curves on figure A1.2 are very nearly parallel to one another, which suggests that there is not a highly significant interaction between the diameter of the hole in the steel support plate and the material. This

possible interaction was included in the design of the Taguchi 2 level experiment, but was found to have a significance of less than the error in the experiment.

### 7.3.2 Depth of bearing plate

The Taguchi multiple level experiment on solid bearing plate designs suggested that the variation of the depth of the bearing plate was a non linear function (table 4.2). The one factor at a time results confirm this with much more detail, and also show that the variation is different for different diameters of hole in the steel support plate. The fact that the curves in figure 4.5 are not parallel to each other shows that there is an interaction between the diameter of the hole in the steel support plate and the depth of the bearing plate. This is an interaction that was not included in the design of the Taguchi experiments. This interaction was suspected because as explained in section 7.2.3 the confirmation test of the multiple level Taguchi experiment on solid bearing plates did not confirm the experiment. As shown by the non parallel curves in figure A1.3, there is also an interaction between the depth of the bearing plate and the diameter of the hole in the steel support plate when evaluated on the basis of load.

Figure 4.5 shows that for each diameter of hole in the steel support plate there is a peak or optimum depth. The optimum value and maximum point of the curve is caused by the fact that the depth of the bearing plate was evaluated by comparing the load / volume. If the bearing plate depth is evaluated by considering the load carried (see figure A1.3), as the bearing plate depth increases the load carried increases. However there is a diminishing return for this increase in depth. At depths of the bearing plate below the optimum, increasing the depth of the bearing plate increases the load carried by more than it increases the plate volume, hence the load / volume increases with an increase in

depth. At depths of the bearing plate above the optimum, increasing the depth still increases the load carried, but the volume is increasing at a greater rate and hence the value of the load / volume decreases with an increase in depth.

Figure 4.5 shows that the smaller the diameter of hole in the steel support plate the smaller is the optimum depth of the bearing plate. Similarly the larger the diameter of hole in the steel support plate, the larger the optimum depth of the bearing plate. This is probably because the larger the diameter of hole in the steel support plate, the greater the proportion of the bearing plate within the hole diameter. Therefore with a larger hole diameter, a larger proportion of the volume increase is within the hole diameter, not outside the hole diameter. Therefore at larger diameters of hole in the steel support plate, the depth of the bearing plate at which the volume increases more than the load increases, is greater. Hence the optimum depth of the bearing plate is greater for larger diameters of hole in the steel support plate.

### 7.3.3 Coned angle

Figure 4.6 shows the variation of coned angle for different diameters of hole in the steel support plate. The fact that the curves in figure 4.6 are not parallel to one another shows that there is an interaction between the coned angle and the diameter of the hole in the steel support plate. This interaction was not included in the design of the Taguchi experiments. This interaction may account for the fact that the confirmation test in the multiple level Taguchi experiment on solid bearing plates did not confirm the experiment.

Figure 4.6 suggests that the greater the diameter of hole in the steel support plate, the smaller is the optimum coned angle. For a small hole in the steel support plate a large coned angle is desirable because this puts a bigger proportion of material within the 55 mm hole diameter region and reduces the amount of material at the outer edges of the bearing plate. However with a larger hole in the steel support plate a high coned angle means that the plate thickness within the diameter of the support plate hole is reduced too much, hence the optimum coned angle is less for a 100 mm hole in the steel support plate than for a 55 mm hole in the steel support plate.

These results may suggest that the region of the bearing plate outside the diameter of the hole in the steel support plate is not very important and is offering very little to the performance of the plate. However it must be remembered that this analysis is a simplification of the situation in the coal mine and is not considering the bearing surface area of the plate on the coal.

#### 7.3.4 Interaction between depth of bearing plate, coned angle and diameter of hole in steel support plate

As figures 4.7, 4.8 and figures A1.4, A1.5 show the optimum coned angle not only varies with the diameter of the hole in the steel support plate but with the depth of the bearing plate. Figure 4.7 shows the variation of load / volume with coned angle for different depths of bearing plates, with a 55 mm hole in the steel support plate as specified in BS 7861. The fact that the curves on this graph are not parallel to each other shows that the depth of the bearing plate and the coned angle are not independent parameters and hence there is an interaction between the coned angle and the depth of the bearing plate. This interaction was not included in the design of the Taguchi experiments (this may also account for the fact that the confirmation test in the multiple

level Taguchi experiment on solid bearing plates, did not confirm the experiment). Also, the variation of load / volume with coned angle for different depths of bearing plates varies for different diameters of hole in the steel support plate (see figures 4.7, 4.8, A1.3 and A1.4). This shows that there is a three way interaction between the diameter of the hole in the steel support plate, the depth of the bearing plates and the coned angle of the bearing plates. This three way interaction was not included in the design of the Taguchi experiments.

Figure A1.5 shows the variation of load / volume with coned angle for different depths of bearing plates with a 100 mm diameter hole in the steel support plate. It also shows that there is an optimum coned angle for each depth of bearing plate. Figure A1.5 shows that for a 100 mm hole in the steel support plate, the optimum coned angle of the bearing plate increases with increasing depth of bearing plates. This is possibly because, a coned angle of  $30^\circ$  reduces the depth of a bearing plate, 20 mm away from the centre by 11.55 mm. Hence for a bearing plate of depth 40 mm the depth 20 mm away from the centre is reduced to 28.45 mm, but for a bearing plate of depth 30 mm the depth 20 mm from the centre is reduced to 18.45 mm. Hence the coned angle reduces the amount of material in a thin plate by more as a fraction of the overall volume than for a thick plate. This may explain why for a greater depth of bearing plate, the optimum coned angle is greater.

Figure A1.6 gives the variation of load / volume with depth of the bearing plate for different coned angles. The peak or optimum depth varies with different coned angles as well as different diameters of hole in the steel support plate. Hence to select the

optimum depth of the bearing plate is not as simple as suggested by figure 4.5, because the optimum depth depends upon the coned angle used.

Figure 4.9 gives the optimum coned angle (determined on the basis of the FE results shown in figures 4.7, 4.8, A1.4 and A1.5) for different depths of bearing plates with different diameters of hole in the steel support plate. The general trend is that the greater the depth of the bearing plates, the greater is the optimum coned angle. Also the greater the diameter of the hole in the steel support plate the smaller is the optimum coned angle. This is the same conclusion suggested by comparing coned bearing plates with only one depth of 30 mm. Also the greater the diameter of hole in the steel support plate the greater is the optimum depth of the bearing plate. This is the same conclusion that was drawn with (non coned) flat bearing plates.

The Finite Element results of varying the thickness and coned angle of the bearing plate suggest that when testing a bearing plate with a 55 mm hole in the steel support plate as much material as possible needs to be within the 55 mm diameter central portion of the bearing plate. Similarly when testing a plate using a 100 mm hole as much material as possible needs to be within the 100 mm diameter central portion.

#### 7.3.5 Increasing thickness above support plate hole

Table 4.4 gives some results comparing designs that have an increased thickness over the edge of the hole in the steel support plate. These are compared with designs that have an increased thickness at the centre of the bearing plate and designs with a constant thickness of the bearing plate. Out of the four designs compared in section 4.5.5, the design with a reduced thickness in the centre (figure 4.12) produced the worst result, on

a load / volume basis. The design with a constant thickness across the diameter of the bearing plate (figure 4.10) was the second worst design. The bearing plate with a constant thickness of 30 mm from the centre to over the edge of the support plate hole and then tapering down to the outside edge (figure 4.11), was better than the plate of constant thickness (figure 4.10). This was due to the decrease in volume of material required in reducing the thickness close to the outside edge. Despite a slight reduction in load carried, due to the decrease in volume of material required, the load / volume increased. The best design seen on a load / volume basis was the coned plates thicker at the centre (figure 4.13) and of reduced thickness further away from the centre. Hence the idea of designs thicker over the edge of the hole in the steel support plate than in the centre, appears not to be a good idea. The results suggest that a bearing plate that is thicker in the centre is preferable to one thicker over the support plate hole edge.

### 7.3.6 Size of nut / volume of nut

#### 7.3.6.1 Comparison of total volume of nut and bearing plate

Most of the results presented are evaluated on the basis of the load / plate volume which considers the most efficient use of material when changing the geometry of the bearing plate. Clearly when varying the diameter of the nut, this is varying the volume of material in the nut not the bearing plate. Hence the total volume of material used needs to be considered. The question of whether it is better to put extra material onto the bearing plate or onto the nut depends partially upon the external diameter of the bearing plate and the depth of the nut, as this effects the volume of material in the bearing plate and nut. The results given in figures A1.7a and A1.7b, show the variation of load / total volume when varying the plate depth and the nut diameter.

The calculations of the effect of adding  $10,000 \text{ mm}^3$  to the nut and bearing plate given in Appendix 1, pg. XI strongly suggests that it is better to add extra material to the nut not the bearing plate. The magnitude of the increases in load of putting extra material onto the nut or the bearing plate depends upon the diameter of the nut and the depth of the bearing plate initially. If the bearing plate is already at the optimum depth, the benefit of increasing the nut diameter is much greater than the benefit of increasing the plate depth. As the diameter of the nut increases the rate of increase in load / total volume carried with increasing diameter of nut decreases. However the calculations on page XI suggest a much larger increase in load when putting extra material on the nut not the bearing plate. As there is such a large difference between the increase in load when adding material to the nut and not the bearing plate, the initial nut diameter and plate depth is perhaps not vital.

A major limitation of this analysis of the total volume of material is that the material used for the bearing plate is not the same as the material used for the nut. The selection of a material for the nut will depend largely upon the properties needed for the threadform. Hence despite the calculations in Appendix 1 suggesting that it is better to put extra material onto the nut rather than the bearing plate, if the material used for the nut is much more expensive than the material used for the bearing plate, it may be better to put the extra material onto the bearing plate.

#### 7.3.6.2 Variation of diameter of nut with different diameters of hole in the steel support plate

Figure 4.14 gives some results comparing the effect of varying the diameter of the nut at different diameters of hole in the steel support plate. It can be seen that the gradient of the curves showing the different diameters of nut with a 70 and 100 mm hole are

parallel to each other. However the gradient of the curve showing the variation of diameter of the nut with a 55 mm hole in the steel support plate is much steeper. This shows there is an interaction between the diameter of the hole in the steel support plate and the diameter of the nut. The interaction may be a localised interaction due to the fact that the 55 mm diameter hole in the steel support plate is around the same size as the nut diameter. This suggests, not surprisingly, that if the nut is close to the same size or larger than the diameter of the hole in the steel support plate, the bearing plate will deflect much less easily.

Figure A1.10 gives some results comparing the difference between the diameter of the hole in the steel support plate and the diameter of the nut used. It can be seen that the general trend is for the load carried to decrease with increasing distance between the edge of the hole in the steel support plate and the edge of the nut. However the gradient of the curve varies with the different diameters of hole in the steel support plate. This suggests that the diameter of the hole in the steel support plate is a more significant parameter than the distance between the edge of the hole in the steel support plate and the nut diameter. This shows that there is an interaction between the diameter of the hole in the steel support plate and the difference between the diameter of hole in the steel support plate and the diameter of the nut. Hence there is an interaction between the diameter of the hole in the steel support plate and the diameter of the nut. This interaction was included in the design of the Taguchi 2 level experiment. However the significance of this interaction in the Taguchi 2 level experiment was below the significance of the error in the experiment. Hence no information can be obtained about the interaction from the Taguchi experiment.

### 7.3.6.3 Further Interactions between diameter of nut and material, coned angle and diameter of hole in the centre of the bearing plate

Figures A1.11 and A1.12 give some further results comparing the variation of diameter of the nut with three different materials. These results are given on a load / plate volume basis and on a load / nut volume basis. Figure A1.12 shows that a higher value of load / nut volume is carried with a smaller diameter of nut. This is because the volume of the nut is considerably reduced with a smaller diameter of nut. Hence despite the decrease in load carried with a smaller diameter of nut, the decrease in nut volume, causes a higher value of load / nut volume for a smaller diameter of nut.

Figure A1.11 shows the variation of the diameter of the nut with three different materials on a load / plate volume basis. It can be seen from figure A1.11 that the curves are very nearly parallel to each other, hence there is not a highly significant interaction between the diameter of the nut and the material. This possible interaction was included in the design of the Taguchi experiment, but was found to have a significance of below the error in the experiment.

Figure A1.8 gives some further results comparing the diameter of the nut for flat plates and for coned plates with different coned angles. It can be seen that for coned plates the gradient of the curve of increasing diameter of nut is steeper than for flat plates. The steeper the coned angle of the bearing plates, the greater is the gradient of the graph of increasing nut diameter. This is possibly because with the coned plates for a given diameter of nut the surface area over which the nut acts is larger than for a flat plate or a shallower coned plate. Results are also given in figure A1.9 which show that when the same results are plotted showing the surface area of the bearing plate that the nut acts

over, the gradient of the curves showing the increase in nut diameter are much closer together. However it should be remembered that the conical seat shape of the bearing plate has not been modelled and hence all that the above results show is that a higher surface area of contact between the nut and bearing plate increases the load carried.

Results are given in figure A1.13 showing the effect of varying the diameter of the nut for different diameters of hole in the centre of the bearing plate. The fact that the curves in figure A1.13 are parallel to each other shows that there is not an interaction between the diameter of the nut and the diameter of the hole in the centre of the bearing plate. This possible interaction was included in the Taguchi 2 level experiment, but was found to have a significance of much less than the error. The fact that the diameter of the central hole in the bearing plate and the diameter of the nut are not highly significant parameters may suggest that there is unlikely to be a highly significant interaction between the two parameters.

### 7.3.7 Diameter of central hole in bearing plate

The one factor at a time results, figure 4.15 suggested that a large hole in the centre of the bearing plate was marginally preferable to a small hole with a 55 mm, 70 mm and 100 mm hole in the steel support plate.

The bearing plate designs were evaluated by comparing the load to cause 1 mm deflection, the maximum deflection was always at the centre of the bearing plate. The method used is possibly not giving a reliable result in evaluating the effect of different diameters of central hole. For a large hole in the centre of the bearing plate the hole edge of the bearing plate is closer to the edge of the hole in the steel support plate and hence

the bearing plate may produce a lower maximum deflection. Also a bearing plate with a small hole in the centre will have the edge of the hole further away from the edge of the hole in the steel support plate, and so may deflect with less load. Hence the bearing plate with a large hole in the centre may perform well when evaluated by the method used here.

The diameter of the central hole in the bearing plate is a much less significant parameter than the depth of the bearing plate. In order to comply with the 18° out of alignment angle design specification, for the depth of the bearing plate to be 35 mm the diameter of the central hole must be at least 34 mm (see figure 2.4). Since the depth of the bearing plate is a much more significant parameter than the diameter of the central hole, it is best to have the depth of the bearing plate at its best level than to have the diameter of the central hole at its best level.

#### 7.3.8 External diameter of bearing plate

The one factor at a time results for external diameter of bearing plate given in table A1.4 agree with the results from the 2 level Taguchi experiment. On a load / volume basis a small external diameter of bearing plate appears best, whereas on a load basis a large external diameter of bearing plate is best.

#### 7.3.9 Number of radial webs

Results are given in figure 4.16 which show the variation of load / volume with number of radial webs for different diameters of hole in the steel support plate. The fact that the curves in figure 4.16 are not parallel to each other shows that there is an interaction between the diameter of the hole in the steel support plate and the number of radial webs. This interaction was not included in the design of the Taguchi experiments.

The results in figure 4.16 show that for small numbers of radial webs, there is a large rate of increase of load / volume with increasing numbers of radial webs. For a 55 mm diameter of hole in the steel support plate the rate of increase in load / volume with increasing number of radial webs is greater than for a 70 mm or 100 mm hole. Beyond around 16 radial webs, the gradient of all three curves is very low signifying very little improvement for the extra webs. The smaller the diameter of the hole in the steel support plate, the larger is the minimum number of radial webs required. Increasing the number of radial webs, adds more material proportionately to the centre of the bearing plate than the outside edge, because the circumference of the plate is greater at the outside edge than at the centre. Hence there is a steeper gradient on the initial portion of figure 4.16 for the curve corresponding to a 55 mm hole in the steel plate than for a 70 mm hole or 100 mm hole. The curve corresponding to a 100 mm hole actual reaches a peak and then the load / volume falls with increasing number of radial webs.

#### 7.3.10 Number of circumferential webs

The results from varying the number and position of the circumferential webs given in Appendix 1 show that the optimum number and position of the circumferential webs depends upon the diameter of the hole in the steel support plate. As can be seen from figure A1.23 designs with the circumferential webs concentrated in the 55 mm hole region perform better when tested with a 55 mm hole in the steel support plate. Similar conclusions can be drawn from figures A1.24 and A1.25 for 70 mm and 100 mm holes respectively. Hence there is an interaction between the number and position of the circumferential webs and the diameter of the hole in the steel support plate. This interaction was not included in the design of the Taguchi experiment.

The results in figures A1.23, A1.24 and A1.25 also show that coned webbed plates perform better on a load / volume basis than flat webbed plates.

The results of varying the number and position of circumferential webs, suggest that when testing with a 55 mm hole in the steel support plate, as big a proportion of the bearing plate's material as possible needs to be concentrated in the central 55 mm of the bearing plate. Similarly when testing with a 100 mm hole in the steel support plate as big a proportion of the bearing plate's material needs to be concentrated in the central 100 mm of the bearing plate. This was the same conclusion reached when investigating the coned angle of the bearing plate, the number of radial webs and looking at the stress levels in the bearing plates.

#### 7.3.11 Thickening of different webs

The results given in figures A1.27, A1.28 and A1.29 show that whether it is better to add extra material to the radial webs or to the circumferential webs depends upon the number of radial and circumferential webs in the design. Hence there is another interaction between the web thickness and the number of radial and circumferential webs. This interaction was not included in the design of the Taguchi experiments.

Figures A1.26 and A1.27 show the effect of varying the web thickness for the same design of bearing plate with a 55 mm and a 100 mm hole in the steel support plate. For a 55 mm hole in the steel support plate, figure A1.27 suggests that it is better to increase the thickness of the radial webs. However figure A1.26 shows that for a 100 mm hole in the steel support plate, it is better to increase the thickness of the circumferential

webs. Hence the results given in Appendix 1 show that whether it is better to add extra material to the circumferential or radial webs depends upon the diameter of the hole in the steel support plate. Hence there is another interaction between the web thickness and the diameter of the hole in the steel support plate. This interaction was not included in the design of the Taguchi experiments.

If there are less than the optimum number of radial webs (see figure A1.27) then the results suggest that thickening the radial webs is more beneficial than thickening the circumferential webs. If there is an optimum number of radial and circumferential webs, then it is equally beneficial to thicken up the radial and circumferential webs. Hence the optimum web thickness depends upon the particular design.

The results given in figures A1.26, A1.27, A1.28 and A1.29 show whether it is better to increase or decrease the web thickness for particular designs away from the standard thickness of 3 mm. The results show that generally it is better to increase the web thickness closer to the centre of the bearing plate and decrease the web thickness further away from the centre of the bearing plate. Hence this fits in with the general trend observed from the coned angle and the position of the circumferential webs; of needing to concentrate the material within the area of the hole in the steel support plate, and in particular close to the centre of the bearing plate.

#### 7.3.12 Comparison of solid and webbed designs

The comparison of solid and webbed designs given in table 4.5, compares a variety of webbed and solid designs including simple flat plates and coned plates, with 55 mm and 100 mm holes in the steel support plate. The webbed plates compared in table 4.5 were

all using the optimum configuration of webs (see figures 4.16, A1.21 and A1.22). In most cases the solid plates compare better than the webbed plates, on a load / volume basis. Clearly the solid plates also perform better than the webbed plates on a load basis. The reduction in volume of the webbed plates does not compensate for the reduction in load carried, so that the solid plates are better than webbed on a load / volume basis. For the flat plates tested with a 55 mm hole in the steel support plate, the webbed plates performed very slightly better than the solid plates. However this only occurred when using a design that had all the circumferential webs concentrated in the centre region. As mentioned in section 7.3.9 adding extra radial webs to a design increases the proportion of material close to the centre more than at the outer edge of the bearing plate, and so the webbed plates compare more favourably with the solid plates with a small hole diameter of 55 mm than with a large hole diameter of 100 mm. Hence the one factor at a time results suggests that a solid bearing plate design is preferable to a webbed bearing plate design when used with a 100 mm hole in the steel support plate.

#### 7.3.13 Materials, Temperature and time effects

The Finite Element Analysis results show that a material with a high value of secant modulus, will carry a larger load before deflecting by 1 mm than a material with a low value of secant modulus. This result is perhaps rather obvious, but by including the material as a parameter in the experiments, an indication of the parameters relative significance in comparison with other parameters was gained.

The results given in figure A1.30 show that there is a reduction in performance when the material is used at 40°C instead of 20°C. This is important because the environment in a coal mine typically has an elevated temperature of up to 40°C. The results in figure

A1.31 also show that there is a reduction in performance when the material is used over an extended period of time. This is important because the bearing plate may be installed in the coal mine for up to 2 years.

The results given in figure A1.30 also show the increase in load carried when reinforced materials are used. This increase in load carried is caused by the increased stiffness of the material. However the criteria for selecting a suitable material are more complicated than to simply look for the maximum value of the secant modulus. Hence a more thorough material selection exercise was required (see Chapter 6).

#### 7.3.14 Design / testing parameters and their interactions

The FE results have shown that there are a large number of parameters concerning the design and testing of a bearing plate and there are many interactions between these parameters. The most significant parameters have been identified. The interactions between the three most significant parameters (diameter of hole in steel support plate, coned angle, depth of bearing plate) have been investigated. Interactions between the diameter of hole in the steel support plate and the parameters in the webbed multiple level Taguchi experiment have been investigated. These interactions were suggested by the Taguchi experiment results. Some other possible interactions have been investigated. The results have demonstrated the main disadvantage of the Taguchi technique (the danger of missed interactions). Further one factor at a time results at many different conditions have been gathered to provide a thorough view of the effect of these parameters and interactions.

The Taguchi and one factor at a time methods were used to give a structured approach to the bearing plate design problem, and to enable all the parameters to be investigated

in a structured manner. However this did not always allow for much creativity in the design concepts. Therefore some designs were modelled just to see if they gave improved results, e.g. plates thickened in different places (section 4.4.5) and positions of circumferential webs (figures A1.14-25). The thickening of bearing plates in different places did not improve the performance, however the different positions of the circumferential webs did improve the design of a webbed bearing plate. Hence this gives an example of the need to allow creativity in design.

## **7.4 Discussion of laboratory bearing plate tests and failed plates from the mines**

The laboratory tests on the bearing plates produced remarkably consistent results. As figure 5.4 shows repeats of tests gave similar results and showed little scatter. BS 2782 on polymer testing and BS 7861 on rockbolting recommends that 5 tests should be carried out on polymer material for each condition. This was not possible with the number of bearing plates available. For some parameters, e.g. diameter of hole in steel support plate, the parameter has such a large effect that the scatter could be considered insignificant. However for parameters which have only a very small effect on the load carried e.g. rate of loading, all that can be concluded is that the parameter does not have a large effect on the load carried.

### **7.4.1 Diameter of hole in steel support plate**

The laboratory testing results of varying the diameter of the hole in the steel support plate for both the Weldgrip and Weidmann bearing plates show that the smaller the diameter of hole in the steel support plate, the higher the load carried by the bearing plate (figure 5.4). This confirms the conclusion reached in the FEA tests (figure 4.3). The laboratory testing results also show different failure mechanisms with different diameters of hole in the steel support plate.

Tests on the Weldgrip bearing plates with a 55 mm, 60 mm and 70 mm hole in the steel support plate and on the Weidmann bearing plate with a 60 mm and 70 mm hole produced a shear failure mechanism (figures 5.1, 5.2 and 7.1). This is a failure mechanism that is not found in the coal mines (figures 2.2, 2.3, 2.4). The shear failure occurred at the edge of the hole in the steel support plate. As shear is not the failure mechanism found in the coal mines, a steel plate with a 55 mm hole (as specified in BS

7861) would appear not to be an appropriate test to evaluate whether bearing plates perform adequately to be used in the coal mines (see figure 7.1). A suitable diameter of hole in the steel support plate for a bearing plate approval test, should have a sufficiently large diameter of hole to ensure that the failure is not by shearing.

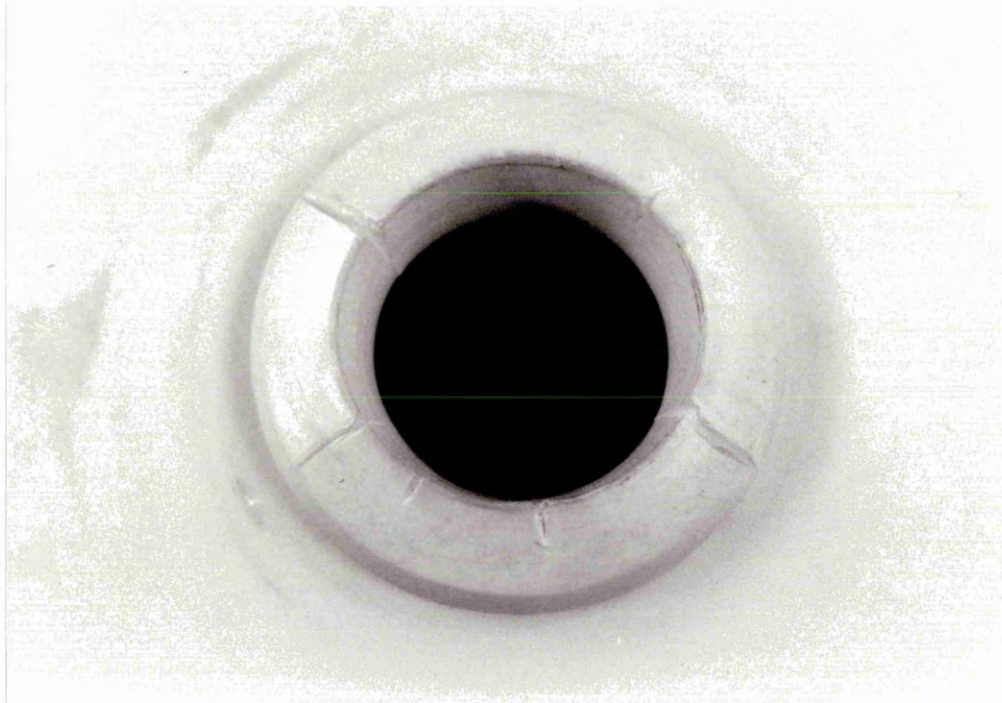


**Figure 7.1** Failure mechanism of Weldgrip bearing plate when tested with 55 mm hole in steel support plate

With an 80 mm hole in the steel support plate, the failure mechanism for the Weldgrip bearing plates was by bending, and for the Weidmann bearing plate was by crack formation caused by bending. Hence the transition from a shear to a bending failure for both the Weldgrip and Weidmann bearing plates occurs between hole diameters in the steel support plate of 70 and 80 mm.

Tests on the Weidmann bearing plate with 80 mm, 100 mm, 120 mm and 140 mm holes in the steel support plate showed that the bearing plate failed by the formation of cracks in the webs after some bending had occurred. However the Weidmann bearing plate

tested with a 100 mm and 80 mm hole in the steel support plate, did show some signs of shear deformation and buckling in the area just above the ring supported by the edge of the steel support plate.

Tests on the Weldgrip bearing plate with a 100 mm and 120 mm hole in the steel support plate showed that the bearing plate underwent a large degree of bending. However on removal of the load the Weldgrip bearing plate returned to almost its original shape (figure 5.7) showing that most of the deformation that had taken place was elastic deformation, not plastic deformation. Plates tested with a 100 mm hole formed small radial cracks on the lower surface of the bearing plate. The plate tested with a 120 mm hole suffered catastrophic failure with the formation of large brittle cracks that spread rapidly through the bearing plate, in the radial direction. This is due to the build up of high tensile circumferential stresses in the bearing plate (perpendicular to the crack) as discussed in section 7.1.4 and predicted by the FE model in figure 4.21. It would appear that the cracks have initiated on the lower surface of the bearing plate.

As shown in figure 4.22, for a standard load, the higher the diameter of hole in the steel support plate, the higher the tensile circumferential stress on the lower surface of the bearing plate. Hence this explains why more and larger radial cracks are produced when bearing plates are tested with larger diameters of hole in the steel support plate.

The laboratory test results (figure 5.4) show that the difference in performance between the Weldgrip and Weidmann bearing plates is greater with a larger diameter of hole in the steel support plate. This suggests an interaction between the diameter of the hole in the steel support plate and another parameter that has changed between the Weldgrip →

Weidmann bearing plate. This is probably due to the change in coned angle. The FEA results suggested an interaction between the diameter of hole in the steel support plate and the coned angle (see figure 4.4).

As shown in figure 5.4 the load carried by the AMS bearing plate is much less than the load carried by the Weldgrip or Weidmann bearing plates. This is compatible with the view of colliery rockbolting engineers that the AMS bearing plate is inadequate for supporting the walls in coal mines.

#### 7.4.2 Radius on edge of hole in steel support plate

Tests on the Weldgrip bearing plates comparing the radius on the edge of the hole in the steel support plate (table 5.1); suggest that the radius on the edge of the hole makes practically no difference to the load carried or to the failure mechanism of the bearing plate. In both cases the failure mechanism was by shearing. The difference in load carried was only 0.8 kN (1.6%), which is probably due to scatter in the results. It is expected that with a larger diameter of hole in the steel support plate the radius on the edge of the hole in the steel support plate would make even less difference to the load carried, because it is bearing plates tested with a small diameter of hole in the steel support plate that fail by shearing. The difference in load carried is so small that the radius on the edge of the hole in the steel support plate probably does not need to be specified in bearing plate tests.

### 7.4.3 Diameter of nut

The laboratory testing results comparing different diameters of nut show that in general the larger the diameter of nut the higher the load carried (table 5.3). This was the same conclusion reached in the FEA tests (figure 4.14).

The laboratory test results also suggest that with a larger diameter of nut, the difference in load carried between different diameters of hole in the steel support plate is greater (table 5.3). This interaction was also suggested by the FE work (figure 4.14).

If the diameter of the nut is larger than the diameter of the hole in the steel support plate, the load carried by the nut as it is pushed through the steel support plate, is clearly a property of the nut, not of the bearing plates. Hence the peak load obtained is the highest load carried by the bearing plate as the tests were stopped before the nut was forced through the steel support plate (if the nut had a larger diameter than the hole in the steel support plate).

### 7.4.4 Diameter of central hole in bearing plate

The laboratory tests on Weldgrip bearing plates with different diameters of hole in the centre of the bearing plate, show that the diameter of the hole in the centre of the bearing plate is a more complicated parameter than was suggested by the FEA results (section 5.5).

With a large standard hole in the centre of the Weldgrip bearing plate and a 100 mm hole in the steel support plate the Mai nut was able to force its way into the centre of the bearing plate, and then caused cracks to be formed suddenly. However these cracks did

not spread all the way to the edge of the bearing plate. With a small hole in the centre of the bearing plate, the Mai nut could not force its way into the centre of the bearing plate and the plate failed catastrophically by breaking in half (figure 5.8). With a large hole in the centre of the bearing plate and a large nut the nut was not able to force its way into the centre of the bearing plate and the plate failed by excessive bending and the production of small cracks.

The different failure mechanisms of the Weldgrip bearing plate with a small and large diameter of hole in the centre of the bearing plate, can be explained by the results shown in table 4.7. The smaller the diameter of hole in the centre of the bearing plate, the larger the tensile circumferential stress. Hence the larger cracks with the smaller diameter of hole.

The laboratory testing results of varying the diameter of the bearing plate central hole demonstrate both the problems and benefits of reducing the hole diameter. Decreasing the hole diameter tends to prevent the nut from being forced into the centre hence increasing the load carried during initial loading. However decreasing the diameter of the central hole can cause catastrophic failure at a lower peak load (table 5.4).

#### 7.4.5 External diameter and shape of bearing plate

The laboratory testing results given in table 5.5 suggest that decreasing the external diameter of the bearing plate, makes a very small reduction in the load carried. This result was also suggested by the FEA work in the 2 level Taguchi experiment (table A1.1) and one factor at a time tests (table A1.4). There appears to be no significant change in load carried between a circular and square shaped bearing plate (table 5.5).

However the real issue concerning the external diameter of the bearing plate is the bearing area over which load is applied. Neither the FEA work or the laboratory test is adequately investigating this issue.

The failure mechanism with different external diameters of bearing plate varies slightly. For a 60 mm hole in the steel support plate the failure is by shearing in an almost identical manner for both diameters of plate, except that with a smaller diameter of bearing plate, a circumferential crack was formed on the upper surface of the bearing plate underneath the nut. For a 70 mm hole in the steel support plate, the failure mechanism is the same for both diameters of plate, except for a circumferential crack underneath the nut in the smaller bearing plate (see figure 7.2). With an 80 mm hole the failure mechanism for both diameters of bearing plate is very similar except with the smaller bearing plate diameter the crack on the lower surface of the bearing plate extends much further to the outer edge of the bearing plate. The failure mechanism of the large circular plate appeared identical to the failure mechanism of the square original shape.



**Figure 7.2** Circumferential crack in Weldgrip bearing plate of external diameter 98 mm when tested with a 70 mm hole in the steel support plate

The difference between the failure mechanism with the different external diameters of bearing plate, could be due to the way in which the edges of the bearing plate tend to ‘lift off’. This occurs with both large and small diameters of bearing plate. However with a small diameter of bearing plate the upwards deflection close to the centre is more than for a large diameter of bearing plate, (see table 4.6). If the deflection in the positive  $y$  direction at a set distance away from the centre of the bearing plate is more, the radial stress in the bearing plate is likely to be more. This was observed in FE models of the Weldgrip bearing plates, as shown in table 4.8. Hence if the tensile radial stress underneath the nut is greater, this would explain the formation of a circumferential crack under the nut in the smaller diameter of bearing plate (figure 7.2). The larger deflection close to the centre may cause the tensile circumferential stress on the lower surface of

the bearing plate to be greater for a smaller diameter of bearing plate, as observed in table 4.8. Hence this may explain why with an 80 mm hole in the steel support plate the radial cracks spread further outwards from the centre of the Weldgrip bearing plate for a small diameter of bearing plate than a large diameter of bearing plate.

#### 7.4.6 Rate of loading of bearing plate

Tests on the Weldgrip bearing plate at different rates of loading (table 5.2) suggest that there is not a large change in load carried with the different rates of loading. However there does appear to be a change in the failure mechanism with different rates of loading. The greater the rate of loading, the more catastrophic the failure mechanism becomes.

It has been observed that decreasing the diameter of the hole in the centre of the bearing plate and increasing the rate of loading both make the failure mechanism of the Weldgrip bearing plate more catastrophic. It is possible that these factors are related because they both increase the rate at which the tensile circumferential stress on the lower surface of the bearing plate increases.

As observed in table 5.7, the smaller the diameter of hole at the centre of the bearing plate, the larger the tensile circumferential stress per 1 mm deflection. Therefore for a constant rate of loading, the rate of increase of tensile circumferential stress is greater for a small hole in the centre of the bearing plate than a large hole. Hence decreasing the diameter of the hole at the centre of the bearing plate and increasing the rate of loading both increase the rate of increase of tensile circumferential stress / strain and make the failure mechanism more catastrophic.

#### 7.4.7 Load applied to bearing plate via bolt

The results given in table 5.6, section 5.7 suggest that applying the load to the bearing plate via the nut directly or via the bolt from above makes negligible difference to the load carried and to the failure mechanism. BS 7861 specifies that the load should be applied to the bearing plate via the bolt by pulling down on the bolt from below; this was not possible with the apparatus available, and the results in table 5.6 suggest that this probably would not have made any difference to the load carried or to the failure mechanism. The Canadian and American standards both specify that the load can be applied to the bearing plate from above or below, via the bolt or via a punch. The test proposal in section 7.4.11 specifies that load is applied via the nut from above as this appears to give as good a representation as any available options.

#### 7.4.8 Bearing plates tested at an inclined angle

The results given in table 5.7 show that the load carried when the bearing plate is supported at an inclined angle of  $10^\circ$  is less than the load carried when the bearing plate is supported flat. This could be because the bearing plate is supported by an elliptical shape which has a maximum dimension of 102 mm and a minimum dimension of 100 mm. It is perhaps more likely to be due to the fact that the load may be applied to the bearing plate unevenly with more load applied to one half than the other half. The non symmetrical bending observed is perhaps compatible with the failure mechanism from the mines. Many bearing plates from the mines displayed non symmetrical bending; this shows that the load being carried in the mines may be less than the expected load predicted by tests where the load is supported flat.

#### 7.4.9 AMS green circular plate

The failure mechanism produced by the AMS bearing plate, was caused by the fact that the AMS end fitting had a very small external diameter of only 40 mm which enabled the end fitting to be forced into the centre of the bearing plate. A similar failure mechanism to the Weldgrip bearing plate and Mai nut except that the cracks were not formed at the time of testing for the AMS bearing plate. Cracks initiated on the lower surface of the AMS bearing plate, weeks after the test had been carried out (figure 5.9). The cracks which formed in the AMS bearing plate suggest the presence of high tensile circumferential stresses on the lower surface of the bearing plate perpendicular to the cracks. Stress relaxation then took place and the cracks formed and grew over several months.

The difference between the failure mechanism of the AMS bearing plate and AMS end fitting (section 5.10, figure 5.9, 5.10) and the Weldgrip bearing plate and Mai nut / AMS end fitting (section 5.5, figure 5.7) is probably because of the greater ductility of the material used in the AMS bearing plate. The AMS bearing plate has a smaller diameter of central hole than the Weldgrip bearing plate. Hence the circumferential stress / strain in the AMS bearing plate with the nut / end fitting forced into the centre will be larger than for the same nut with the Weldgrip bearing plate. Hence it must be the difference in material behaviour that causes the different failure mechanisms. The AMS bearing plate material (high density polyethylene) has a lower Young's modulus than the Weldgrip bearing plate material but may have a better ductility, (see table 6.1 for material selection criteria required for bearing plate).

#### 7.4.10 Bearing plates failed in collieries

The failure mechanism of the Mai bearing plate used in the mines is different from that of the Weldgrip plate used in the mines (figures 2.2, 2.3 and 2.4). The Weldgrip bearing plate has failed by bending and by allowing the nut to be forced through the centre of the bearing plate. The Mai bearing plate has failed by large cracks forming and breaking the bearing plate in half. This is almost certainly due to the different materials used in the bearing plates, not the different shapes. The Mai plate shows some signs of initial bending but has failed catastrophically, probably because the Mai plate is made from much more brittle material (glassfibre). The failure mechanism of the Weldgrip bearing plate is preferred by colliery rockbolting engineers to the failure mechanism of the Mai bearing plate because it is less sudden and catastrophic.

Failure in the coal mines of Weldgrip bearing plates always involves bending of the bearing plate with the centre of the bearing plate deflecting downwards (into the coal face) see figure 2.2. A very unusual failure mechanism is for the bearing plate to form cracks extending radially outwards from the centre of the bearing plate in addition to the bending observed (figure 2.3). Inspection of this crack in the Weldgrip bearing plate suggests that it initiated on the lower surface of the bearing plate. FE models of the Weldgrip bearing plate support this theory, figure 4.21. The FE models of the Weldgrip bearing plate predicted compressive circumferential strains on the upper surface of the bearing plate, and tensile strains on the lower surface of the bearing plate (figure 4.21). Weldgrip bearing plates tested with large holes in the steel support plate also formed cracks which initiated on the lower surface of the bearing plate.

The Weldgrip bearing plate deformation during testing appeared similar to the bending encountered in failed plates from the mines, apart from the fact that the bending in the

laboratory was more symmetrical. Weldgrip bearing plates used in coal mines had large amounts of localised plastic deformation at the centre of the bearing plate. Weldgrip bearing plates tested in the laboratory did not display this deformation. One of the main differences between the bearing plates tested with a 100 mm / 120 mm hole in the steel support plate and the bearing plates that failed in the mines, is the fact that the plates used in the mine were tested over a long period of time and hence had time for creep or stress relaxation to take place, whilst the bearing plates in the laboratory were tested over a very short period of time at a rate of 5 mm/min. This could partially explain the difference in the appearance of the failed laboratory tested and colliery used plates.

The loading and support conditions encountered in the mine are more complex than that simulated in the laboratory. In the mine a hole of approximately 28 mm is drilled in the rock (coal). A plywood plate with a central hole of 25 mm diameter is used. Clearly the hole in the rock will not be a perfect hole and the plywood bearing plate may not be supported at a diameter of 28 mm. Also the coal surface will be very uneven and hence parts of the bearing plate will be supported initially whilst other parts will not. The coal itself has quite a low compressive strength ( $30 \text{ MN/m}^2$ ), hence as the load on the plate increases the coal itself may fail and cause the bearing plate to be supported further away from the centre (see Appendix 4 for calculations of the load to cause crushing of the coal). Clearly the failure of the coal is almost impossible to simulate in the laboratory. Douglas (1983) suggests the use of resin spread onto the rock / coal before the bearing plate is installed to enable the load to be spread more evenly.

The fact that the corners of the Weldgrip bearing plates that failed in the mines are free from scratches, suggests that they had 'lifted off' and were not in contact with the coal

or plywood plates. Bearing plates tested in the laboratory and modelled using FEA also ‘lifted off’ at the edges (see table 4.6).

#### 7.4.11 Laboratory bearing plate test proposal

As figure 5.4 shows, the diameter of the hole in the steel support plate greatly affects the peak load carried by the bearing plate. Hence to be able to compare different designs of bearing plate they must be tested with a standard diameter of hole in the steel support plate. However the current BS 7861 diameter of 55 mm has been shown not to give a realistic representation of the failure mechanism encountered in the mine.

A test using a steel support plate with a 100 mm diameter hole would appear to be more appropriate than a steel support plate with a 55 mm hole, because the failure mechanism with a 100 mm hole is by bending whereas with a 55 mm hole the failure is by shearing (figures 5.1, 5.2 and 7.1). The failure encountered in the coal mines (figures 2.2, 2.3) is a bending type failure. The exact choice of hole diameter is perhaps not absolutely critical as long as the failure is by bending rather than by shear.

As the laboratory testing and FEA results show, the difference in performance between different bearing plates varies with small and large diameters of hole in the steel support plate (see figures 5.4 and 4.4). Therefore it is necessary for a bearing plate approval test to simulate as closely as possible the loading conditions encountered in the mines so that a bearing plate that performs well in the laboratory test will also perform well in the coal mine.

Figure 7.3 shows a proposed test for non metallic rockbolt bearing plates, which has been shown to produce a failure mechanism which is closer to the failure mechanism encountered in coal mines than the current BS 7861 test.

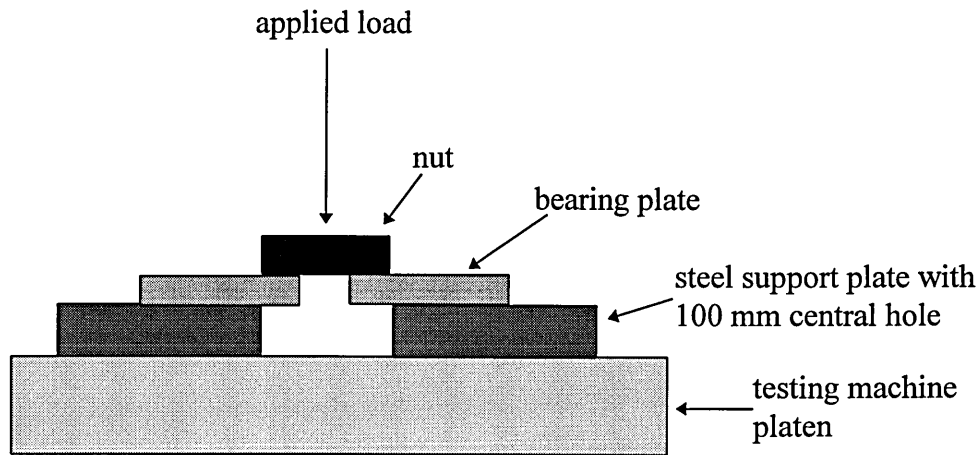


**Figure 7.3** Proposed test on non metallic rockbolt bearing plates for use in coal mines

The bearing plate should be centrally positioned on the steel support plate.

Despite the fact that the results shown in table 5.2 suggest that the rate of loading does not greatly change the load carried; to enable valid comparisons to be made between test results a standard rate of loading is proposed. A rate of loading of 5 mm/min would appear to be a sensible choice.

As there is some scatter produced on tests of polymeric components ideally at least five bearing plates should be tested. As this research has shown that the external diameter of the nut alters the load carried by a bearing plate (table 5.3), the nut that will be used with the bearing plate down the coal mine should be used to test the bearing plate.

The peak load carried in the test should be recorded and the failure mechanism noted. A slow gradual failure mechanism is preferable to a sudden catastrophic failure.

There are a number of limitations to the above test proposal. Performance over a long period of time is not considered, because results are usually required quickly not in two years time. Also the above test does not include a test on the threadform used. As the hole diameter specified in figure 7.3 is much larger than that specified by BS 7861, the load carried to cause failure is reduced. Hence it is perhaps unlikely that the threadform would fail before the bearing plate. Hence a separate test is required to test the rockbolt threadform and the nut threadform. The above test does not consider the issue of out of alignment angles of bearing plates.

A bearing plate that withstands a load of at least 40 kN with a 100 mm hole in the steel support plate would perform better in the coal mine than the best bearing plate currently available (see figure 5.4). However as shown in figure 5.4, a minimum requirement of 16 kN would ensure that the Weldgrip would pass this test and a minimum load of 35 kN would ensure that the Weidmann bearing plate would pass this test. The current requirement in BS 7861 is 50 kN with a 55 mm hole in the steel support plate. To ensure that bearing plates currently used will pass the test, a load of 16 kN with a 100 mm hole is proposed.

BS 7861 does not include a test on the larger plywood bearing plates or header plates that are used in conjunction with bearing plates in UK coal mines. As plywood bearing plates have been observed to fail down coal mines, it would appear to be sensible to include a test on the plywood plates. The test proposed in figure 7.3 for smaller polymeric bearing plates may not be suitable for large plywood plates. A test with a larger hole in the steel support plate of around 150 mm as specified by the Canadian Standard, may be suitable, although further work would be needed to establish this.

### **7.5 Material selection**

The FE modelling of the three main materials investigated showed polypropylene to perform better than polycarbonate or polyamide 6 (see figures A1.2, A1.11 and A1.12). Most of the FE work was based upon the load to cause 1 mm deflection, hence the material that performs best will be the one with the highest stiffness or secant modulus. The FE modelling was all carried out at low stress and strain levels. Figure 6.4 shows that at low levels of strain the polypropylene has the highest secant modulus, however at high levels of strain the polycarbonate and polyamide 6 have higher values of secant modulus than the polypropylene. Hence the relative performance of the different materials depends upon the level of the performance criteria chosen. If 2 or 3 mm deflection had been chosen instead of 1 mm for the performance comparison, the polyamide and polycarbonate may have been shown to perform better than the polypropylene. Hence this shows that simply looking at one value of secant modulus for the material is a simplistic approach.

The terms polyamide, polypropylene and polycarbonate cover a broad range of different materials. The results showing polypropylene with the greatest stiffness are based upon the particular grades chosen from the Campus database.

The material selection charts (figures 6.1, A3.2, A3.3 and A3.4) also suggest polypropylene as a suitable material. Polypropylene appears to have an acceptable level of Young's modulus, ductility, cost per unit volume, anti flammatory properties and maximum service temperature. However it is recognised that there is a large variety of materials with different strengths and stiffness, which can be classified under the broad term polypropylene. When choosing a specific grade the above properties need to be

considered and also the creep properties and performance at elevated temperatures of up to 40°C investigated. Software packages such as Plascams could be used to find a specific grade of material for use in a bearing plate.

## 7.6 Summary of how results can be used to design bearing plates for use in coal mines

### 7.6.1 Design specification

BS 7861 on rockbolting gives minimum performance levels for bearing plates and rockbolting components to be used in coal mines. As shown in Chapter 5 the BS 7861 test to evaluate bearing plates does not produce the same failure mechanism as is encountered in the coal mines. Table 7.1 gives a specification for a bearing plate to comply with BS 7861, and a modified version for a bearing plate to be used in the coal mines, based on this research and consultations with mining engineers. The proposed test produces a bending type failure mechanism as encountered in the coal mines, whereas the existing BS 7861 test produces a shear failure mechanism.

	BS 7861 specification	Proposed specification - design for colliery
Performance	50 kN when tested with 55 mm hole in steel support plate allows an out of alignment angle of at least 18°	40 kN when tested with 100 mm hole in steel support plate allows an out of alignment angle of at least 18°
Materials	non-metallic	non-metallic
Target product cost	not specified	target price - 80p
Life in service	not specified	up to 2 years
Size	not specified	spreading load over as large an area as possible minimum 0.016 m <sup>2</sup>
Safety	flame retardancy properties anti-sparking properties nut fails before bearing plate	flame retardancy properties anti-sparking properties nut fails before bearing plate bearing plate in full contact with rock after yielding
Environment	not specified	temperature 20 - 40 °C

**Table 7.1** Design Specification for non metallic bearing plates

Laboratory tests on bearing plates have shown that using a 100 mm diameter hole in the steel support plate is a more representative test on bearing plates than using a 55 mm hole (see figures 5.1, 5.2 and 5.7). Hence the proposed specification is based upon the

performance of the bearing plates with a 100 mm hole in the steel support plate. The suggested load to be carried by the bearing plate is reduced to 40 kN from 50 kN. Despite the reduction in load requirement, with the change in diameter of the hole in the steel support plate, the proposed test is more stringent than the existing BS 7861 test (see figure 5.4). Since the load that is applied to the bearing plates in the coal mines is unknown, it is not simple to define a minimum load for the bearing plate to be able to carry. However it is known that the bearing plate which performs best in the coal mines according to colliery rockbolting engineers (Weidmann webbed bearing plate) carries a load of 37 kN with a 100 mm hole in the steel support plate (see figure 5.4). The Weidmann bearing plate tends to fail completely in only 5 % of cases (table 2.1), and exhibits signs of failure in around 50 % of cases. Hence a bearing plate which carried a minimum load of more than 40 kN when tested in the laboratory with a 100 mm hole in the steel support plate would produce a better performance than the best product currently available.

BS 7861 does not specify a minimum bearing area or size of the bearing plates. However from a Rock Mechanics perspective the bearing plate is required to have as large a surface area as possible in order to spread the load over as large an area of the rock as possible. As shown by equations 1.1 and 1.2 the larger the surface area of the bearing plate, the larger the stiffness of the rockbolt on the mine wall. Plywood plates are used in conjunction with polymeric bearing plates to enable the load to be spread over a larger area of the rock. If a bearing plate of a large diameter (around 300 mm) could be produced, which did not 'lift off' at the edges, there would be no need for the plywood plate, which would give a large cost advantage by only requiring one bearing

plate. However a larger bearing area is of no use if the corners of the bearing plate simply lift away at the edges.

BS 7861 includes flame retardant and anti-sparking property requirements because of the danger of sparks and fire down the mines. BS 7861 does not mention the length of time that the bearing plate may be used for or the temperature it will be subjected to. Two years in service and a temperature of 40°C are taken as the worst cases likely to be encountered.

The fact that the bearing plate may be in service for up to 2 years suggests that creep of the polymer material may be a problem. However discussions with colliery rockbolting engineers established that the load on the bearing plate was not applied steadily over the two year period. In practice the load on the bearing plate increases due to excavation of coal nearby increasing the loading on the coal still to be mined and hence increasing load on the rockbolt and bearing plate. Another factor which can cause the load to be increased include mine workings above or below the roadway.

BS 7861 also specifies that the polymeric nut should still be intact after the failure of the bearing plate, and that the failure mechanism should be progressive, without sudden catastrophic failure. If the performance of the bearing plate is greatly increased, the polymeric nut may fail before the bearing plate.

### 7.6.2 Design guidelines

The diameter of hole in the steel support plate has been found to be the most significant parameter concerning the design and testing of bearing plates. It has also been found

that the optimum level of many other parameters depends upon the diameter of hole in the steel support plate. Therefore before designing a bearing plate using the results given in this thesis it is necessary to establish what diameter of hole in the steel support plate is applicable. As shown in section 5.2 and discussed in section 7.4 a 100 mm diameter of hole in the steel support plate gives a reasonable approximation of the mine behaviour, although the actual support diameter will vary greatly for individual bearing plates, depending upon the compressive strength of the coal (see Appendix 4). Hence when using the results in this thesis to design a bearing plate for use in a coal mine, results with a 100 mm hole in the steel support plate should be used. However as shown in Appendix 4, if the coal has a very low compressive strength, results with a 120 mm hole in the steel support plate are more akin to real situation.

The depth of the bearing plate and the coned angle have been found to be the second and third most significant parameters respectively. Figure A1.5 shows the variation of coned angle for different depths of bearing plate for a 100 mm hole in the steel support plate. Figure A1.6 shows the variation of depth of bearing plate for different coned angles with a 100 mm hole in the steel support plate. These two graphs both show that in general a large depth of bearing plate and a large coned angle give a more efficient design on a load / volume basis, which considers the efficient distribution of material. However an efficient design does not carry much more load than is necessary and so an efficient design for use in the coal mine is not the same thing as an efficient design on a load / volume basis.

To design a bearing plate for use in a coal mine, results presented in Chapter 4 and Appendix 1 for a 100 mm hole in the steel support plate should be used. The results in

figure A1.5 can be used to suggest dimensions for reasonably efficient (not optimum) designs. From figure A1.5 it can be seen that a depth of 30 mm and coned angle of  $30^\circ$  would be a reasonable design. If a larger stronger design was required a bearing plate of depth 35 mm and coned angle  $35^\circ$  would be suitable. If an even larger stronger bearing plate was required a depth of 40 mm and coned angle of  $40^\circ$  or a depth of 45 mm and coned angle of  $45^\circ$  is recommended. These suggested bearing plate dimensions are compared with existing designs in table 7.2. A major problem with the method used is that the load carried by the FE models is not the load carried to cause failure in laboratory tests. Hence it is not known what the designs suggested will carry in real laboratory tests. The only way to determine the failure load of the new designs is to produce samples and carry out real laboratory tests.

Table 7.2 gives a simple comparison of the load and load / volume carried by different bearing plate designs in FE tests using a 100 mm hole in the steel support plate using the Weldgrip and Weidmann material data respectively. Table 7.2 shows that the new designs are much stiffer than existing designs, requiring a higher load to cause 1 mm deflection. In practice, although new designs are much stiffer than existing designs, the new designs may fail due to excessive tensile circumferential stress on the lower surface of the bearing plate.

Bearing plate	Load to cause 1 mm deflection	Load / volume to cause 1 mm deflection (N/mm <sup>3</sup> )
Weldgrip	0.944 kN	0.006267
Weidmann	1.699 kN	0.008665
depth 30 mm coned angle 30°	3.93 kN, 3.2 kN	0.02055, 0.01671
depth 35 mm coned angle 35°	5.52 kN, 4.44 kN	0.02613, 0.02103
depth 40 mm coned angle 40°	6.95 kN, 5.659 kN	0.03061, 0.02491

**Table 7.2** Load carried by bearing plate FE models with a 100 mm hole in the steel support plate

The new designs of bearing plate appear to perform much better than the Weldgrip bearing plate when evaluated using FEA. It can be seen that as the depth and coned angle increases the efficiency on a load / volume basis increases.

The advantage in performance of the new designs compared to the Weldgrip designs is partially due to the different designs at the centre of the bearing plate, not just the different depths and coned angles. The practice of creating a conical seat for the nut to sit in and allow out of alignment, means that material thickness is reduced at the centre of the bearing plate where it is needed most.

The choice of material is very important for bearing plate performance. Chapter 6 gives some materials selection criteria, the points highlighted in Chapter 6 need to be carefully considered before choosing a material for the bearing plate. The material selection charts (figures 6.1, A3.2, A3.3 and A3.4) suggest that polypropylene is a suitable material although this is a large category with a large range of material properties.

It has been shown (figure 4.12) that the larger the external diameter of the nut the more load the bearing plate will carry. Calculations in Appendix 1 have shown that in general it is better to add extra material to increase the nut diameter and not the bearing plate depth. However clearly the nut diameter should not be increased infinitely and the limits of this calculation have not been established. The results in table 7.2 are based upon a nut diameter of 56 mm which is the largest nut currently available.

The FE results are thought not to be giving a clear indication of the best values for the diameter of the hole in the centre of the bearing plate. As discussed in section 7.3.7 the performance comparison chosen perhaps hinders the interpretation of this parameter. However it is recognised that the depth of the bearing plate is a much more significant parameter than the central hole in the bearing plate. To ensure that the 18° out of alignment angle specified by BS 7861 is possible, once the depth of the bearing plate has been chosen; the minimum diameter of bearing plate central hole to allow 18° out of alignment can be read off figure 2.5. Assuming that no more than 18° out of alignment is required the minimum values of bearing plate central hole diameter given in figure 2.5 is probably a sensible choice of hole diameter, as if the bearing plate central hole diameter is too large or the nut too small the nut will simply pull through the bearing plate. However as shown in figure 2.5 to allow an out of alignment angle of 18° with large diameters of bolt, requires a large hole in the centre of the bearing plate.

The FE results suggested that a solid bearing plate is preferable to a webbed bearing plate. However it should be remembered that the FEA does not consider the problem of moulding polymeric components with large thickness. If a bearing plate design is to be webbed, 12 radial webs appears to be a suitable number as shown in figure 4.14. Five

circumferential webs with the web positions shown in webbed designs 5 and 8 (figures A1.18, A1.21) appears suitable. The best web thickness for each portion of the webbed bearing plate can be read off figure A1.28. A general trend throughout the FEA tests is that material needs to be concentrated in the area within the diameter of hole in the steel support plate. Hence the coned shape of the bearing plate and for webbed bearing plates concentrating webs close to the centre.

The results in this thesis have shown that is best for a coned shaped bearing plate to have straight sides.

The 2 level Taguchi experiment and one factor at a time results both suggested that on a load / volume basis a bearing plate with a small external diameter is best; but on the basis of load a large external diameter is best (table 4.1, A1.1, A1.4). However the method used in this thesis does not consider the advantages of the bearing plate performance in terms of area of rock / coal that load is transferred over. This is a limitation of this work. As shown in equations 1.1 and 1.2 the larger the surface area of the bearing plate the greater the support offered by the bearing plate to the rock.

The laboratory testing results shown in table 5.5 suggest that the load carried is not significantly affected by a circular or square shape to the bearing plate. Hence on a load / volume basis a circular shape is probably best, because a circular shape does not have wasted material at the corners a long way from the centre. However it could be argued that the corners of the square bearing plate are increasing the area of the bearing plate in contact with the rock and hence a square bearing plate (of the same dimension as the diameter of a circular plate) is better, although this is increasing the amount of material

required. The shape that is easiest / cheapest to manufacture is probably the most sensible option.

This thesis has looked principally at the non metallic bearing plate used in conjunction with GRP rockbolts in UK coal mines. However it is perhaps a mistake to look solely at one aspect of a rockbolting system without considering the entire rockbolting system. As previously identified by O'Grady (1994) the load carried by a bearing plate is limited by the bearing plate design and by the compressive strength of the coal itself. Whilst there is scope for improving the design of the bearing plate, the compressive strength of the coal itself is a limiting factor as shown in Appendix 4. As identified by Fabjanczyk (1992) poor load transfer between the resin and rock and between the resin and bolt leads to higher forces on the bearing plate and end fitting. Consideration therefore needs to be given to other aspects of the rockbolting system including the resin / grout used and the surface of the rockbolt.

## CHAPTER 8

### 8. CONCLUSIONS

#### 8.1 Geometry of bearing plate

This thesis appears to be the first time that either Finite Element Analysis or Taguchi experimental design methods have been applied to the design of bearing plates. This appears to be the first study comparing testing methods and failure mechanisms of non metallic bearing plates. Although design work on bearing plates has been carried out by various manufacturers already, this is the first time that the work has been made publicly available.

The results from the FE and laboratory tests on the bearing plate produced some basic conclusions which are included below for completeness.

- The smaller the diameter of the hole in the steel support plate, the more load the bearing plate will carry. This was observed in both the FEA and laboratory testing results.
- Increasing the depth of the bearing plate increases the load carried.
- A flat plate is preferable to a coned plate of the same central depth when comparing the load carried.
- A larger diameter of nut increases the load that the bearing plate will carry. This was observed in both the FEA and laboratory testing results.
- A solid design of bearing plate is preferable to a webbed design when comparing the load carried.

The FE and laboratory testing also produced some conclusions that were not expected before the study.

1. As the depth of the bearing plate increases, the rate of increase of load with increasing depth decreases. If the bearing plate depth is evaluated on the basis of the load / volume,

there is a peak or optimum depth, this depth depends upon the diameter of the hole in the steel support plate. The larger the diameter of hole in the steel support plate, the larger the optimum depth of the bearing plate.

2. If the load / volume is considered it is best to have a coned plate. The optimum value of the coned angle depends upon the diameter of the hole in the steel support plate and the central depth of the bearing plate. The smaller the diameter of the hole in the steel support plate, the larger the optimum coned angle. The larger the depth of the bearing plate, the larger the optimum coned angle.

3. Designs that are thicker at the centre of the bearing plate are preferable to designs that are thicker over the edge of the hole in the steel support plate.

4. A smaller external diameter of bearing plate produced a slightly smaller load than a larger diameter of bearing plate, this was observed in the FEA tests and the laboratory tests.

5. If comparing the load / volume a solid plate performs better than a webbed plate in the vast majority of cases. With a small hole in the steel support plate, with webs concentrated close to the centre of the bearing plate and with an efficient web thickness the webbed plate sometimes performs better. In a webbed design the optimum number of radial webs depends upon the diameter of the hole in the steel support plate. Similarly the optimum number and position of the circumferential webs depends upon the diameter of the hole in the steel support plate. In general for a webbed design of bearing plate, the webs close to the centre and around the restraint should be as thick as possible. Webs at diameters greater than the diameter of hole in the steel support plate should be

as thin as possible to increase efficiency on a load / volume basis. Whether it is best to increase the thickness of the radial webs or the circumferential webs depends upon the number of radial and circumferential webs in the design. The optimum web thickness of a webbed design depends upon the diameter of the hole in the steel support plate.

6. Material is more efficiently used if it is added to the nut rather than the bearing plate, assuming that the cost of the material used in the nut is the same as the cost of the material used in the bearing plate.

7. The methodology used showed that it was best to concentrate the material in the central region of the bearing plate within the area of the hole in the steel support plate. However the British Standard test and the method used in this thesis does not consider the design of the outer region of the bearing plate.

## **8.2 Laboratory testing parameters**

The most important conclusion from the laboratory tests is that a new test for bearing plates is required. The current diameter of hole in the steel support plate specified in BS 7861 (55 mm) does not correspond with the failure mechanism in the coal mines, as a shear failure mechanism is produced. A larger hole diameter of 100 mm produces a bending failure, which gives a better representation of the failure mechanism encountered in the coal mines. Hence a hole diameter of 100 mm is proposed.

A number of further conclusions can be drawn from the results of testing bearing plates in the laboratory:-

1. Small diameters of hole in the steel support plate produce a shear failure of the bearing plates. Large diameters of hole in the steel support plate produce a bending failure.
2. The rate of loading used when testing bearing plates in the laboratory has a negligible effect on the load carried by the bearing plate.
3. The radius on the edge of the hole in the steel support plate caused a difference of less than 2 % to the load carried by the bearing plate and no change in the failure mechanism.
4. Bearing plates tested with an out of alignment angle of  $10^\circ$  carried 8 % less load than bearing plates tested flat.

### **8.3 Stress / strain distribution in bearing plate**

Stress levels in regions of the bearing plate greater than the support plate hole diameter are very low usually less than  $2 \text{ MN/m}^2$ .

Loading of the bearing plates creates tensile circumferential stress on the lower surface of the bearing plate and compressive circumferential stress on the upper surface of the bearing plate. The stress distribution produced by FE models of the Weldgrip bearing plate is compatible with the laboratory and coal mine failure mechanism of the Weldgrip bearing plates.

### **8.4 Methodology**

The main disadvantage of the Taguchi method (not including all possible interactions in the experiment) has been demonstrated in this thesis. However by using the Taguchi method the number of FE models required in the initial screening process was reduced

from 256 to 16 FE models. Hence on balance the Taguchi method provided a good starting point.

### **8.5 Materials**

The material selection exercise described in Chapter 6 suggested polypropylene as an appropriate material for a bearing plate. Clearly the choice of materials is limited to what is currently available. The particular grade used needs to be carefully chosen considering the points raised in Chapter 6.

### **8.6 Further Work**

1. As mentioned in Chapter 6 the suitability of a design for injection moulding could be investigated using Moldflow injection moulding software. This software can be used to determine whether a mould will fill satisfactorily and the cooling times required before going to the expense of producing a mould.

2. Solid and webbed designs of bearing plate have both been investigated in this thesis. However combined solid and webbed designs - solid in the centre and webbed at outer regions of bearing plate have not been investigated. Combined solid and webbed designs may be beneficial because the results in this thesis have shown that it is best to increase the amount of material at the centre of the bearing plate rather than the outer edges of the bearing plate.

3. The concave upper surface at the centre of the bearing plate for the nut to sit in has not been investigated. As the results in this thesis have shown that it is best to concentrate material close to the centre of the bearing plate, the effect of taking material away from this region to allow for the movement of the nut and conical seat is likely to be highly significant.

4. There are a number of possible interactions that have not been investigated:-

Coned angle v Number of radial webs

Coned angle v Number of circumferential webs

Coned angle v Web thickness

Depth of bearing plate v Number of radial webs

Depth of bearing plate v Number of circumferential webs

Depth of bearing plate v Web thickness

Number of radial webs v Number of circumferential webs

As the results in this thesis have suggested that a solid plate is preferable to a webbed plate these interactions are not relevant. However if for manufacturing reasons a webbed design of bearing plate is required, these interactions should be investigated.

5. As mentioned in Chapter 6 very limited creep material data is available and creep needs to be carefully considered when choosing a particular grade of material. As the bearing plate may be used underground for up to 2 years, creep behaviour is an important consideration.

6. The advantages of a larger diameter of bearing plate and the extra support that this offers to the coal wall have not been investigated. The design of the outer regions of the bearing plate and the required thickness of bearing plate to offer sufficient support to the coal has not been investigated. This requires detailed consideration of the problem from a Rock Mechanics perspective.

7. BS 7861 does not include a test for the large plywood plates used in conjunction with the polymeric plates. The suitability of the test included in the Canadian Standard, with a 150 mm hole in the steel support plate could be investigated and a new test proposal made if appropriate.

## References

- ABAQUS (1994) User's Manual 1, version 5.4, Hibbitt, Karlsson and Sorensen, Inc.
- American Standard (1983) Specification for Roof and Rock Bolts, and accessories, F432
- AROA (1992) Applied research of Australia party Ltd, Private Communication
- Ashby M.F. (1992) Materials Selection in Mechanical Design, Pergamon Press, 1st edition.
- Ashby M.F. (1992) Materials Selection in Mechanical Design, Materials and Process Selection Charts, Pergamon Press.
- Bell F.G. (1992) Engineering in Rock Masses, Butterworth-Heindemann Ltd
- Benmokrane B., Xu H., Bellavance E. (1996) Bond Strength of cement grouted Glassfibre reinforced Plastic (GFRP) anchor bolts. International Journal of Rock Mechanics, Mining Sciences and Geomechanics Abstracts, v 33 n 5 pp 455-465
- Bigby D.N. (1997) Developments in British Rockbolting Technology, Coal International, May, pp 111 - 116
- Boresi A.P., Schmidt R.J., Sidebottom O.M. (1993) Advanced Mechanics of Materials, 5th edition, John Wiley and Sons
- Brady B.H.G., Brown E.T. (1993) Rock Mechanics for underground Mining 2nd edition, Chapman & Hall.
- Brown E.T., Bray J.W., Ladanyi B., Hoek E. (1983) Ground response curves for Rock Tunnels, Journal of Geotechnical Engineering v109 n1 January 1983 pp 15-39
- British Coal Operating Instructions OI/30 (1993) Rockbolting in Mines.
- British Coal Code of Practice, Cable bolting for Roof Support
- British Standard 7861 (1996) Strata reinforcement support system components used in coal mines. Part 1 Specification for Rockbolting, Part 2 Specification for Birdcaged Cablebolting.
- BS 2782 (1976) Methods of testing plastics. Part 3. Mechanical properties. Method 320C
- Cambridge Material Selector, version 2.0
- Canadian Standard (1990) Roof and Rock bolts, and accessories
- Conley N., Priest S.D. (1992) Tests make the case for "Plastic" Roof Bolts, Colliery Guardian, v240 n2 March 1992 pp 72-80.

- Davies R.A. (1977) A catalogue of strength properties of some coal measures rocks, National Coal Board Internal Report
- Daws G. (1978) Resin Anchors, Civil Engineering October 1978, pp71-75
- Daws G. (1987) Coal Mine Roofbolting, Mining Engineer v147 n313 pp 147-154
- Daws G. (1988) Roofbolting in the mining industry, Mine and Quarry v17 n11 pp17-20
- Daws G. (1991) Cable Bolting, Mining Engineer v150 n353 pp 261-266
- Daws G. (1991) The use of pumped resins for Rockbolt anchorage at Pen y Clip.
- Daws G. (1994) Letter to the editor and author's response (Rockbolting), Coal International v242 n6 November 1994
- Daws G. (1995) APEX Report, Testing of Cable bolts
- Douglas T.H., Arthur L.J. (1983) Guide to the use of Rock Reinforcement in underground excavations CIRIA 101 Construction Industry Research and Information Association.
- Dunham R.K., Pugh W.L. (1991) Rockbolt trials in the Ince Six Feet Seam, Golborne Section, Bickershaw colliery complex, Mining Engineer, v 150 n 355
- Eaton J.C. (1988) Roofbolting for Retreat, Colliery Guardian, September 1988 pp 320 - 322
- Eaton J.C. (1993) Roofbolting supply side technology, Mining Engineer, v153 n383 August 1993, pp 35 - 42.
- Fabjanczyk M.W., Tarrant G.C. (1992) Load Transfer mechanisms in Reinforcing Tendons, 11th International conference on ground control in mining, University of Wollongong, N.S.W. July 1992, pp 212 - 219
- Freire J.L.F., Riley W.F. (1980) Yield behaviour of Photoplastic Materials, Experimental Mechanics, v20 pp 118 -125
- German Standard (1993) DIN 21521, Rock bolts for mining and tunnel support; general specification for steel bolts; tests and testing methods
- Hardy A. (1995) Private Communication, Union of Democratic Mineworkers
- Hassani F.P. (1995) Private Communication, Department of Mining and Metallurgical Engineering, McGill University, Montreal
- Health and Safety Executive (1996a) Guidance on the use of cablebolts to support roadways in coal mines, Deep Mined Coal Industry Advisory Committee

Health and Safety Executive (1996b) Guidance on the use of rockbolts to support roadways in coal mines, Deep Mined Coal Industry Advisory Committee

Hoechst (1994) Designing with plastics the fundamentals, Hoechst UK limited Polymers Division.

Howarth D.F., Renwick M.T. (1992) Innovative Rock Reinforcement Hardware, 11<sup>th</sup> International Conference on Ground Control in Mining, The University of Wollongong, N.S.W. pp 220 - 229

Hurt K. (1994) New developments in Rockbolting, Colliery Guardian July 1994, pp 133 - 140

Lang S. (1995) Private Communication, Whitemoor colliery

Lewis P.E., Ward J.P. (1991) The Finite Element Method - Principles and application, Addison Wesley

Logothetis N., Wynn H.P. (1989) Quality Through Design - Experimental design, off line quality control and Taguchi's contributions, Clarendon Press

Ludwig B. (1983) Shear tests on rockbolts, Proceedings of the International Symposium on rockbolting, Abisko, Sweden pp 113-123

Mears D.R., Pae K.D., Sauer J.A. (1969) Effects of Hydrostatic pressure on the Mechanical behaviour of Polyethylene and Polypropylene, Journal of Applied Physics, v40 n11 pp 4229 -4237

Mietz J., Rueckert J., Isecke B. (1997) Electrochemical investigations on austenitic and duplex stainless steels for use as ground anchor materials, Materials Science Forum, v247 pp 25-36

Mills N.J. (1993) Plastics Microstructure and Engineering applications, 2nd edition, Edward Arnold.

Moldflow injection moulding software

Naylor J. (1994) Underground applications of polymer mining grid, Mining Engineer v154 n398 November 1994, pp141 - 143

Norris C., Yearby M. (1981) Roof Bolt Developments, Colliery Guardian International, July 1981 v229 n7, pp 22 - 30

Ogata Y., Fujimoto K. (1985) On the strength and its testing method of steel plate for Rock bolt, Mining and Safety (Japan) v31 n6 pp 281-290.

O'Grady P., Fuller P.G. (1992) Design considerations for cable truss secondary support in roadways of underground collieries, 11th International conference on Ground Control in Mining, The University of Wollongong NSW July 1992, pp 63 - 69.

O'Grady P., Fuller P., Dight P. (1994) Cable bolting in Australian Coal Mines - Current Practice and Design Considerations. *Mining Engineer* v 154 n396 pp 63-69

Oreste P.P., Peila D. (1996) Radial Passive Rockbolting in Tunnelling design with a new convergence-confinement model, *International Journal of Rock Mechanics, Mining Sciences and Geomechanics Abstracts* v33 n5 pp 443-454

Pakalnis R., Peterson D., Poulin R. (1994) Evaluation of glassfibre bolts for mining applications, *Mining Engineer (Colorado)* v46 n 12, pp 53 - 57

Patran (1993) User's Manual, version 3, PDA Engineering

Raghava R., Caddel R.M., Yeh G.S.Y. (1973) The Macroscopic yield behaviour of Polymers, *Journal of Materials Science* v8 pp 225 -232

Reddish D.J., Dunham R.K., Adkins G. (1994) Glass Fibre Rock Reinforcement, pp 133 - 153

Reznik Y.M. (1996) Minimizing Uncertainties in Geotechnical Investigations, *Uncertainty in Geologic Environment*, American Society of Civil Engineers v58 n1 pp149-166

Ross P.J. (1988) Taguchi techniques for Quality Engineering, McGraw Hill

Rukovodstvo P. (1977) Guidelines to SNIP II-15-74, CIS

Schach R., Garshol K., Heltzen A.M. (1979) Rock bolting - a practical handbook, Norwegian Institute of Rock Blasting techniques.

Tague D., Aziz A., Smart B.G.D., (1990) The Evolution of Australian Bolting Practice, *Mining Engineer*, v 149 n 342

Trofimenkov Y.G., Piarnpuu Z.K., Mariupolsky, L.G. (1983) Relationship between Bearing Plate and Pressuremeter Deformation Moduli, *Fundamenty i Mekhanika Gruntov*, Moacow, CIS, n4 pp 19-22

Watermann N.A. (1991) Materials engineering for deep mining applications - an International view, *Materials and Design* v 12 n1

Williams P. (1994) The development of rockbolting in UK coal mines, *Mining Engineer* v153 n392 May 1994, pp 307 - 312

Wronski A.S., Pick M. (1977) Pyramidal yield criteria for epoxides, *Journal of Materials Science*, v 12 pp 28 -34

Zienkiewicz O.C. (1977) *The Finite Element Method*, 3rd edition, McGraw Hill

## Contents of Appendices

	page
<b>Appendix 1</b>	
Taguchi 2 level experiment	II
Multiple level Taguchi experiment for webbed bearing plates	III
Variation of diameter of hole in steel support plate	V
Variation of depth of bearing plate	VII
Variation of coned angle for different depths of bearing plate	VIII
Variation of nut diameter	X
External diameter of bearing plate	XVI
Variation of number and positions of circumferential webs	XXVI
Variation of web thickness	XXIX
Materials	XXXII
<b>Appendix 2</b>	
Orthogonal arrays and drawings of bearing plates used in 2 level and multiple level Taguchi experiments	XXXIV
<b>Appendix 3</b>	
Dimensions of tensile testing specimens	XXXVII
Material selection charts from Cambridge Material selector software	XXXVIII
List of abbreviations of material names	XLI
<b>Appendix 4</b>	
Calculations of load to cause crushing of coal	XLII

**APPENDIX 1 - Further results from FEA using Taguchi and one factor at a time experimentation**

**Taguchi 2 level experiment**

Table A1.1 gives the results from the Taguchi 2 level experiment, when evaluated by comparing the load carried. The results are given in the order of significance found in the experiment.

	best level	worst level	confidence level
B - Depth of bearing plate at the centre	35 mm	10 mm	< 90 %
D - Webbed or solid	Solid	Webbed	< 90 %
H - External diameter of bearing plate	200 mm	150 mm	< 90 %
F - Diameter of hole in steel support plate	55 mm	100 mm	< 90 %
E - Material	Polypropylene	Polyamide 6	< 90 %
Error			< 90 %
C - Coned or flat shape	Coned	Flat	< 90 %
A - Diameter of central hole in bearing plate	25.85 mm	34 mm	< 90 %
G - External diameter of nut	56 mm	40 mm	< 90 %

**Table A1.1** Results from two level Taguchi experiment

In the two level Taguchi experiment evaluated on the basis of the load carried, none of the parameters had a confidence level of 90 % or above.

**Multiple level Taguchi experiment for webbed bearing plates**

Table A1.2 gives some results from the multiple level Taguchi experiment for webbed bearing plates when using a 55 mm hole in the steel support plate. The parameters are given in order of significance, and were evaluated by comparing the load / volume.

	best level	intermediate level	worst level	confidence level
K - Number of radial webs	20	12	4	95 %
E - Material	polypropylene	polyamide 6	polycarbonate	< 90 %
L - Web thickness	5 mm	4 mm	3 mm	< 90 %
M - Number of circumferential webs	4	3	5	< 90 %

**Table A1.2** Results from multiple level Taguchi experiment on webbed bearing plates, using a 55 mm hole in the steel support plate

Table A1.3 gives some results from the webbed multiple level Taguchi experiment, in order of significance where only the webs close to the centre were thickened. The innermost circumferential web was thickened and the portion of the radial webs between the innermost and second circumferential webs was thickened. These results were obtained using a 55 mm hole in the steel support plate.

	best level	intermediate level	worst level	confidence level
K - Number of radial webs	12	20	4	< 90 %
L - Web thickness	5 mm	4 mm	3 mm	< 90 %
E - Material	polypropylene	polyamide 6	polycarbonate	< 90 %
M - Number of circumferential webs	4	3	5	< 90 %

**Table A1.3** Results from multiple level Taguchi experiment on webbed bearing plates, with only the two centre webs thickened

Comparisons of the results in tables A1.2 and A1.3 show that the web thickness is a more significant parameter when only the central two webs are thickened than when all the webs are thickened.

### Variation of diameter of hole in steel support plate

Figure A1.1 shows the variation of load / volume with diameter of hole in the steel support plate when used with a webbed bearing plate. The webbed model used for this one factor at a time comparison was the confirmation model from the two level Taguchi experiment (see figure A2.17).

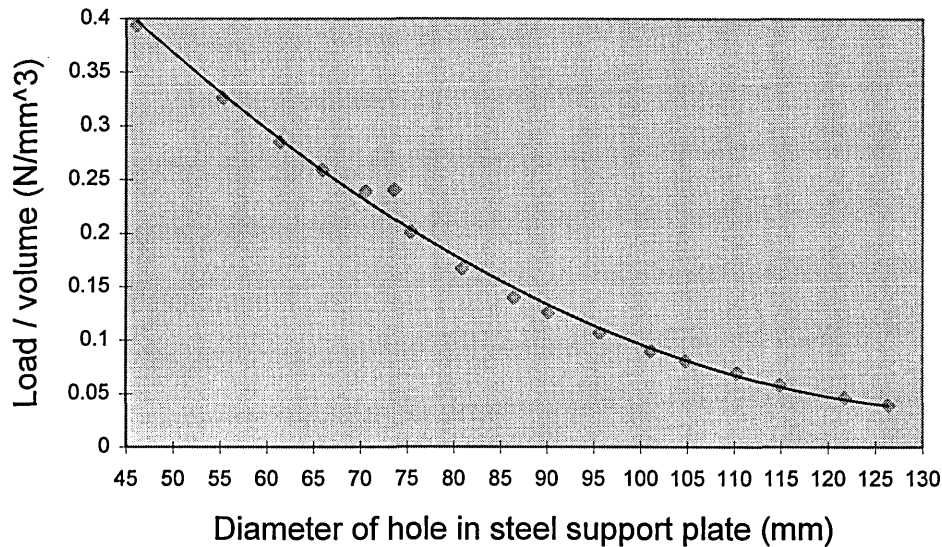


**Figure A1.1** Variation of load / volume with diameter of hole in steel support plate for a webbed bearing plate

Diameters of 73.6 mm and 110.34 mm correspond to positions of circumferential webs. It can be seen in figure A1.1 that the result at a diameter of 73.6 mm does not fit the curve very well.

Figure A1.2 shows the variation of load / volume with diameter of hole in the steel support plate for three different materials. The bearing plate used was a flat plate of depth 10 mm. It can be seen that the curves in figure A1.2 are not completely parallel. It can be seen from figure A1.2 that the polypropylene plate carries the highest load, the

polyamide the next highest and the polycarbonate the least. The difference between the three materials is not as great with a large hole in the steel support plate as with a small hole in the steel support plate.

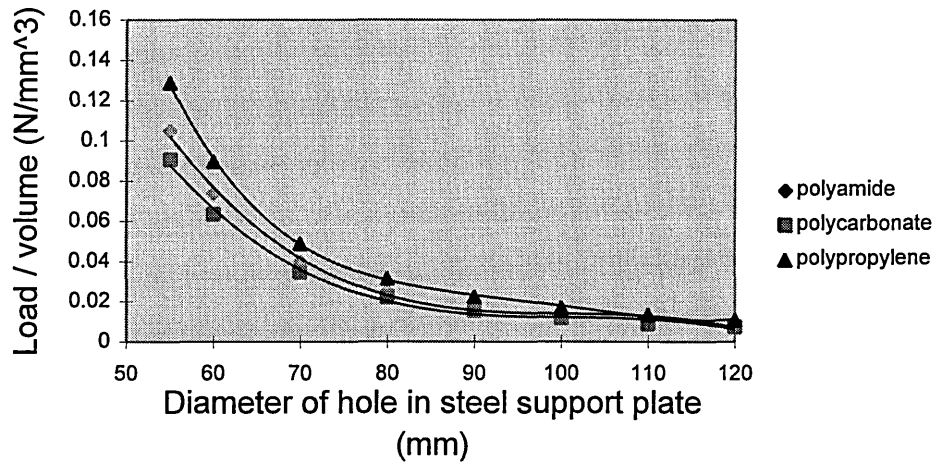


**Figure A1.2** Variation of load / volume with diameter of hole in steel support plate for three different materials.

### Variation of depth of bearing plate

Figure A1.3 shows the variation of load / volume with depth of bearing plate for five different diameters of hole in the steel support plate, when compared on the basis of load carried.

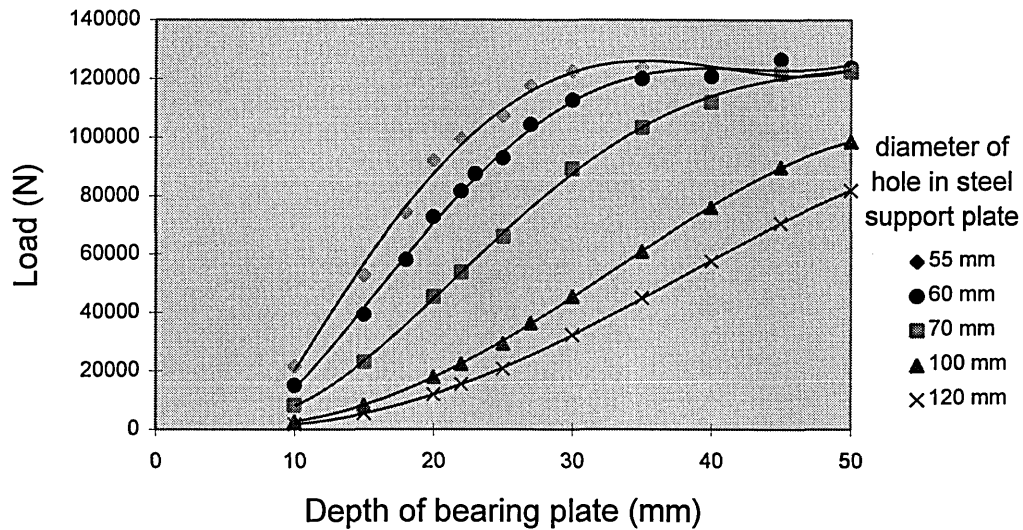
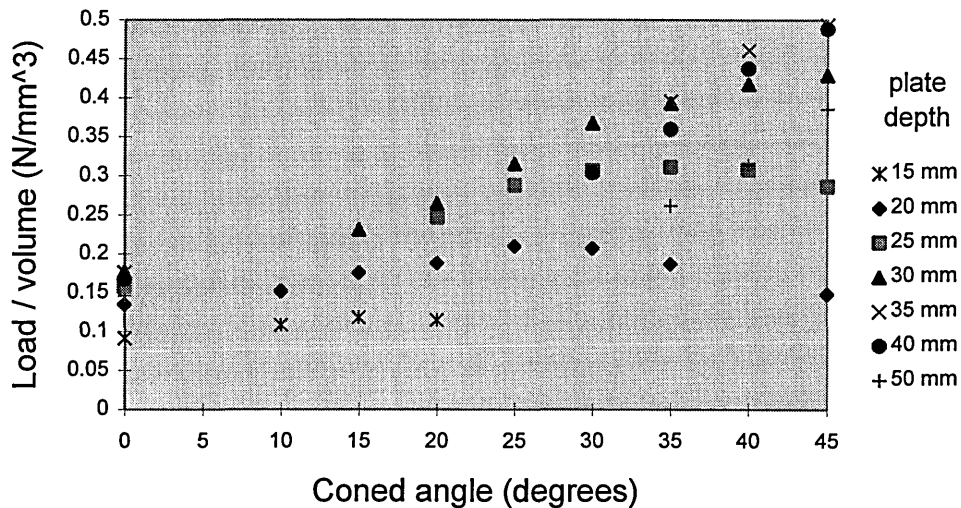


**Figure A1.3** Variation of load / volume with depth of bearing plate

The results in figure A1.3 clearly show that as the depth of the bearing plate increases, the load carried increases. However as the depth increases, the rate of increase in load carried with increasing depth of bearing plate decreases.

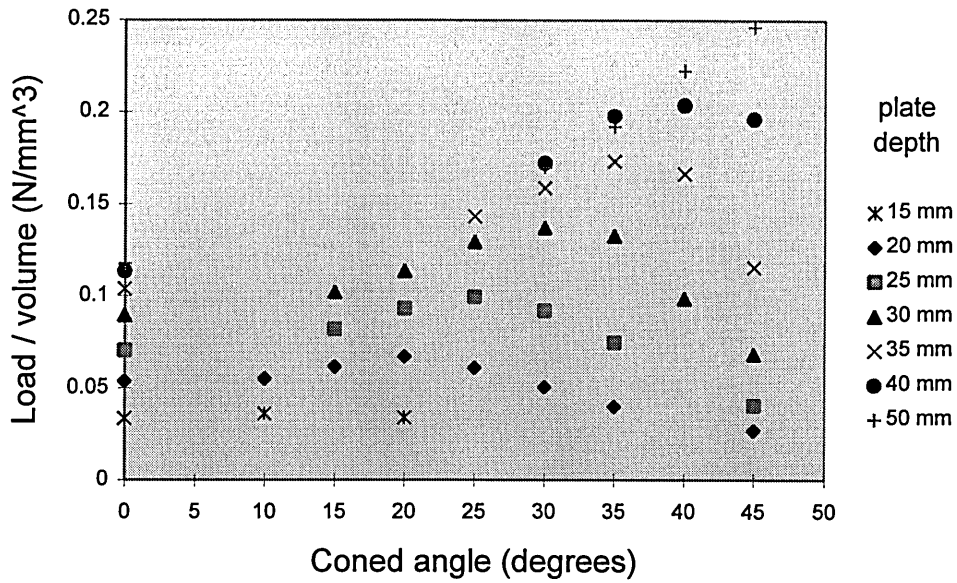
### Variation of coned angle for different depths of bearing plate

Figure A1.4 shows the variation of load / volume with coned angle for seven different depths of bearing plate for a 70 mm hole in the steel support plate. The coned angle of zero corresponds to a flat bearing plate of constant thickness.



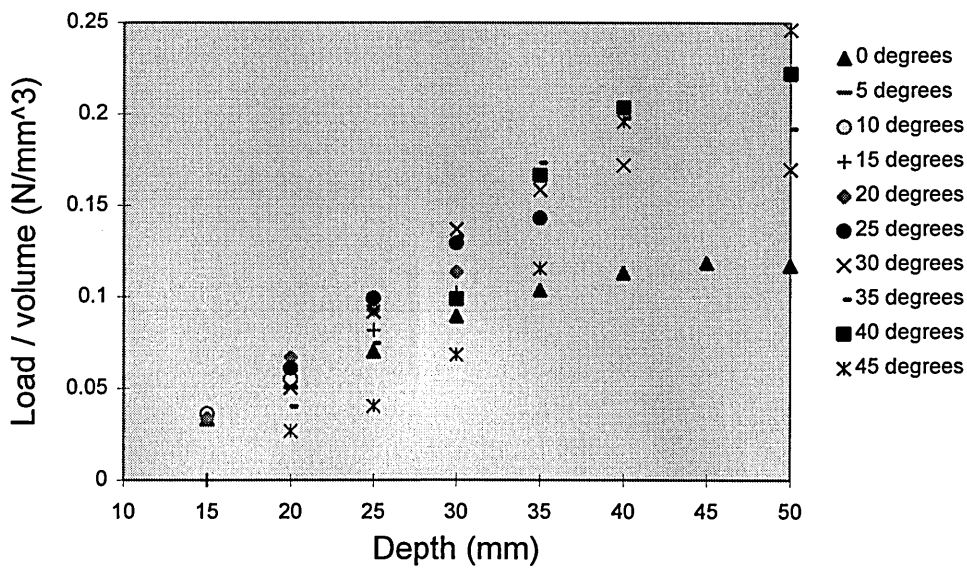
**Figure A1.4** Variation of load / volume with coned angle for different depths of bearing plate with a 70 mm hole in the steel support plate

Figure A1.5 shows the variation of load / volume with coned angle for different depths of bearing plate with a 100 mm hole in the steel support plate. It can be clearly seen in figures A1.4 and A1.5 that the curves for the different diameters of hole in the steel support plate are not parallel to each other. It can also be seen that the values of load / volume in figure A1.4 corresponding to a 70 mm hole in the steel support plate are much higher than the values in figure A1.5 corresponding to a 100 mm hole in the steel support plate.



**Figure A1.5** Variation of load / volume with coned angle with different depths of bearing plate with a 100 mm hole in the steel support plate

Figure A1.6 shows the variation of load / volume with depth of bearing plates for different coned angles, when using a 100 mm hole in the steel support plate. This is the same data as plotted in figure A1.5.



**Figure A1.6** Variation of load / volume with depth of bearing plate for different coned angles with a 100 mm hole in the steel support plate

### Variation of nut diameter

Figure A1.7 shows the variation of load / volume with diameter of the nut and the depth of the bearing plate, when considering the total volume of material used in the nut and bearing plate. These results were obtained for flat plates of external diameter 150 mm. The depth of the nut was taken as 40 mm. Figure A1.7a shows results obtained with a 100 mm hole in the steel support plate and figure A1.7b shows results obtained with a 55 mm hole in the steel support plate.

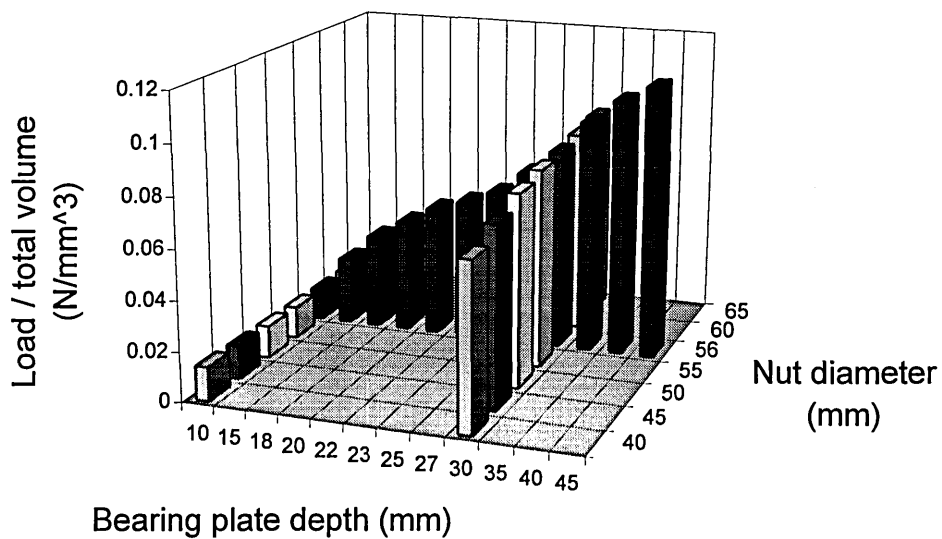


**Figure A1.7a** Variation of load / total volume with bearing plate depth and nut diameter for 100 mm hole in the steel support plate

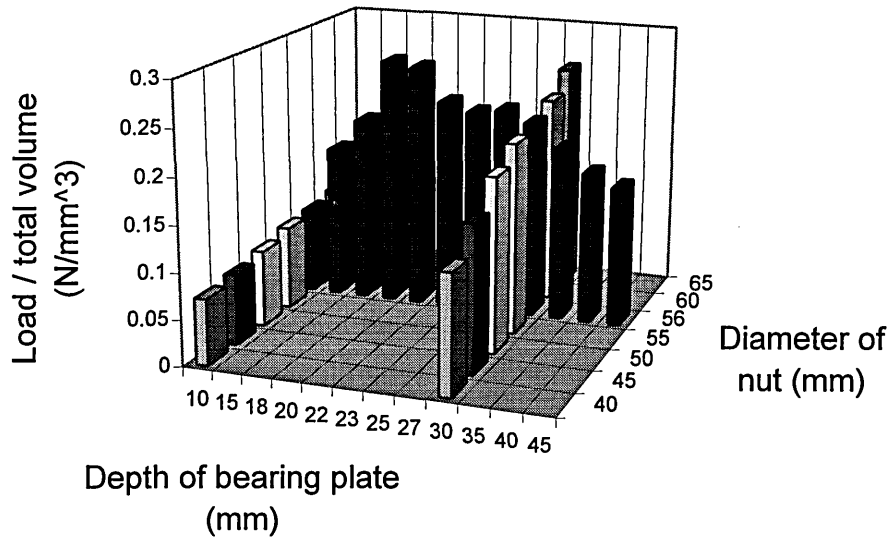


**Figure A1.7b** Variation of load / total volume with bearing plate depth and nut diameter for 55 mm hole in the steel support plate

The results given below are a comparison of the effect of adding 10,000 mm<sup>3</sup> of material to the nut or to the bearing plate. The load carried was interpolated from the results given in figures A1.7a for the bearing plate change in depth, and a separate test was carried out for the change in nut diameter. The calculated volumes are based upon a nut depth of 40 mm and a bearing plate external diameter of 150 mm.

Initial conditions :-

100 mm diameter hole in steel support plate

Plate depth 30 mm

Nut diameter 56 mm

Plate volume 502,905 mm<sup>3</sup>

Nut volume 61,326 mm<sup>3</sup>

Total volume 564,231 mm<sup>3</sup>

Load carried 45.6 kN

Effect of adding  $10,000 \text{ mm}^3$  to the bearing plate

New depth of bearing plate 30.59 mm

New load carried 47.4 kN

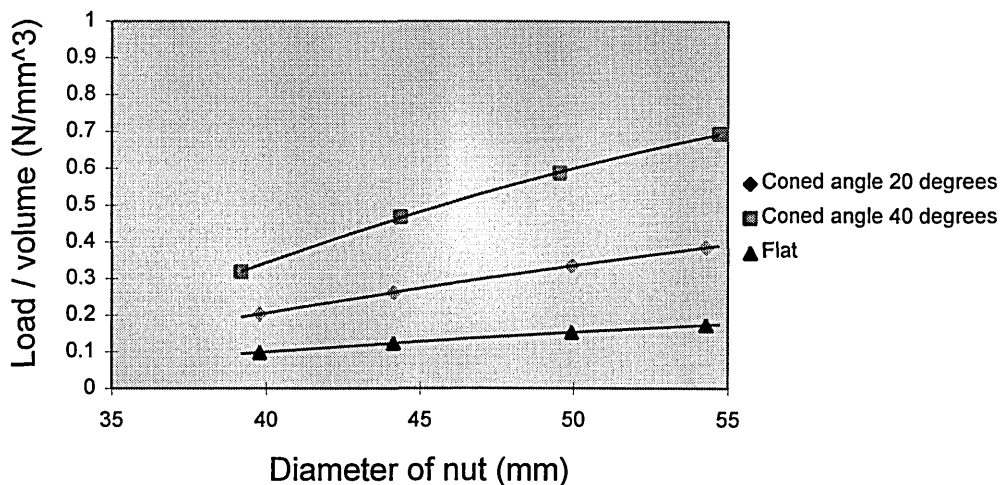
Effect of adding  $10,000 \text{ mm}^3$  to the nut

New diameter of nut 79.32 mm

New load carried 59.2 kN

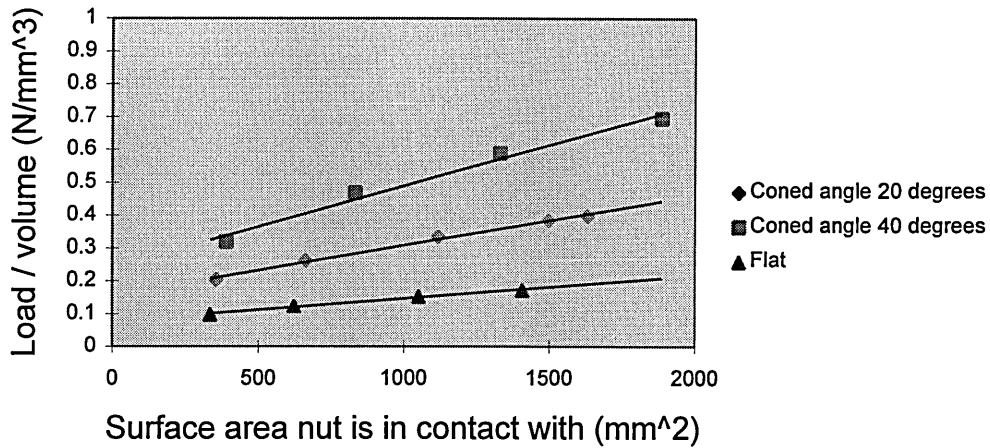
Clearly adding  $10,000 \text{ mm}^3$  of material to the nut increases the nut diameter more than adding  $10,000 \text{ mm}^3$  of material to the bearing plate increases the bearing plate depth. This is because the nut has a depth of only 40 mm while the bearing plate has an external diameter of 150 mm. For the example given, the  $10,000 \text{ mm}^3$  of material added to the nut allows an increase in load of 13.6 kN. Whereas the  $10,000 \text{ mm}^3$  of material added to the bearing plate allows an increase in load of only 1.8 kN. Hence the results suggest that it is better to add extra material to the nut rather than the bearing plate.

Figure A1.8 shows the variation of load / volume with nut diameter for coned plates with  $20^\circ$  and  $40^\circ$  coned angles and flat plates, all of depth 30 mm. The hole in the steel support plate used was 55 mm. The curves shown in figure A1.8 are clearly not parallel to one another.



**Figure A1.8** Variation of load / volume with nut diameter for coned and flat plates

Figure A1.9 shows the same results as figure A1.8, but the variation in load / volume is plotted against the surface area of the bearing plate that the load is applied over.



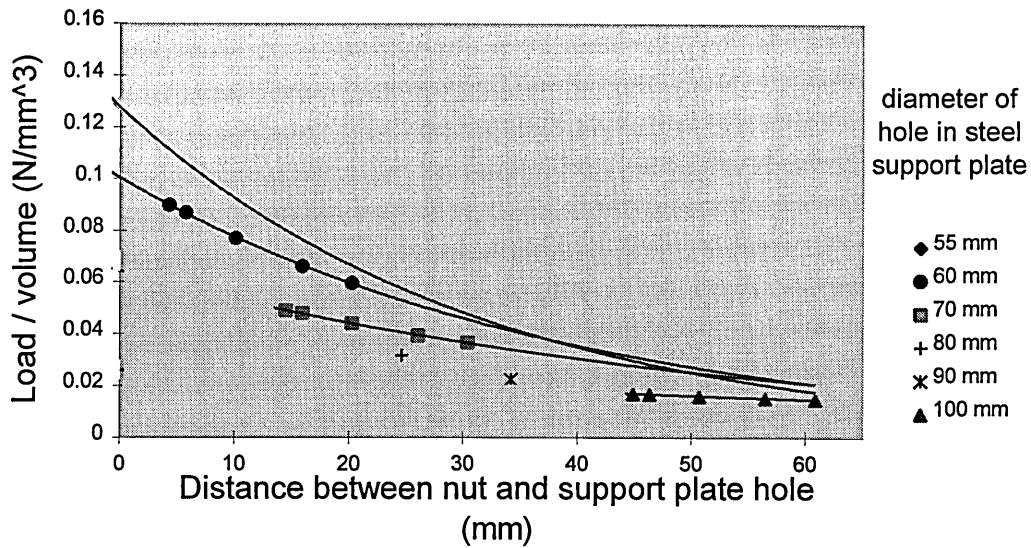
**Figure A1.9** Variation of load / volume with surface area load is applied over for coned and flat plates

The curves shown in figure A1.9 are not completely parallel to each other, but they are more parallel than the curves shown in figure A1.8.

Figure A1.10 shows the variation of load / volume with distance 'r' where :-

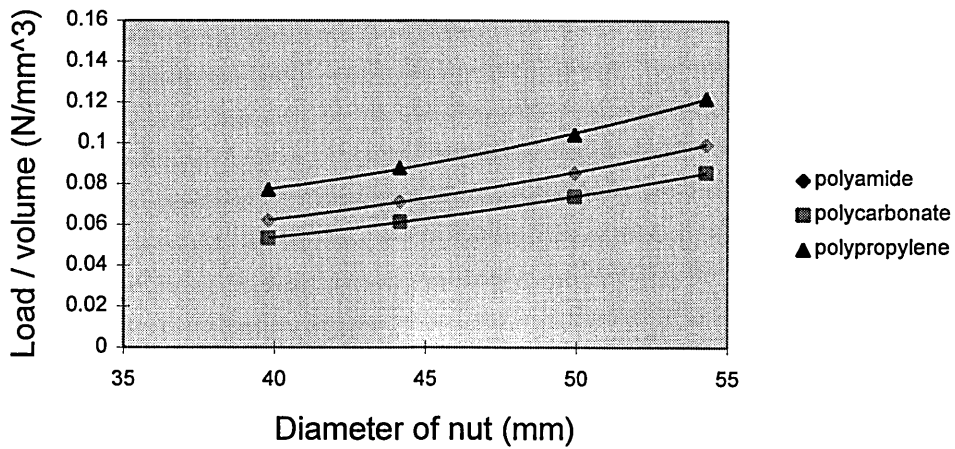
$r = \text{Diameter of hole in steel support plate} - \text{Diameter of nut}$

for six different diameters of hole in the steel support plate. These results were obtained using a simple flat bearing plate of depth 10 mm.



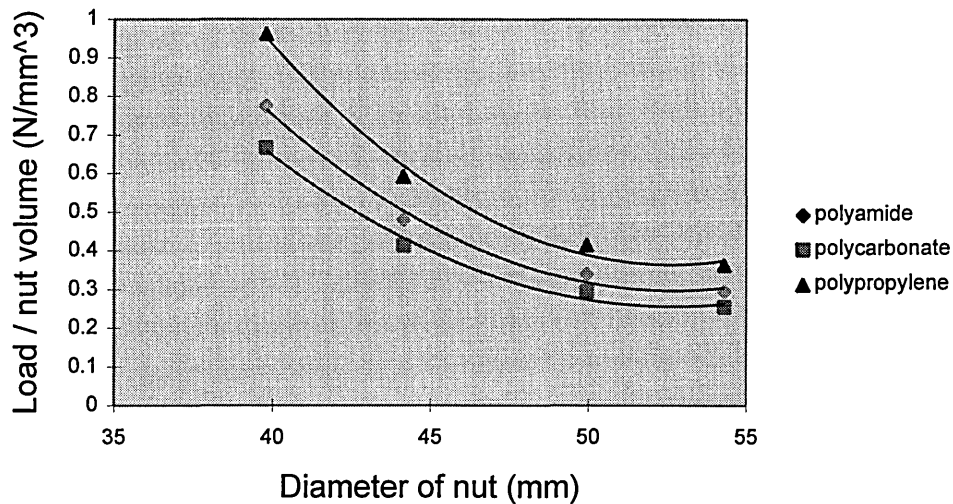
**Figure A1.10** Variation of load / volume with distance ‘r’

Figure A1.11 shows the variation of load / volume with diameter of the nut for three different materials, with a 55 mm hole in the steel support plate. The bearing plate used was a flat plate of depth 10 mm. Figure A1.11 shows the variation on a load / plate volume basis, which is the same basis used to evaluate all of the other parameters.



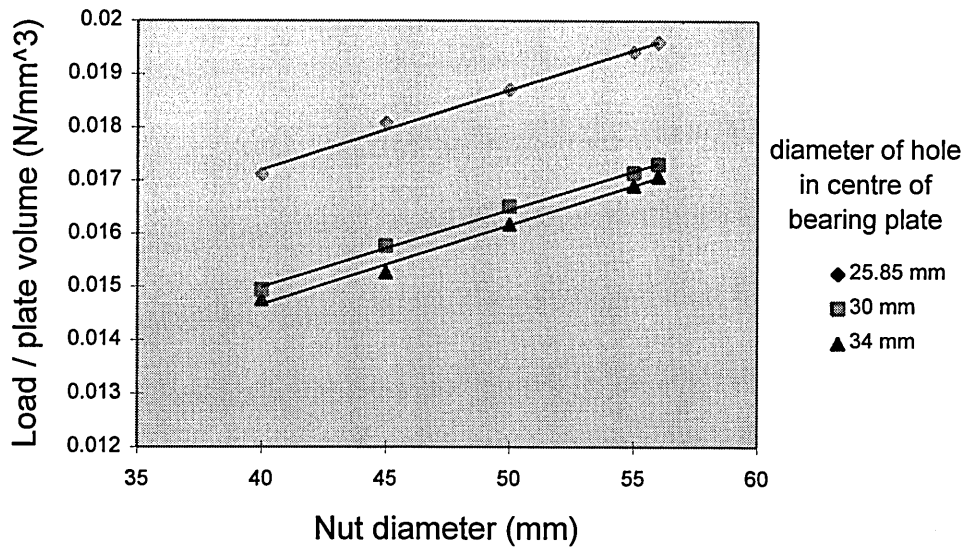
**Figure A1.11** Variation of load / volume with nut diameter for three different materials

Figure A1.12 shows the same results as figure A1.11 but the results are evaluated on a load / nut volume basis. Figure A1.12 shows that a higher load / nut volume is carried with a smaller diameter of nut.



**Figure A1.12** Variation of load / nut volume with nut diameter for three different materials

Figure A1.13 shows the variation of load / volume with nut diameter for three different diameters of hole in the centre of the bearing plate, for a 100 mm hole in the steel support plate. Figure A1.13 shows the variation on the basis of load / plate volume. The curves in figure A1.13 can be seen to be parallel to each other. It can be seen that the smaller the diameter of the hole in the centre of the bearing plate, the larger the amount of load / plate volume. It can also be seen that the bearing plate with a 25.85 mm central hole carries much more load / volume than the bearing plate with a 30 mm hole. However the difference between the bearing plate with a 30 mm central hole and a 34 mm central hole is not so great.



**Figure A1.13** Variation of load / volume with nut diameter for different diameters of hole in the centre of the bearing plate

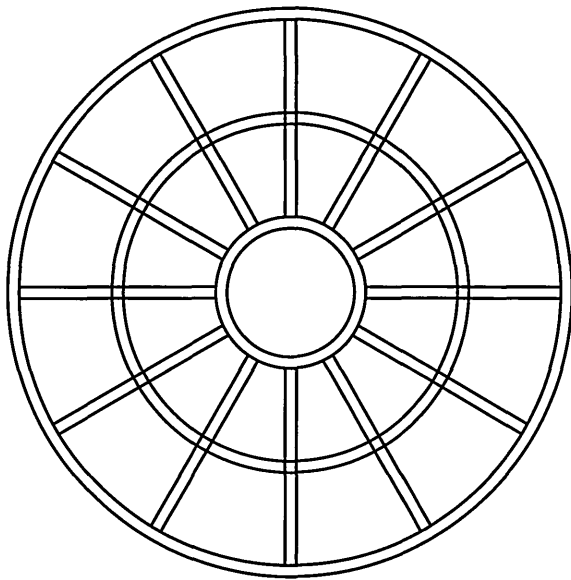
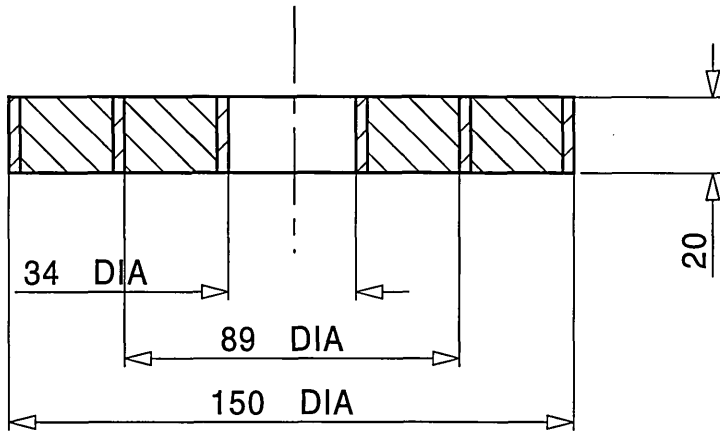
**External diameter of bearing plate**

Table A1.4 compares the load carried and load / volume by a simple bearing plate of depth 10 mm with different external diameters of bearing plate.

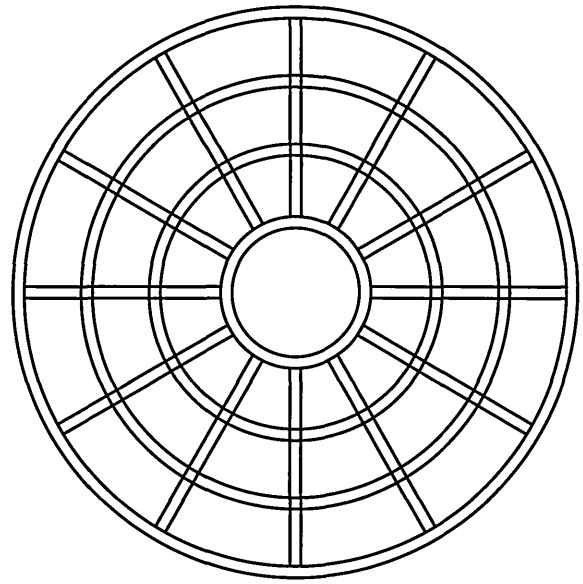
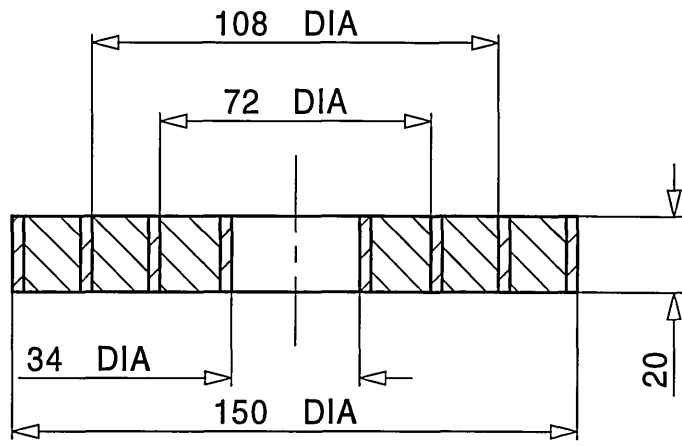
	110 mm	150 mm
load (N)	2520	2864
load / volume (N/mm <sup>3</sup> )	0.02932	0.01708

**Table A1.4** Load carried by flat bearing plate of depth 10 mm with different external diameters

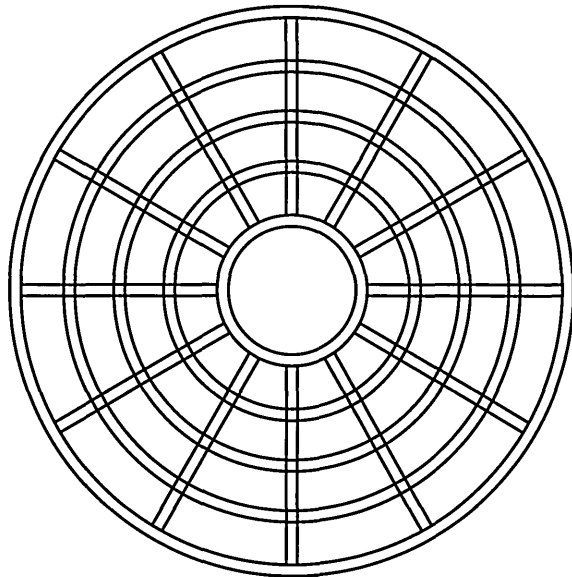
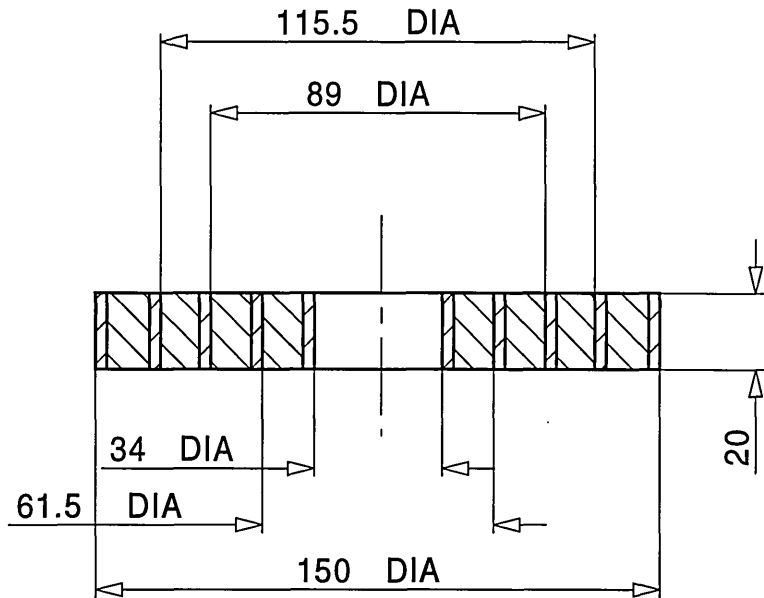
The results suggest that when comparing the load carried a larger diameter of bearing plate is best. However when comparing the load / volume a smaller diameter of bearing plate is best.

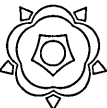


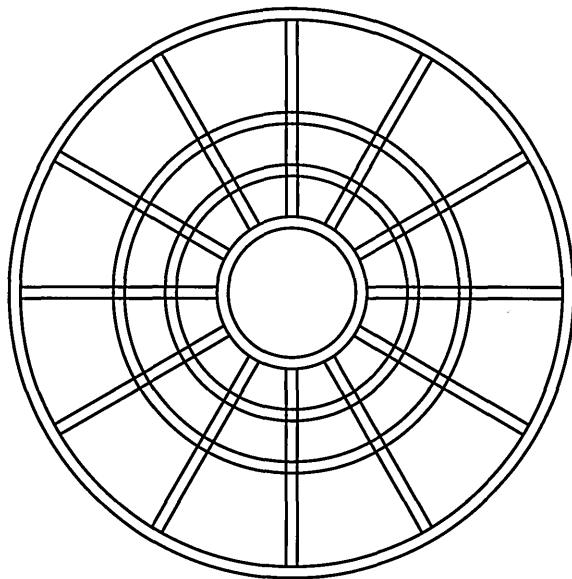
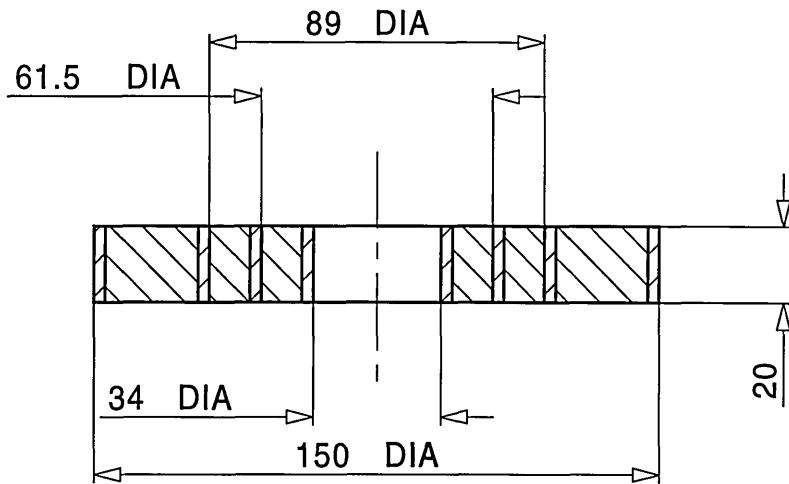
	 School of Engineering Sheffield Hallam University		
	TITLE <b>Webbed design number 1</b>		
Date 17 3 97	PROJECT <b>A4</b>	DWG <b>Figure A1.14</b>	ISSUE <b>A</b>
Date -	SCALE <b>1 : 2</b>		SHEET - OF -



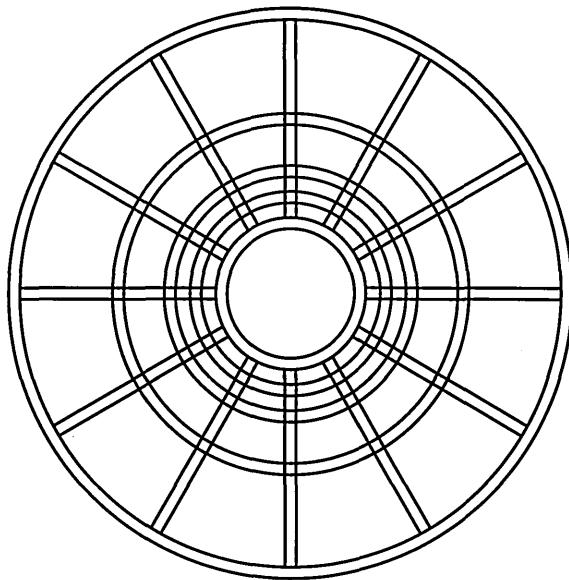
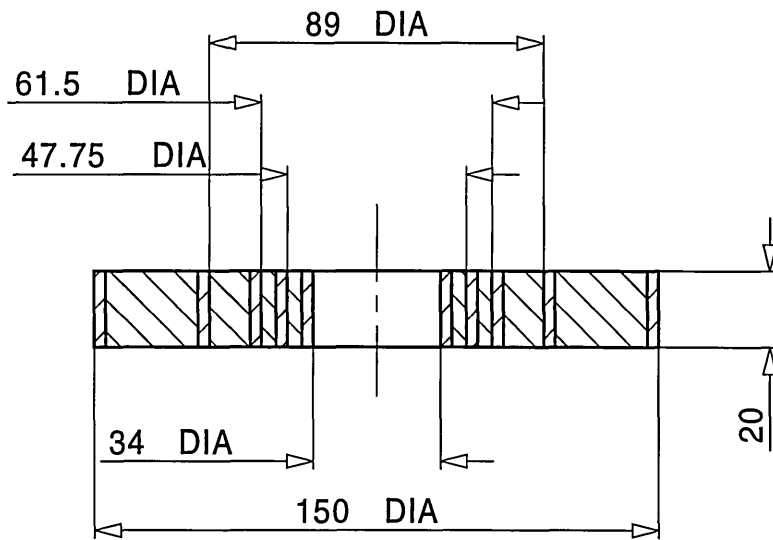
	 School of Engineering Sheffield Hallam University		
	TITLE <b>Webbed design number 2</b>		
Date 17 3 97	PROJECT <b>A4</b>	DWG <b>Figure A1.15</b>	ISSUE <b>A</b>
Date -	SCALE <b>1 : 2</b>		SHEET - OF -



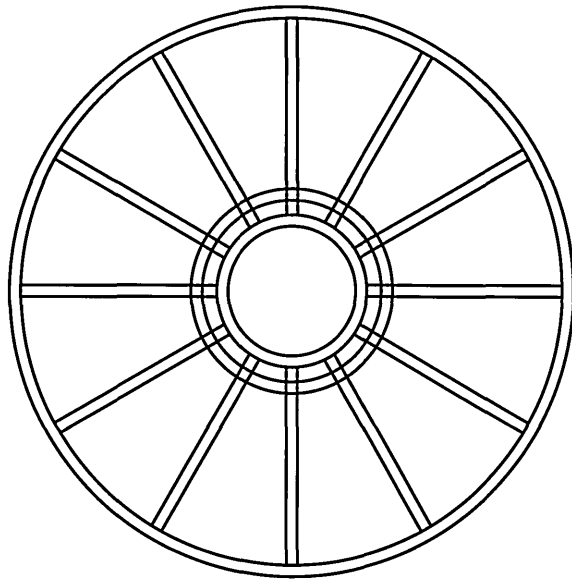
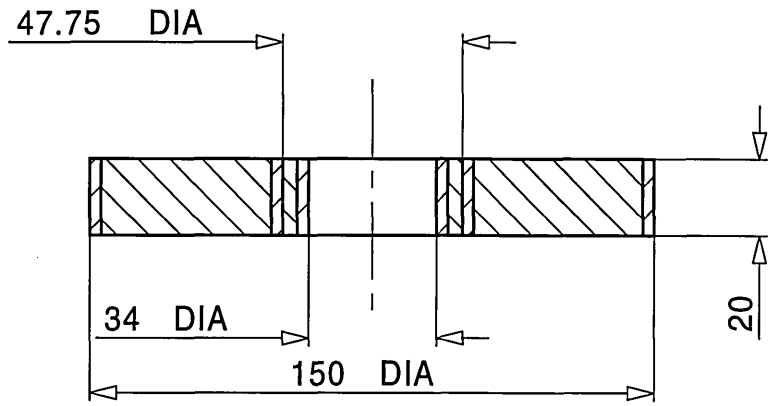
	 School of Engineering Sheffield Hallam University		
	<b>TITLE</b> Webbed design number 3		
Date 17 3 97	<b>A4</b> PROJECT	DWG Figure A1.16	ISSUE A
Date -	<b>SCALE</b> 1 : 2	SHEET - OF -	



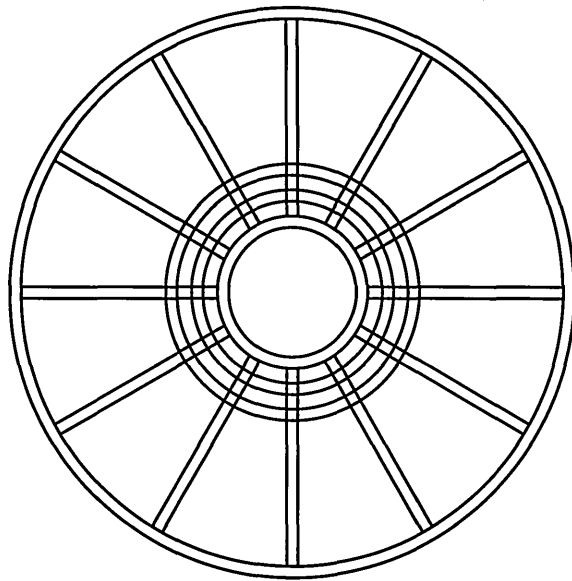
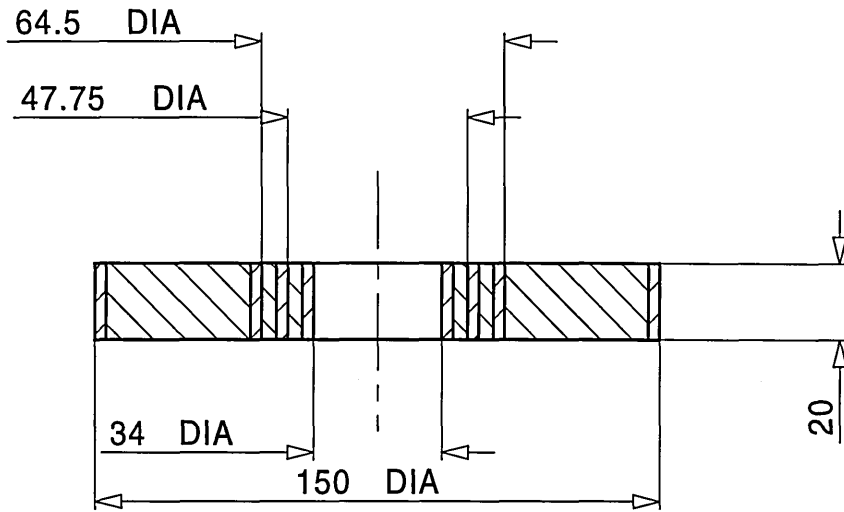
	 School of Engineering Sheffield Hallam University		
	TITLE <b>Webbed design number 4</b>		
Date 17 3 97	PROJECT <b>A4</b>	DWG <b>Figure A1.17</b>	ISSUE <b>A</b>
Date -	SCALE <b>1 : 2</b>		SHEET - OF -



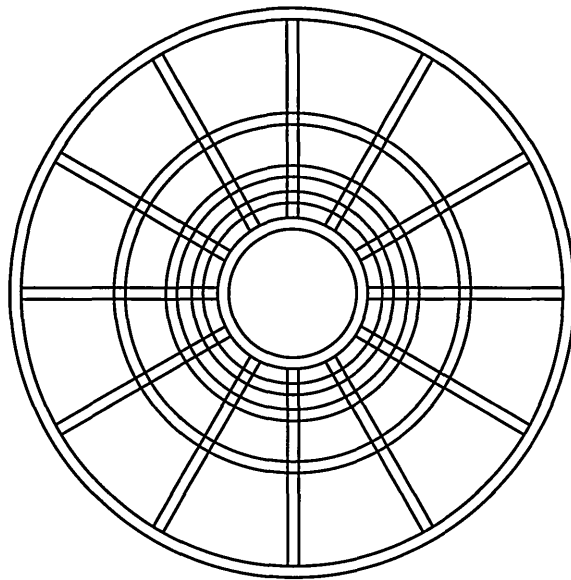
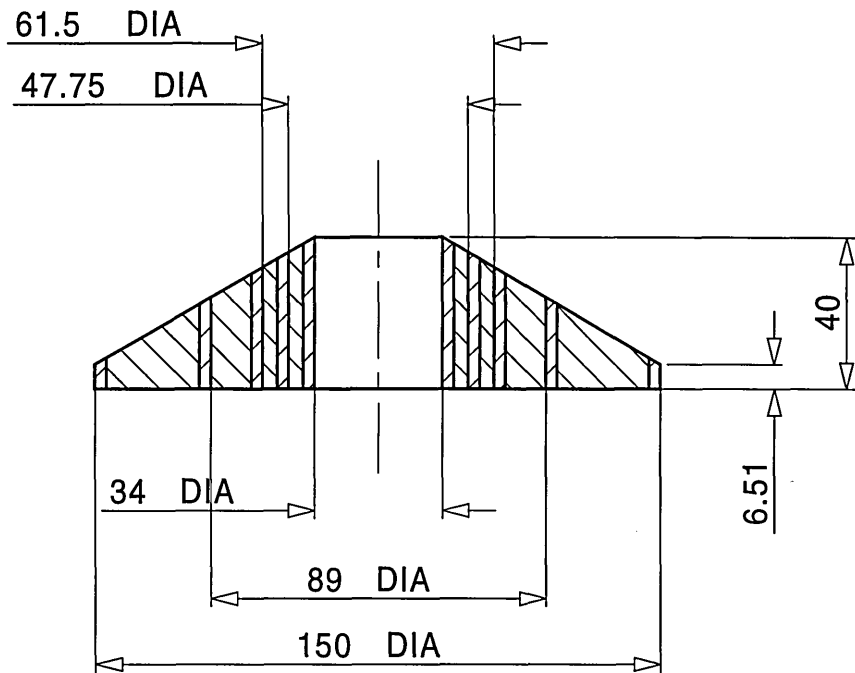
	 School of Engineering Sheffield Hallam University		
	TITLE <b>Webbed design number 5</b>		
Date 17 3 97	PROJECT <b>A4</b>	DWG <b>Figure A1.18</b>	ISSUE <b>A</b>
Date -	SCALE <b>1 : 2</b>		SHEET - OF -



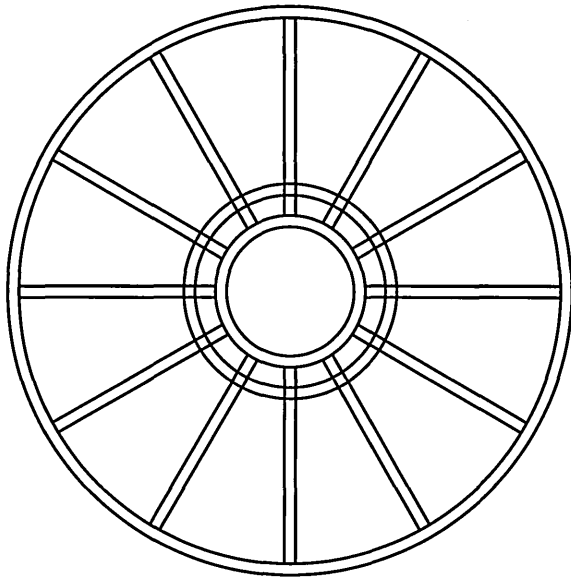
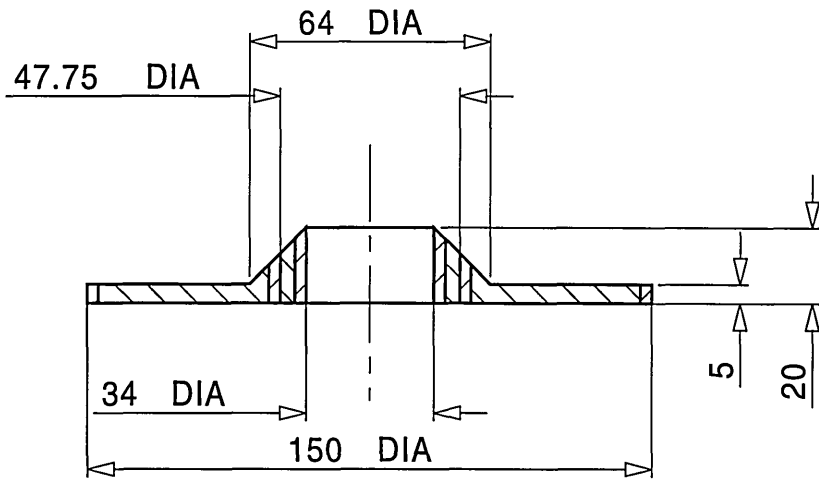
	 School of Engineering Sheffield Hallam University		
	TITLE <b>Webbed design number 6</b>		
Date 20 3 97	PROJECT <b>A4</b>	DWG <b>Figure A1.19</b>	ISSUE <b>A</b>
Date -	SCALE <b>1 : 2</b>		SHEET - OF -



	 School of Engineering Sheffield Hallam University		
	TITLE <b>Webbed design number 7</b>		
Date 20 3 97	PROJECT <b>A4</b>	DWG <b>Figure A1.20</b>	ISSUE <b>A</b>
Date -	SCALE <b>1 : 2</b>		SHEET - OF -



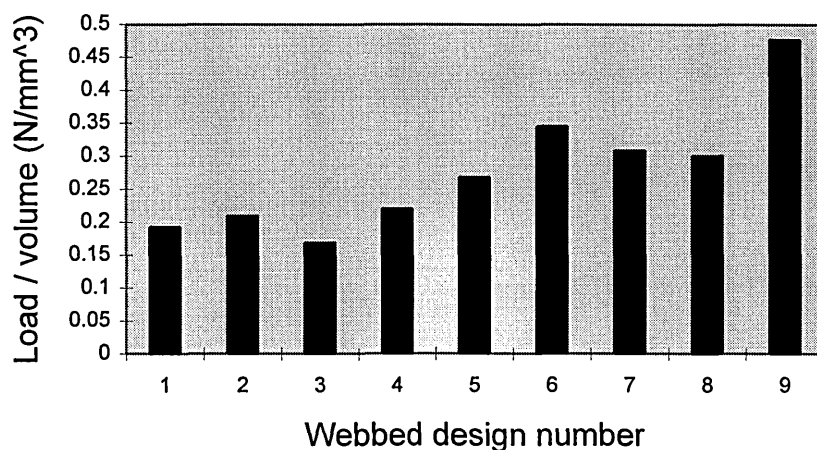
	 School of Engineering Sheffield Hallam University		
	TITLE <b>Webbed design number 8</b>		
Checked by KMW	Date 21 3 97	PROJECT <b>A4</b>	DWG <b>Figure A1.21</b>
-	Date -	SCALE <b>1 : 2</b>	
		SHEET - OF -	ISSUE <b>A</b>



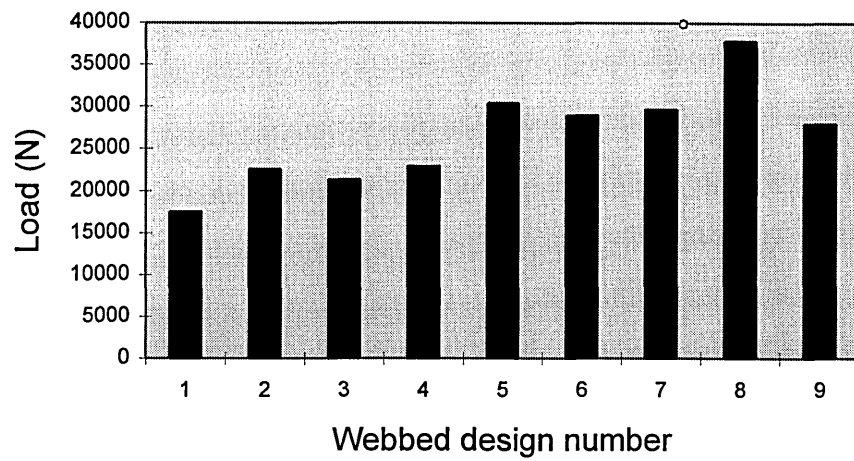
	 School of Engineering Sheffield Hallam University		
	TITLE <b>Webbed design number 9</b>		
Date 17 4 97	PROJECT <b>A4</b>	DWG <b>Figure A1.22</b>	ISSUE <b>A</b>
Date -	SCALE <b>1 : 2</b>		SHEET - OF -

### Variation of number and position of circumferential webs

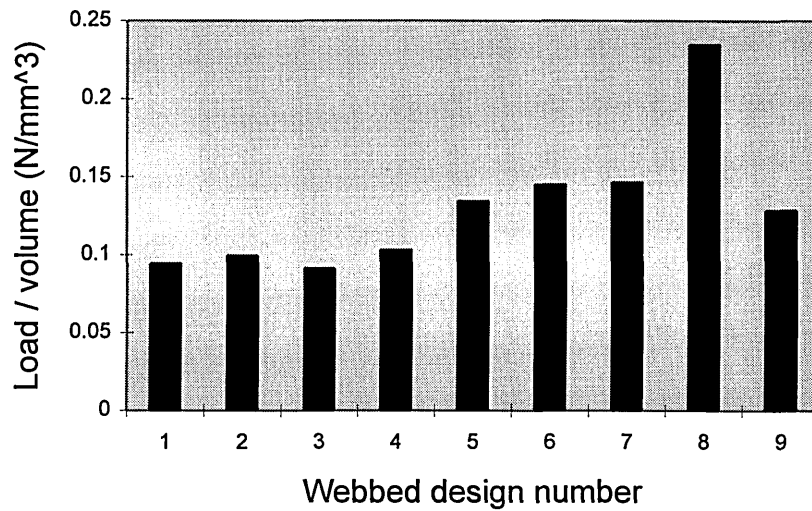
The circumferential webs investigated in the multiple level Taguchi experiment were all equally spaced webs. Figures A1.14-22 show nine designs of webbed bearing plates that were investigated, some of which have webs positioned closer to the centre. Webbed designs 1 -7 are all flat (not coned) webbed plates of depth 20 mm, with 12 radial webs. Hence the only difference between designs 1 - 7 is the number and position of circumferential webs. Webbed designs 8 and 9 are designs produced on the basis of the best position of circumferential webs and also the best number of radial webs, the best coned angle and the best depth of the bearing plate according to the results given in figures 4.5, 4.6 and 4.16 for a 100 mm and 55 mm hole in the steel support plate. Figure A1.23 compares the performance of these webbed designs when using a 55 mm hole in the steel support plate. Figure A1.24 compares the performance of these webbed designs when using a 70 mm hole in the steel support plate. Figure A1.25 compares the performance of these webbed designs when using a 100 mm hole in the steel support plate.



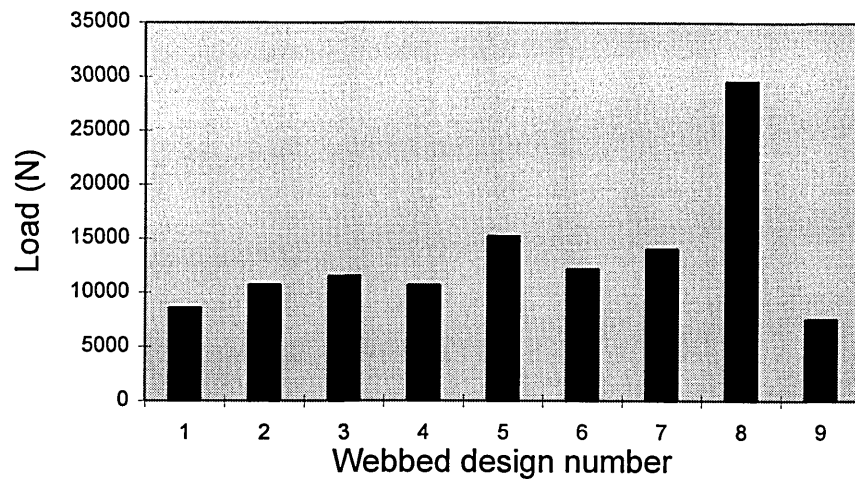
**Figure A1.23a** Comparison of webbed designs 1 - 9 using a 55 mm hole in the steel support plate, evaluated on basis of load / volume



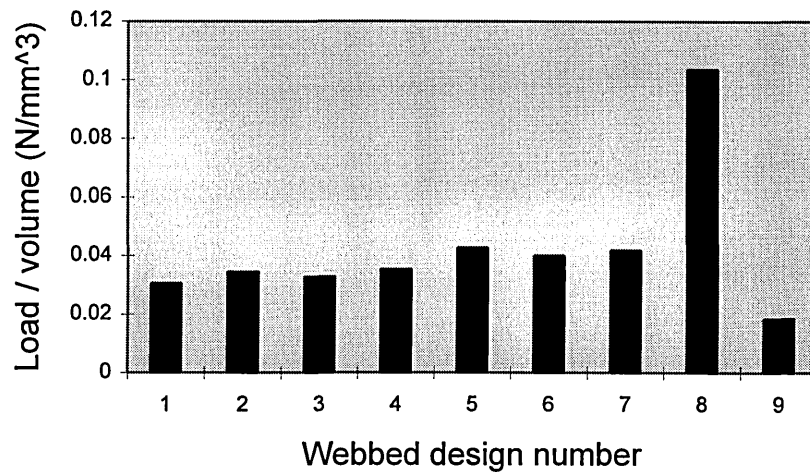
**Figure A1.23b** Comparison of webbed designs 1 - 9 using a 55 mm hole in the steel support plate, evaluated on basis of load



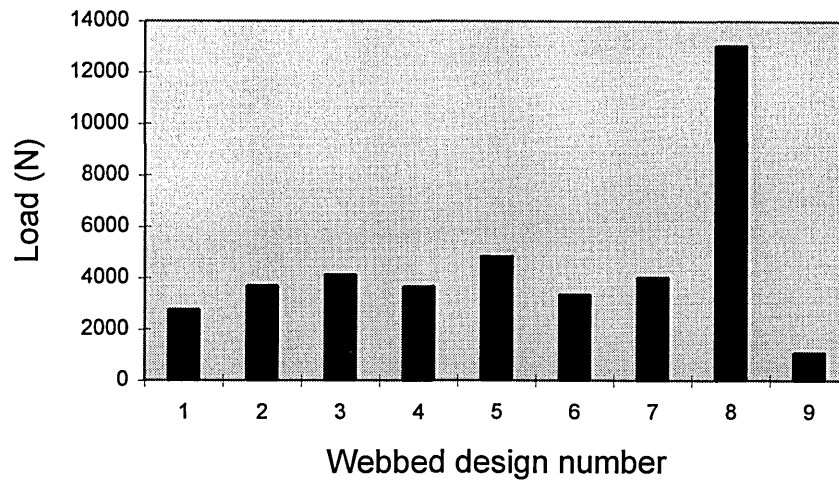
**Figure A1.24a** Comparison of webbed designs 1 - 9 using a 70 mm hole in the steel support plate, evaluated on basis of load / volume



**Figure A1.24b** Comparison of webbed designs 1 - 9 using a 70 mm hole in the steel support plate, evaluated on basis of load



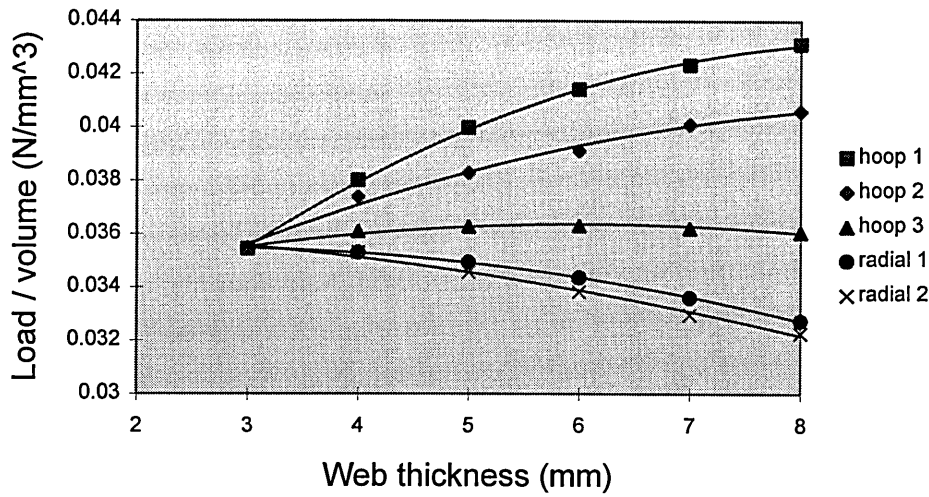
**Figure A1.25a** Comparison of webbed designs 1 - 9 using a 100 mm hole in the steel support plate, evaluated on basis of load / volume



**Figure A1.25b** Comparison of webbed designs 1 - 9 using a 100 mm hole in the steel support plate, evaluated on basis of load

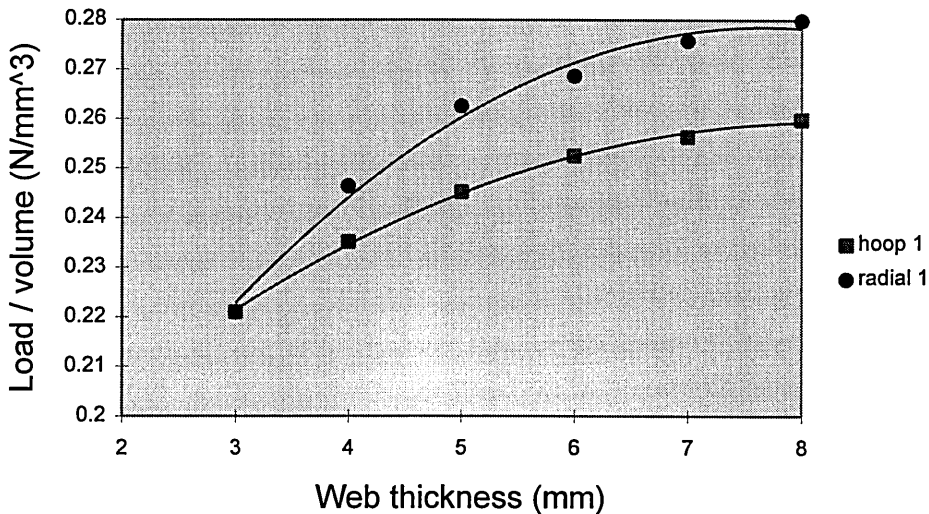
### Variation of Web thickness

The effect of increasing and decreasing the thickness of the webs in a webbed design of bearing plate was investigated, using a one factor at a time approach. The webs in the radial direction were split into radial 1, radial 2 and radial 3. Radial 1 was the portion of the radial web between the first and second circumferential web. Radial 2 was the portion of the radial web between the second and third circumferential webs etc. Hoop 1 was the first circumferential web from the centre of the bearing plate, hoop 2 was the second circumferential web from the centre of the bearing plate. The web thickness of a portion of the plate was increased or decreased, whilst all other webs were held at a constant thickness of 3 mm. The 3 mm web thickness was an arbitrary thickness held constant to enable comparison. Figures A1.26 and A1.27 refer to the increase and decrease of the web thickness for the design given in figure A1.17, when tested with 55 mm and 100 mm holes in the steel support plate respectively .



**Figure A1.26** Variation of load / volume with web thickness for webbed design number 4 (figure A1.17) with a 100 mm hole in the steel support plate

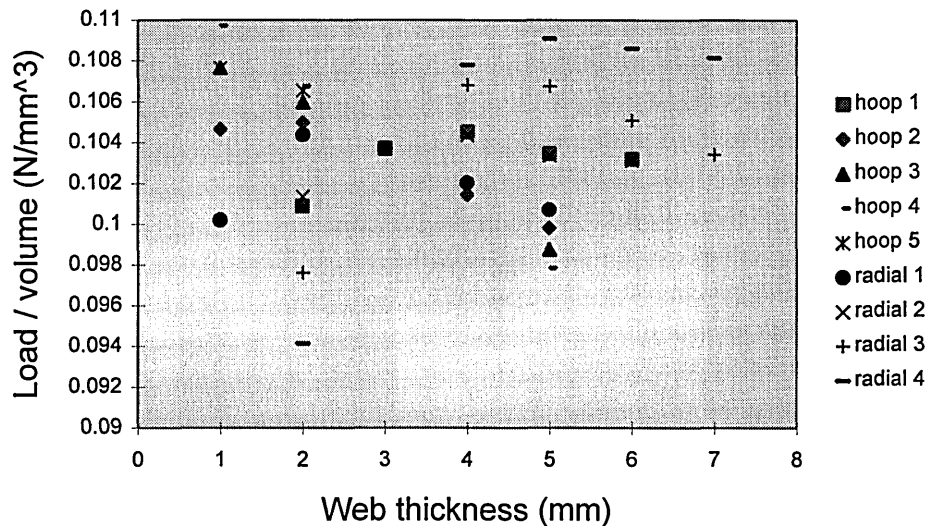
The curves shown in figure A1.26 for different parts of the webbed bearing plate are clearly not parallel to each other. The results given in figures A1.26 and A1.27 for the same design of bearing plate but with different diameters of hole in the steel support plate are clearly not the same.



**Figure A1.27** Variation of load / volume with web thickness for webbed design number 4 (figure A1.17) with a 55 mm hole in the steel support plate

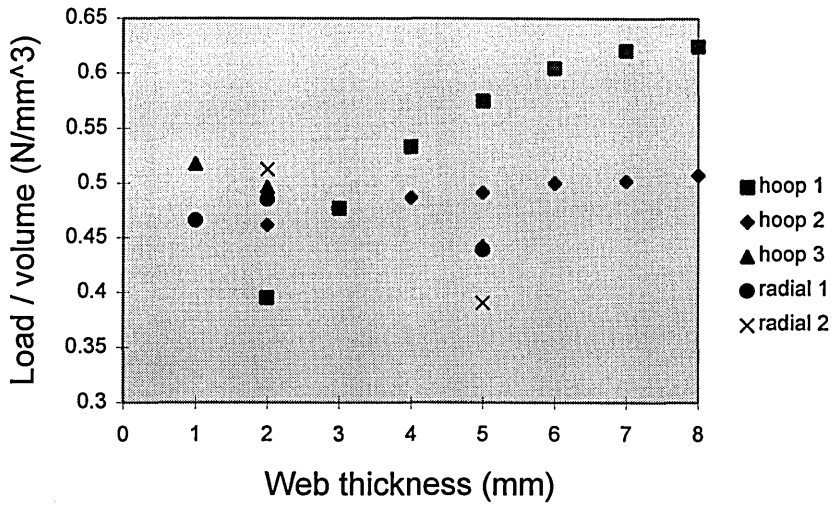
Webbed design number 4 shown in figure A1.17 has only 12 radial webs. As figure 4.14 shows, 12 radial webs is less than the optimum number required for a 55 mm hole in the steel support plate. Hence the fact that the design has less than the optimum number of radial webs, may account for the high significance of increasing the thickness of the radial webs as shown in figure A1.27.

Figure A1.28 shows the variation of load / volume with web thickness for webbed design number 8 (figure A1.21) with a 100 mm hole in the steel support plate



**Figure A1.28** Variation of load / volume with web thickness for webbed design number 8 (figure A1.21) with a 100 mm hole in the steel support plate

Figure A1.29 shows the variation of load / volume with web thickness for webbed design number 9 (figure A1.22) with a 55 mm hole in the steel support plate.



**Figure A1.29** Variation of load / volume with web thickness for webbed design number 9 (figure A1.22) with a 55 mm hole in the steel support plate

**Materials**

Figure A1.30 gives a comparison of some materials at 25°C and at an elevated temperature of 40°C. This was obtained by using material data obtained at different temperatures from the Campus material database.

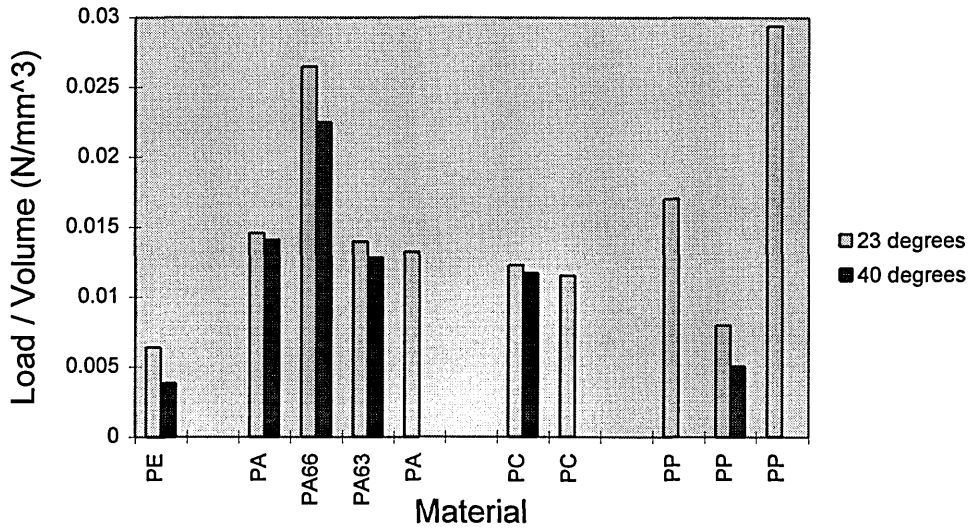


**Figure A1.30** Comparison of materials at 25°C and 40°C

The results in figure A1.30 show that the material does not perform as well at 40°C as at 23°C. The decrease in performance at increased temperature appears larger for polyethylene and polypropylene than for polyamide and polycarbonate. The results in figure A1.31 show that the materials perform much worse over extended periods of time than over short periods of time. These results give a brief indication of the relative significance of the material parameters compared to other parameters.

Figure A1.31 gives a comparison of some materials used over different periods of time.

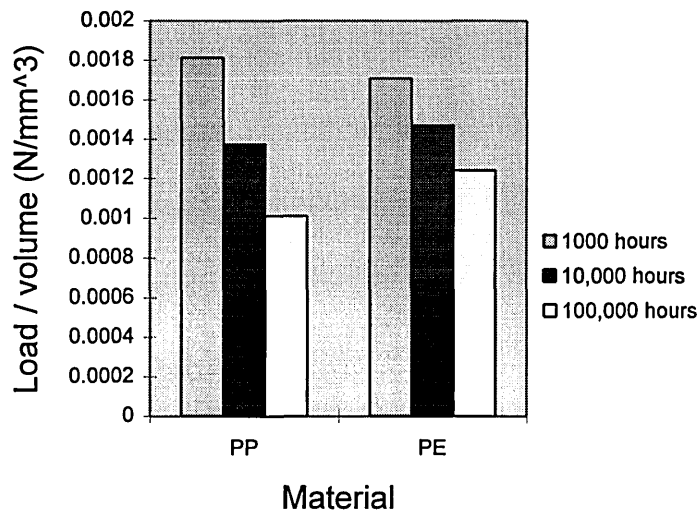


**Figure A1.31** Comparison of materials used over different periods of time

## APPENDIX 2 - Orthogonal arrays and drawings of bearing plate designs

### 2 level Taguchi experiment

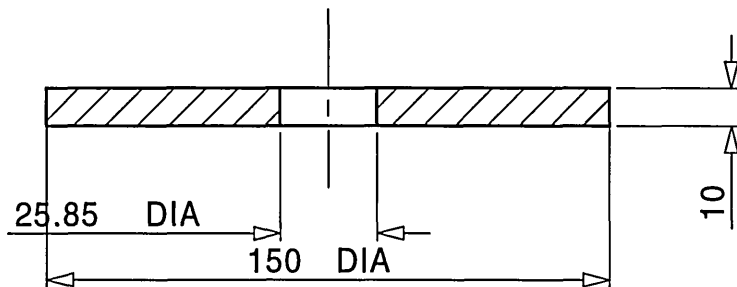
Table A2.1 shows an L16 orthogonal array that was used for the two level Taguchi experiment. The eight parameters have each been assigned to columns. Each of the 16 numbered rows in the orthogonal array refer to a Taguchi test (FE model). The numbers 1 or 2 in the array give the level of each parameter (column) for each test (row).

Test number	Parameters							
	G	E	F	B	A	C	D	H
1	1	1	1	1	1	1	1	1
2	1	1	1	1	2	2	2	2
3	1	1	2	2	1	1	1	2
4	1	1	2	2	2	2	2	1
5	1	2	1	2	1	2	2	1
6	1	2	1	2	2	1	1	2
7	1	2	2	1	1	2	2	2
8	1	2	2	1	2	1	1	1
9	2	1	1	2	1	1	2	1
10	2	1	1	2	2	2	1	2
11	2	1	2	1	1	1	2	2
12	2	1	2	1	2	2	1	1
13	2	2	1	1	1	2	1	1
14	2	2	1	1	2	1	2	2
15	2	2	2	2	1	2	1	2
16	2	2	2	2	2	1	2	1

**Table A2.1** L16 Orthogonal array used in 2 level Taguchi experiment

Table A2.1 is a simplified version of the orthogonal array used for the FE work, the analysis of the experiment was performed using a more complex orthogonal array which included the interactions.

Figures A2.1 - A2.17 are drawings of the 16 models and the confirmation test used in the Taguchi 2 level experiment.



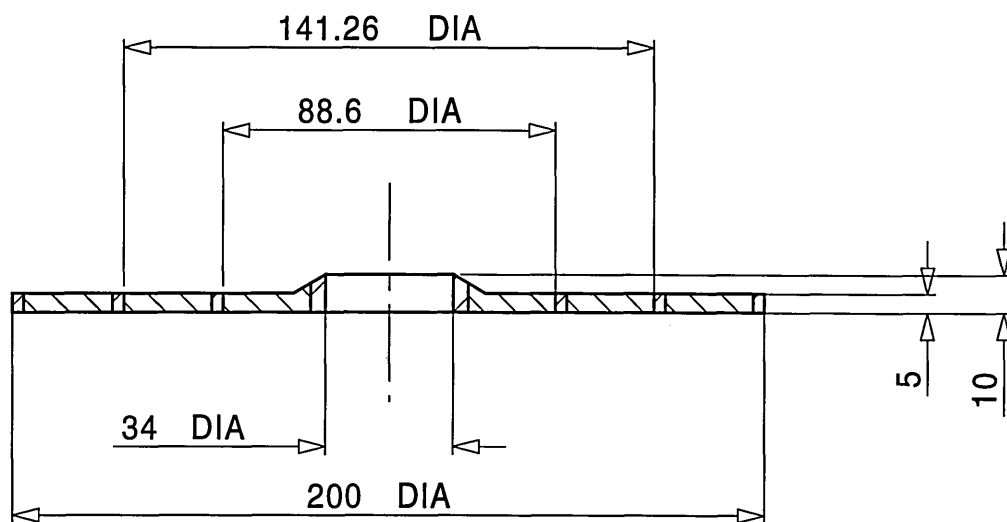
Nut diameter - 40 mm

55 mm hole in steel support plate

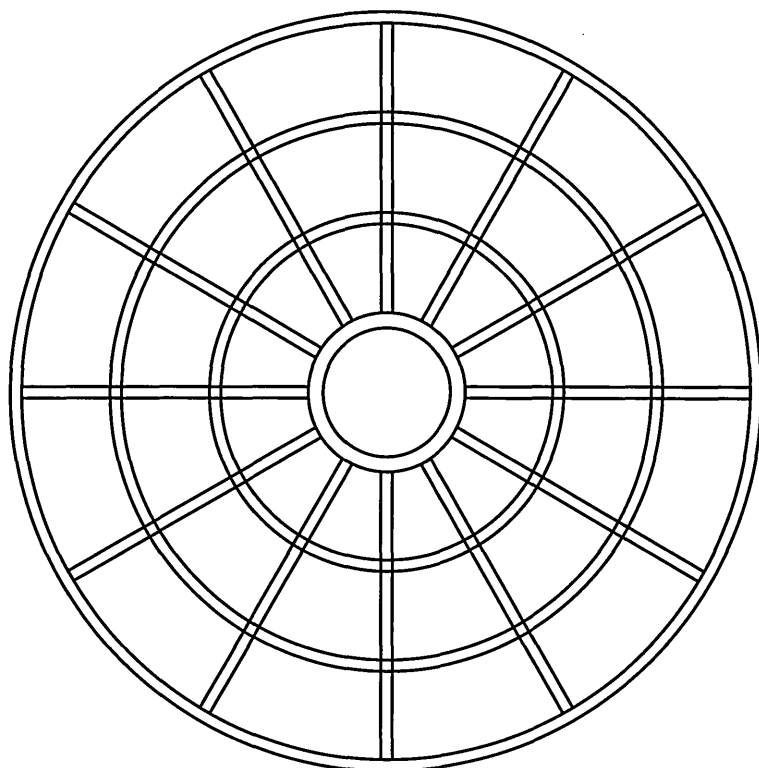
Material - Polypropylene

		 School of Engineering Sheffield Hallam University		
		TITLE <b>Taguchi test 1</b>		
Date <b>KMW</b>	Date <b>06 03 97</b>	PROJECT <b>A4</b>	DWG <b>Figure A2.1</b>	ISSUE <b>A</b>
Checked by -	Date -	SCALE <b>1:1</b>		SHEET - OF -

Nut diameter - 56 mm

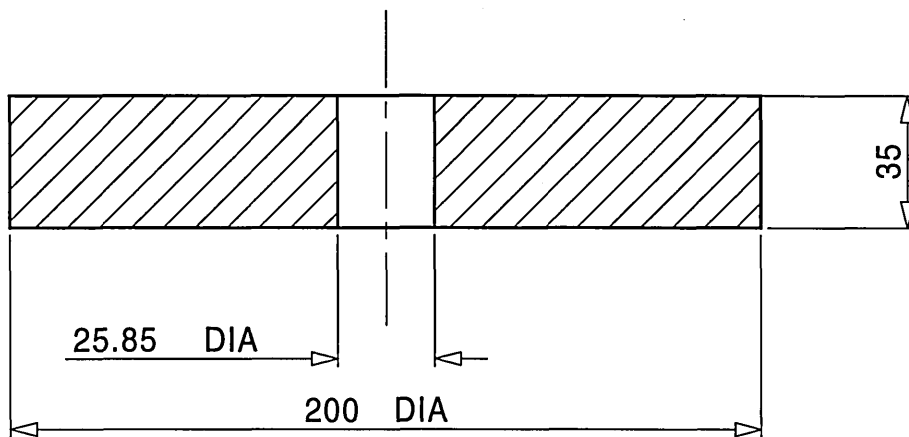


55 mm hole in steel support plate



Material - Polypropylene

		School of Engineering Sheffield Hallam University		
		TITLE Taguchi test 2		
Date 13 3 97	PROJECT A4	DWG Figure A2.2	ISSUE A	
Date -	SCALE 1 : 2	SHEET - OF -		



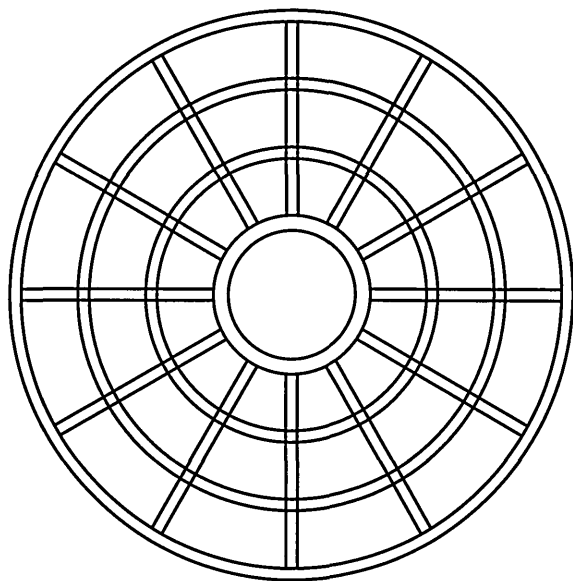
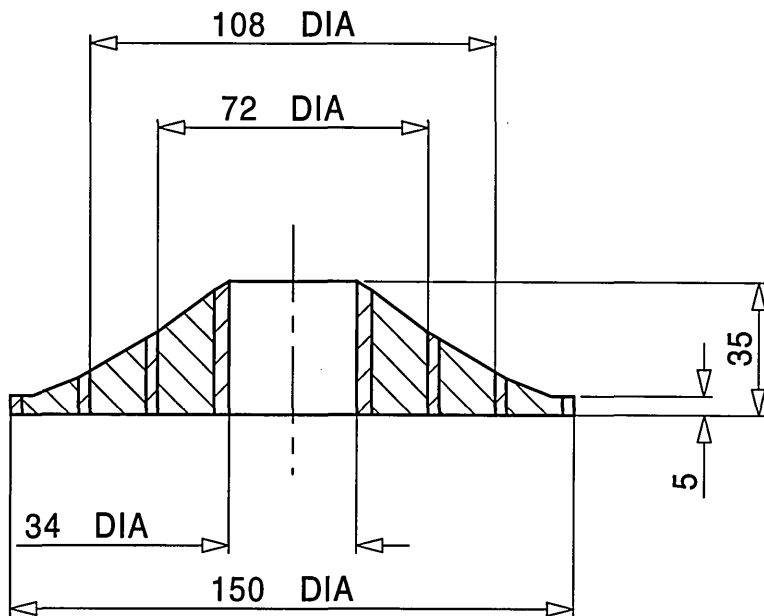
Nut diameter - 56 mm

100 mm hole in steel support plate

Material - Polypropylene

		 School of Engineering Sheffield Hallam University	
		TITLE <b>Taguchi test 3</b>	
Date KMW 06 03 97	PROJECT <b>A4</b>	DWG <b>Figure A2.3</b>	ISSUE <b>A</b>
Date - -	SCALE <b>1 : 2</b>		SHEET - OF -

Nut diameter - 40 mm

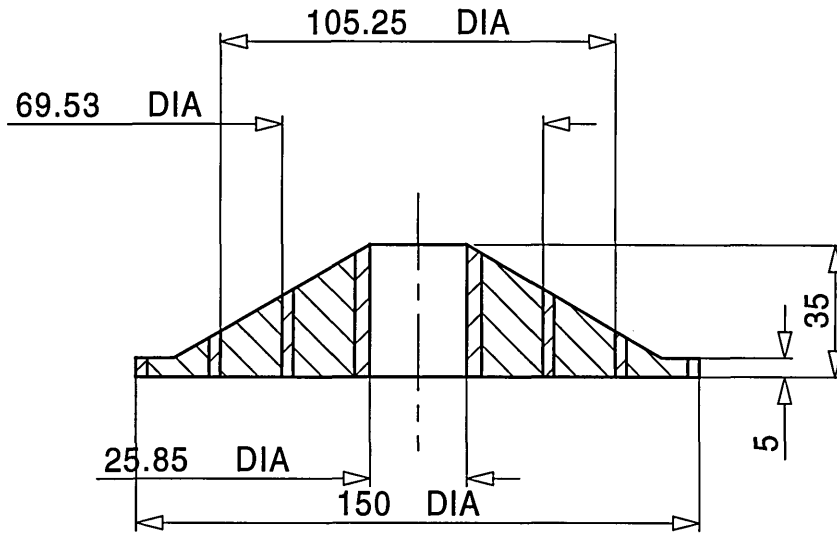


100 mm hole in steel support plate

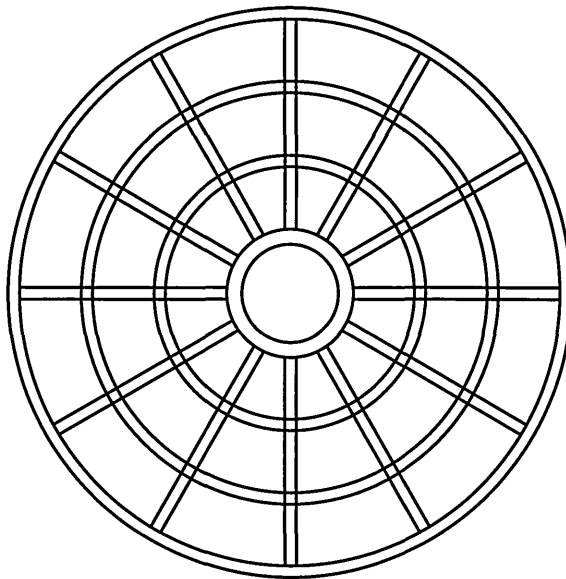
Material - Polypropylene

	 School of Engineering Sheffield Hallam University		
	TITLE <b>Taguchi test 4</b>		
Date 14 3 97	PROJECT <b>A4</b>	DWG <b>Figure A2.4</b>	ISSUE <b>A</b>
Date -	SCALE <b>1 : 2</b>		SHEET - OF -

Nut diameter - 40 mm

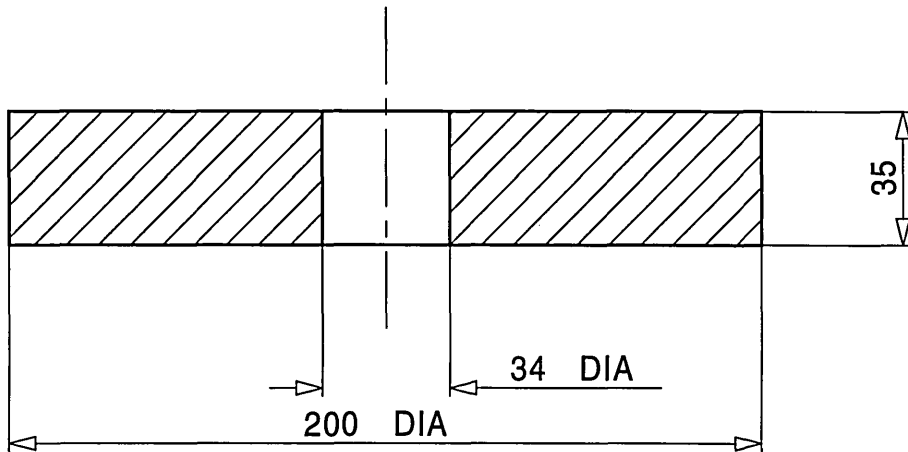


55 mm hole in steel support plate



Material polyamide 6

		School of Engineering Sheffield Hallam University		
		TITLE Taguchi test 5		
KMW	Date 14 3 97	PROJECT A4	DWG Figure A2.5	ISSUE A
-	Date -	SCALE 1 : 2	SHEET - OF -	



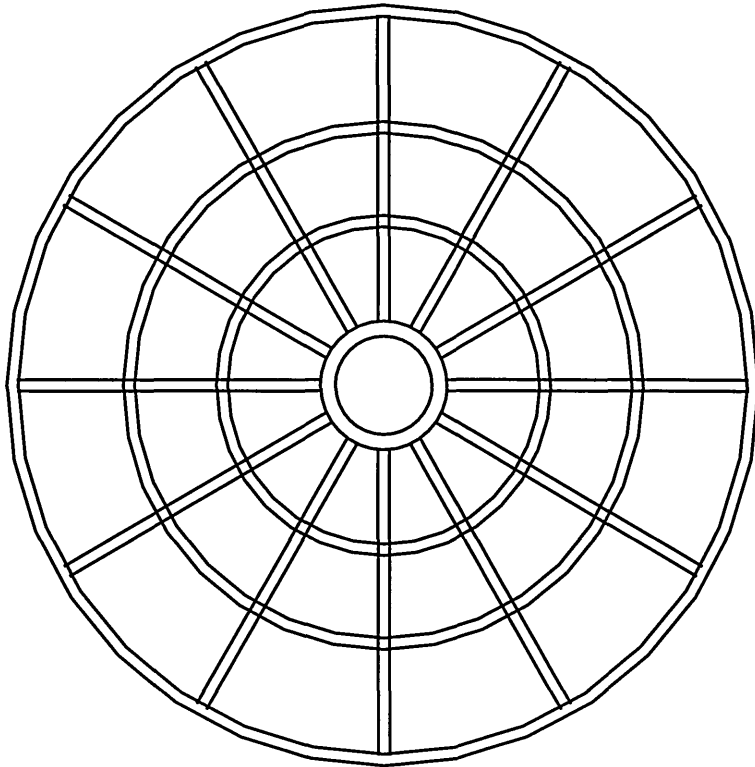
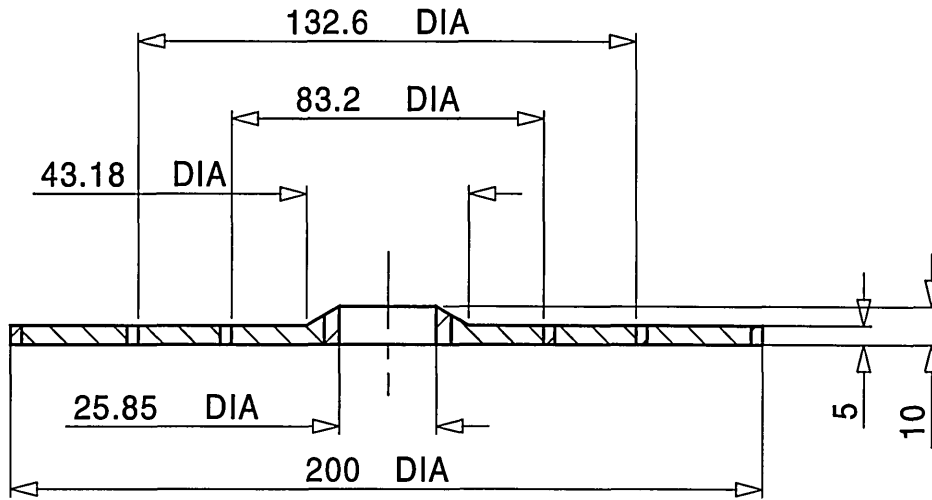
Nut diameter - 40 mm

55 mm hole in steel support plate

Material - Polyamide 6

	 School of Engineering Sheffield Hallam University		
	<b>TITLE</b> <b>Taguchi test 6</b>		
Date 06 03 97	<b>A4</b> PROJECT	DWG <b>Figure A2.6</b>	ISSUE <b>A</b>
Date -	SCALE <b>1 : 2</b>		SHEET - OF -

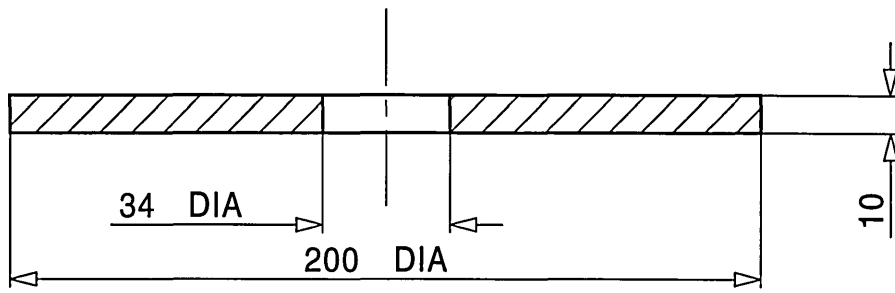
Nut diameter - 40 mm



100 mm hole in steel support plate

Material - Polyamide 6

<b>MEDUSA</b>	 School of Engineering Sheffield Hallam University		
	TITLE <b>Taguchi test 7</b>		
Date 14 3 97	PROJECT <b>A4</b>	DWG <b>Figure A2.7</b>	ISSUE <b>A</b>
Date -	SCALE <b>1 : 2</b>		SHEET - OF -

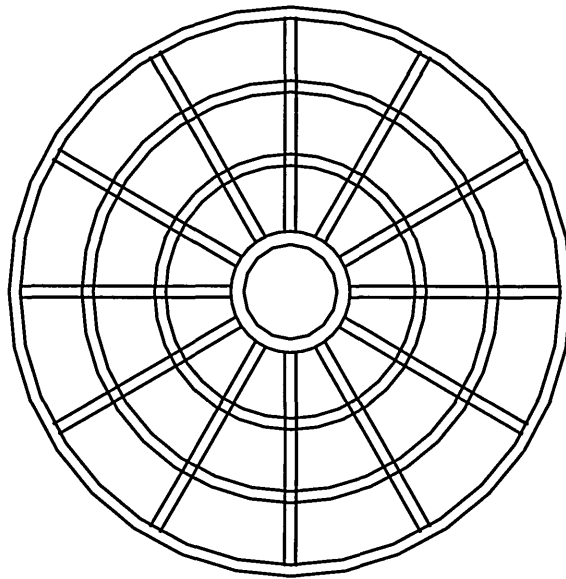
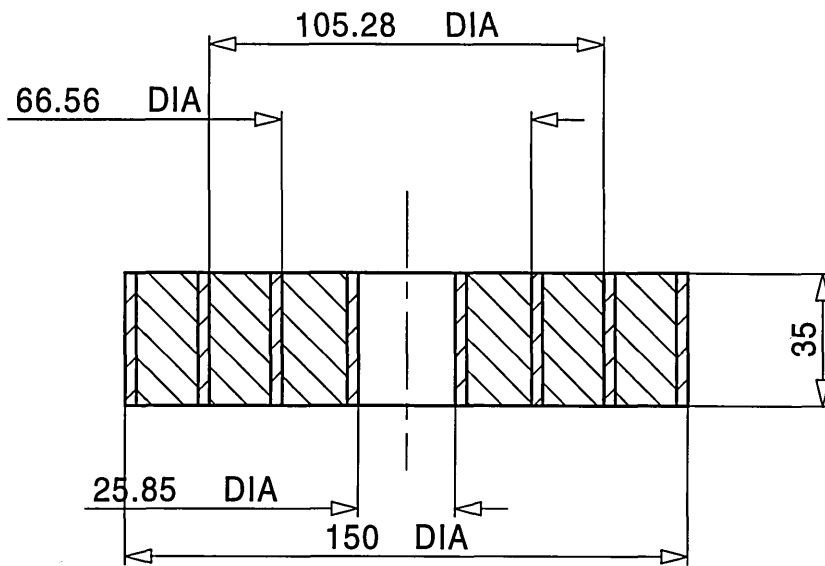


Nut diameter - 40 mm

100 mm hole in steel support plate

Material - Polyamide 6

	 School of Engineering Sheffield Hallam University		
	TITLE <b>Taguchi test 8</b>		
Date 07 03 97	PROJECT <b>A4</b>	DWG <b>Figure A2.8</b>	ISSUE <b>A</b>
Date -	SCALE <b>1 : 2</b>		SHEET - OF -

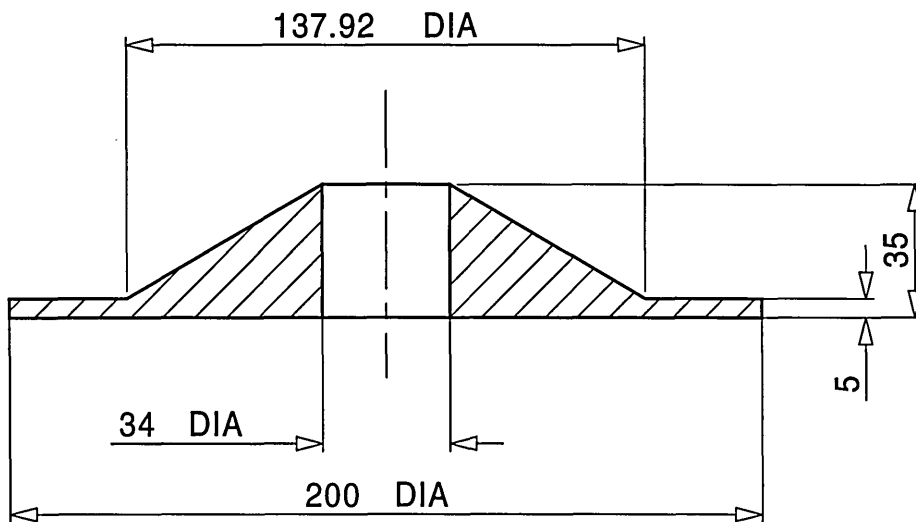


Nut diameter - 56 mm

55 mm hole in steel support plate

Material - Polypropylene

				School of Engineering Sheffield Hallam University	
	TITLE <b>Taguchi test 9</b>				
Date 12 3 97	PROJECT <b>A4</b>	DWG <b>Figure A2.9</b>	ISSUE <b>A</b>		
Date -	SCALE <b>1 : 2</b>		SHEET - OF -		



Nut diameter - 56 mm

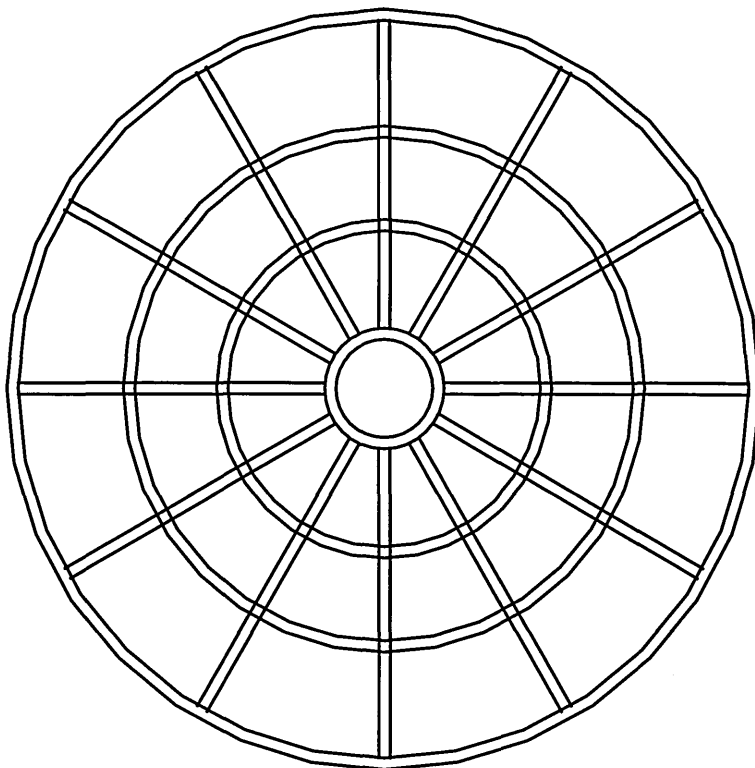
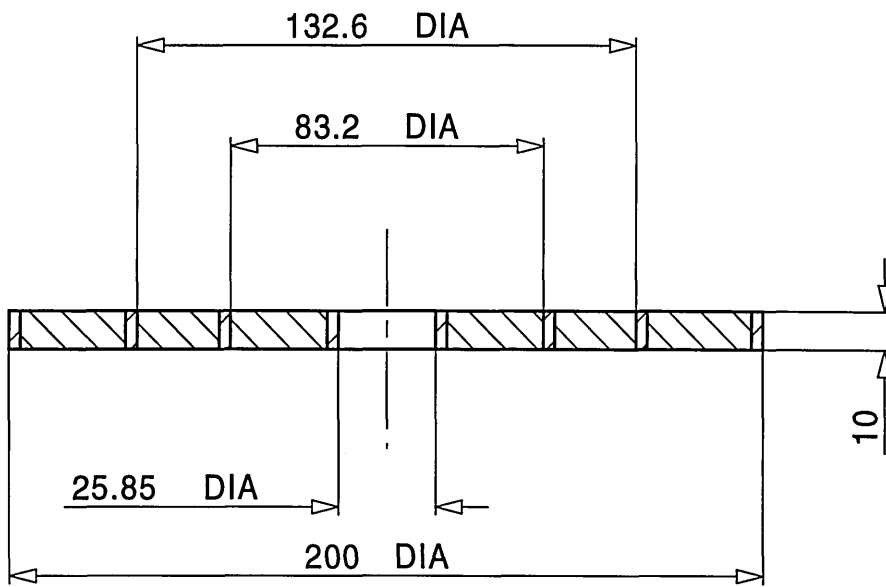
55 mm hole in steel support plate

Material - Polypropylene

	 School of Engineering Sheffield Hallam University		
	TITLE <b>Taguchi test 10</b>		
Date 07 03 97	PROJECT <b>A4</b>	DWG <b>Figure A2.10</b>	ISSUE <b>A</b>
Date -	SCALE <b>1 : 2</b>		SHEET - OF -

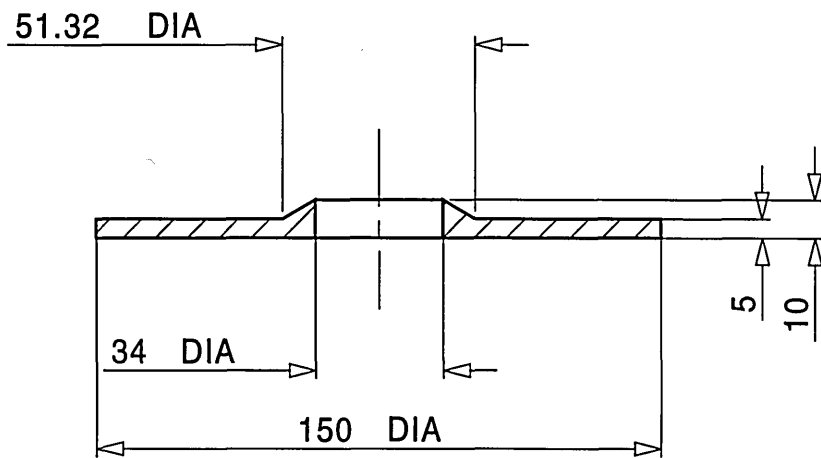
Nut diameter - 56 mm

100 mm hole in steel support plate



Material - Polypropylene

		School of Engineering Sheffield Hallam University		
		TITLE <b>Taguchi test 11</b>		
Checked by KMW	Date 12 3 97	PROJECT <b>A4</b>	DWG <b>Figure A2.11</b>	ISSUE <b>A</b>
SCALE 1 : 2		SHEET - OF -		

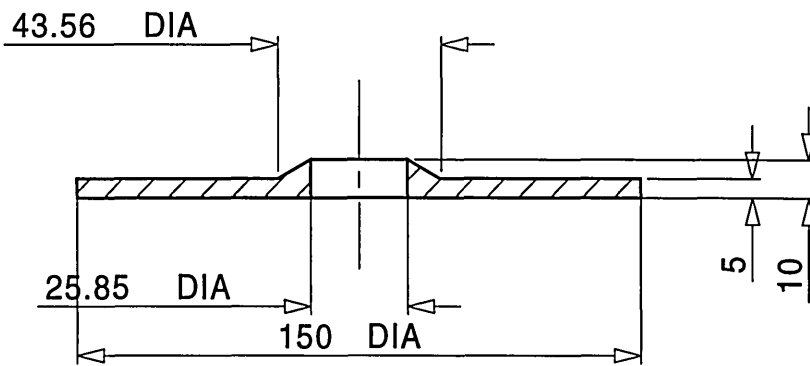


Nut diameter - 56 mm

100 mm hole in steel support plate

Material - Polypropylene

	 School of Engineering Sheffield Hallam University		
	TITLE <b>Taguchi test 12</b>		
Date 07 03 97	PROJECT <b>A4</b>	DWG <b>Figure A2.12</b>	ISSUE <b>A</b>
Date -	SCALE <b>1 : 2</b>		SHEET - OF -



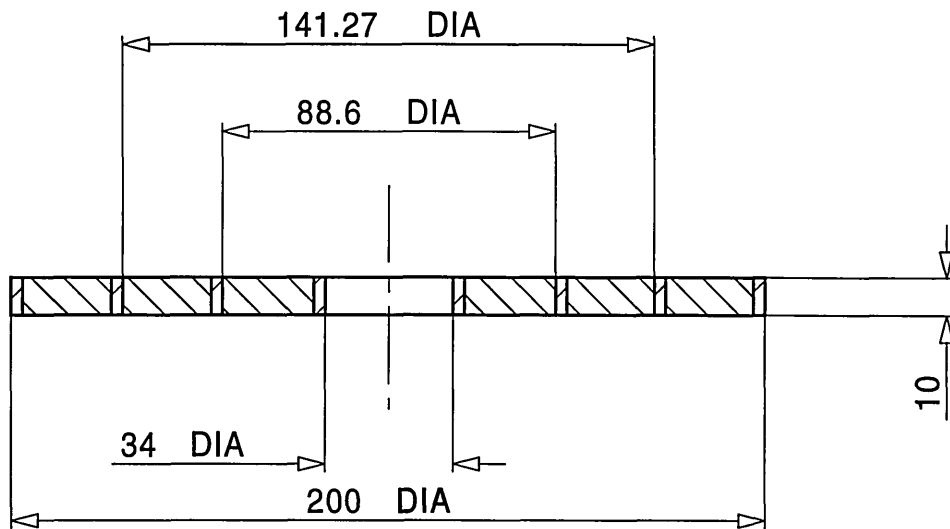
Nut diameter - 56 mm

55 mm hole in steel support plate

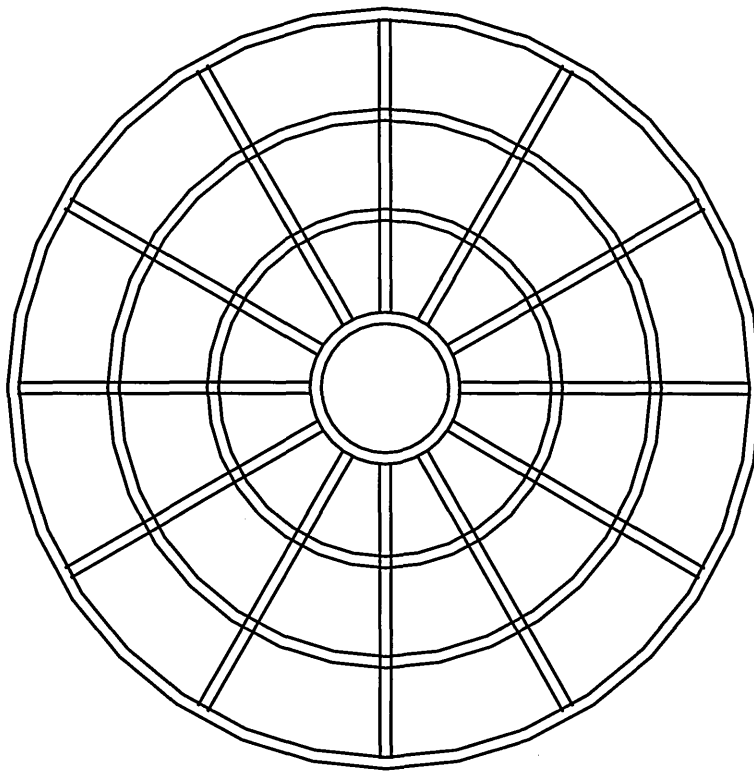
Material - Polyamide 6

	 School of Engineering Sheffield Hallam University		
	TITLE <b>Taguchi test 13</b>		
Date 07 03 97	PROJECT <b>A4</b>	DWG <b>Figure A2.13</b>	ISSUE <b>A</b>
Date -	SCALE <b>1 : 2</b>		SHEET - OF -

Nut diameter - 56 mm

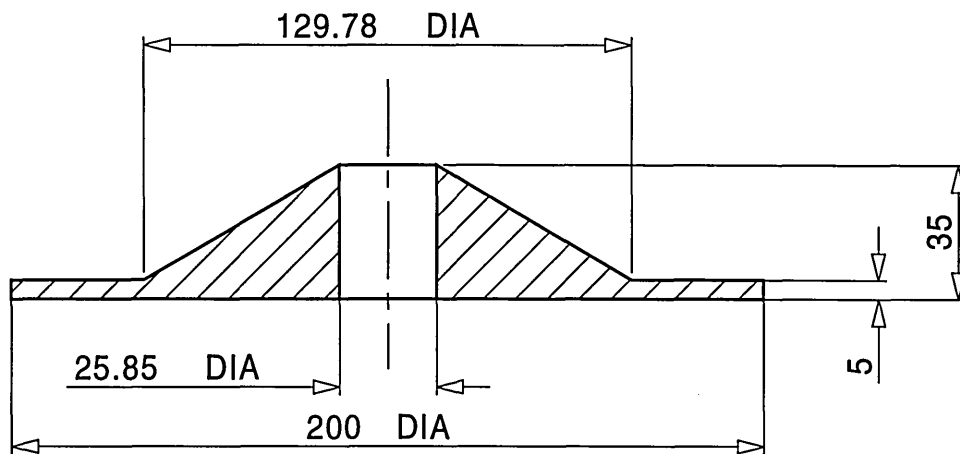


55 mm hole in steel support plate



Material - Polyamide 6

<b>MEDUSA</b>	 School of Engineering Sheffield Hallam University		
	TITLE <b>Taguchi test 14</b>		
Date 12 3 97	PROJECT <b>A4</b>	DWG <b>Figure A2.14</b>	ISSUE <b>A</b>
Date -	SCALE <b>1 : 2</b>	SHEET - OF -	



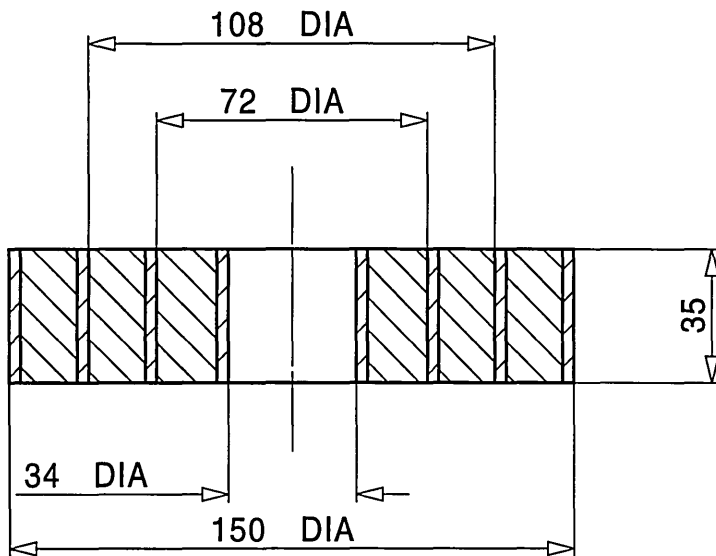
Nut diameter - 56 mm

100 mm hole in steel support plate

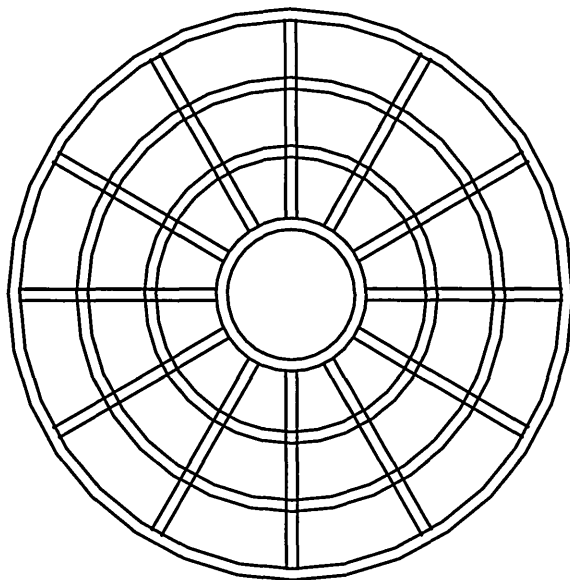
Material - Polyamide 6

		 School of Engineering Sheffield Hallam University		
		TITLE <b>Taguchi test 15</b>		
Date <b>KMW</b>	Date <b>07 03 97</b>	PROJECT <b>A4</b>	DWG <b>Figure A2.15</b>	ISSUE <b>A</b>
Date -		SCALE <b>1 : 2</b>		SHEET - OF -

Nut diameter - 56 mm

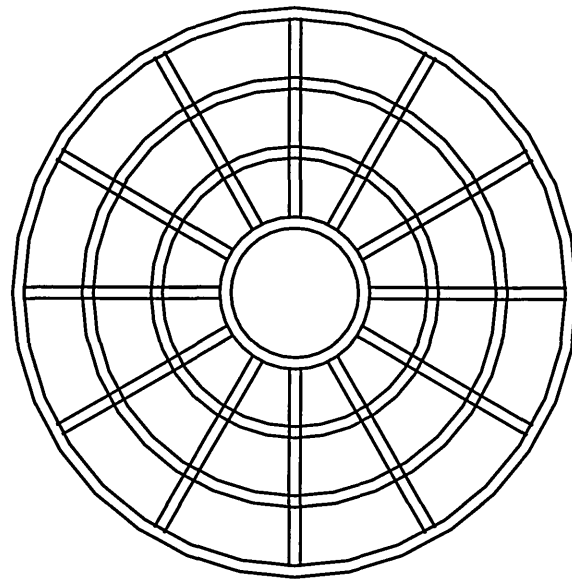
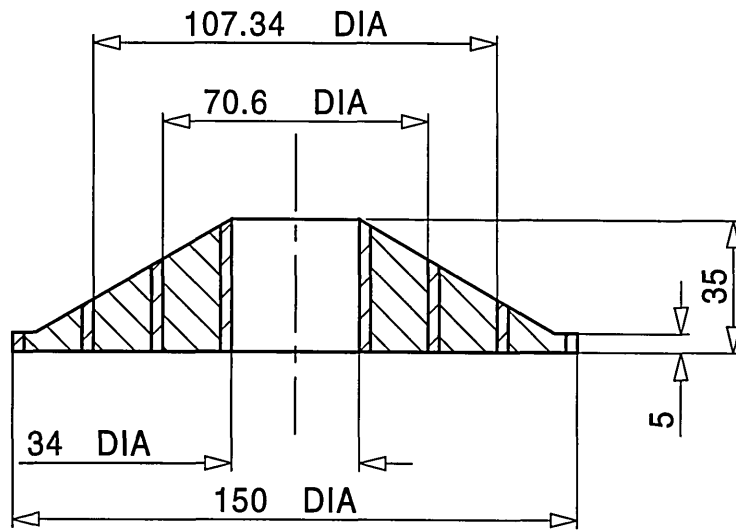


100 mm hole in steel support plate



Material - Polyamide 6

		School of Engineering Sheffield Hallam University		
		TITLE Taguchi test 16		
KMW	Date 13 3 97	PROJECT A4	DWG Figure A2.16	ISSUE A
-	Date -	SCALE 1 : 2	SHEET - OF -	



Material - Polypropylene

55 mm hole in steel support plate

Nut diameter - 40 mm

		 School of Engineering Sheffield Hallam University		
		TITLE <b>Taguchi 2 level confirmation</b>		
Date <b>KMW</b>	Date <b>21 3 97</b>	PROJECT <b>A4</b>	DWG <b>Figure A2.17</b>	ISSUE <b>A</b>
Checked by -		SCALE <b>1 : 2</b>		SHEET - OF -

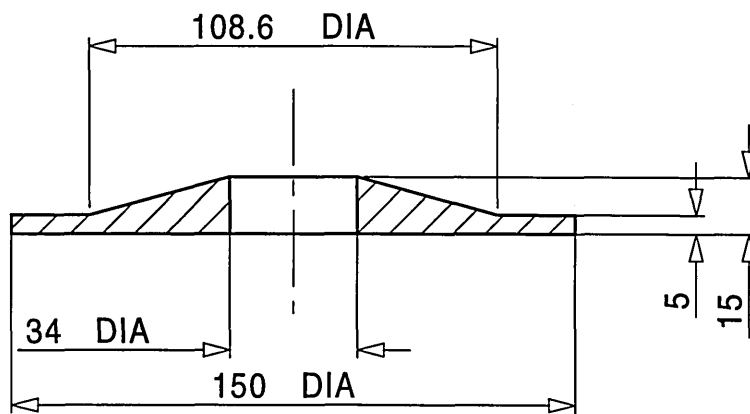
**Multiple level Taguchi experiment for solid bearing plate designs**

Table A2.2 shows an orthogonal array that was used for the multiple level Taguchi experiment on solid bearing plates. This orthogonal array required 9 tests (FE models) to be carried out. The numbers 1, 2 or 3 in the orthogonal array give the level of each parameter for each test. There were 3 levels investigated in this multiple level Taguchi experiment.

Test number	Parameters			
	F	B	I	J
1	1	1	1	1
2	1	2	2	2
3	1	3	3	3
4	2	1	2	3
5	2	2	3	1
6	2	3	1	2
7	3	1	3	2
8	3	2	1	3
9	3	3	2	1

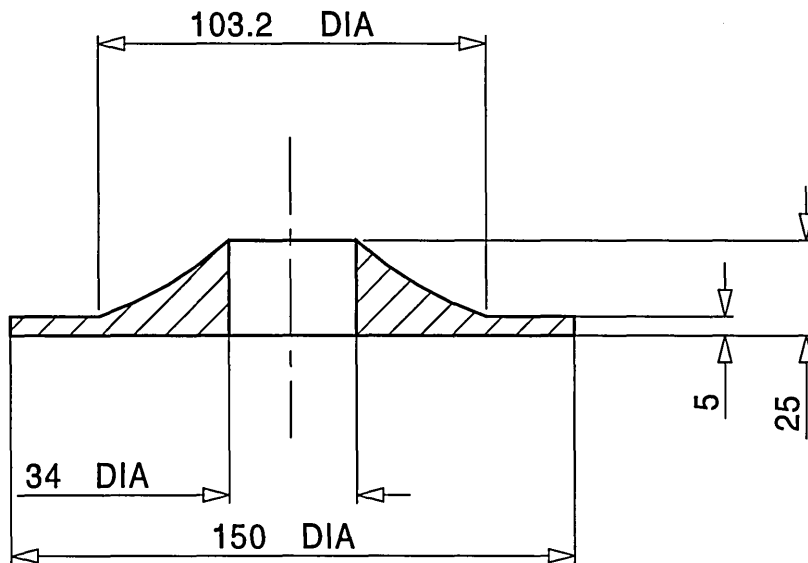
**Table A2.2** L9 orthogonal array used in multiple level Taguchi experiment on solid bearing plate designs

Figures A2.18 - A2.27 are drawings of the 9 models and the confirmation test used in the multiple level Taguchi experiment on solid bearing plate designs.



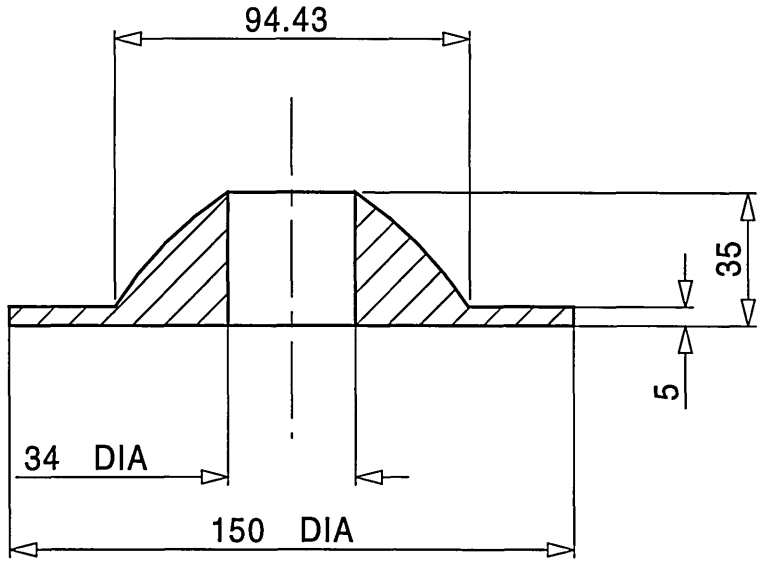
55 mm hole in steel support plate

		 School of Engineering Sheffield Hallam University		
		TITLE <b>Multiple level test 1</b>		
Date <b>KMW</b>	Date <b>07 03 97</b>	PROJECT <b>A4</b>	DWG <b>Figure A2.18</b>	ISSUE <b>A</b>
Date -		SCALE <b>1 : 2</b>		SHEET - OF -



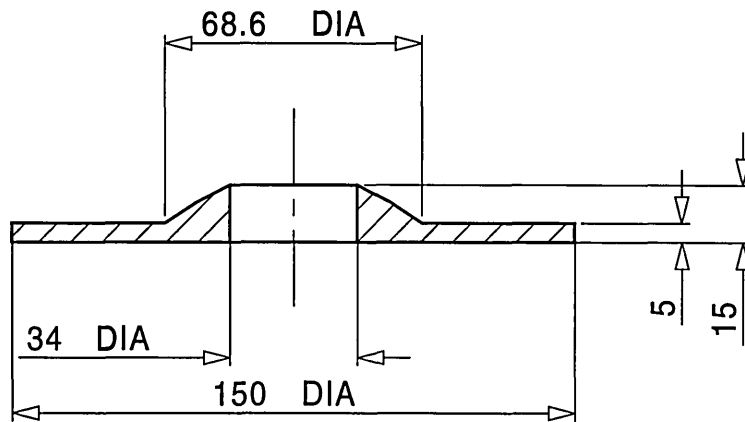
55 mm hole in steel support plate

		 School of Engineering Sheffield Hallam University			
				TITLE Multiple level test 2	
KMW	Date 07 03 97	A4	PROJECT Figure A2.19	DWG	ISSUE A
	Date -	SCALE 1 : 2	SHEET - OF -		



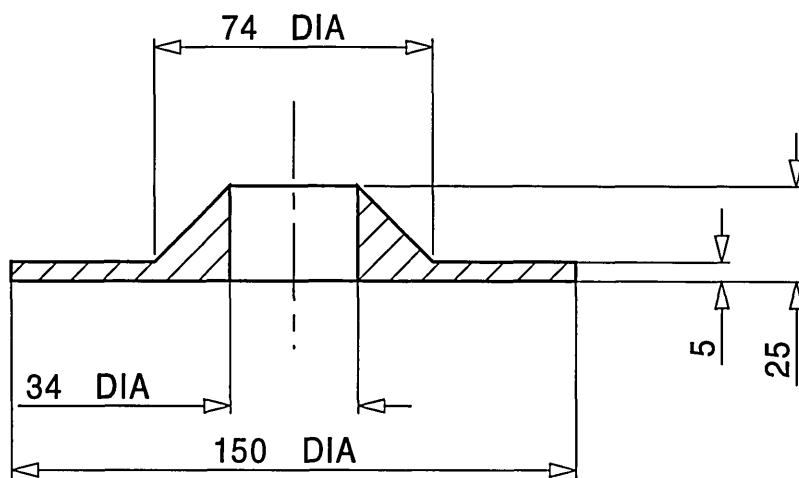
55 mm hole in steel support plate

	 School of Engineering Sheffield Hallam University		
	TITLE <b>Multiple level test 3</b>		
Date 8 5 97	PROJECT <b>A4</b>	DWG <b>Figure A2.20</b>	ISSUE <b>A</b>
Date -	SCALE <b>1 : 2</b>		SHEET - OF -



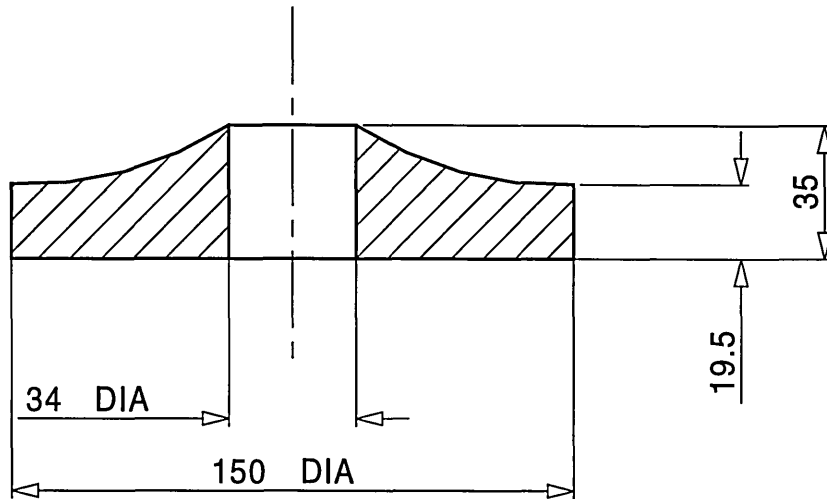
65 mm hole in steel support plate

	 School of Engineering Sheffield Hallam University		
	TITLE <b>Multiple level test 4</b>		
Date 8 5 97	PROJECT <b>A4</b>	DWG <b>Figure A2.21</b>	ISSUE <b>A</b>
Date -	SCALE <b>1 : 2</b>		SHEET - OF -



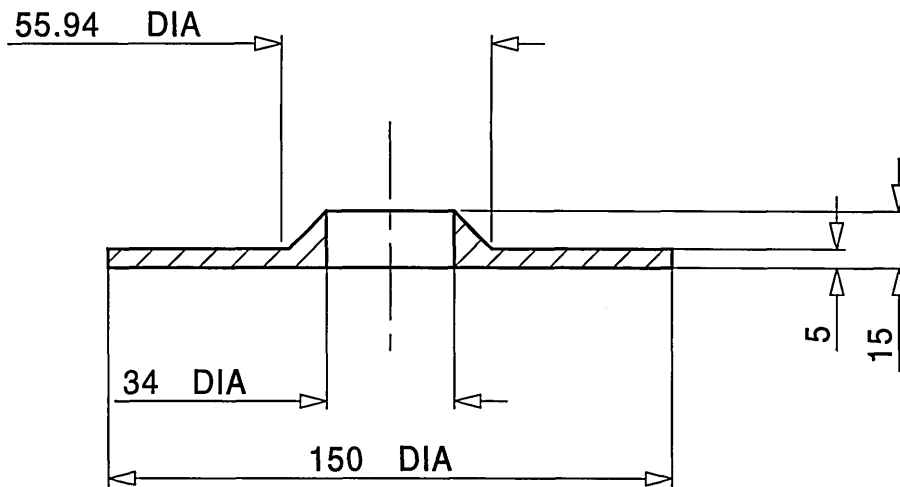
65 mm hole in steel support plate

	 School of Engineering Sheffield Hallam University		
	<b>TITLE</b> Multiple level test 5		
Date 07 03 97	<b>A4</b> PROJECT	DWG Figure A2.22	ISSUE A
Date -	<b>SCALE</b> 1 : 2		SHEET - OF -



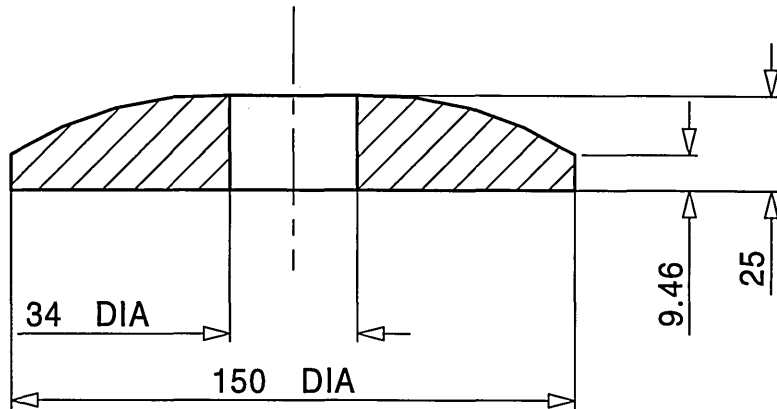
65 mm hole in steel support plate

	 School of Engineering Sheffield Hallam University		
	TITLE <b>Multiple level test 6</b>		
Date 8 5 97	PROJECT <b>A4</b>	DWG <b>Figure A2.23</b>	ISSUE <b>A</b>
Date -	SCALE <b>1 : 2</b>		SHEET - OF -



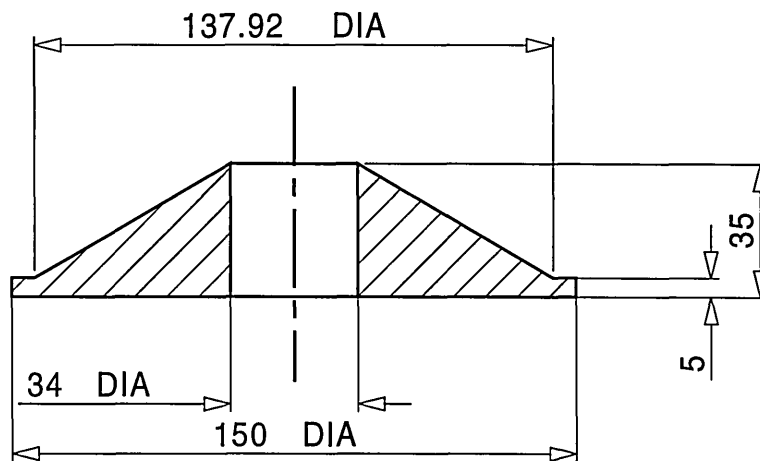
75 mm hole in steel support plate

	 School of Engineering Sheffield Hallam University		
	<b>TITLE</b> Multiple level test 7		
Date 8 5 97	<b>A4</b> PROJECT	DWG Figure A2.24	ISSUE A
Date -	<b>SCALE</b> 1 : 2		<b>SHEET</b> - <b>OF</b> -



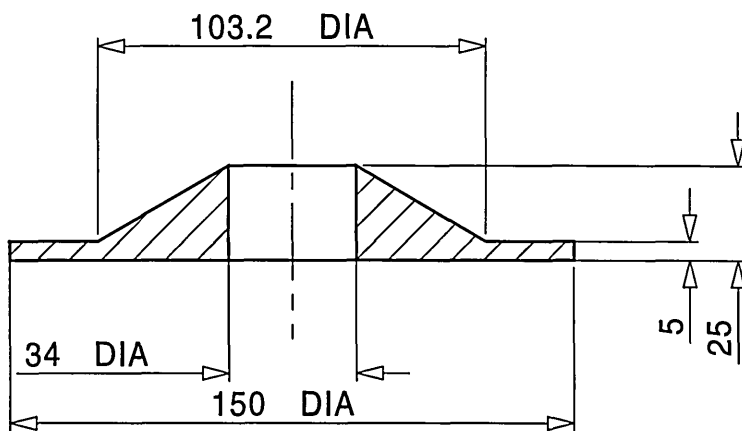
75 mm hole in steel support plate

	 School of Engineering Sheffield Hallam University		
	TITLE <b>Multiple level test 8</b>		
Date 8 5 97	PROJECT <b>A4</b>	DWG <b>Figure A2.25</b>	ISSUE <b>A</b>
Date -	SCALE <b>1 : 2</b>		SHEET - OF -



75 mm hole in steel support plate

		 School of Engineering Sheffield Hallam University		
		TITLE <b>Multiple level test 9</b>		
KMW	Date 10 03 97	PROJECT <b>A4</b>	DWG <b>Figure A2.26</b>	ISSUE <b>A</b>
Checked by -	Date -	SCALE <b>1 : 2</b>		SHEET - OF -



55 mm hole in steel support plate

		 School of Engineering Sheffield Hallam University		
				TITLE Multiple level confirmation
KMW Checked by -	Date 10 03 97 Date -	PROJECT A4 SCALE 1 : 2	DWG Figure A2.27	ISSUE A SHEET - OF -

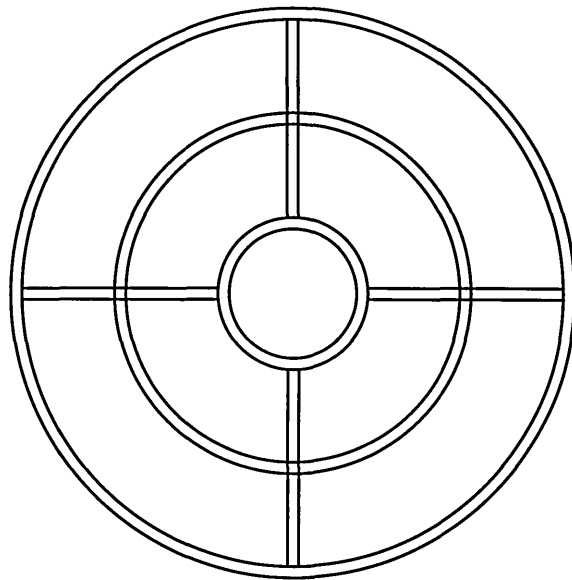
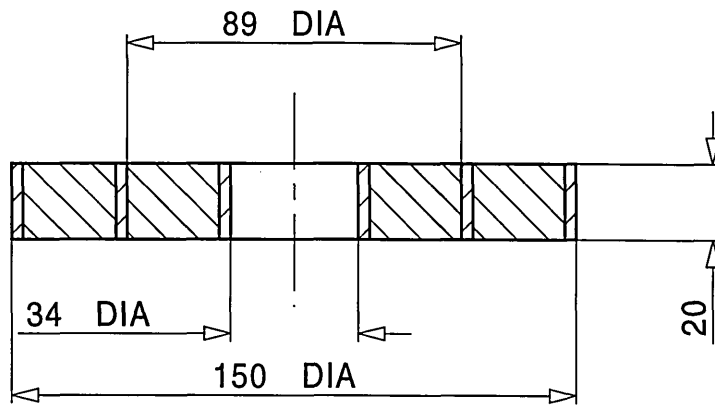
**Multiple level Taguchi experiment on webbed bearing plates**

Table A2.3 shows an L9 orthogonal array that was used for the multiple level Taguchi experiment on webbed bearing plates.

Test number	Parameters			
	K	L	M	E
1	1	1	1	1
2	1	2	2	2
3	1	3	3	3
4	2	1	2	3
5	2	2	3	1
6	2	3	1	2
7	3	1	3	2
8	3	2	1	3
9	3	3	2	1

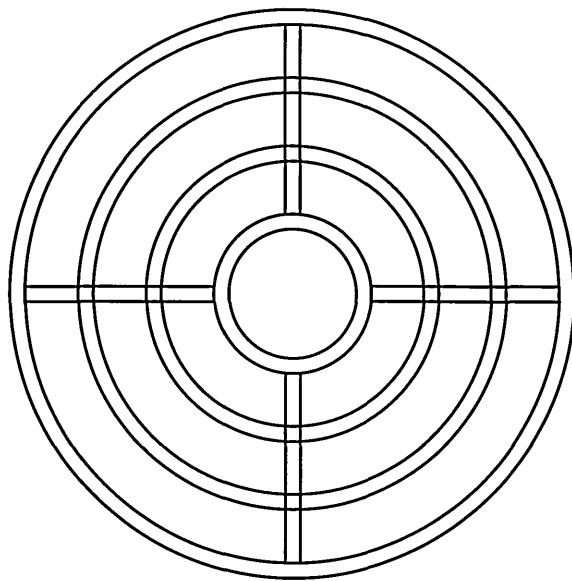
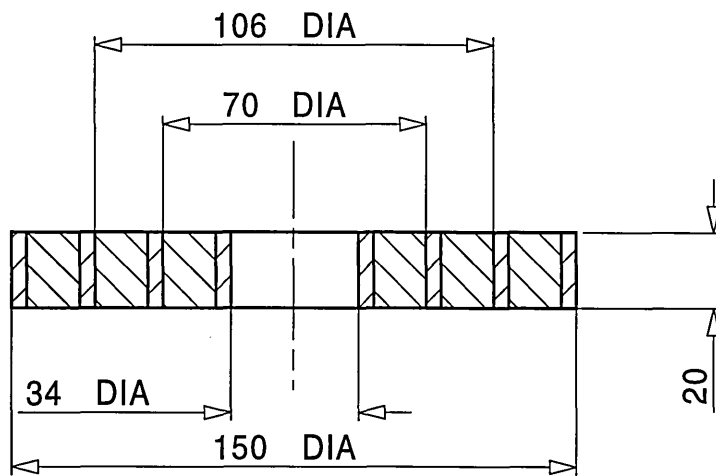
**Table A2.3** L9 orthogonal array used in multiple level Taguchi experiment on webbed bearing plate designs

Figures A2.28 - A2.38 are drawings of the 9 webbed models and confirmation tests used for the multiple level Taguchi experiment on webbed bearing plates.



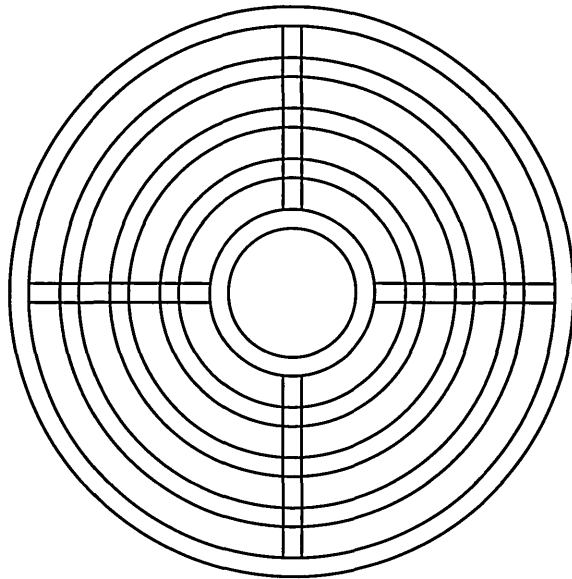
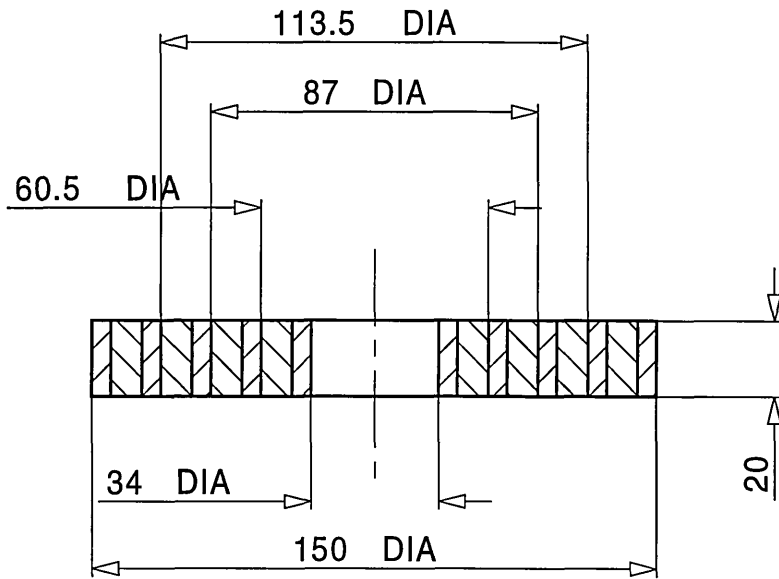
Material - polypropylene

	 School of Engineering Sheffield Hallam University		
	<b>TITLE</b> Multiple level webbed test 1		
<b>KMW</b> Checked by	Date 24 4 97	<b>A4</b> PROJECT	DWG <b>Figure A2.28</b>
-	Date -	<b>SCALE</b> 1 : 2	
		SHEET - OF -	ISSUE <b>A</b>



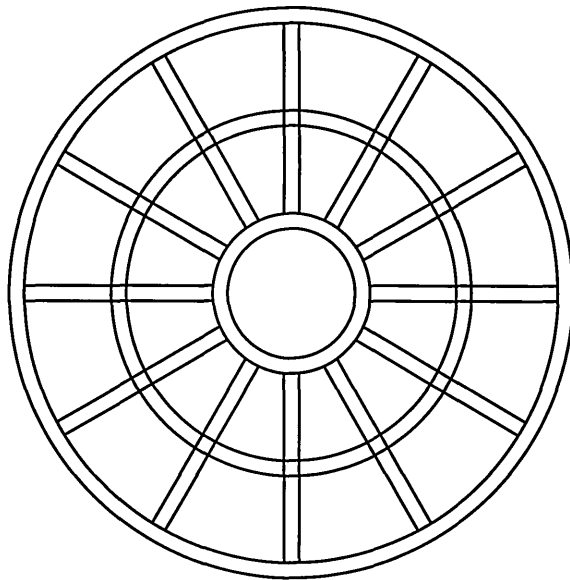
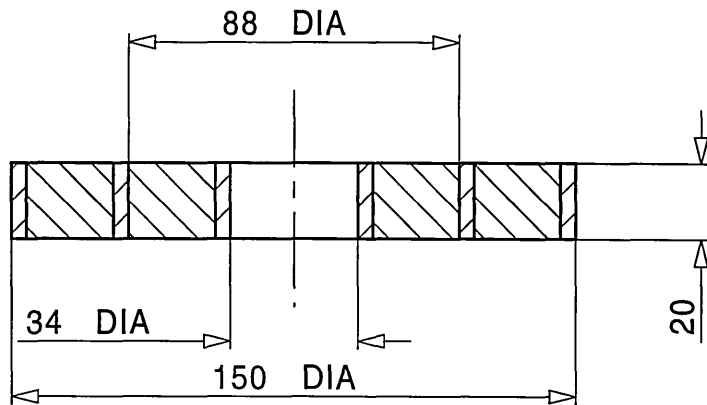
Material - polyamide 6

	 School of Engineering Sheffield Hallam University		
	<b>TITLE</b> Multiple level webbed test 2		
Date 24 4 97	<b>A4</b> PROJECT	DWG Figure A2.29	ISSUE A
Date -	<b>SCALE</b> 1 : 2		SHEET - OF -



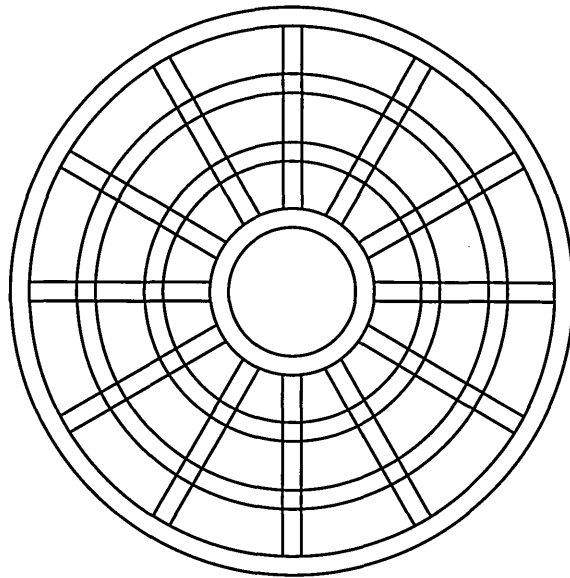
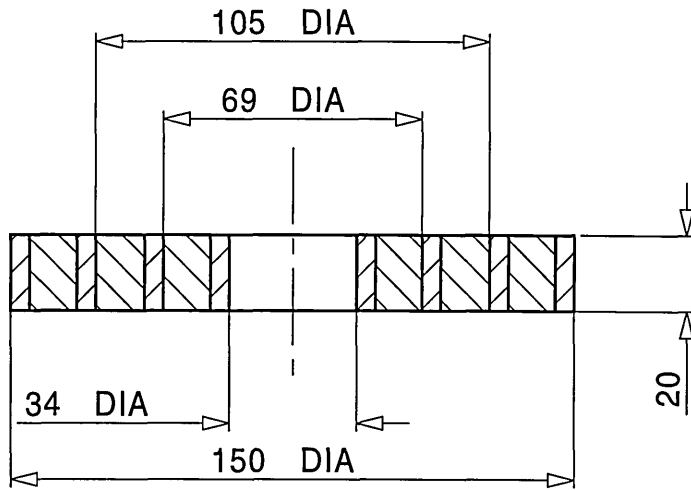
Material - polycarbonate

	 School of Engineering Sheffield Hallam University		
	<b>TITLE</b> Multiple level webbed test 3		
Date 24 4 97	<b>A4</b> PROJECT	DWG Figure A2.30	ISSUE A
Date -	SCALE 1 : 2	SHEET - OF -	



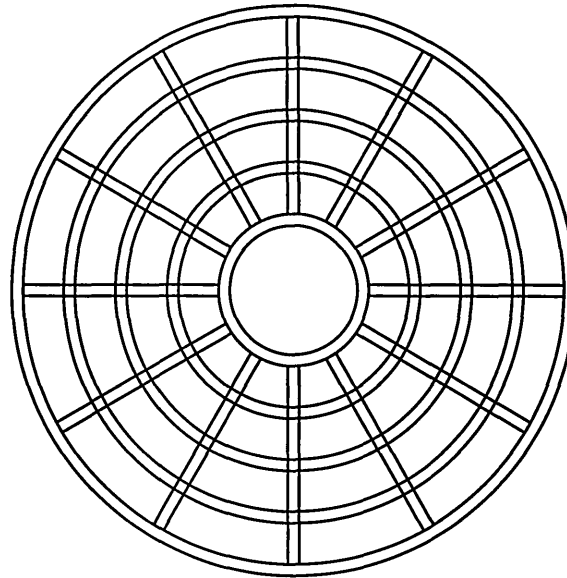
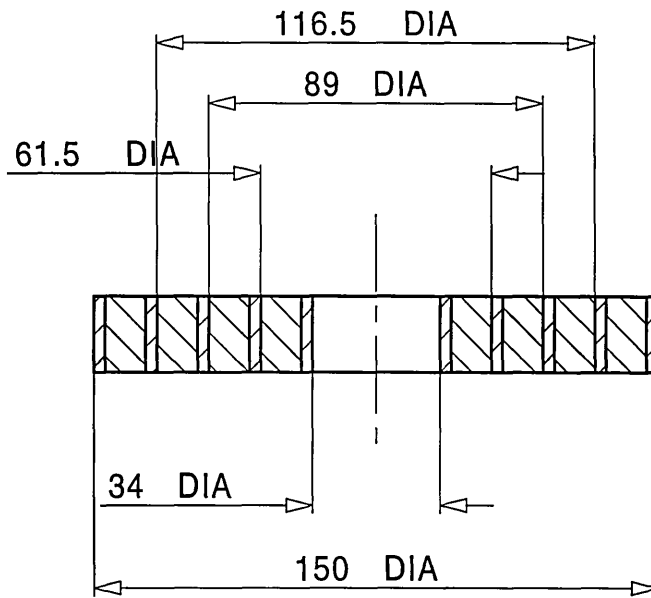
Material - polycarbonate

	 School of Engineering Sheffield Hallam University		
	TITLE <b>Multiple level webbed test 4</b>		
Date 28 4 97	PROJECT <b>A4</b>	DWG <b>Figure A2.31</b>	ISSUE <b>A</b>
Date -	SCALE <b>1 : 2</b>		SHEET - OF -



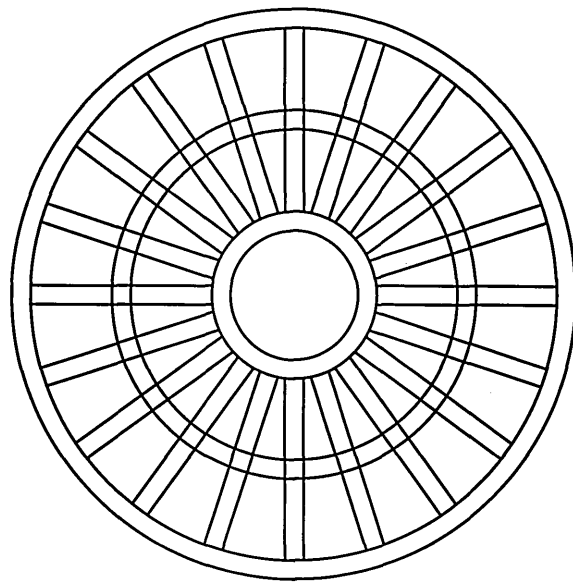
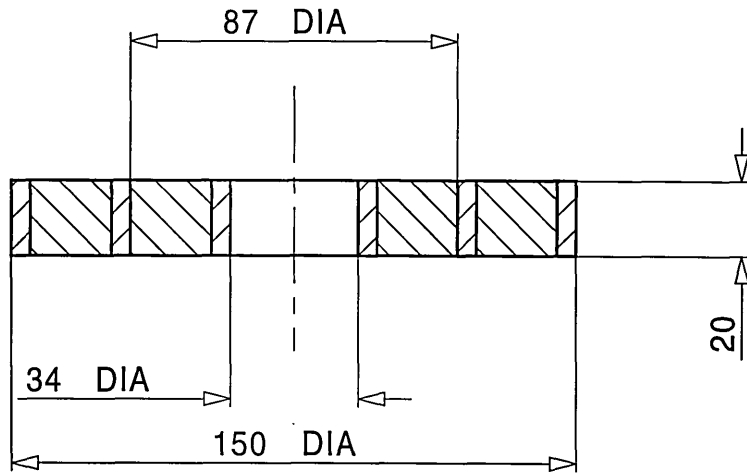
Material - polypropylene

	 School of Engineering Sheffield Hallam University		
	TITLE <b>Multiple level webbed test 5</b>		
Date 28 4 97	PROJECT <b>A4</b>	DWG <b>Figure A2.32</b>	ISSUE <b>A</b>
Date -	SCALE <b>1 : 2</b>	SHEET - OF -	



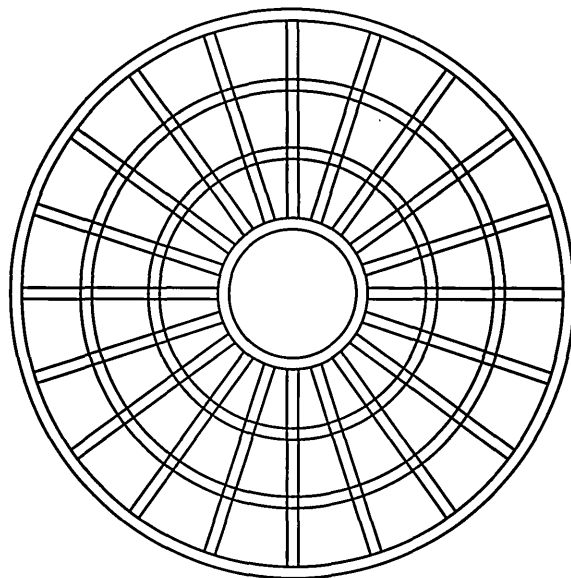
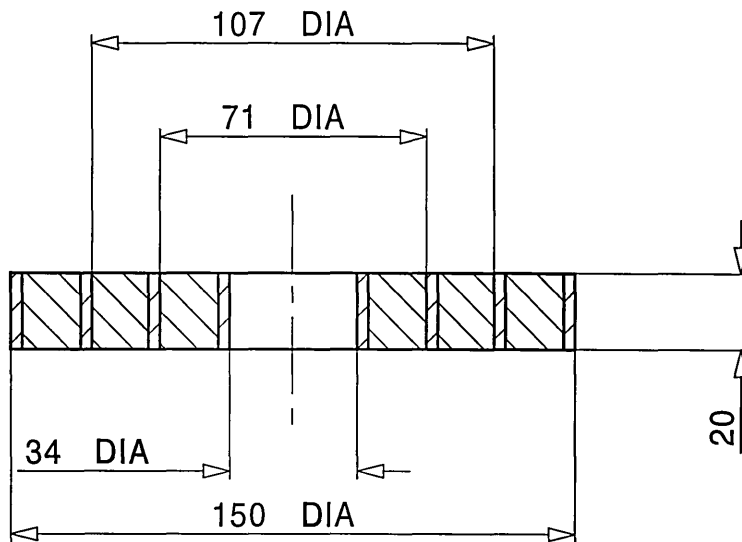
Material - polyamide 6

	 School of Engineering Sheffield Hallam University		
	<b>TITLE</b> Multiple level webbed test 6		
Date 28 4 97	<b>A4</b> PROJECT	DWG <b>Figure A2.33</b>	ISSUE <b>A</b>
Date -	<b>SCALE</b> 1 : 2		SHEET - OF -

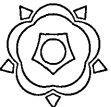


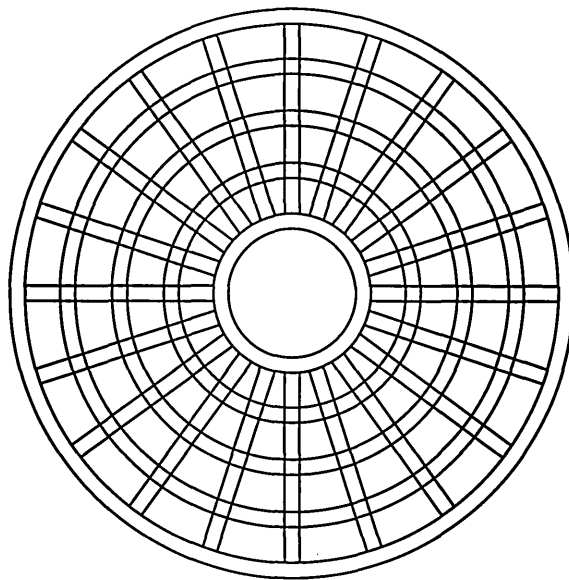
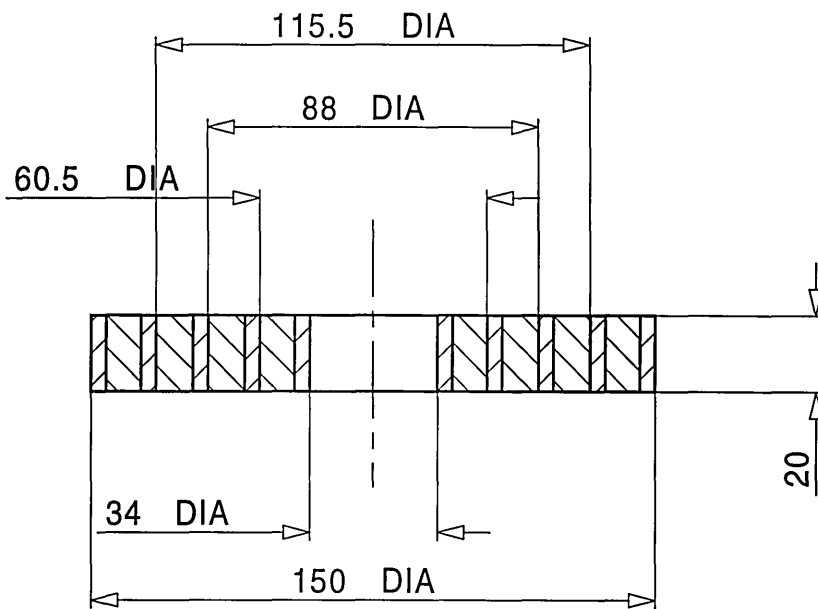
Material - polyamide 6

	 School of Engineering Sheffield Hallam University		
	TITLE <b>Multiple level webbed test 7</b>		
Date 15 97	PROJECT <b>A4</b>	DWG <b>Figure A2.34</b>	ISSUE <b>A</b>
Date -	SCALE <b>1 : 2</b>		SHEET - OF -



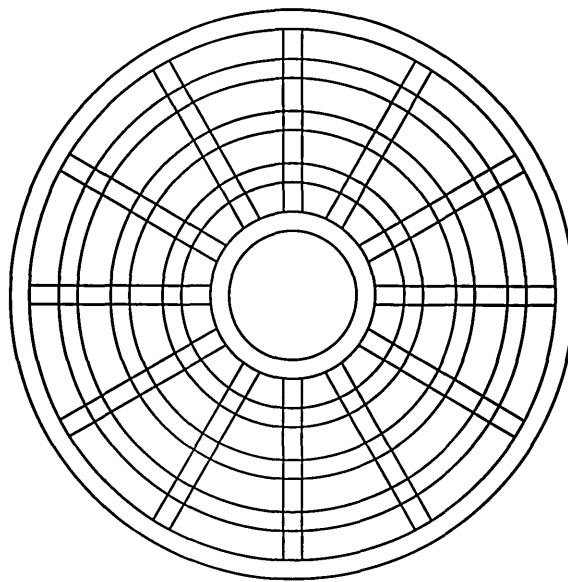
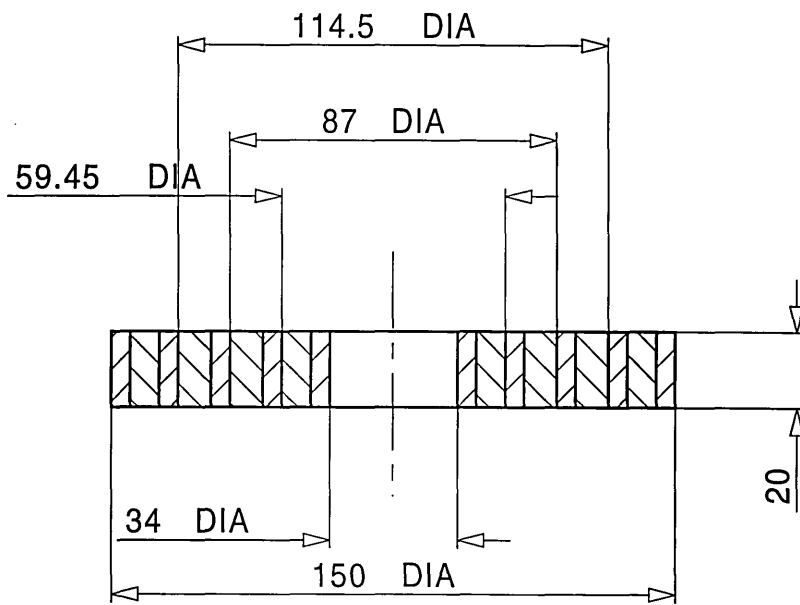
Material - polycarbonate

	 School of Engineering Sheffield Hallam University		
	TITLE <b>Multiple level webbed test 8</b>		
KMW	Date 1 5 97	PROJECT <b>A4</b>	DWG <b>Figure A2.35</b>
-	Date -	SCALE 1 : 2	ISSUE <b>A</b>
		SHEET - OF -	



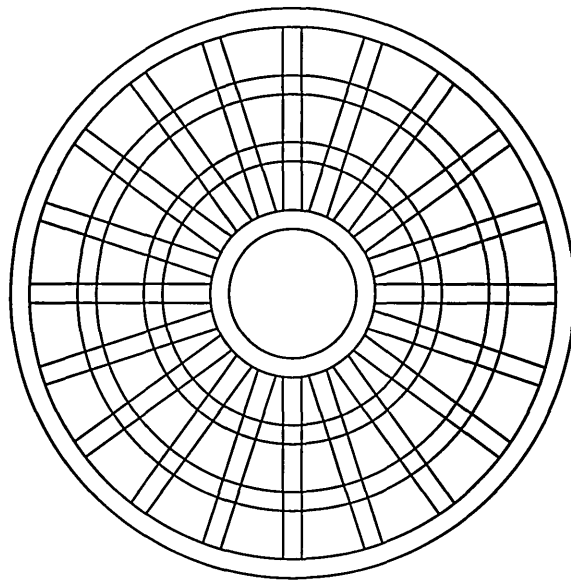
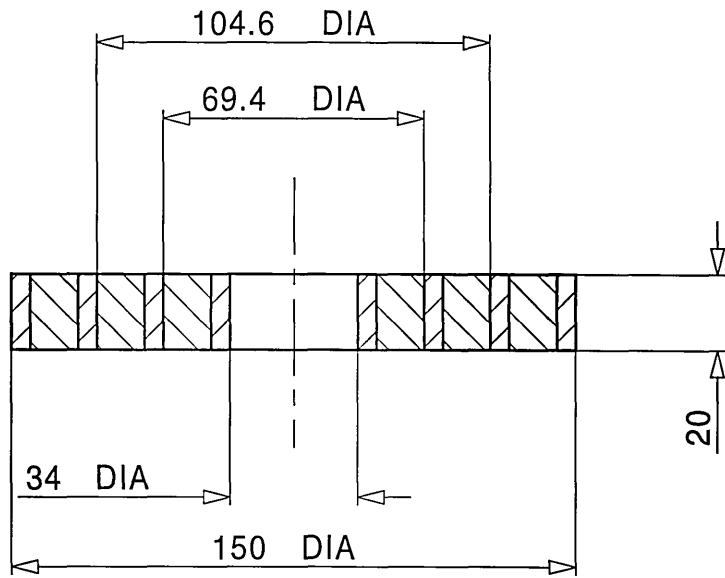
Material - polypropylene

	 School of Engineering Sheffield Hallam University		
	TITLE Multiple level webbed test 9		
Date 1 5 97	PROJECT A4	DWG Figure A2.36	ISSUE A
Date -	SCALE 1 : 2		SHEET - OF -



Material - Polypropylene

				School of Engineering Sheffield Hallam University
	TITLE <b>Confirmation test 100mm hole</b>			
Date 8 5 97	PROJECT <b>A4</b>	DWG <b>Figure A2.37</b>	ISSUE <b>A</b>	
Date -	SCALE <b>1 : 2</b>		SHEET - OF -	



Material - Polypropylene

				School of Engineering Sheffield Hallam University	
	TITLE <b>Confirmation test 55mm hole</b>				
Date 8 5 97	PROJECT <b>A4</b>	DWG <b>Figure A2.38</b>	ISSUE <b>A</b>		
Date -	SCALE <b>1 : 2</b>		SHEET - OF -		

## **APPENDIX 3 - Material data**

### **Weldgrip and Weidmann bearing plate material**

To be able to model existing designs of bearing plates using FEA, material data was required. Figure A3.1 shows the dimensions of the tensile testing specimens used to produce the material data. The dimensions are as specified by BS 2782.

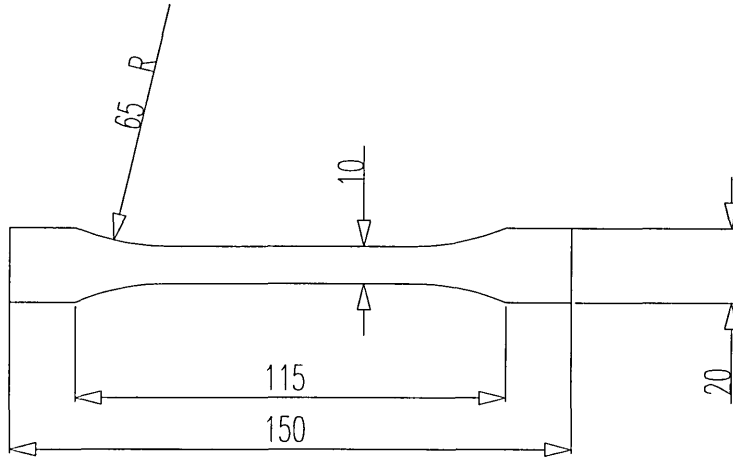


**Figure A3.1** Tensile testing specimens

The thickness of the Weldgrip tensile testing specimens was approximately 6.6 mm and the Weidmann tensile testing specimens approximately 6 mm. The allowable range specified by BS 2782 was 1 - 10 mm.

Figure A3.2 is a material selector chart from the cambridge material selector software package, showing ductility and Young's modulus. Figure A3.3 is another materials selector chart showing flammability and Young's modulus. Figure A3.4 shows tensile strength and maximum service temperature.

Figure A3.2 Material selection chart showing ductility and Young's Modulus

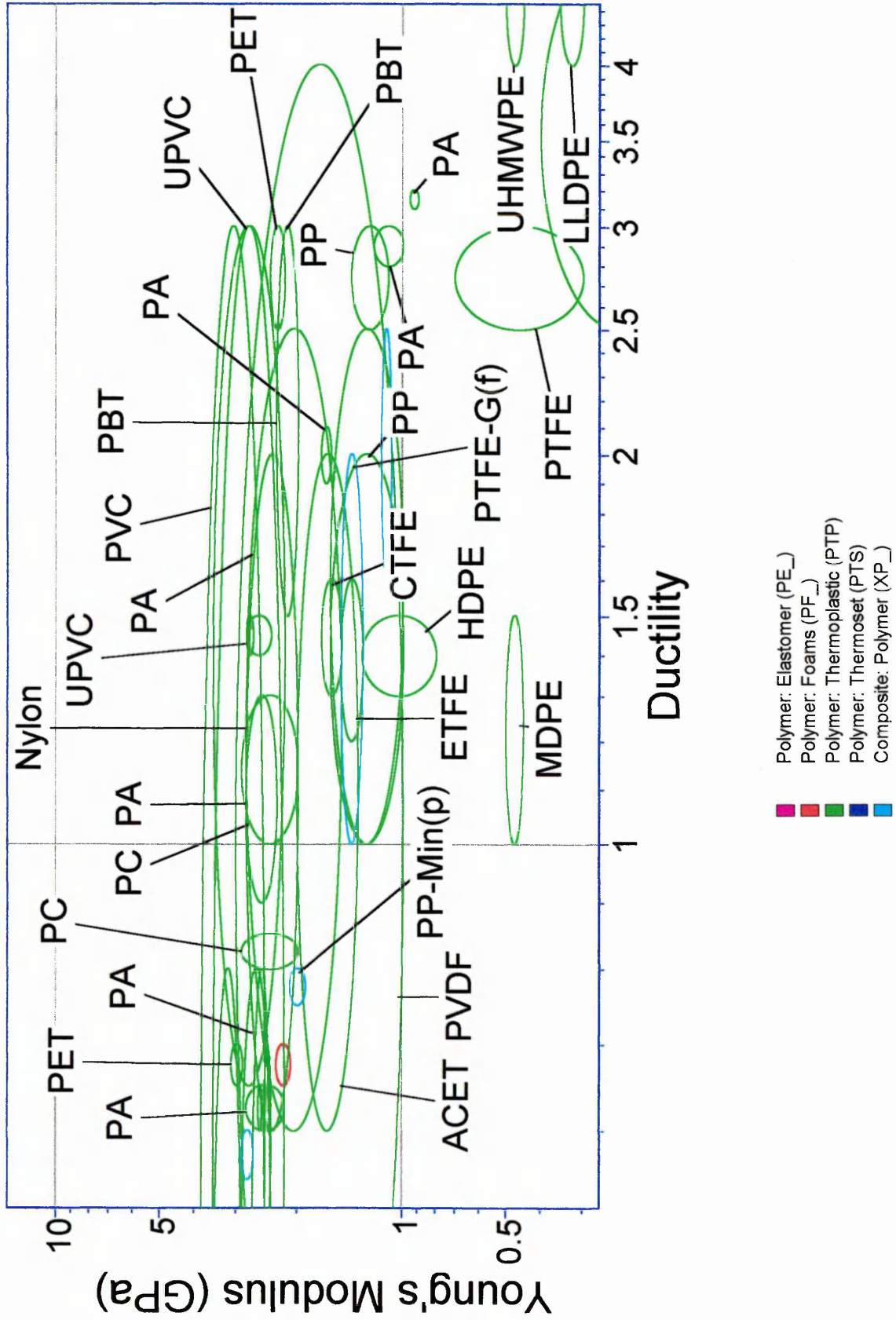
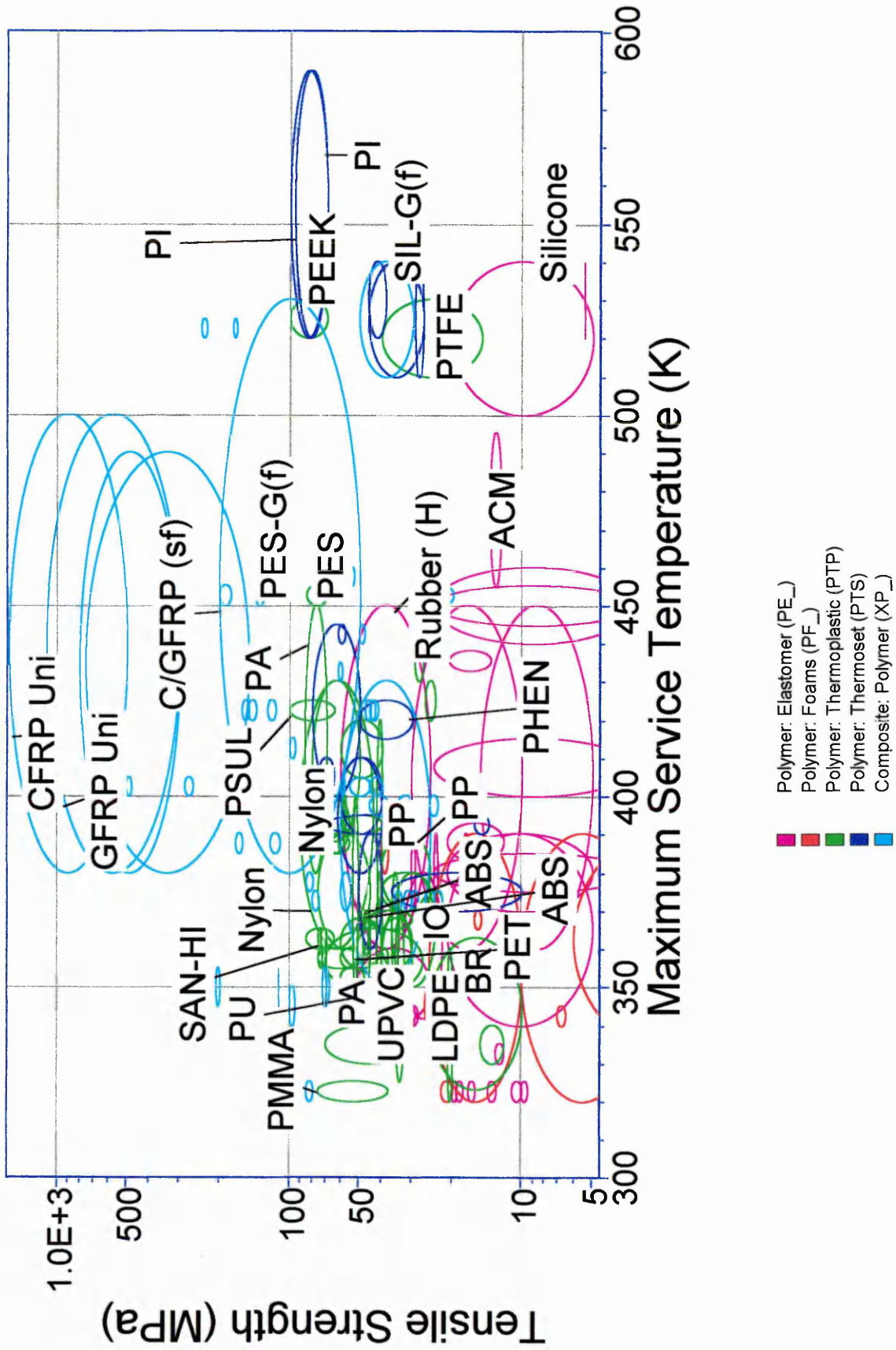




Figure A3.4 Tensile strength and maximum service temperature



**List of abbreviations of material names**

ABS	acrylobutadienestyrene
ACET	acetal
ACM	polyacrylate
Alk	alkyds
BR	butadiene
CAB	cellulose acetate butyrate
CFRP	carbon fibre reinforced polymer
CPE	chlorinated polyethylene
CSM	chloro sulfonated polyethylene
EP	epoxy resin
EPDM	ethylene propylene terpolymer
ETFE	ethylene tetra fluoro ethylene
EVA	ethyl vinyl acetate
GFRP	glass fibre reinforced polymer
HDPE	high density polyethylene
IO	ionomer
LDPE	low density polyethylene
MDPE	medium density polyethylene
PA	polyamide
PBT	poly butyl terephthalate
PC	polycarbonate
PEEK	polyether ether ketone
PES	polyester
PET	polyethylene terephthalate
PHEN	phenolic
PMMA	poly methyl methacrylate
PP	polypropylene
PPO	polyphenyleneoxide
PS	polystyrene
PSUL	polysulphone
PTFE	poly tetra fluoro ethylene
PU	polyurethane
PUTS	polyurethane thermoset
PVC	polyvinyl chloride
PVDF	polyvinylidene fluoride
SAN	styrene acrylonitrile
SBR	styrene butadiene rubber
SIL	silicone
UPVC	polyvinyl chloride

## APPENDIX 4 - Calculations of load to cause crushing of coal

Table A4.1 gives some values of the compressive strength of coal, it can be seen that there is a large variation in the compressive strength.

	mean (MN/m <sup>2</sup> )	variance	standard deviation	minimum value	maximum value	range	no in sample
Coal	30.4	154.3	12.4	11.9	55	43.1	53

**Table A4.1** Compressive strength of coal (Davies (1977))

Table A4.2 gives the loads on bearing plates that would cause coal of different compressive strengths to be crushed when supported at different diameters. It is assumed that the bearing plate is supported at the specified diameters plus an annulus of 2.5 mm around the circumference at the specified diameter. The magnitude of the 2.5 mm annulus was chosen based on observations of the way in which edges of bearing plates modelled using FEA lifted off. The load at which the Weldgrip and Weidmann bearing plate failed at in laboratory tests of specified diameter of hole in steel support plate is given in bold type.

Compressive strength of coal (MN/m <sup>2</sup> )	80 mm diameter extending to 85 mm	100 mm diameter extending to 105 mm	120 mm diameter extending to 125 mm
11.9	7.7 kN	9.6 kN	11.4 kN
20	12.9 kN	16.1 kN	19.2 kN
30	19.4 kN	24.1 kN	28.9 kN
40	25.9 kN	32.2 kN	38.5 kN
50	32.4 kN	40.2 kN	48.1 kN
55	35.6 kN	44.3 kN	52.9 kN
Weldgrip	<b>30.9 kN</b>	<b>17.6 kN</b>	<b>11.6 kN</b>
Weidmann	<b>48.6 kN</b>	<b>37 kN</b>	<b>24.8 kN</b>

**Table A4.2** Calculation of load to cause crushing of coal, when bearing plate is supported at different diameters and load carried by Weldgrip and Weidmann bearing plates in laboratory tests

It can be seen from the results in table A4.2 that with an 80 mm diameter support, the bearing plates (Weldgrip and Weidmann) are stronger than most of the coal and hence the coal fails and the support diameter is increased. For a 100 mm diameter the failure load of the Weldgrip and Weidmann bearing plate is within the range of the failure of the coal and hence the bearing plate may fail or the coal may fail. With a 120 mm diameter of support most of the coal carries more load than the bearing plate and hence the bearing plate fails. Hence this is compatible with the observations given in section 5.2 that a 100 mm hole in the steel support plate gives a reasonable representation of the behaviour in the mine.